Understanding Reaction Mechanisms and Structure/Reactivity Relationships in the Electrophilic Fluorination of Enol Esters

Susanna Helen Wood

Submitted in part fulfilment of the requirements of the degree of Doctor of Philosophy

April 2019

Department of Pure and Applied Chemistry

University of Strathclyde

Thomas Graham Building

295 Cathedral Street

Glasgow

G1 1XL

Declaration

'This thesis is the result of the author's original research. It has been composed by the author and has not been previously submitted for examination which has led to the award of a degree.'

'The copyright of this thesis belongs to the author under the terms of the United Kingdom Copyright Acts as qualified by University of Strathclyde Regulation 3.50. Due acknowledgement must always be made of the use of any material contained in, or derived from, this thesis.'

Signed:

Date:

Abstract

Since the invention of the first fluorinated drug molecule in 1954 fluorinated pharmaceutical compounds have improved the health of many people throughout the world. This is due to the many ways in which fluorine can influence the behaviour, structure and physical properties of organic molecules. An essential aspect of ensuring the access to drug molecules by those who need them is the ability for these compounds to be synthesised efficiently and safely. The near complete lack of natural organofluorine molecules has necessitated the invention of a number of synthetic methods for the introduction of fluorine atom(s) into organic molecules, including nucleophilic and electrophilic fluorinating methods. A complete understanding of the mechanisms in operation in any given synthetic methodology is of high importance in ensuring that the synthetic procedures can be carried out in the most efficient manner possible.

Enol esters have been widely utilised in electrophilic fluorination reactions using the SelectFluor reagent in order to synthesise 6α-fluorosteroid drug molecules. Despite the prevalence of this procedure in the patent literature the reaction mechanism of the electrophilic fluorination of enol esters was hitherto unexplored. Particularly, the addition of acidic and basic compounds to the fluorination reaction is commonplace in order to achieve high α/β ratios however the source of this high diastereoselectivity is unknown.

Investigations into the reaction mechanism of the electrophilic fluorination of simple cyclic enol esters using SelectFluor have been undertaken. Once a feasible mechanistic rationale for the fluorination of these simple substrates had been established a number of steroid-like and steroidal substrates were examined in order to determine whether the mechanism is conserved throughout the different substrate classes. Finally, the role of the additives was examined to determine whether they allow the reaction to proceed *via* a divergent reaction mechanism or if their role is purely to aid crystallisation of the desired 6α-product from the reaction mixture in high purity.

What can't be mended may still be tended

Margaret Atwood, The Year of the Flood

Acknowledgements

Abbreviations

(acac) = Acetylacetone

(DHQ)$_2$AQN = hydroquinine anthraquinone-1,4-diyl diether

(DHQ)$_2$PHAL = hydroquinine 1,4-phthalazinediyl diether

μM = micromolar

2-MeTHF = 2-Methyltetrahydrofuran

5-HT = 5-hydroxytryptamine

Å = Ångstrom

Ac = Acetyl

Ar = Aryl

ax = Axial

Bz = Benzoyl

CNS = central nervous system

COPD = chronic obstructive pulmonary disease

COSY = Correlated Spectroscopy

CYP450 = cytochrome P450

d = doublet

DABCO = 1,4-diazabicyclo[2.2.2]octane

DBN = 1,5-Diazabicyclo[4.3.0]non-5-ene

DBU = 1,8-Diazabicyclo[5.4.0]undec-7-ene

DCM = Dichloromethane

dd = doublet of doublets

ddd = doublet of doublet of doublets

DDQ = 2,3-Dichloro-5,6-dicyano-1,4-benzoquinone

DFT = Density functional theory

DHQB = dihydroquinine 4-chlorobenzoate

DMAP = 4-Dimethylaminopyridine

DMF = dimethylformamide

dt = doublet of triplets

EC_{50} = Half-maximal effective concentration

ED_{50} = Half-maximal effective dose

EPR = Electron Paramagnetic Resonance

eq = Equatorial

Equiv. = Equivalent

ESI-MS = electrospray ionisation/mass spectrometry

Et = Ethyl

FDA = Food and Drug Administration

FDG = fluorodeoxyglucose

FDOPA = fluoro-L-dopa

G = Gibb's Free Energy

g = gram

GC/MS = Gas Chromatography/Mass Spectrometry

GSK = GlaxoSmithKline

H = Enthalpy

h = Planck's constant, $6.62607004 \times 10^{-34} \ m^2 \, kg^{-1} \, s^{-1}$

hERG = Human Ether-a-go-go Related Gene

HMBC = Heteronuclear Multiple Bond Correlation

HPA = hypothalamic-pituitary-adrenal

HPLC = High performance liquid chromatography

HRMS = High Resolution Mass Spectrometry

HSQC = Heteronuclear Single Quantum Coherence

Hz = Hertz

IC_{50} = Half-maximal inhibitory concentration

^{i}Pr = *iso*-Propyl

IR = Infra-Red

K = Kelvin

k = rate of reaction

k_b = Botlzmann constant, $1.38064852 \times 10\text{-}23 \text{ m}^2 \text{ kg s}^{-2} \text{ K}^{-1}$

$Kcal \text{ mol}^{-1}$ = kilocalorie per mole

Kg = kilogram

KIE = Kinetic Isotope Effect

KSP = kinesin spindle protein

LC/MS = Liquid Chromatography/Mass Spectrometry

LDA = Lithium diisopropylamide

LiHMDS = lithium hexamethyldisilyazide

M = molar

m = Multiplet

mbar = Millibar

mCPBA = *meta*-Chloroperoxybenzoic acid

MDAP = Mass Directed Autopurification

Me = Methyl

Mg = milligram

mGluR1 = metabotropic glutamate receptor 1

min = minutes

mL = Millilitre

MsOH = Methanesulfonic Acid

N-FPy = *N*-Fluoropyridinium tetrafluoroborate

NAD^+ = Nicotinamide adenine dinucleotide

NaHMDS = Sodium hexamethyldisilyazide

NFSI = *N*-Fluorobenzenesulfonimide

nM = Nanomolar

NMR = Nuclear Magnetic Resonance

NXS = *N*-Halosuccinimide

Pd(dppf)Cl$_2$ = [1,1'-Bis(diphenylphosphino)ferrocene]dichloropalladium(II)

PET = positron emission tomography

Ph = Phenyl

PMP = *para*-Methoxyphenyl

ppm = Parts Per Million

PTC = Phase Transfer Catalyst

Py = Pyridine

R = Gas constant, 8.314 4621 J mol^{-1} K^{-1}

rt = Room temperature (*ca.* 19-21 ˚C)

S = Entropy

s = Seconds

SAR = Structure Activity Relationship

SDS = sodium dodecyl sulfate

SET = Single Electron Transfer

S$_N$1 = Unimolecular Substitution Reaction

S$_N$2 = Bimolecular nuclear substitution

T = temperature

t = triplet

*t*Bu = *tert*-Butyl

td = triplet of doublets

TEMPO = 2,2,6,6-Tetramethyl-1-piperidinyloxy free radical

THF = Tetrahydrofuran

TMPDA = *N,N,N',N',*-tetramethyl-*p*0phenylenediamine

TMS = Trimethylsilyl

TREAT-HF = Triethylamine trihydrofluoride

TsOH = *p*-Toluenesulfonic acid

UV/vis = Ultraviolet/visible

WHO = World Health Organization

Table of Contents

1. Introduction

1.1. Fluorine in Medicinal Chemistry

Modern medicine has had a beneficial impact on quality of life for many people all over the world, with life expectancies in western countries continuing to rise. In 2017, the World Health Organization (WHO) updated their list of essential medicines such that it now includes 433 medical treatments.[1] This illustrates the importance of the development of new medicines which necessitates drug research and development by medicinal chemists. Fluorine can have a dramatic effect on the properties of biologically active molecules and has therefore found its way into many drug molecules.[2] Indeed, in 2016 as many as 12% of the top 200 prescribed drugs in the USA contained at least one fluorine atom (*Figure 1*).[3,4]

Top 100 Prescribed US Drugs 2016

Approvals 2009-2018

- ■ No fluorines   ■ 1 fluorine
- ■ 2 fluorines   ■ 3 fluorines
- ■ 4 or more fluorines

■ Non-Fluorinated   ■ Fluorinated
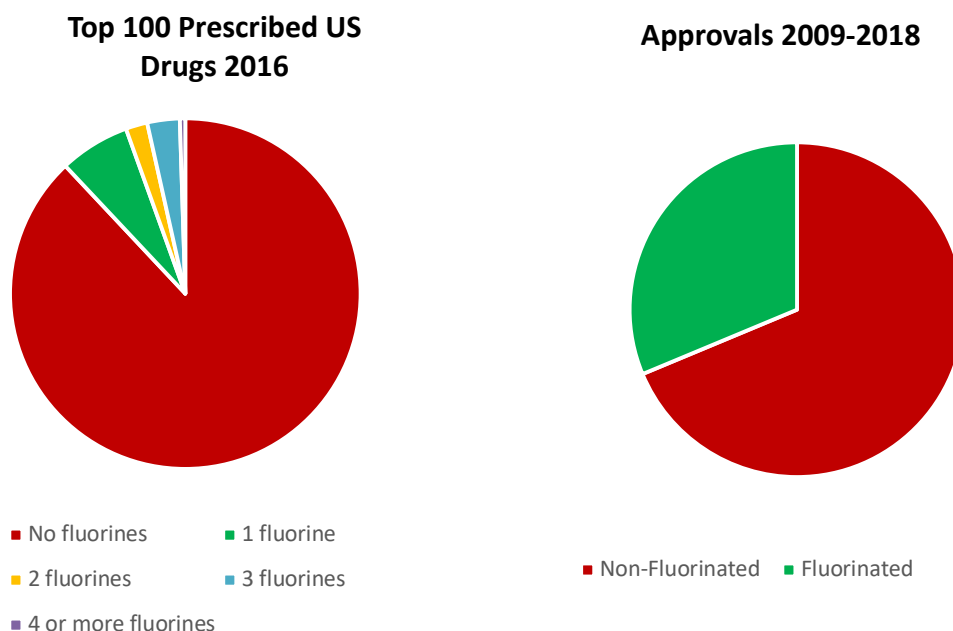
Figure 1: Top Prescribed US Dugs in 2016 (left), Drug Approvals from 2009-2018 (right)

Discovery of novel biologically active fluorinated molecules is not slowing down either; a search of the ChEMBL drug database indicated that of the 179 new approvals of

synthetic small molecule drugs in the last decade 56 of these contained at least one fluorine atom, making up 31% of all new approvals in this time.[5]
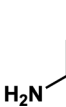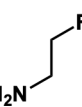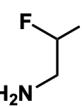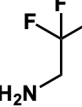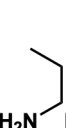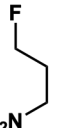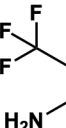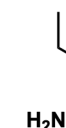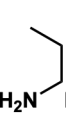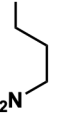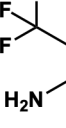
1.1.1. Influence of Fluorination on pK_a

Another prevalent structural motif within drug molecules is a basic nitrogen. The protonation state of a basic molecule can impact its pharmacological behaviour, changing its lipophilicity,[6] permeability,[7] solubility[8] and biological activity at the target.[7,9] The basicity of the nitrogen can also cause problems, such as increased activity at antitargets such as human Ether-a-go-go Related Gene (hERG).[10,11,12] The control of pK_a is therefore a vital tool for the medicinal chemist. There are a number of different ways to achieve this,[9] with fluorination being one. The modulation of the properties of a molecule using fluorine is an attractive prospect given that after hydrogen, fluorine is the smallest possible substituent making it least likely to have a detrimental effect on biological activity. Carbon-fluorine bonds are amongst the strongest bonds due to highly effective orbital overlap between fluorine and carbon. In addition to this the fluorine lone pairs and negative dipole on fluorine shield the carbon centre from nucleophilic attack.[13] These features allow a degree of confidence in the stability of the resulting compound. Fluorination reduces pK_a by withdrawing electron density inductively, lowering the basicity of the nitrogen centre. Introducing a fluorine atom at the β-position in open chain aliphatic amines has the most drastic effect, with pK_a being lowered by *ca*. 1.7 units. This effect is continued for further additions of β-fluorine.[9] Introduction of fluorine at positions further removed from the nitrogen can also lower the pK_a, though to a lesser extent, and the further the fluorine is from the basic nitrogen, the smaller the effect is.[9] *Table 1* shows the expected pK_a decrease for fluorine substituted amines, depending on the fluorine position. The addition of two fluorines to ethylamine allowed the pK_a to be tuned to physiological pH.

Table 1: Influence of Fluorination on Acyclic Amine pK$_a$

Fluorine Position	pK$_a$
F-α	-1.7
F-β	-0.7
F-γ	-0.3
F-δ	-0.1

pK$_a$ =   10.7   9.0   7.3   5.6

pK$_a$ =   10.7   9.9   8.7   10.7   9.7

In cyclic amines, fluorination can decrease the pK$_a$ in a manner similar to that observed in acyclic amines. The situation is complicated by the fact that the molecule is constrained by the ring system, therefore the fluorine can either occupy the axial or equatorial position. In addition to the distance from the basic centre, the geometry of the fluorinated ring can have an effect on pK$_a$. When fluorine occupies the axial position, the influence on pK$_a$ is less marked than would be predicted from the values for open chain amines whilst for equatorial fluorines the effect is more pronounced. For example, in 3-fluoropiperidine (*Figure 2*), the fluorine is in the β-position on one side and the δ-position on the other side, relative to the nitrogen, therefore the decrease in pK$_a$ (from *Table 1*) would be expected to be 2.0 units. In practice, the pK$_a$ decrease is observed to be 1.8 units.[9] Conversely, when the pK$_a$ of a polyhydroxylated piperidine, known to contain an equatorial fluorine in the β-position, was measured, the decrease compared to the non-fluorinated compound was found to be 2.25 units.[14]

Lankin *et al.*[15] performed NMR experiments to observe the behaviour of a number of fluorinated piperidines which uncovered an effect on conformation of the piperidines dependent on protonation state. They found that when 3-fluoropiperidinium hydrochloride was analysed in D$_2$O solution, the only conformer observed was the one

in which the fluorine adopts an axial orientation. Conversely, when the molecule was analysed under basic conditions (1 N NaOD in D_2O) where it is converted to the free base, only the equatorial conformer was observed. The behaviour observed for 3-fluoropiperidinum hydrochloride was also observed for its N-methylpiperidinium and N,N-dimethylpiperidinium counterparts.[16] It was suggested that it is possible for the molecule to form favourable charge-dipole interactions when fluorine is in the axial position[9,15,16] when the piperidine is positively charged. These additional interactions are thought to stabilize the axial N-H bond in the cation which can account for the unexpectedly small pK_a decrease for mono-fluorinated piperidines.

Medicinal chemists have been able to use the effect of fluorination on pK_a to great advantage. Van Niel and co-workers developed a series of basic-nitrogen containing compounds when investigating the synthesis of 5-hydroxytryptamine receptor 1D (5-HT$_{1D}$) selective agonists for the treatment of migraine.[17] Compound **1** (*Figure 3*) which was identified as a starting point for SAR generation, had a high affinity for 5-HT$_{1D}$ (IC$_{50}$ 0.14 nM) but was found to be unselective, also binding to 5-HT$_{1B}$ with an IC$_{50}$ of 11 nM. Attempts to attenuate the promiscuity of the molecule found that a second piperazinyl nitrogen was unnecessary for the binding of **1** to either of the 5-HT receptors as piperidinyl analogue **2** had almost identical affinity. However, it was discovered that while compound **1** was very readily absorbed and highly orally bioavailable, **2** did not have such properties.
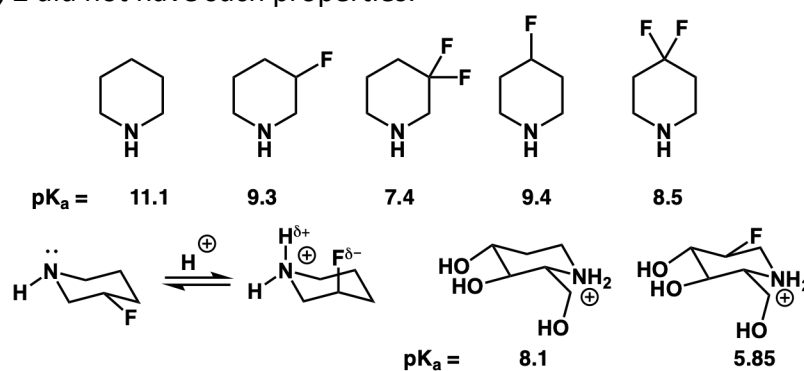
Figure 2: Influence of Fluorination on pK_a of Cyclic Amines
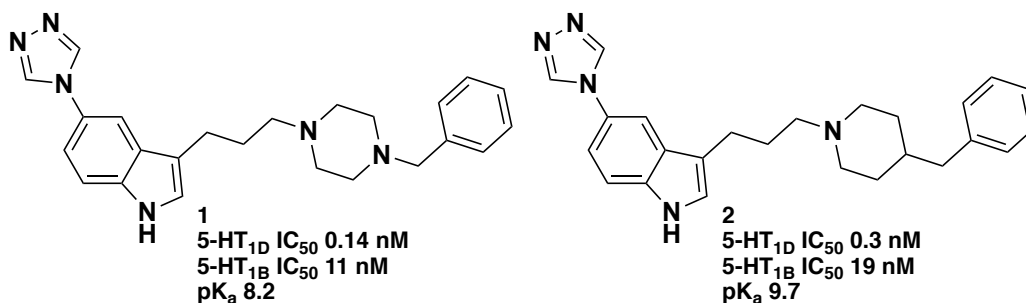
Figure 3: Compounds *1* and *2*

The difference in physiochemical properties was attributed to the reduced basicity of the piperizinyl nitrogen. Modulation of the pK_a was then investigated *via* fluorination of compound **2** and related analogues. Fluorination of **2** in the 4-position (as in **3**, *Figure 4*) afforded the desired decrease in pK_a to a value more comparable to that of **1**; however, there was no improvement in selectivity for the target. Relocation of the fluorine to the linker between the indole and the piperidine in **4** proved to be more fruitful. This structural modification resulted not only in a more desirable pK_a value but also in higher selectivity between the 5-HT receptors. The development of **4** illustrates nicely how fluorination can have dual positive consequences in biologically active molecules.
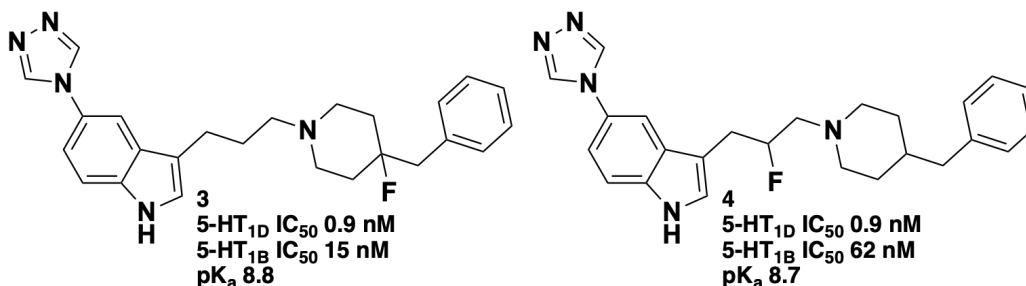
Figure 4: Compounds *3* and *4*

Cox *et al.*[18] also ran into selectivity issues with their intended kinesin spindle protein (KSP) inhibitors for the treatment of cancer; on this occasion the issue was blockade of the hERG potassium ion channel found in the heart. Drugs have been withdrawn from the market due to hERG interaction as it has been implicated in undesirable cardiovascular side effects.[10] It is therefore critical that any potential drug molecule has minimal interaction with this protein. The starting point for this work was compound **5** (*Figure 5*) which had been identified as having a high affinity for KSP in

binding assays (IC$_{50}$ 6 nM) as well as *in vivo* potency in the mouse xenograft cancer model.[18] Unfortunately, **5** also exhibited unacceptably high hERG inhibition (IC$_{50}$ 14.6 μM), probably due to the high pK$_a$ of the piperidine nitrogen. Again, fluorination was employed to great effect in lowering the pK$_a$. Introduction of fluorine in the 3-position of the piperidine generated two diastereoisomers: **6** which features an axial fluorine and **7** in which the fluorine is equatorial. This example demonstrates the drastic difference between the pK$_a$'s of piperidines containing equatorial and axial fluorines. Axial diastereoisomer **6** exhibits a drop in pK$_a$ of 1.2 units, while in **7** the decrease is much bigger at 2.2 units. These compounds with lowered pK$_a$ also had lower activity at hERG whilst also maintaining activity at the KSP target. The above examples provide just two instances from the literature where fluorination has been utilised to great effect by the medicinal chemist in lowering the basicity of amines; however, many more examples exist.[19–21]

5
KSP IC$_{50}$ 6 nM
hERG IC$_{50}$ 14.6 μM
pK$_a$ 8.8

6
KSP IC$_{50}$ 2.2 nM
hERG IC$_{50}$ 20.5 μM
pK$_a$ 7.6

7
KSP IC$_{50}$ 11.5 nM
hERG IC$_{50}$ 36.9 μM
pK$_a$ 6.6
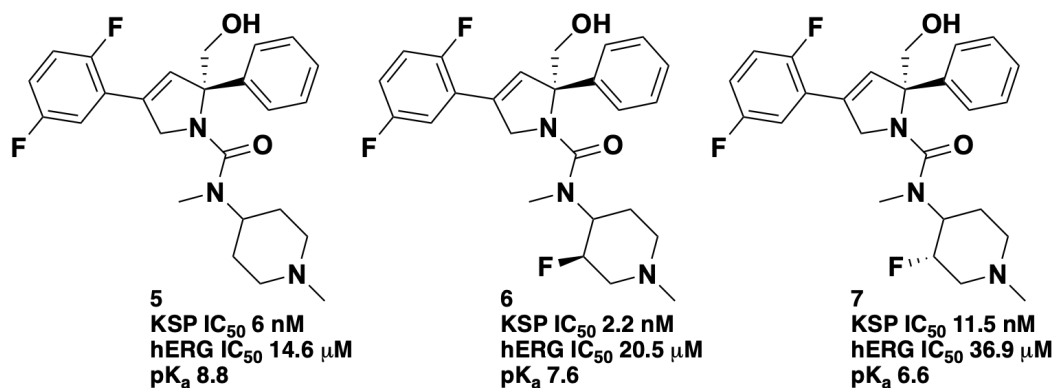
Figure 5: Compounds 5-7

It is not only basic functionality which can have its pK$_a$ modified by the introduction of a fluorine atom nearby. In 1993, Maren and Conroy were investigating carbonic anhydrase inhibitors. It had long been known that weakly acidic sulfonamide **8** (*Figure 6*) was a carbonic anhydrase inhibitor and it had been found that anionic functionality was critical for activity. It was proposed that a high affinity molecule would be identified if the pK$_a$ of **8** (pK$_a$ 10.5) could be lowered. Indeed, when the fluorinated analogue **9** was tested, it exhibited not only the lower pK$_a$ desired, but also improved

affinity in a binding assay. Compound **9** also had the added advantage over its unfluorinated counterpart in that it was highly soluble in aqueous media.[22]

8
Carbonic anydrase K$_i$ >10000 nM
pK$_a$ 10.5

9
Carbonic anydrase K$_i$ 2 nM
pK$_a$ 5.9
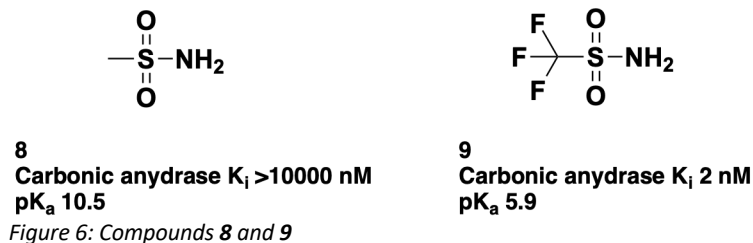
*Figure 6: Compounds **8** and **9***

1.1.2. Influence of Fluorine on Conformation

Fluorine is the most electronegative element in the periodic table, so carbon-fluorine bonds are highly polarised and the resulting dipole can have a profound effect on the conformation of fluorine-containing molecules.[23] O'Hagan and co-workers[24] observed in 1999 that α-fluoroamides preferentially adopted a conformation in which the C-F bond was orientated *trans*-to the amide carbonyl due to dipole-dipole repulsion
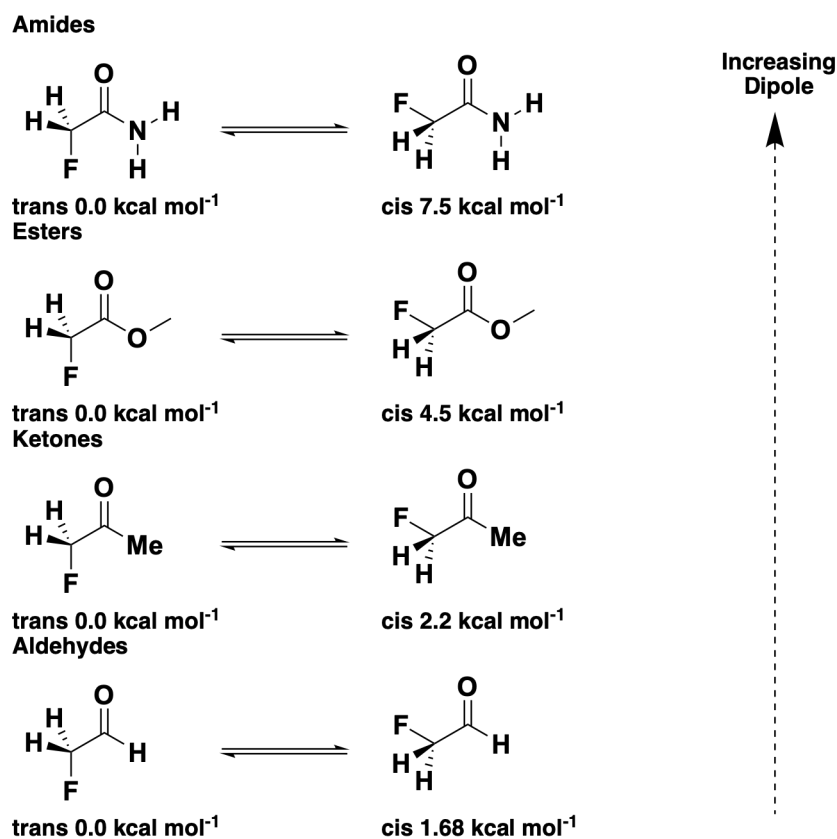
Figure 7: Conformational Preferences of α-Fluorocarbonyl Compounds

7

(*Figure 7*). The effect was also observed in other carbonyl containing compounds, but was less pronounced as the carbonyl dipole weakened.[25–27]

It is not only through repulsive interactions that the fluorine-carbon dipole can have an influence on the conformation of a molecule. Given that peptides exist in equilibrium between the cisoid and transoid geometries around the amide bond, there has long been interest in the substitution of an alkene for an amide unit in biologically relevant molecules, both to further understand active conformation of a peptide and for the generation of more long-lived biologically active species.[28,29] An obstacle is presented by the fact that an unsubstituted alkene lacks the polarity and hydrogen bond-making capabilities of the amide it replaces. This can result in loss of activity at the biological target. However, it is possible for a fluoroalkene moiety to act as a mimic for the amide functional group, due to the highly polarised nature of the carbon-fluorine bond (*Figure 8*). While this motif does not have the same hydrogen bond forming capabilities as the amide, it has been found that the direction of the dipole is similar enough for it to behave as a convincing bioisotere.[30–33]

Figure 8: Comparison of Amide and Fluoroalkene

Compounds that contain fluorine in the position β-to a protonated heteroatom preferentially adopt a *gauche* conformation. This effect is the result of the same stabilising interactions that explain the preferential axial orientation of fluorine in 3-fluoropiperidines (page 4).[15,16,23,34]
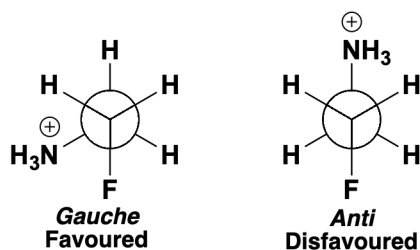
Figure 9: Gauche *and* Anti *Conformations*

In amines, the *gauche* conformation is only slightly favoured due to a weak intramolecular N-H…C-F hydrogen bond, according to density functional theory calculations carried out by O'Hagan and colleagues (*Figure 9*).[34]

The conformational restrictions which appropriately placed fluorine atoms can exert on a molecule have the potential to elucidate the preferred conformation of known ligands when they bind to biological targets. Hunter *et al*. have investigated the effect of difluorinated γ-amino acids can have on the geometry of peptides,[35–37] demonstrating how fluorination could be employed to control the conformation of unguisin A (*Figure 10*).[38]
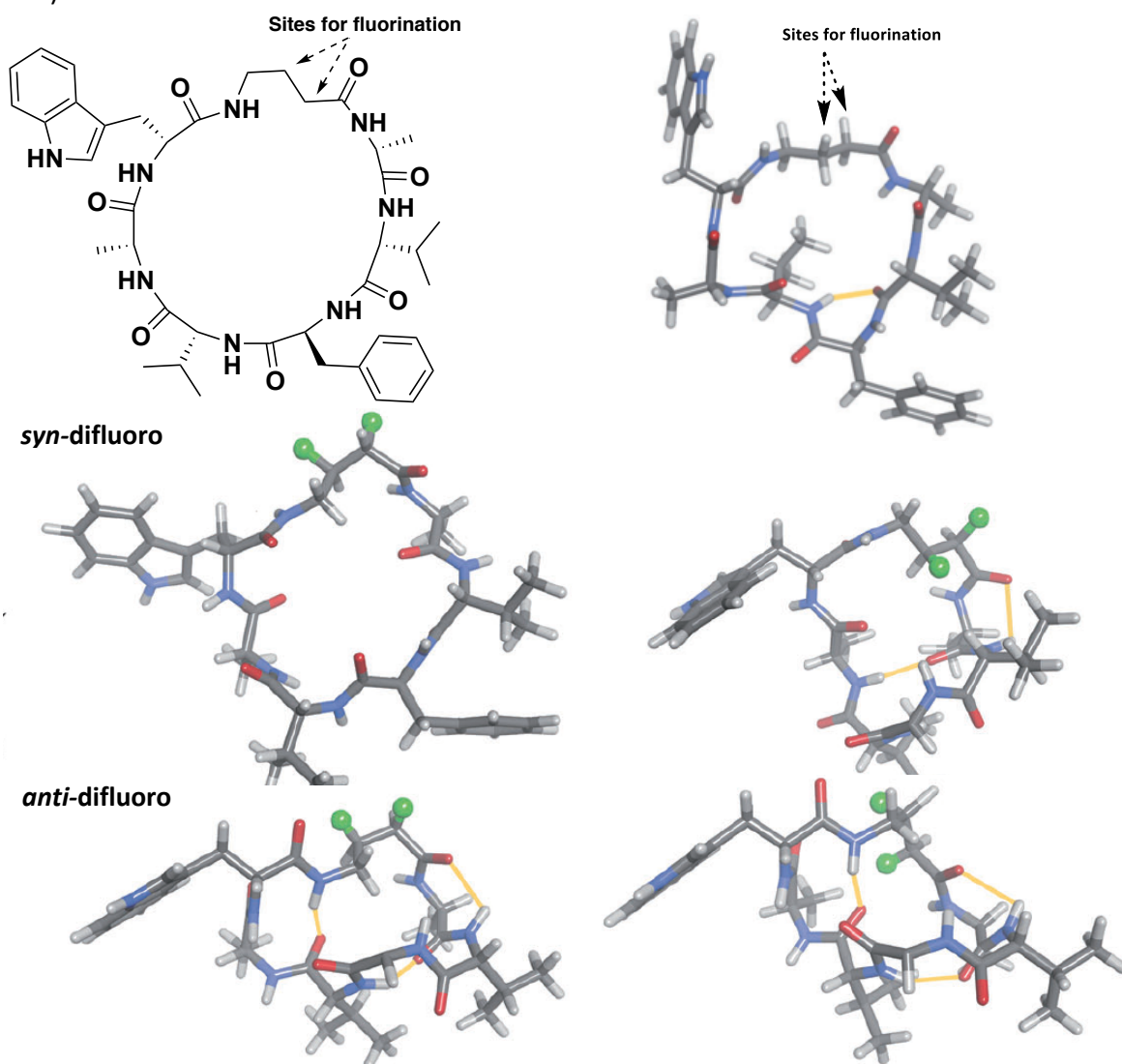
Figure 10: Unguisin A Conformations

Four fluorinated analogues of the natural peptide were synthesized. ^{1}H NMR experiments in conjunction with DFT energy minimization calculations on the structures revealed that fluorination had indeed changed the geometry of the parent peptide, allowing varying degrees of intramolecular hydrogen bonding.

1.1.3. Influence of Fluorine on Metabolic Stability

It is of vital importance that a drug molecule gets to its site of action intact so that it can carry out its function. Unfortunately, organisms have developed efficient ways of metabolising organic molecules so that they can be excreted. If a biologically active molecule is easily metabolized, only a small amount will reach the site of action, which would necessitate high doses in order to observe the desired effect. With higher doses, the risk of unwanted side effects is increased. In other cases, drug molecules can be metabolized into toxic compounds which not only do not carry out the function the drug was originally designed for but also have harmful effects on the patient.
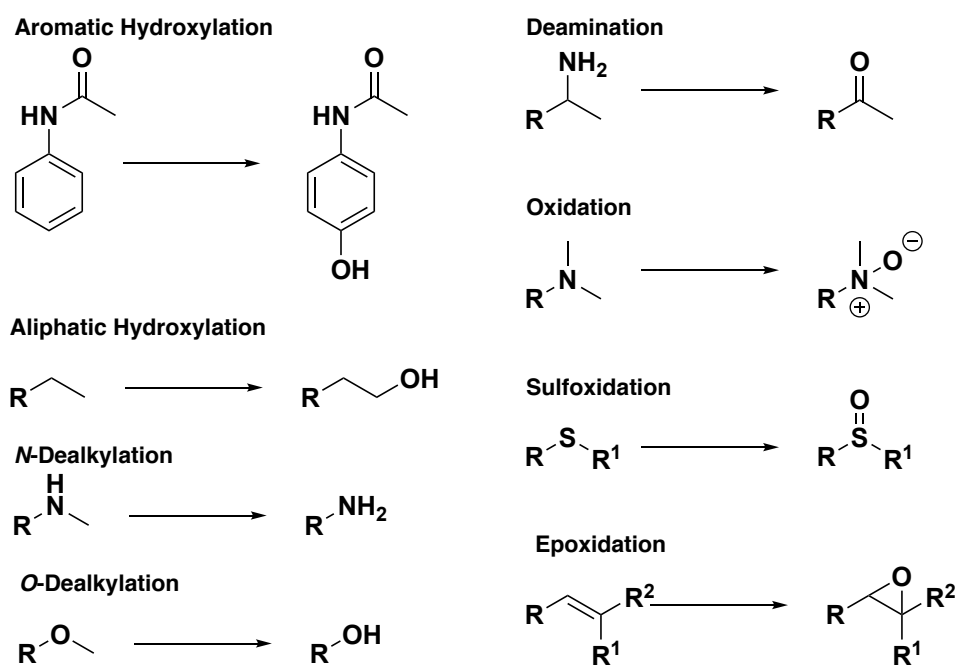
Figure 11: Common CYP450 Metabolism Pathways

This highlights the need to understand what happens to a molecule once it is inside the body and for strategies to prevent undesired metabolic pathways. Transformations of drug molecules during metabolism are generally divided into two categories which are Phase I and Phase II. The majority of the Phase I metabolic events are performed by Cytochrome P450 (CYP450) enzymes (*Figure 11*); these tend to be oxidative processes, involving the introduction of polar functionality into molecules, often providing substrates for Phase II metabolism.

Common Phase I transformations are aromatic hydroxylation, aliphatic hydroxylation, *N*-dealkylation, *O*-dealkylation, deamination, oxidation and sulfoxidation. Unsaturated molecules can be metabolised via epoxidation followed by hydrolysis to dihydroxylated products. Phase II metabolism involves conjugation reactions in which a solubilising group is attached to the molecule.[39]

Fluorination has been identified as a useful means of blocking undesirable metabolism of a drug molecule. Research at Schering-Plough into cholesterol absorption inhibitors for the treatment of heart disease resulted in the design and synthesis of **10** (*Figure 12*); unfortunately, studies of its metabolic profile predicted that it would be transformed into a complex mixture of metabolites. It was then found that the mixture of metabolites was a more potent inhibitor of cholesterol absorption than **10** itself. Analysis of **10** suggested that there were several metabolically labile positions. A selection of the potential metabolic products was synthesized in an attempt to identify which modifications were associated with the increased activity. Aliphatic hydroxylation in the benzylic position along with *O*-dealkylation of one methoxy group increased biological activity. In contrast, aromatic hydroxylation and *O*-dealkylation of the other methoxy group were found to lower activity. These findings led to the design of a more active and more metabolically stable analogue of **10**; alcohol **11** showed a 50-fold improvement in *in vivo* activity compared to the parent compound, attributed to a combination of improved binding and increased metabolic stability.[13,40]

O-Dealkylation sites

Hydroxylation sites

10
ED$_{50}$ 2.2 mg kg^{-1} day^{-1}

11
ED$_{50}$ 0.04 mg kg^{-1} day^{-1}
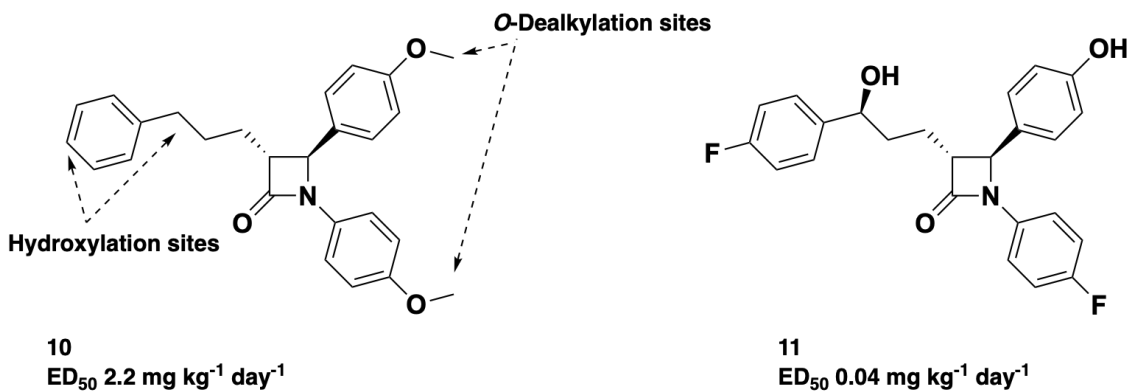
Figure 12: Compounds 10 and 11

Whilst simply blocking the metabolically labile site with fluorine has been employed to great effect, it is also possible to suppress metabolism of a molecule by fluorinating adjacent to a vulnerable functional group. Many of the metabolic pathways discussed above proceed *via* a partially positively charged intermediate; introduction of fluorine can inhibit the formation of such intermediates. A fluorine atom is strongly inductively electron-withdrawing so formation of a positive charge nearby is disfavoured.[13]

9α-Fluorocortisol (**13**) is a much more potent analogue of the natural product cortisol (**12**). When cortisol is metabolised, the 11β-hydroxy group is oxidized to an inactive ketone by NAD$^+$. This process involves the formation of a partial positive charge. In the 9α-fluoro derivative, this oxidation does not occur due to the inductive electron withdrawing effects of fluorine destabilizing the positive charge.[13,41,42] The above examples are but two of the many instances where fluorination of a biologically active but metabolically susceptible species has been employed to improve *in vivo* stability.[43–51]

12
Cortisol

13
9α–Fluorocortisol
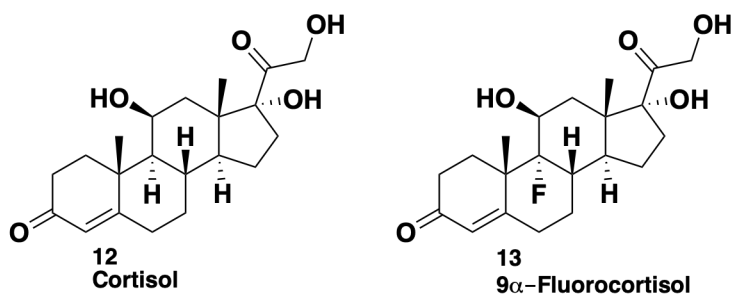
Figure 13: Cortisol (12) and 9α-Fluorocortisol (13)

1.1.4. Influence of Fluorination on Target Binding

The previous sections have discussed how fluorination can be used to influence the behaviour of biologically active molecules to solve a particular problem, often with fortuitous improvements in biological activity. The unique properties of the fluorine atom can also be exploited to improve binding or activity, and form additional interactions with a target protein. A fluorine atom is an interesting substituent in medicinal chemistry, because it allows "polar lipophilicity" to be introduced into a molecule. Fluorine is capable of behaving as a weak hydrogen bond acceptor. Calculations predict the strength of the F...H hydrogen bonds to be between 1.9 and 3.2 kcal mol^{-1}.[52] This is considerably weaker than O...H hydrogen bonds which tend to fall within the range of 5 to 10 kcal mol^{-1}.[53] In 1996, O'Hagan and co-workers[53] analysed all the crystal structures which contained fluorinated molecules in the Cambridge Structural Database System, in order to determine whether these molecules were forming hydrogen bonds and whether fluorine was capable of replicating the hydrogen bonding observed in HO...H interactions. The analysis revealed that though very few fluorinated molecules were forming short contact hydrogen bonds, it was possible. It also demonstrated that C(sp^2)-F...H hydrogen bonds (1.48 kcal mol^{-1}) were much weaker than C(sp^3)-F...H hydrogen bonds (2.38 kcal mol^{-1}).[53]

Due to the high electronegativity of fluorine, substitution of hydrogen for fluorine on an aromatic ring inductively withdraws electron density from the aromatic system, in turn increasing the polarisation of the remaining hydrogens on the ring. This allows them to better participate in CH-π interactions with – for example – aromatic amino acids in proteins.[13,54] Fluorination can also alter the behaviour of substituents on an aromatic ring. In anisole, the methyl group lies in the plane of the ring as the p-type lone pair of the oxygen is in conjugation with the ring π-electrons (*Figure 14*). When the methoxy group is replaced with a trifluoromethoxy, the trifluoromethyl is no longer in the plane of the ring.[55,56] The alteration of geometry when compared to anisole is surprising, given

that not only is the stabilising p-type lone pair to π-system lost, but the electronegative fluorine atoms are orientated facing the electron rich π-cloud.
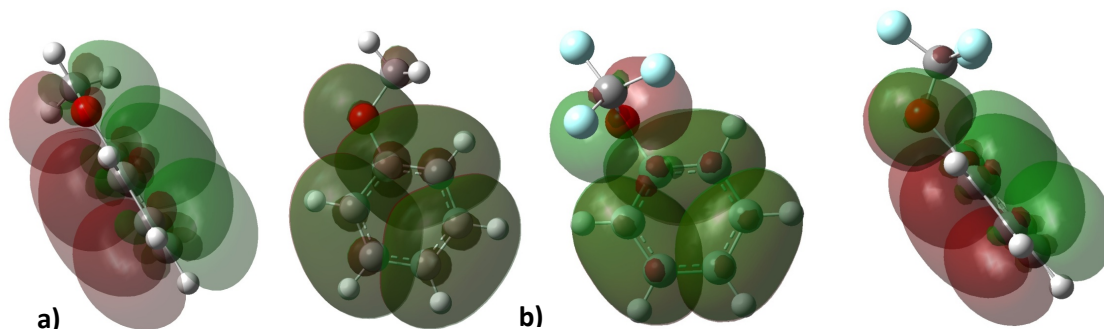
Figure 14: Orbital Overlap in Anisole (a) and Trifluoroanisole (b)

Caminati and co-workers postulated that the fluorine atoms were potentially forming favourable interactions with the adjacent hydrogens on the aromatic ring, indeed the distance between the fluorine and hydrogen is in keeping with that of a weak hydrogen bond.[55] In addition to the changed geometry of the molecule, the C-F bond in trifluoromethoxybenzene is lengthened when compared to α,α,α-trifluorotoluene as one of the oxygen lone pairs can donate into the σ*-orbital of the C-F bond resulting in lengthening of the C-F bond.[56]

Another key means in which fluorine can interact with biological targets is *via* dipole-dipole interactions. Whilst the ability of fluorine as a hydrogen bond acceptor is moderate, it has been discovered that fluorine can participate in dipole-dipole attractive interactions with the carbon of carbonyl groups.   This ability allows favourable interactions between fluorinated molecules and the amide backbone of proteins. This phenomenon is not restricted to aliphatic fluorines but is also observed for aromatic fluorines and trifluoromethyl groups. Repulsive dipole-dipole interactions can also occur, resulting in fluorinated moieties preferentially binding so that they need not interact with electron rich functional groups, such as the electron rich indole of the amino acid tryptophan.[56,57]

An example of fluorine acting as a hydrogen bond acceptor and participating in intramolecular hydrogen bonds can be found in the isomeric adrenoreceptor ligands **14** and **15** (*Figure 15*). Compounds **14** and **15** are fluorinated analogues of the endogenous adrenoreceptor ligand norepinephrine.   The fluorine on the aromatic ring forms a hydrogen bond with the benzylic hydroxyl group. Depending on the regiochemistry of the fluorine the molecule adopts a different conformation. Surprisingly, compound **14** is a β-agonist and **15** is an α-agonist.[13,58]

Norepinephrine

14
α−**Adrenic activity EC$_{50}$ 110 μM**
β−**Adrenic activity EC$_{50}$ 0.7 μM**

15
α−**Adrenic activity EC$_{50}$ 2.6 μM**
β−**Adrenic activity EC$_{50}$ 72 μM**
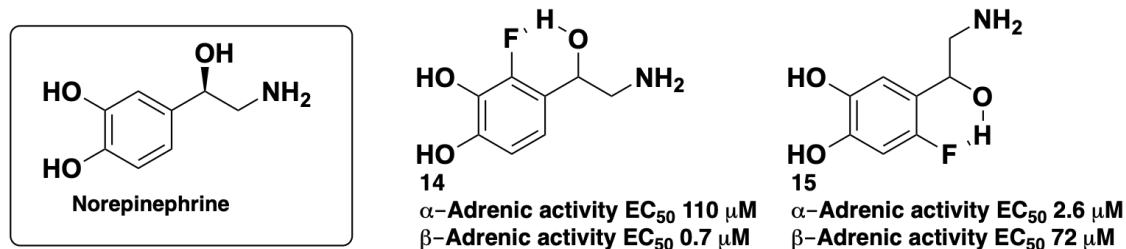
*Figure 15: Compounds **14** and **15***

It has been discovered that the thrombin receptor can be activated by a seven amino acid sequence at the *N*-terminus of the protein. This heptapeptide has also been found to be active in the absence of the rest of the protein. Site directed mutagenesis on the *N*-terminal heptapeptide revealed a phenylalanine residue to be critical for activation of the receptor. Further research conducted by Shimohigashi *et al.*[59] into modification of the heptapeptide showed that the activity of the peptide could be improved by the substitution of phenylalanine by *para*-fluorophenylalanine. Further investigation into substituting fluorine atoms for the hydrogens on phenylalanine provided some interesting results. Substitution of all the hydrogens on the phenyl ring of the phenylalanine residue resulted in complete loss of activity, indicating that the presence of at least some of the aromatic hydrogens was important for activity. Comparable activity to the *para*-fluorophenylalanine derivative was observed for the 2,4-difluorophenylalanine (**16**) and 3,4-difluorophenylalanine (**17**) analogues. It was postulated that the reason for the high activity observed was CH/π edge-to-face interactions, as shown in *Figure 16*.[60]
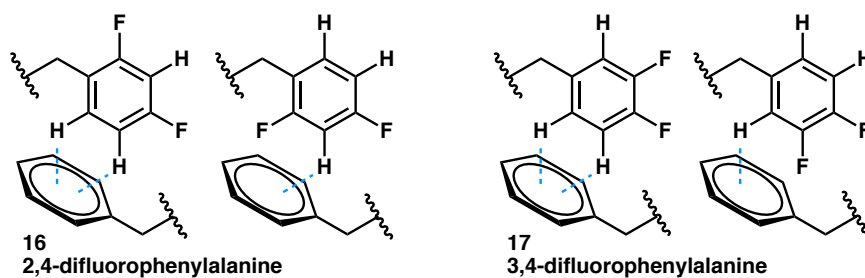
Figure 16: Interactions of Phenylalanine Compounds 16 and 17

Thrombin plays a key role in blood clotting processes[61] and therefore has become the target for drug research and development into inhibitors which produce an anticoagulant effect.[62]   In conducting research into possible thrombin inhibitors, Diederich and co-workers uncovered interesting insight into the interaction of organo-fluorine molecules with proteins.[63] They found that electronegative fluorine was able to form a weak attractive interaction with carbonyl carbons of the amide backbone. One such example of this is found in compound **18** (*Figure 17*). The 4-fluoro-aryl moiety is in close proximity to a carbonyl carbon of the amide backbone of thrombin, potentially forming an attractive interaction.
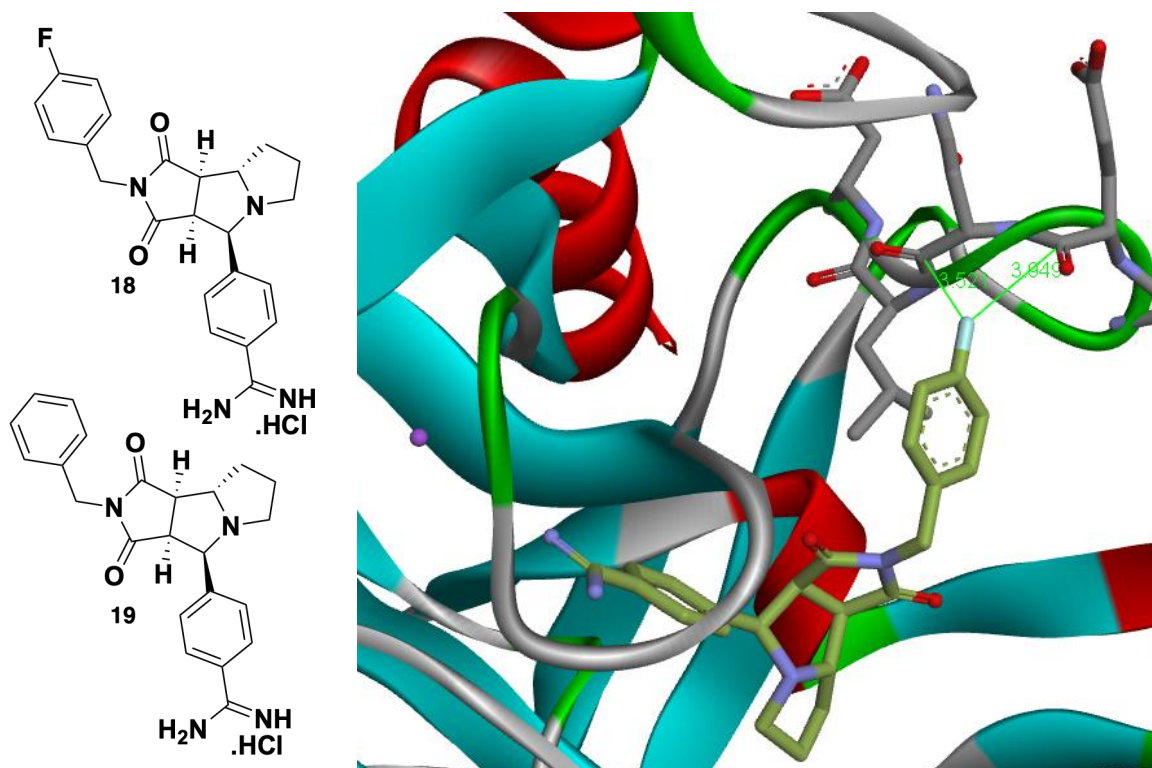
Figure 17: Compounds 18 and 19 (left) Compound 18 Binding to Thrombin (right)

The fluorinated compound **18** exhibited enhanced activity (K_i 0.057 μM) at thrombin compared to the non-fluorinated analogue **19** (K_i 0.31 μM) and it was postulated that this was at least in part due to this attractive interaction.[63]

1.1.5. Applications of ^{18}F in Medicine

The ^{18}F radioisotope has found application in medical diagnostics. ^{18}F is a positron emitter and has therefore been exploited in positron emission tomography (PET). ^{18}F has a half-life of 109.8 minutes, which is favourable when compared with radioisotopes of other nuclei commonly found in biologically active molecules (the half-lives of ^{15}O, ^{13}N and ^{11}C are 2 minutes, 10 minutes and 20 minutes respectively). ^{18}F is prepared in a cyclotron as either $[^{18}F]F_2$ or $[^{18}F]$fluoride. These can be used directly in the synthesis of radioligands or for the production of fluorination reagents.[64]

Due to these useful radioisotopic properties, ^{18}F has been used to label a number of different molecules for use in medical diagnostics. In the field of oncology ^{18}F labelled molecules are widely applied. PET imaging can be used to determine the location of any cancerous tissue to aid diagnosis, to identify if a treatment of a patient is complete, or to determine disease progression. Increased glucose metabolism has long been known to be an indication of cancerous tissue,[65] and this knowledge led to the design of 2-deoxy-D-glucose in 1960. 2-Deoxy-D-glucose can be phosphorylated as for glucose; however, once inside the cell, further metabolism is impossible so it accumulates. The synthesis of $[^{18}F]$fluorodeoxyglucose (FDG, **20**, *Figure 18*) then allowed the study of glucose metabolism *via* PET. Although it was first applied to imaging of cardiac and brain tissue, $[^{18}F]$FDG is now widely used for imaging of cancerous tissue. $[^{18}F]$FDG PET imaging is not without its disadvantages, and can on occasion give misleading results. Cancerous cells are not alone in their elevated uptake of $[^{18}F]$FDG; cells associated with inflammatory responses, for example, are more glucose-hungry than cancer cells and therefore accumulate even more $[^{18}F]$FDG than cells in a tumour.[66]

Another important fluorinated PET ligand is [18F]fluoro-L-dopa (FDOPA, **21**, *Figure 18*). In patients with Parkinson's disease, the ability to convert the natural amino acid L-dopa to dopamine is diminished. It is possible to use PET imaging to measure [18F]FDOPA uptake as a determination of the ability for L-dopa conversion to dopamine in the brain.[67,68] Furthermore, patients can be dopamine-deficient in the brain for some time before symptoms present, so PET imaging using [18F]FDOPA has the potential to allow the diagnosis and treatment of Parkinson's disease to begin before the quality of life of the patient has begun to deteriorate, hopefully resulting in better clinical outcomes.[69]
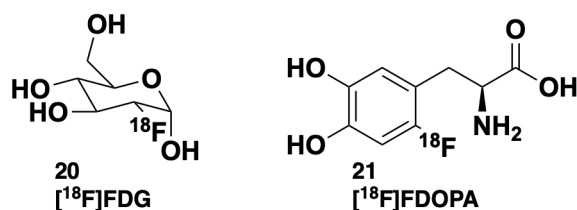
Figure 18: [18F]Fluorodeoxyglucose (20) and [18F]F-dopa (21)

PET ligands are also useful in confirming that a proposed drug is getting to the site of action. For example, a compound designed to treat a neurological condition is most likely to exert its action in the brain so it must be able to cross the blood/brain barrier to reach the site of action. If there is a suitable PET biomarker for the condition, it is possible to determine if it has been displaced by the proposed drug molecule, thus confirming CNS penetration.

An example of this technique in action was described by Elmenhorst *et al.*,[70] when examining the occupancy of the A_1 receptor by caffeine. It is thought that caffeine exerts its stimulant effect *via* antagonism of the adenosine receptors in the brain. Whilst knockout studies in animal models suggested that the effects of caffeine are predominantly mediated by the A_{2a} receptor, due to the differences in receptor concentration and distribution, questions have been raised as to whether these translate to the effects observed in humans. Therefore, it was necessary to examine the binding of caffeine to the A_1 receptor, the most abundant of the adenosine receptors found in

the human brain. This was achieved by monitoring the displacement of an ^{18}F labelled A$_1$ ligand using PET imaging (*Figure 19*).

It was discovered that caffeine is capable of displacing the radioligand in order to bind to the receptor at concentrations which equate to the same amount of caffeine in 4-5 cups of coffee. It was therefore postulated that the amount of caffeine regularly consumed by many people on a daily basis is capable of having an antagonistic effect on the adenosine A$_1$ receptor.[70]
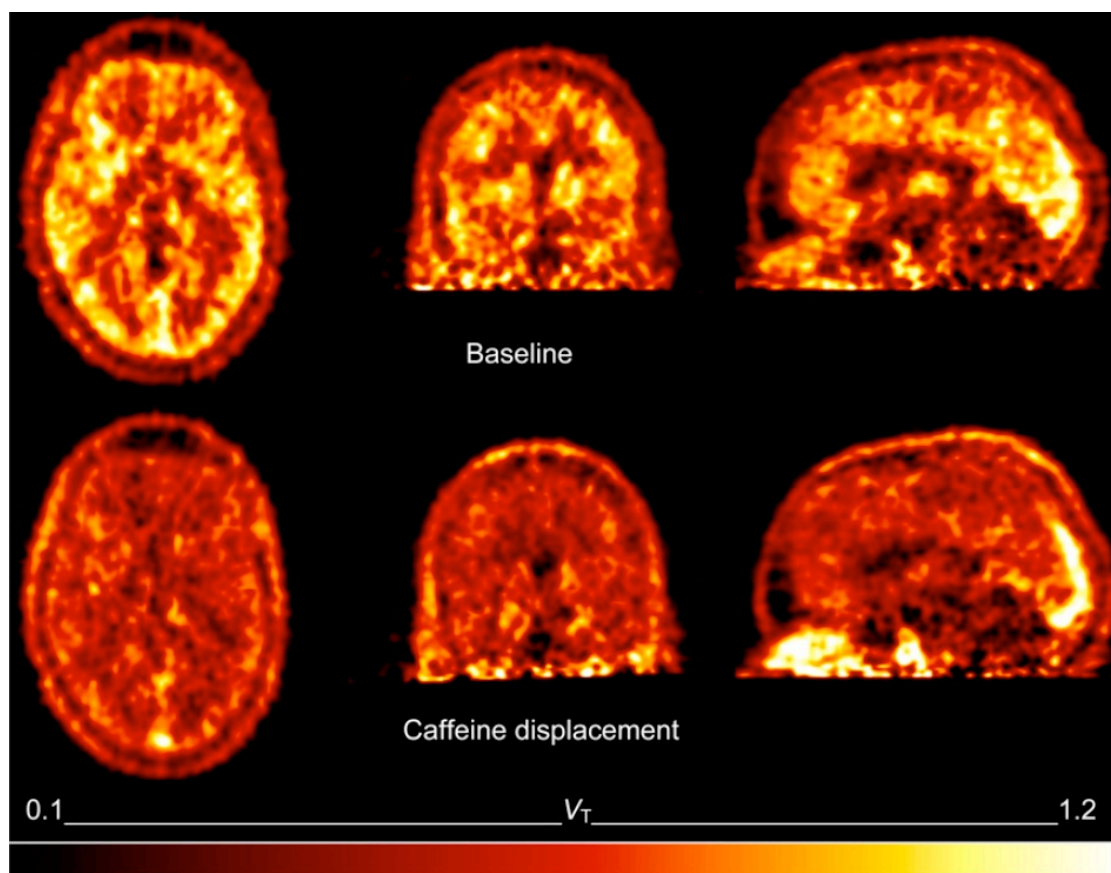
Figure 19: Displacement of [^{18}F]Radioligand by Caffeine

1.1.6. Fluorinated Steroids in Medicinal Chemistry

The first approved fluorinated drug molecule was 9α-fluorocortisol (**13**), approved in 1955 by the FDA in America.[3] It was first reported in 1954 by Sabo and Fried, who found that incorporation of a halogen in the 9α-position increased the

glucocorticoid activity over that of the endogenous steroid cortisol. The 9α-chloro-analogue was four times more potent than cortisol, but was surpassed by the 9α-fluoro-derivative which had ten times the activity of cortisol.[71] 9α-Fluorocortisol is prescribed for adrenocortical insufficiency and is important enough to be on the WHO's essential medicines list.[1] Since then, fluorinated steroids have continued to make a valuable contribution to healthcare; 21% of FDA approved (up until 2013) fluorinated drugs are based on steroidal structures.[72] Fluorinated steroids have made their biggest impact as antiflammatory agents; 80% of approved fluorinated steroid medicines are used as treatments for inflammation, e.g. diflorasone, ciobetasol and flunisolide (*Figure 20*).
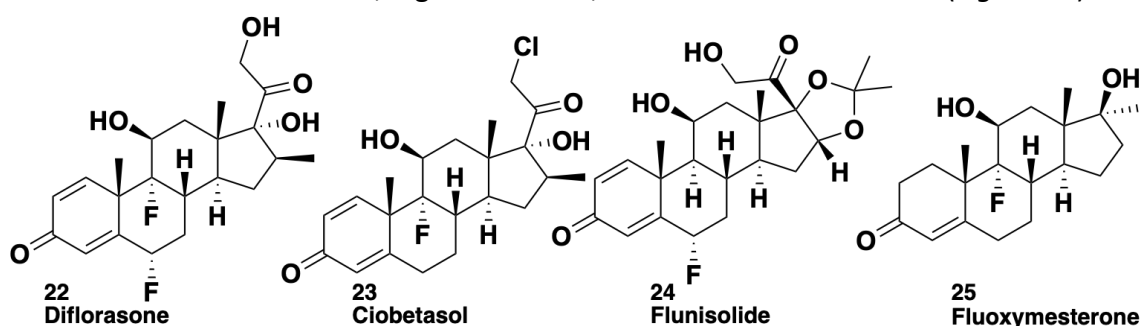
Figure 20: Compounds Fluorinated on Steroid Core

Fluoxymethasone (*Figure 20*) and fulvestrant (*Figure 21*) are used to treat cancer,[3,73] rather than for the treatment of inflammation. Fluoxymethasone has also found illicit use amongst athletes due to its anabolic androgenic effects.[74] Dutasteride (*Figure 21*) is used to treat enlarged prostate in men.[75]
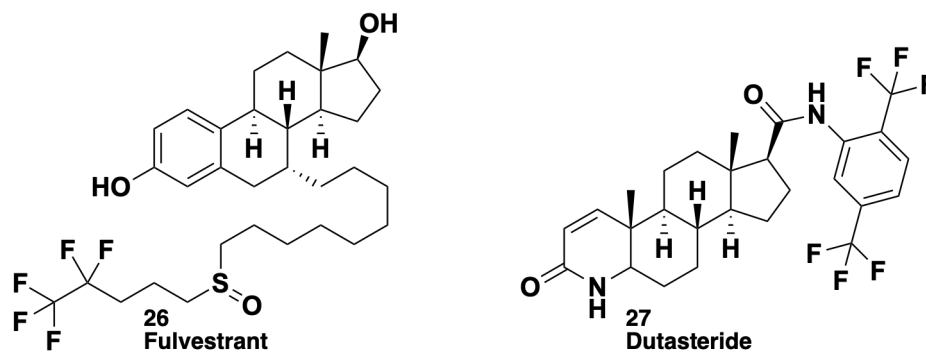
Figure 21: Compounds with Fluorinated Pendant Groups

A key structural motif common to almost all fluorinated drugs based on steroidal structures is fluorination in the 9α-position. This is likely to be due to the favourable effect on metabolic stability (*vide supra*). Another common feature is fluorination in the

6α-position. In fact, dutasteride and fulvestrant are alone in not containing either of these common features.

In 1954, Sabo and Fried employed anhydrous HF in chloroform at 0 ˚C to open the epoxide in 13a in their original synthesis of 9α-fluorocortisol (*Scheme 1*). This method produced **13** in 50% yield).[71] This method was also employed in the synthesis of ciobetasol, affording the fluorinated product.[76]
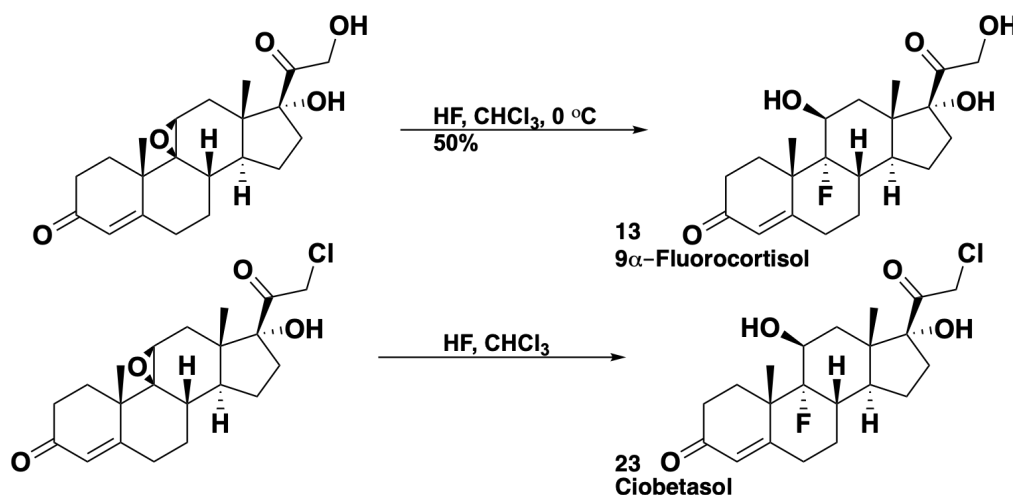
Scheme 1: Fluorination Steps in the Synthesis of 9-Fluorocortisol (**13**) and Ciobetasol (**23**)

The first approved fluorinated steroid to feature the 6α-fluorine moiety was fluocinolone acetonide (**28**); the synthesis was first reported in 1960 by Mills and co-workers *(Scheme 2)*.[77] Again, the fluorine atom was installed *via* the opening of an epoxide with a source of nucleophilic fluoride; however this synthesis required several steps to then remove the hydroxyl group generated by the epoxide opening step. On this occasion, boron trifluoride etherate was used as the fluoride source. Once fluorine was installed in the axial position, it was then necessary to oxidise the alcohol on the A ring to the ketone. Treatment with HCl eliminated water and epimerised the α-position, converting the intermediate to the equatorial fluoride. Final product **28** was produced following six further steps.[77]
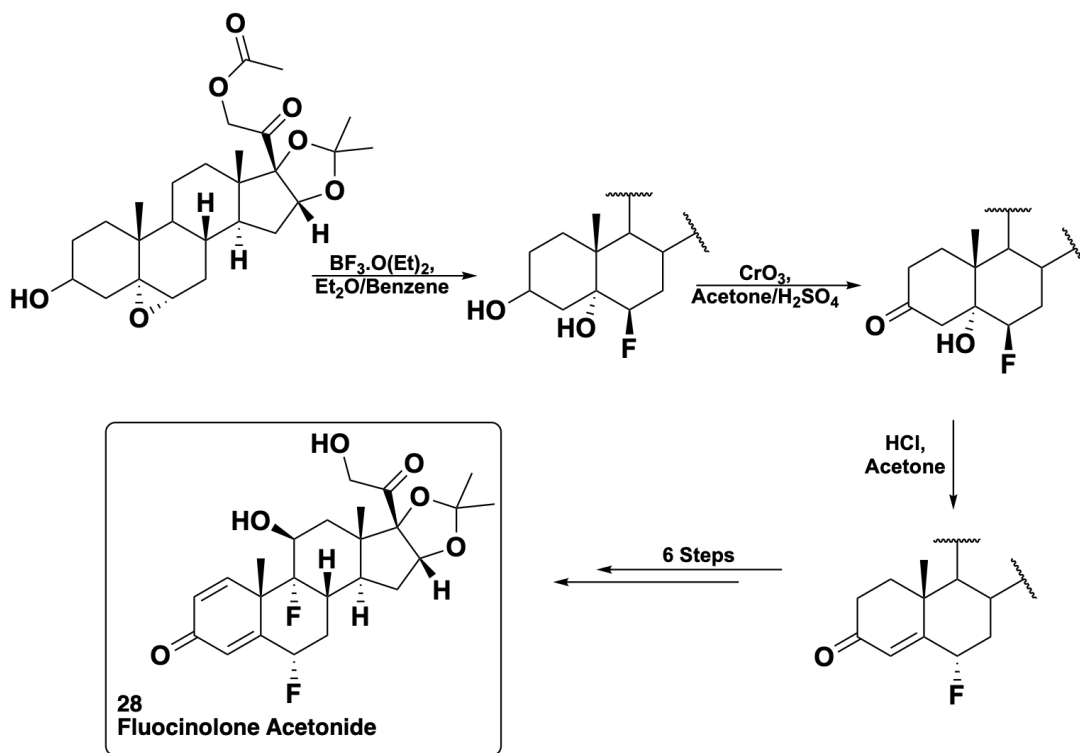
Scheme 2: Synthesis of Fluocinolone acetonide (**28**)

1.1.6.1.   Fluticasone Propionate and Related Compounds

Fluticasone propionate (**29**) is one of the most significant fluorinated steroids on the market. It is formulated with β_2-adrenoreceptor agonist salmeterol, sold as Advair by GlaxoSmithKline (GSK), and used as a treatment for asthma.[78] Advair (*Figure 22*[79]) is an inhaled asthma medication and was the 2nd highest selling fluorinated drug and the 13th highest selling drug overall in the United States in 2016.[3]

Figure 22: Advair Diskus

Fluticasone propionate **29** (*Figure 23*) was first reported in 1994 by Phillipps and co-workers; a number of steroidal analogues were investigated to determine their effectiveness as anti-inflammatory agents. Twenty-three steroidal molecules were synthesised and tested in order to determine their anti-inflammatory and vasoconstrictive properties as well as to determine whether they exhibited any undesirable hypothalamic-pituitary-adrenal (HPA) suppression or not. The identities of the substituents were varied in the 6α- and 9α- positions as well as the terminal substituent on the thio- or seleno-ester.

28
Fluocinolone Acetonide
V activity (human) 100
AI activity (mouse) 100
HPA activity (mouse) 100

29
Fluticasone Propionate
V activity (human) 945
AI activity (mouse) 113
HPA activity (mouse) 1

30
V activity (human) 1984
AI activity (mouse) 63
HPA activity (mouse) 149

31
V activity (human) 1388
AI activity (mouse) 67
HPA activity (mouse) n/a

32
V activity (human) 1469
AI activity (mouse) 41
HPA activity (mouse) 44

33
V activity (human) 1262
AI activity (mouse) 89
HPA activity (mouse) 450

34
V activity (human) 1497
AI activity (mouse) 41
HPA activity (mouse) 44

35
V activity (human) 1048
AI activity (mouse) 197
HPA activity (mouse) >100

*Figure 23: Steroidal Compounds **28-35***

The properties of these molecules were quantified relative to those of fluocinolone acetonide. Whilst analogues **30-35** were more active than **29** in the vasoconstriction assay, they all exhibited increased HPA suppression. Compound **29** was identified as the species with the greatest vasoconstrictive and anti-inflammatory activity whilst also avoiding HPA suppression.[80]

Fluticasone furoate **36** (*figure 24*) differs only from **29** in the identity of the ester substituent on the 17-oxygen; **36** incorporates a furoate moiety instead of the characteristic propionate ester found in **29**. Analogue **36** is prescribed to patients suffering from chronic obstructive pulmonary disease (COPD).[81] The manufacturers of **36** state that **36** is metabolised five times faster than **29**. It is suggested that this would mean that **36** would be safer with patients receiving reduced systemic exposure compared to **29**, allowing **36** to be dosed once daily which is more convenient to the patient.[82]

36
Fluticasone Furoate
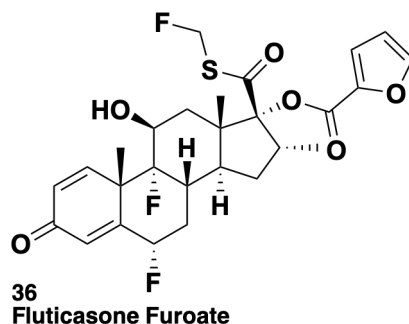
Figure 24: Fluticasone Furoate 36

The identity of the substituent on the thioester is important for activity as shown by the SAR associated with compounds **29**-**36**. The fluoromethyl group can be installed by alkylating the sulfur using bromofluoromethane (*Scheme 3*).[83] Once again, the 9α-fluorine was installed by epoxide opening using a nucleophilic fluoride source such as HF. Notable in its absence is any mention of the installation of the 6α-fluorine in the original literature surrounding compounds **29** and **36**.[80,83–87] Since the discovery of these molecules developments have been made in the fluorination at the 6-position (*vide infra*).

36a

BrCH$_2$F, NaHCO$_3$,
DMF, -20 °C 88%

36
Fluticasone Furoate
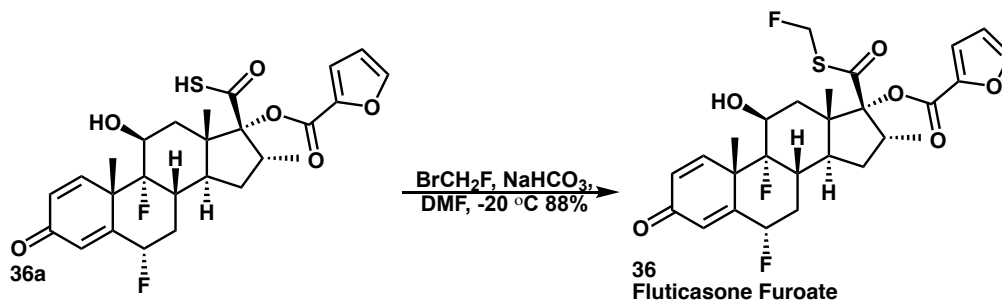
Scheme 3: Installation of Fluoromethyl Group

1.2. Electrophilic Fluorination

The majority of C-F bond formation processes proceed *via* the reaction of an electrophilic carbon centre and a nucleophilic source of fluorine, given that fluorine is so electronegative. It is desirable to be able to introduce functionality to a molecule through reaction with either electrophilic or nucleophilic carbon for the synthetic chemist. Great strides have been made in the design and application of electrophilic fluorinating agents which allow fluorination at a variety of centres and adjacent to many functional groups.

1.2.1. Early Electrophilic Fluorinating Agents

Xenon difluoride, one of the first reagents to be used in electrophilic fluorination reactions, was discovered in 1962.[88] Shaw and co-workers had been investigating syntheses of fluorobenzene with limited success when it was discovered that when xenon difluoride was combined with benzene in carbon tetrachloride, fluorobenzene could be formed in moderate yield.[89] In addition to its ability to be a source of electrophilic fluorine, xenon difluoride is also strongly oxidising making it an inappropriate participant in reactions of molecules containing sensitive functionality.[90,91] Whilst xenon difluoride is available commercially, the cost of the reagent at £16,015 per mol is somewhat prohibitive for large scale use.[92]

With the advent of fluorinated steroids, the ability to perform industrial scale fluorinations became a pressing issue. The first electrophilic fluorinating agent to be used industrially for this was perchloryl fluoride ($FClO_3$).[13] Perchloryl fluoride can be used to fluorinate steroids selectively without interfering with the rest of the molecule.[93] However, the reagent is particularly difficult to handle. It is a gas at room temperature, toxic by inhalation and reacts with common organic solvents to yield shock sensitive products causing a significant explosion risk.[94]

Other early electrophilic fluorinating reagents include hypofluorite reagents. These molecules are characterised by a bond between fluorine and oxygen, making for highly reactive species. Like perchloryl fluoride, hypofluorites tend to be highly toxic and volatile, and some of them are gases at room temperature. Again, these reagents are plagued by their propensity for forming explosive by-products upon contact with organic solvents, precluding application in industry.[13] One area where hypofluorites have found good use is in the synthesis of [^{18}F]FDG (*Scheme 4*). Given that time is of the essence in radiotracer synthesis, the use of a highly reactive reagent is an advantage. In this case, acetyl hypofluorite can be synthesised rapidly from [^{18}F]F$_2$, ready to participate in the formation of [^{18}F]FDG.[95]
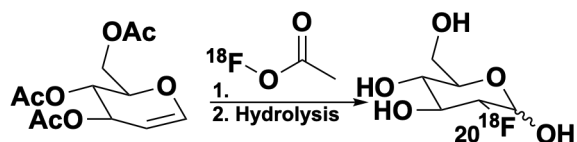
Scheme 4: Synthesis of [18F]FDG with Acetyl Hypofluorite

1.2.2. *N*-F Reagents

Up until the 1980's, all of the available electrophilic fluorinating reagents presented significant hazards. Extensive research was underway to discover an electrophilic fluorinating reagent with sufficient reactivity to afford fluorinated products in a timely manner but that was not so reactive that it would pose significant risks to the user. It was discovered that is possible to synthesise molecules where the fluorine is bonded to a nitrogen; these formed the basis of modern *N*-F reagents.

1.2.2.1.   *N*-F Pyridinium Reagents

The first *N*-F type reagents to be discovered were based on pyridine structures. When fluorine is reacted with pyridine at -70°C in chloroform, a white suspension is formed. After analysis, the substance was identified as *N*-fluoropyridinium fluoride which decomposed on warming.[96] These observations were made in the 1960's by Meinert;[97] however it was not until the late 1980's that the first bench stable *N*-

fluoropyridinium salt was prepared by Umemoto and co-workers, achieved by changing the counterion from fluoride to triflate or tetrafluoroborate.[98–100] These molecules are stable enough to be commercially available at £14,336 per mol for the triflate[101] and £8,887 per mol for the tetrafluoroborate.[102]

In 2003, the crystal structure of *N*-fluoropyridinium triflate was published by Banks and co-workers.[103] The crystal structure shows the bond length of the N-F bond to be 1.357 Å, consistent with the calculated length of 1.363 Å (generated using Gaussian 09 software using the B3LYP/6-31+G(d,p) level of theory). It is thought that this bond length is indicative of π-backdonation from fluorine to the nitrogen in the ring.[96] When the orbitals are visualised (from the above geometry calculation), one of the fluorine lone pairs lies in the same plane as the π-system (*Figure 25*).
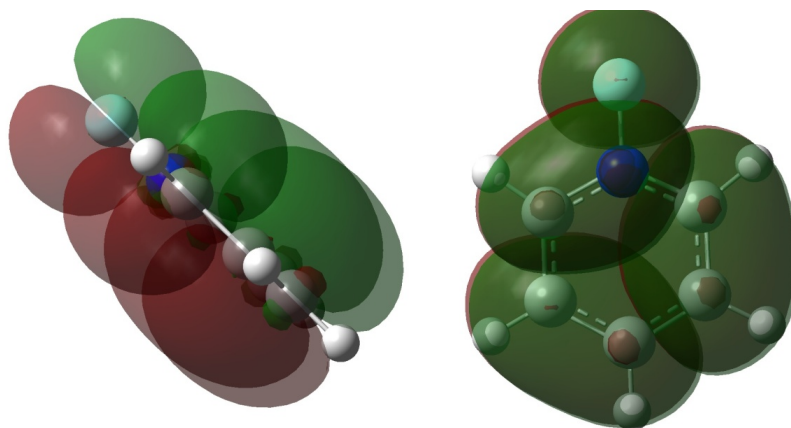
Figure 25: Overlap of Fluorine Lone Pair with Aromatic Ring in N-*Fluoropyridinium*

N-Fluoropyridinium reagents can be varied not only in the identity of the counterion but also in the nature of the heterocycle. A number of different *N*-F pyridinium molecules have been synthesised and examined to determine their power as electrophilic fluorinating reagents. Altering the substituents on the pyridine ring can have a dramatic impact on the reactivity of these *N*-F pyridinium reagents (*Scheme 5*). It comes as no surprise that increasing the number of electron withdrawing substituents increases the electrophilic fluorinating power of the reagent whilst electron donating reagents lower the reactivity of these compounds. Indeed, it was discovered that the

2,3,4,5,6-pentachloro derivative (**38**) reacted with anisole much more efficiently than the unsubstituted (**37**) or 2,4,6-trimethyl analogue (**39**), which required elevated temperatures and long reaction times (*Scheme 5*).[99]

Fluorinating Agent	37	38	39
Temperature	120 °C	rt	147 °C
Time	18 hours	0.25 hours	10 hours
Conversion	71%	91%	68%

Scheme 5: Reactivity of N-Fluoropyridinium Reagents
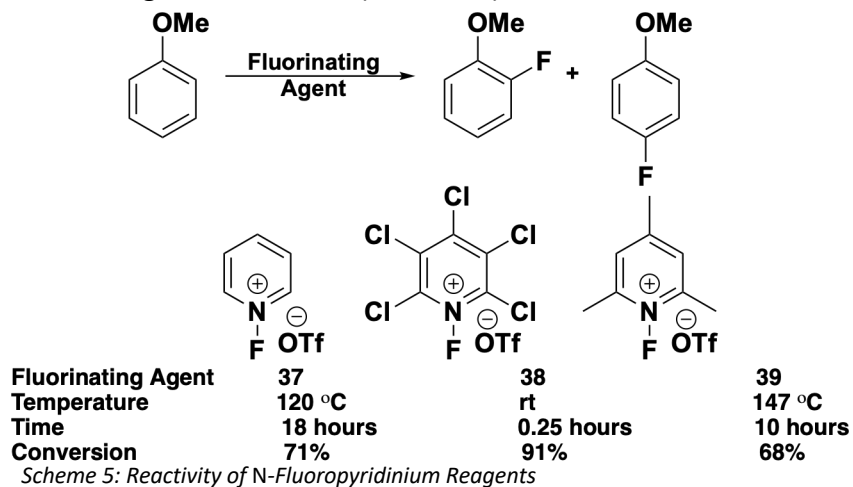
Umemoto and co-workers went on to develop their *N*-F pyridinium reagents further, incorporating the counterion into the pyridine ring, generating zwitterionic species of the type **40**. These reagents showed interesting reactivity. Whilst **37**-**39** tended to give a mixture of *ortho*- and *para*- substituted products when reacted with phenol, **40** only afforded the *ortho*- functionalised product. It is thought that this is due to the molecules orientating themselves such that the phenyl rings can participate in π-stacking and the negatively charged sulfonate can form a hydrogen bond with the phenolic hydroxyl group, as shown in *Figure 26*.
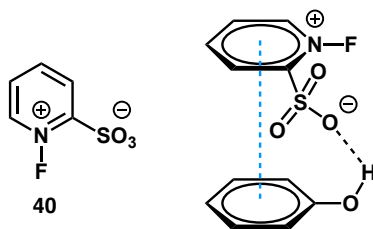
Figure 26: Compound 40

1.2.2.1.1. Mechanism of Fluorination with *N*-Fluoropyridinium Reagents

The mechanism of fluorination reactions using *N*-fluoropyridinium reagents is not yet well understood. Umemoto suggests that a radical mechanism is possible, in which the *N*-fluoropyridinium accepts a single electron followed by fluorine radical transfer to

the nucleophile. It was argued that the hypothesis is corroborated by the observed difference in reactivity of *N*-fluoropyridinium reagents with organolithium and Grignard reagents. The reaction with organolithium reagents yielded no fluorinated products whilst the reaction with Grignard reagent did.[99] This argument is not conclusive because although Grignard reagents are capable of reacting *via* single electron transfer (SET) mechanisms, they have also been proven to participate in reactions through a S_N2 mechanism.[104] Furthermore, the statement that organolithium reagents are unable to react through SET pathways is thrown into doubt when viewed alongside Yamataka's investigations from 1989 which show that organolithium reagents are capable of SET.[105]

The difference in reactivity between *N*-fluoropyridinium reagents and organolithium/magnesium reagents has not entirely been explained. One hypothesis is based on the proposal that for Grignard reagents, the rate determining step for SET pathways is the reorganisation of radicals, whilst for organolithium reagents it is the electron transfer itself. The electron transfer from organolithium reagents happens so quickly that the fluorine radical generated reacts preferentially with the solvent to form HF, explaining why the expected fluorinated products are not observed and supporting the initial assertion that *N*-fluoropyridinium reagents react through SET.[106] Kochi and co-workers investigated the ability of a variety of pyridinium compounds to act as electron acceptors and discovered that *N*-fluoropyridinium reagents can indeed accept an electron to form a coloured charge transfer complex (*Scheme 5*).[107,108] It is therefore suggested that fluorination of aromatic and olefinic substrates with *N*-fluoropyridinium reagents proceeds *via* a charge transfer complex intermediate.[106]
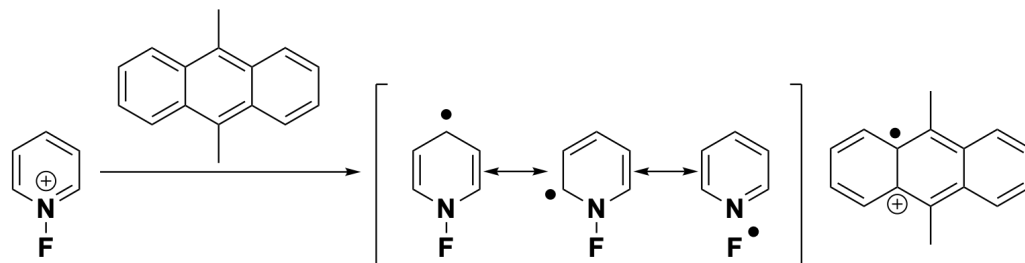
Scheme 5: Charge transfer to N-*Fluoropyridinium compound*

N-Fluoropyridinium reagents have also found use beyond electrophilic fluorination reactions. Kiselyov and co-workers were trying to prepare fluorinated nitroalkanes *via* fluorination with *N*-fluoropyridinium tetrafluoroborate. To their surprise, the only products isolated were substituted pyridines.[96] Ito *et al.* used this reactivity to great effect in the synthesis of metabotropic glutamate receptor 1 (mGluR1) ligands; reacting the *N*-fluoropyridinium reagent with sodium azide afforded a pyridine with an azide in the 2-position which could then be cyclised to form the triazole compound (*Scheme 6*).[109] Further examples of *N*-fluoropyridinium reagents reacting in this manner have also been published.[110–112]
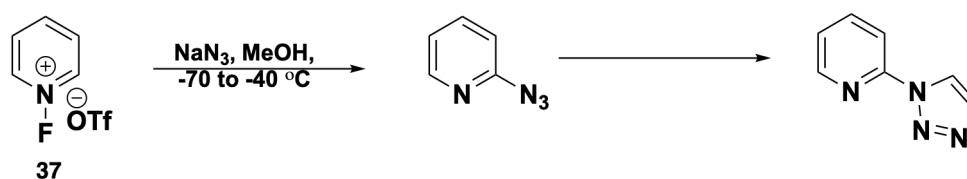
Scheme 6: Reaction of N-*Fluoropyridinium with Sodium Azide*

N-fluoropyridinium reagents also undergo interesting transformations in basic conditions. When *N*-fluoropyridinium triflate is placed under basic conditions in dichloromethane three products are produced: 2-chloropyridine, 2-fluoropyridine and 2-pyridyl triflate. A number of organic or inorganic bases can be used, resulting in the production of these adducts in varying quantities. Altering the solvent resulted in the formation of various 2-substituted pyridine products. The 2-substituent was derived from the solvent, counterion or the substituent was fluorine itself. This reactivity has been attributed to a carbene intermediate which forms as a result of hydrogen abstraction (*Scheme 7*).[113]
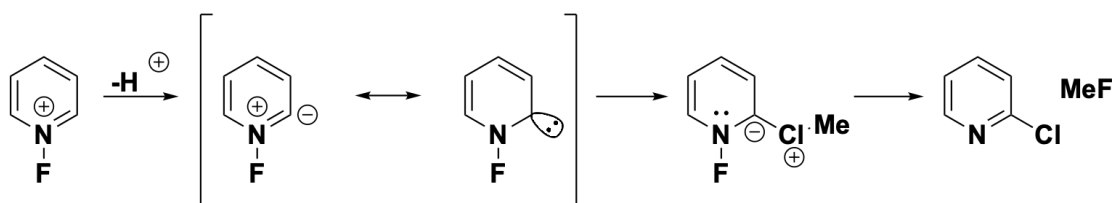
Scheme 7: N-*Fluoropyridinium Reacting* via *a Carbene Intermediate*

1.2.2.2. *N*-F Reagents Based On Tertiary Alkyl Amines

Another important class of electrophilic fluorinating reagents are those based on a tertiary amine core. The first *N*-F compound of this type to be isolated was *N*-fluoroquinuclidinium fluoride, synthesised by Banks and co-workers in the 1980's. Unlike *N*-fluoropyridinium fluoride, *N*-fluoroquinuclidinium fluoride is stable and can be stored for extended periods provided the atmosphere under which it is stored is dry. The solid is hygroscopic, increasing in weight upon contact with air, and is soluble in water and other polar solvents such as alcohols. This compound was used in the fluorination of various carbon nucleophiles at room temperature or below in low to moderate yields. Whilst this reagent holds an advantage over those of the *N*-fluoropyridinium class given that it cannot undergo unwanted side reactions, the problems with storage posed by the hygroscopic nature of the compound combined with fluorination reactions not providing high yields of product show that this is far from the ideal reagent.[114]

Evidently, further research into these reagents was required to understand the factors that control reactivity and stability in order to produce a reagent that is simultaneously a reactive electrophilic fluorinating reagent and bench stable and easy-to-handle. Perhaps the reagent class which have made the biggest impact on the usability of electrophilic fluorination as a route to fluorine containing molecules are those based on the 1,4-diazabicyclo[2.2.2]octane (DABCO) amine skeleton – the so called SelectFluor reagents.

1.2.2.2.1. SelectFluor

The original SelectFluor reagent (**41**) is a non-hygroscopic, bench stable, colourless solid. It is commercially available (£910 per mol) and safe to handle.[115] Synthesis of this reagent is achieved by reaction of the parent amine with dichloromethane; after exchange of the chloride counterion for tetrafluoroborate, the

monocationic species can be fluorinated with elemental fluorine diluted in nitrogen to give the final compound (*Scheme 8*).[106]

Scheme 8: Synthesis of SelectFluor (41)
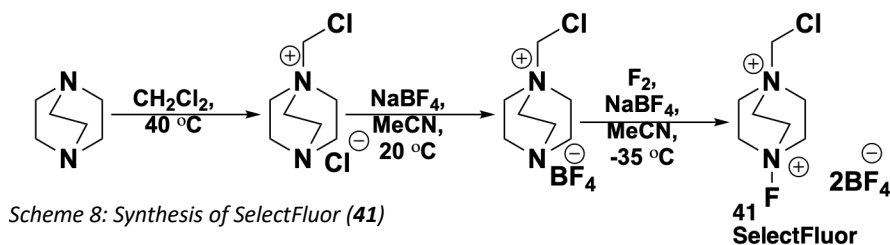
As a readily available, safe reagent SelectFluor has been applied in a number of fluorination reactions. It is capable of reacting with a number of carbon nucleophiles to produce fluorinated products. It has been shown to react with aromatic substrates, alkenes, enol ethers and esters and many more.[13,106,116] A drawback to the use of SelectFluor, however, is its poor solubility in organic solvents. It is very soluble in water (176 g per litre)[116] and slightly soluble in acetonitrile (50 g per litre)[116] and other polar solvents such as methanol but in less polar solvents the solubility is low, precluding its use on a number of substrates.

SelectFluor has found application in the synthesis of α-fluoro carbonyl compounds. Solladié-Cavallo and co-workers[117] were investigating the use of chiral α-fluorocarbonyl compounds as catalysts for epoxidation. The synthesis of these molecules was achieved *via* the fluorination of silyl enol ethers (**42a** and **43a**) to furnish the appropriate fluorocarbonyl compounds (**42** and **43**, *Scheme 10*). The fluorination reactions were carried out at 0 °C in DMF, affording fluorinated products in 80 and 81% yield. Fluorination of these compounds occurred enantioselectively. Analysis of compound **43** by X-ray diffraction of a single crystal showed that the fluorine occupied the axial position. Comparing the NMR spectra of compound **43** (of which the crystal structure had been determined) and compound **42** allowed the assignment of the fluorine in **42** as equatorial. The source of the enantioselectivity is not discussed in the original publication however it is notable that in this instance the fluorine is installed on the opposite face to that of the methyl group, likely due to the large size of the SelectFluor reagent.
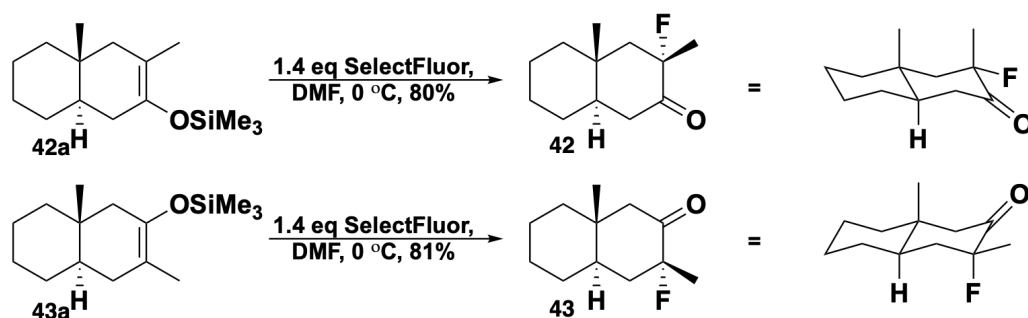
Scheme 10: Fluorination of Silyl Enol Ethers with SelectFluor

Researchers at Columbia University published a patent on research into analogues of erastin, a small molecule known to induce cell death in certain types of cancerous cell.[118] One of the compounds declared in the patent contains an α-fluoro carbonyl moiety. This was installed *via* the electrophilic fluorination of lithium enolate **44b** with SelectFluor (*Scheme 11*). The enolate was generated through the deprotonation of ketone **44a** with LiHMDS. Following this the reaction mixture was concentrated and then suspended in acetonitrile. SelectFluor was then added to this mixture to yield fluoroketone **44** in 55% yield.[119]
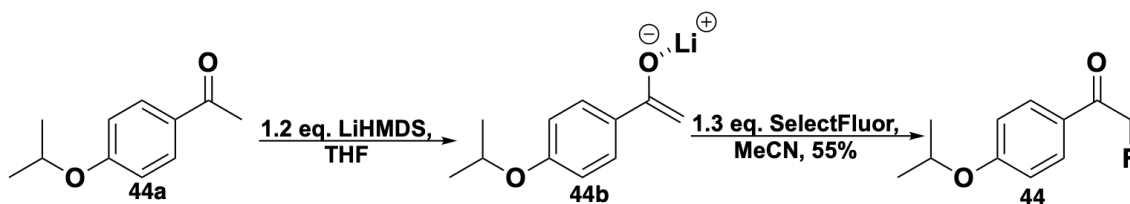
Scheme 11: Fluorination of a Lithium Enolate with Selectfluor

Ramírez and colleagues[120] were investigating the biological effects of synthetic analogues of naturally occurring brassinosteroids. Brassinosteroids have been found to promote growth in crops. It was decided that fluorinated analogues of the natural steroids would be of interest given the impact fluorination of steroids has had in medicinal chemistry. Introduction of fluorine at the 2-position, α to a hydroxyl was targeted. In order to install the fluorine the enol acetate (**45a**, *Scheme 12*) of the corresponding ketone compound was synthesised. Fluorination of this with SelectFluor in acetonitrile afforded α-fluoroketones (**45b**) which were then subjected to reduction to yield the desired brassinosteroid analogues (**45-1** and **45-2**).
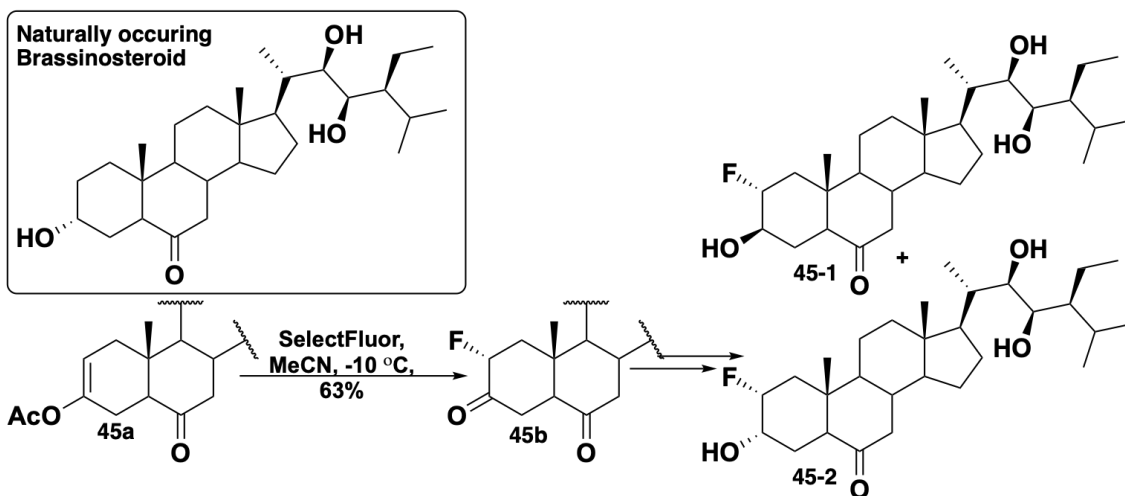
Scheme 12: Fluorination of an Enol Ester in the Synthesis of Fluorinated Brassinosteroids

Toste and co-workers hypothesised that the addition of an anionic phase transfer catalyst (PTC) may be beneficial in order to facilitate fluorination of substrates with poor solubility in polar solvents traditionally used for SelectFluor fluorinations. The addition of a chiral phosphate not only allowed the fluorination to take place in non-polar solvents such as fluorobenzene, but also conferred stereoselectivity during the synthesis of fluorinated spiro-oxazoline compounds (*Scheme 13*).[121]
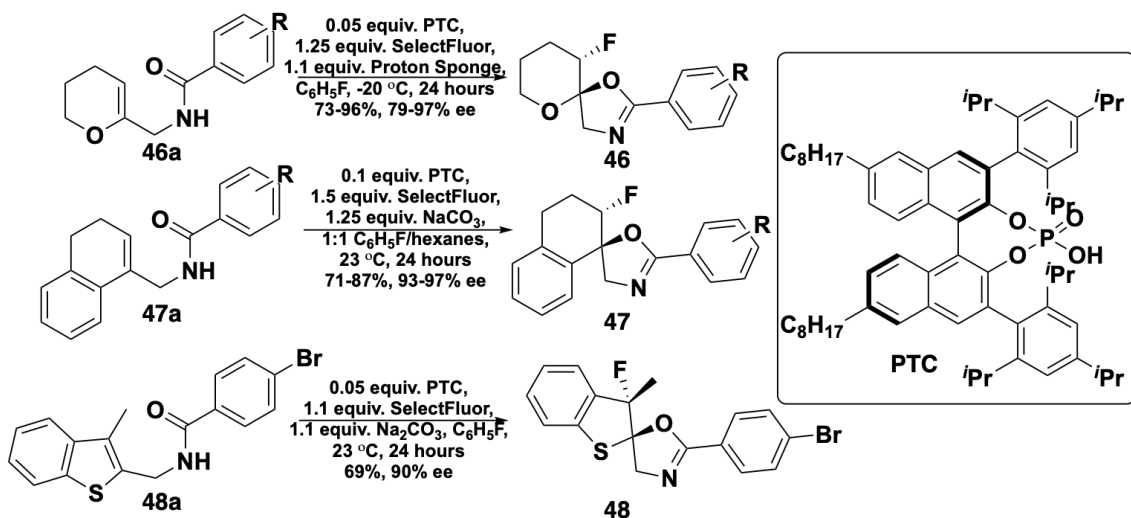
Scheme 13: Fluorination with SelectFluor in Non-Polar Solvents Facilitated by PTC

It was postulated that the improvement to the reaction was due to the chiral phase transfer catalyst (PTC) acting as the counterion for SelectFluor, delivering the

fluorine source to the substrate in a mild and controlled manner. Through this methodology, complex, chiral, fluorinated molecules can be built up from relatively simple, achiral substrates in a single step. After optimisation of conditions, it was found that the addition of [1,8-bis(dimethylamino)naphthalene] (proton sponge) to the reaction mixture made the process more efficient by neutralising the equivalent of acid produced as well as allowing the anionic phase transfer catalyst to be generated *in situ* from the parent phosphonic acid, although sodium carbonate as base appears to work equally as well. This methodology was applied to a range of alkene substrates, from electron rich alkenes of the type **46a** to less electron rich substrates, **47a**. Interestingly, when the synthesis of **48a** is attempted under "normal" SelectFluor fluorination conditions (1.1 equivalents of SelectFluor in acetonitrile), a complex mixture is obtained, and very little of this is the desired product. However, under Toste's newly developed anionic phase transfer conditions the reaction proceeds smoothly to the desired product in good yield.

Leading on from these promising results, Hamashima and co-workers sought to apply this methodology to alternative substrates to synthesise other heterocycles. In the fluorolactonization reaction illustrated in *Scheme*, it was discovered that the phosphate anionic phase transfer catalyst developed by Toste was not as effective. Two hypotheses were proposed as an explanation for the lack of selectivity in this case. One was that, given that the substrate itself is anionic, it could in fact be acting as the phase transfer catalyst, allowing the reaction to proceed but with no stereochemical information, resulting in a racemic product.
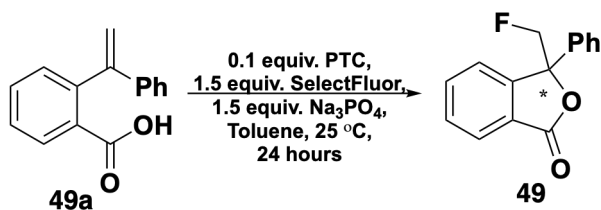
*Scheme 14: Fluorolactonisation of **49a***

The other hypothesis was that the counterion of Toste's phase transfer catalyst was also forming a complex with the substrate anion, resulting in a loose ion pair and as a result no enantioselectivity.[122]

In the light of the first hypothesis, the researchers set about designing an alternative phase transfer catalyst which incorporated the acidic functionality of the substrate. It was thought to be important for these substrates than not only the fluorinating reagent but also the substrate formed interactions with the phase transfer catalyst to get high enantioselectivity. These considerations led to the design of the alternative bifunctional phase transfer catalyst (shown in *Scheme 15*). The novel phase transfer catalyst incorporates a carboxylate functional group to bind the SelectFluor as well as a hydroxyl, thought to be able to interact with the carboxylate of the substrate. The reaction conditions were investigated and the best results were obtained when sodium sulfate was used as base and a drying agent (Na_2SO_4) was added to the reaction mixture.
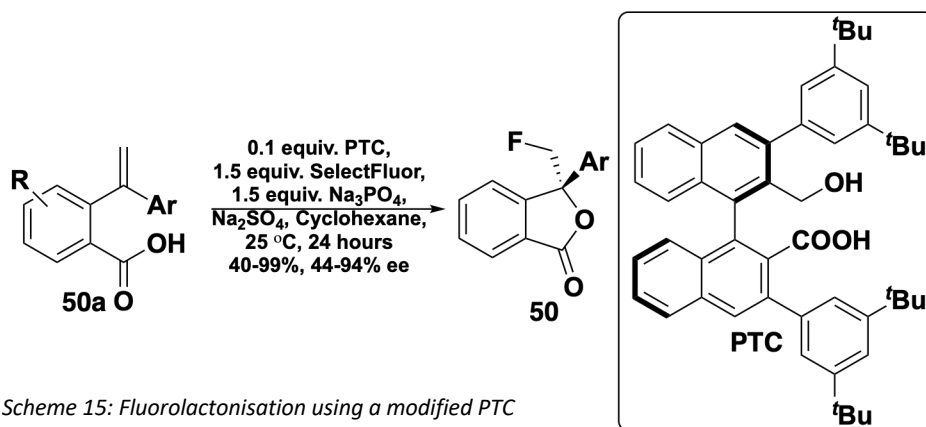
Scheme 15: Fluorolactonisation using a modified PTC

Surfactants have been used to solubilise organic substrates in aqueous media so that fluorination can be achieved in water. Stavber and co-workers found that without any solubilising additives, the reaction of indanone (**51**) with SelectFluor in water went to 58% conversion in 12 hours at 80 ˚C. Surfactants which contained cationic functionality to interact with the water were found to be ineffective as were neutral surfactants. When sodium dodecyl sulfate (SDS) was used the reaction proceeded to 100% conversion under the same conditions (*Scheme 16*).[123]
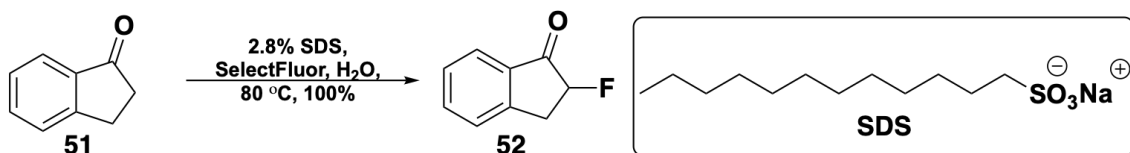
Scheme 16: Fluorination in Water using SelectFluor and Sufactants

The ability to perform reactions in water could lead to more sustainable chemistry; other developments of this type have occurred. In 2002, work by Laali and Borodkin was published in which fluorination of aromatic molecules was achieved using ionic liquid solvents. The ionic liquid can then be recycled and used again in further fluorinations.[124] Since then, there have been many further publications in which ionic liquids have been used as solvent for SelectFluor mediated fluorinations.[125–133] For example, the fluorination of phenolic steroid **53** gives regioisomeric products **54** and **55** as shown in *Scheme 17*.[134]
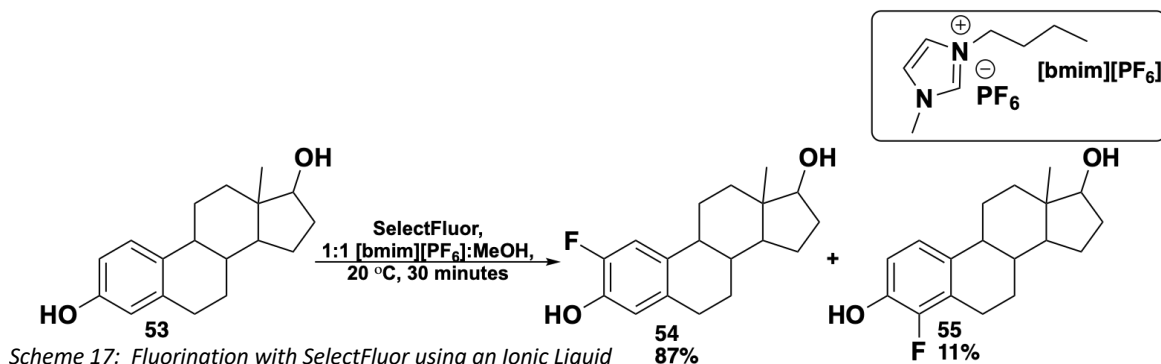
Scheme 17: Fluorination with SelectFluor using an Ionic Liquid

1.2.2.2.2. Mechanism of Fluorination with SelectFluor

It is evident that electrophilic fluorination with SelectFluor enables a wide range of products to be synthesised. What is not clear, however, is the mechanism that these reactions proceed through. When developing a synthesis of fluorinated sugars, Wong and co-workers decided to investigate the mechanism through which their reactions proceeded. They devised an experiment whereby a SET process would yield one product (**57**) and a two electron process would give another (**56**). When the reaction was carried out, 45% conversion to only the expected two electron reaction product was observed whilst none of the starting material (**56a**) was recovered (*Scheme 18*).[135] Whilst this did appear to show that a two electron mechanism is possible, the lack of clarification as to

what happened to the rest of the material does not rule out that a one electron mechanism could also be possible but that the products of this pathway are either unstable or irretrievable from the reaction mixture.
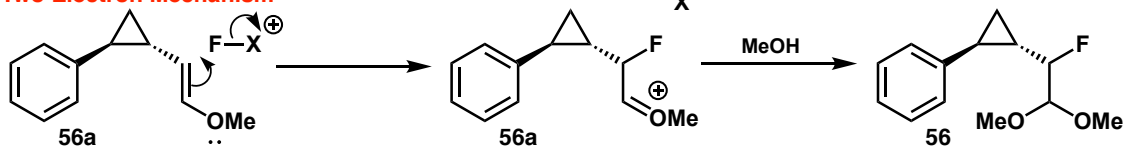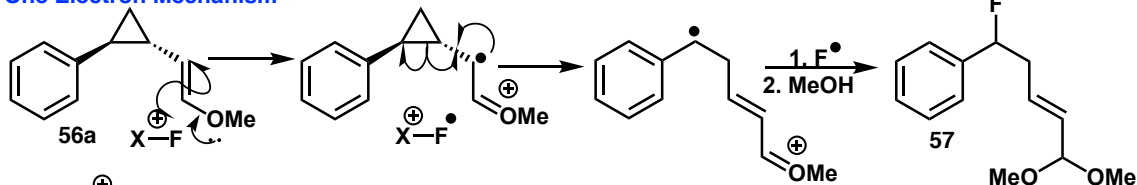
Scheme 18: Possible fluorination mechanisms of **56a**

Whilst this work appeared to provide some evidence for a two electron mechanism in the fluorination with SelectFluor, work by Guo *et al.*[136] exposes evidence for a SET process being involved in the fluorination of alkenes. When the reactions were monitored by electrospray ionization/mass spectrometry (ESI-MS), radical cationic intermediates were detected. It has been shown that the ions produced by ESI are a generally a good reflection of the ions present in the solution sample and that ionisation by this method does not tend to induce side reactions.[137,138] Furthermore, these species were not observed during control experiments, where the alkene substrates were analysed by ESI-MS without the presence of SelectFluor. The mechanism proposed for these reactions is detailed in *Scheme 19*. The alkene substrate (**58a**) undergoes a one electron oxidation to form the radical cation (**58b**) which is stabilised in both positions by the adjacent phenyl groups, SelectFluor can then deliver a fluorine radical to this species, forming a cationic intermediate (**58c**) which is then quenched with methanol to form **58**.[136]
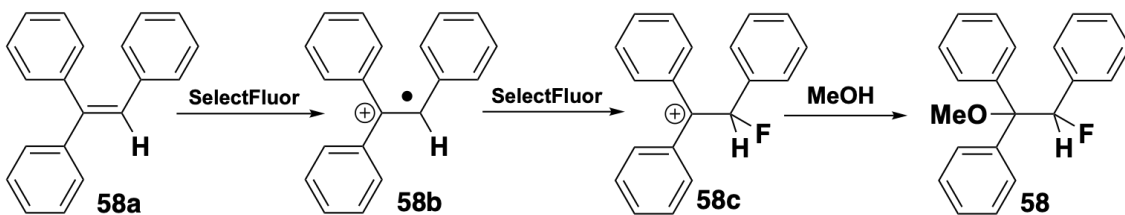
Scheme 19: Transformation of **58a** to **58** using SelectFluor via a SET Mechanism

38

Further to this, Serguchev and co-workers published a study in 2010 in which the reaction of SelectFluor with alkene substrates was examined both experimentally and computationally in order to identify a plausible reaction mechanism. The reaction of SelectFluor with isobutene was modelled. The first step was predicted to involve the formation of complex **C** (shown in *Figure 27*) which is accompanied by charge-transfer from the alkene to SelectFluor. The charge transfer was predicted to populate the antibonding LUMO associated with the N-F bond, resulting in bond lengthening (**TS**).
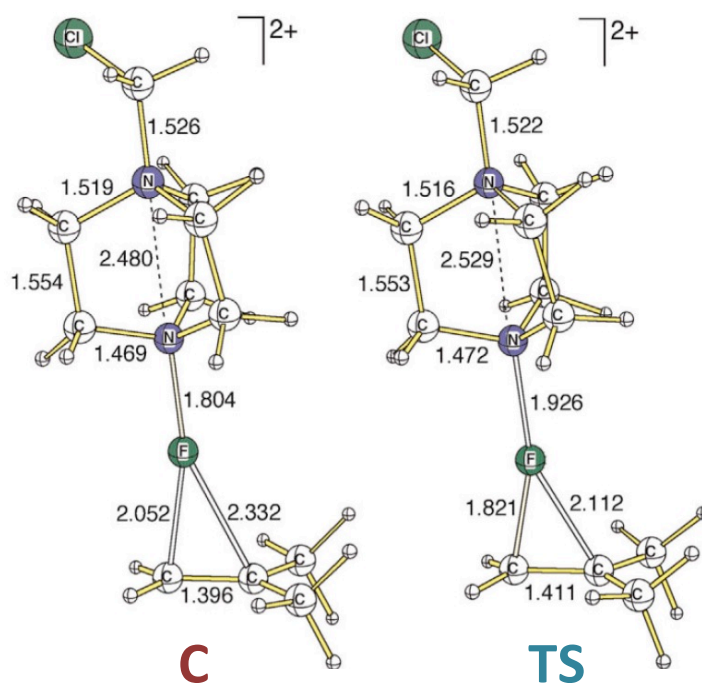
*Figure 27: Complex **C** and Transition State **TS** (image from Serguchev et al.[139])*

The outcome of this was that the predicted energy difference between this complex and the transition state becomes small. In order to clarify whether this process proceeds *via* an electrophilic, concerted or radical mechanism three models of the SelectFluor reaction were examined. The electrophilic model featured the reaction of the 'fluorine cation'-water complex with isobutene, the concerted model was the reaction of F_2 with isobutene and the radical model was the reaction of a fluorine radical alone with isobutene. The transition states for the electrophilic and concerted models

bore very little resemblance to **TS** predicted for the SelectFluor fluorination whilst the radical model was in good agreement with this.[139]

In previous work, Serguchev has described the electrophilic cyclisation reaction of bicyclo[3.3.1]nonane dienes by *N*-halosuccinimides (NXS). This reaction produces a cationic intermediate (**59**) which can then be quenched with a nucleophile (in this case fluoride or water). The electrophilic halogen has been shown to always add in the same position (*Scheme 20*).[140] In contrast to this, when SelectFluor is reacted with bicyclo(3.3.1)nonane dienes different reactivity is observed. The fluorine has been shown to be incorporated in a different position (**60**). Xenon difluoride also exhibits similar reactivity with this type of substrate. Fluorination takes place in the same position as SelectFluor and the cation is formed in the same position when SelectFluor or xenon difluoride are used.[139] Xenon difluoride is known to be able to operate *via* a single electron transfer mechanism.[141–144] The authors postulated that this, when taken in combination with their computational results rules out an electrophilic mechanism and points towards a SET process, involving the formation of a charge transfer complex.[139]
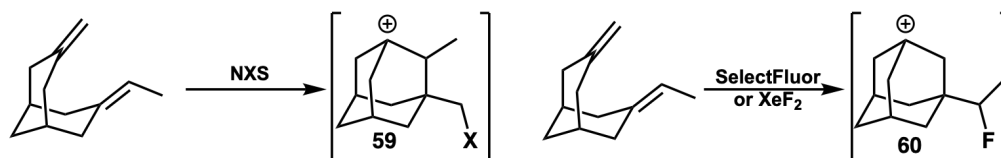
Scheme 20: Reaction of Bicyclo(3.3.1)nonanes with NXS and SelectFluor or XeF₂

Inspired by work from Li *et al.*,[145] in which alkyl boronate complexes were fluorinated by a silver-fluorine complex generated by the reaction of silver with SelectFluor, Aggarwal and co-workers set about developing fluorination reactions of boronate complexes which did not require precious metal intervention (*Scheme 21*). The work by Li was thought to proceed *via* a radical mechanism, resulting in racemic products. Aggarwal and co-workers endeavoured to design a process which would involve a two electron reaction, resulting in inversion of configuration, to yield enantioentriched products. In the initial experiments, the stereoselectivity was poor,

leading the authors to suggest that the reaction was predominantly progressing *via* a SET pathway. It was thought that by changing the nature of the boronate complex the reactivity could be altered to proceed through a two electron mechanism. It was possible that the introduction of electron withdrawing groups on the aryl ring attached to boron would reduce the reduction potential of the boronate complex which should push the reactivity towards a two electron process rather than SET. Unfortunately, the use of boronate complex **62** did not result in a significant improvement in enantiospecificity. It was not until styrene complex **63** was fluorinated that a significant improvement was observed. It was postulated that this alteration to the reactivity could be due to the alkene substituent on the styrene participating in some way. To determine whether this was likely, 1.3 equivalents of styrene was added to the reaction of the original boronate complex **61**. This led to a dramatic increase in enantiospecificity. To explain the changed reactivity with the addition of styrene it was proposed that styrene acts as a radical scavenger, trapping a radical propagating species. This allows the reaction to proceed *via* the two electron process, giving the desired products.[146]
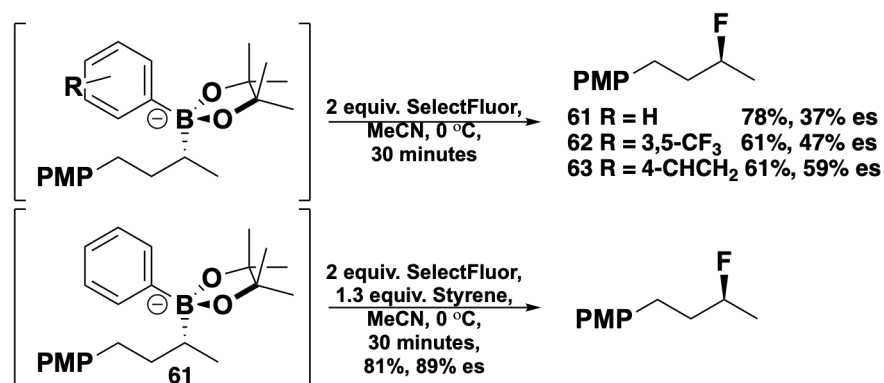
Scheme 21: Reactions of Boronate Complexes with Selectfluor

In 2016 Liu and Wu published an investigation into the synthesis of α-fluoroketones *via* fluorination of vinyl azides with SelectFluor.[147] Two possible fluorination mechanisms were postulated, one which proceeds through a polar mechanism similar to that established for the acidic hydrolysis of vinyl azides[148] or a single electron charge transfer mechanism. The two possible mechanisms proposed are shown in *Scheme 22*. The two electron mechanism involves direct nucleophilic attack by

the alkene on the fluorine atom of SelectFluor with simultaneous cleavage of the N-F bond, resulting in the formation of a cationic intermediate which can be stabilised through resonance. Hydrolysis of this intermediate by water affords the desired ketone product. The single electron mechanism involves electron transfer to the fluorinating reagent to form a radical cation species which can then recombine with the radical-bearing fluorine to form the same cationic intermediate as the one implicated in the polar mechanism.
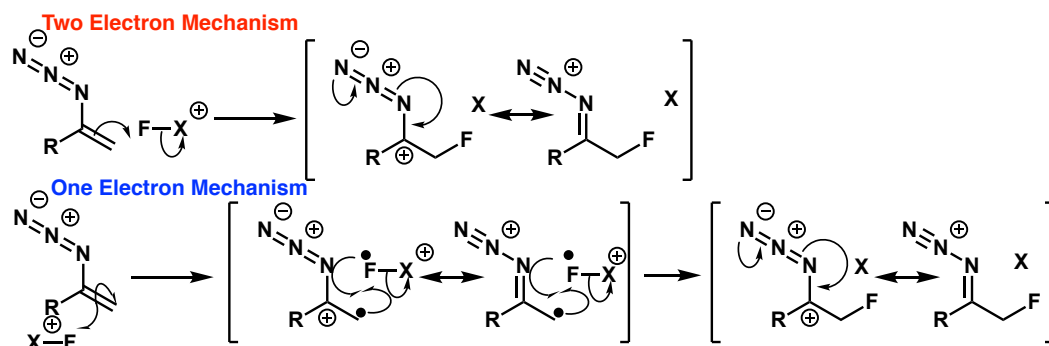
Scheme 22: Proposed possible mechanisms for the fluorination of vinyl azides

In order to probe the likelihood of the participation of radical species, the radical scavenger TEMPO was added to the fluorination reaction. This intervention resulted in the isolation of none of the fluorinated product along with two adducts of the starting material with TEMPO (**64b** and **64c**, *Scheme 23*) albeit in modest yield, providing evidence for the possible participation of radical intermediates. Under the same reaction conditions, but in the absence of SelectFluor, no reaction of the starting material was observed, clearly indicating that SelectFluor is essential for the formation of the substrate-TEMPO adducts. Reaction of **64a** in the presence of alternative radical scavenger 1,1-diphenylethene proceeded smoothly to yield only fluorinated product **64**, providing no further evidence for a single electron reaction mechanism. In a further attempt to elucidate the reaction mechanism, cyclopropane substrate **65a** was synthesised with the proposal that ring opening would be observed if a radical intermediate was formed. The reaction yielded only the α-fluoroketone product **65** in 80% yield with no evidence of the formation of ring-opened products. Regardless, the

authors suggested that the fluorination of vinyl azides with SelectFluor proceeds *via* the single electron transfer process shown in *Scheme 22*.
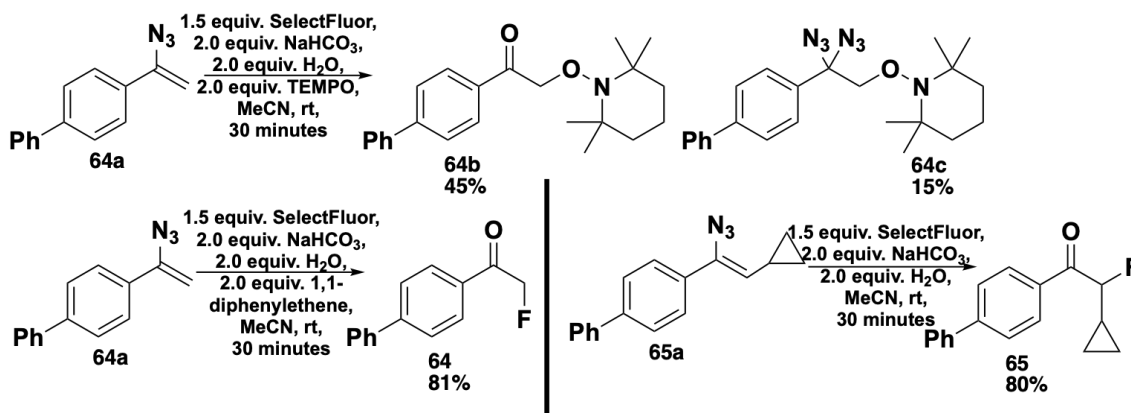
Scheme 23: Reaction of vinyl azide with TEMPO and fluorination with SelectFluor to give fluoroketones

Continuing their work on the fluorination of vinyl azides Liu *et al.* turned their attention to the generation of azidofluoronitriles (*Scheme 24*).[149] The reaction conditions for this transformation were similar to those employed for the generation of fluoroketones from vinyl azides, instead utilising a cyanide source to quench the positive charge generated rather than using water.
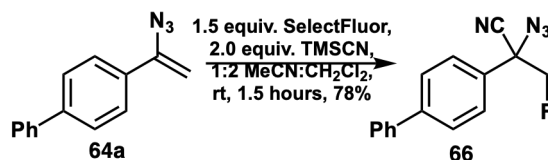
Scheme 24: Generation of azidofluoronitriles from vinyl azides

Once again, when TEMPO was included in the reaction mixture an adduct with the substrate was the only product isolated even if only in 12% yield. On this occasion cyclopropyl substrate **67a** did react to form ring-opened product **67** in 70% yield (*Scheme 25*). The authors observed that during the reaction a yellow colour was generated from their previously colourless starting materials; this, alongside the radical trapping experiments, led them to propose a single electron transfer mechanism resulting in the formation of a charge-transfer complex. The radicals can then rapidly recombine to yield the cationic intermediate proposed in *Scheme 24* above which in turn reacts with trimethylsilylcyanide to yield the desired products.
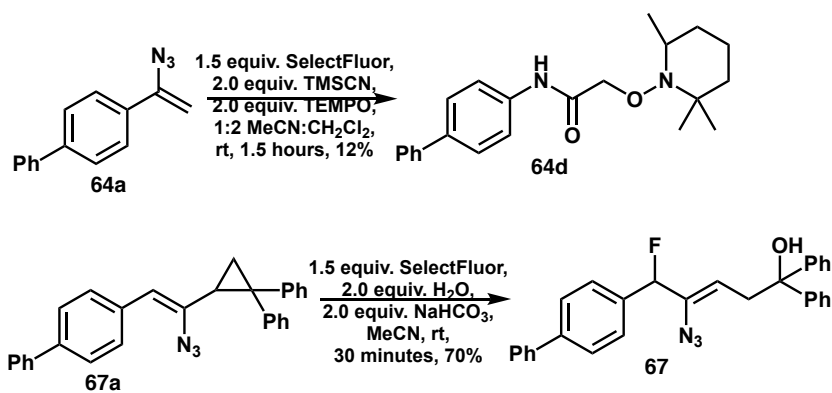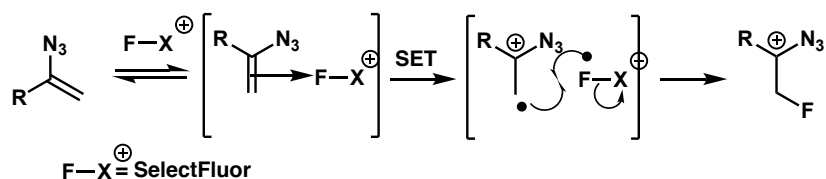
Scheme 25: Evidence For Radical Involvement in the Fluorination of Vinyl Azides

In order to quantify the reactivity of *N*-F electrophilic fluorinating reagents the Mayr research group measured the rate of reactions of SelectFluor with a number of enamine substrates of known nucleophilicity (*Scheme 26*).[150] They found SelectFluor to be the most electrophilic of the fluorinating reagents studied.
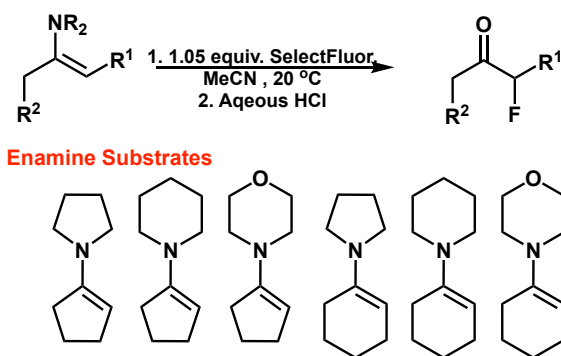
Scheme 26: Fluorination of enamines

To further understand the reaction mechanism, the experimentally determined energy barrier to fluorination was compared with the Gibb's energy of single electron transfer from the substrates. This was calculated using the anodic peak potentials of the substrates determined by Schoeller and Niemann[151] and peak reduction potentials determined by Lal *et al.*[152] for SelectFluor. It was determined that the Gibb's energy of

electron transfer was 16-19 kcal mol^{-1} higher for each of the substrates analysed. Given that the energy barrier to a single electron transfer mechanism is likely to be higher than the Gibb's energy of electron transfer the researchers came to the conclusion that it was more likely that a different (polar) mechanism was in operation. This behaviour was common across all of the fluorinating reagents studied, suggesting a shared mechanism for these substrates.

Hodgson *et al.* similarly performed kinetic studies to attempt to quantify and understand the reactivity of *N*-F electrophilic fluorinating reagents (*Scheme 27*).[153] In this study 1,3-diketone substrates were reacted with an excess of SelectFluor in acetonitrile to obtain the pseudo-first order reaction rates. The substrates studied exist predominantly in the enol form in acetonitrile solution and it is proposed that it is this tautomer that participates in the fluorination reaction. A number of substrates bearing both electron donating and electron withdrawing groups on the aryl ring were tested and a clear correlation between the electronic properties of the substrate and the rate of fluorination were observed, with more electron rich substrates reacting faster than those that were more electron deficient. It was therefore concluded that a polar mechanism was likely to be in operation. This behaviour was also observed for the other fluorinating reagents studied, indicative of a common reaction mechanism with this substrate class.
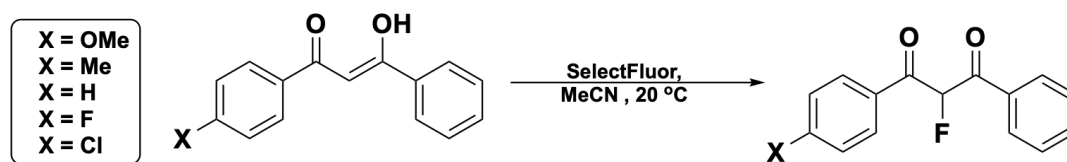
Scheme 27: Generation of fluorinated 1,3-diketones

It is clear that whilst evidence exists for SelectFluor participating in both SET and two electron mechanisms it is likely that the reagent is able to react in either manner; which mechanism is dominant depends highly on substrate and reaction conditions. A definitive explanation of how this molecule reacts is yet to be provided.

1.2.2.2.3.   Second Generation Alkyl *N*-F Reagents

Beyond SelectFluor itself, a number of related fluorinating reagents have been developed. Most closely related is the SelectFluor II reagent (**69**) which is commercially available at £12,153 per mol.[154] It differs only from SelectFluor itself in that the terminal chlorine is absent.   Examples in the literature of the use of SelectFluor II show similar behaviour to that observed for the original SelectFluor reagent.[155] In a similar vein, AccuFluor reagent (**71**) incorporates a hydroxyl group on the nitrogen rather than an alkyl group (*Scheme 28*). Again, reactivity similar to SelectFluor is observed.[156]
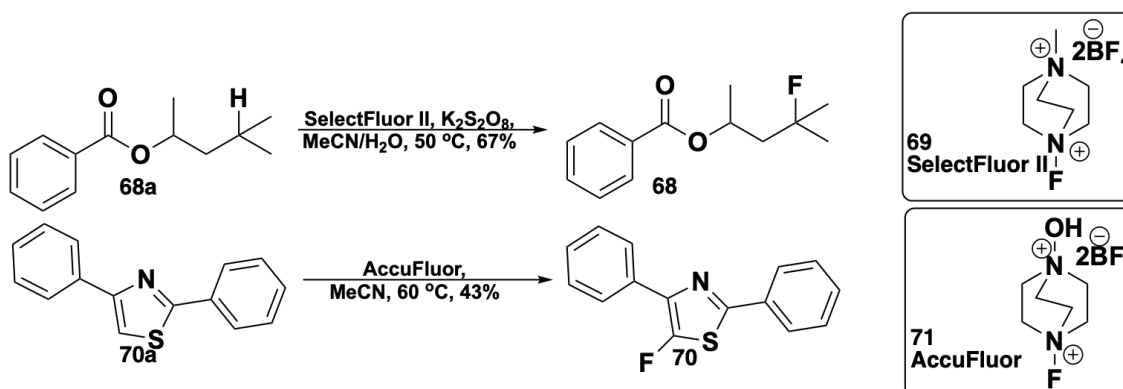
Scheme 28: Fluorination with SelectFluor II and AccuFluor

An interesting innovation in the field of alkyl *N*-F reagents is the use of chiral amines as the core of the fluorine transfer agent. First described by Cahard *et al.* in 2000, *cinchona* alkaloids (for example **72a**, *Scheme 29*) were fluorinated at nitrogen with SelectFluor. This yielded novel *N*-F compounds (e.g. **72**) which could then themselves be used in fluorination reactions.   Four *cinchona* alkaloid based compounds were synthesised in this manner and their usefulness as fluorinating reagents examined.[157]
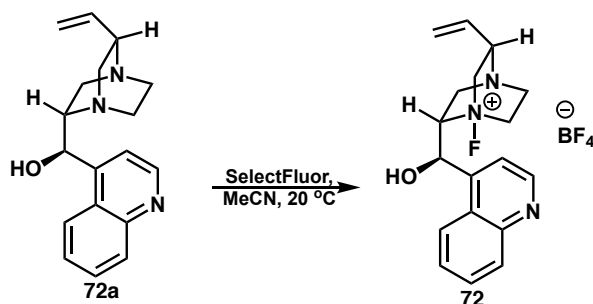
Scheme 29: Synthesis of a Chiral N-F Reagent from SelectFluor

The first reaction these novel reagents were applied to was the fluorination of 2-methyl tetralone enolate. It was observed that the stereochemistry of the product could be influenced by which isomer of fluorinating agent was used. Though the enantiomeric excesses recorded in this initial study were somewhat modest, a promising first step had been made.[157] Shibata and co-workers published further investigations into enantioselective fluorinations using chiral amine-based fluorinating agents (*Scheme 30*).
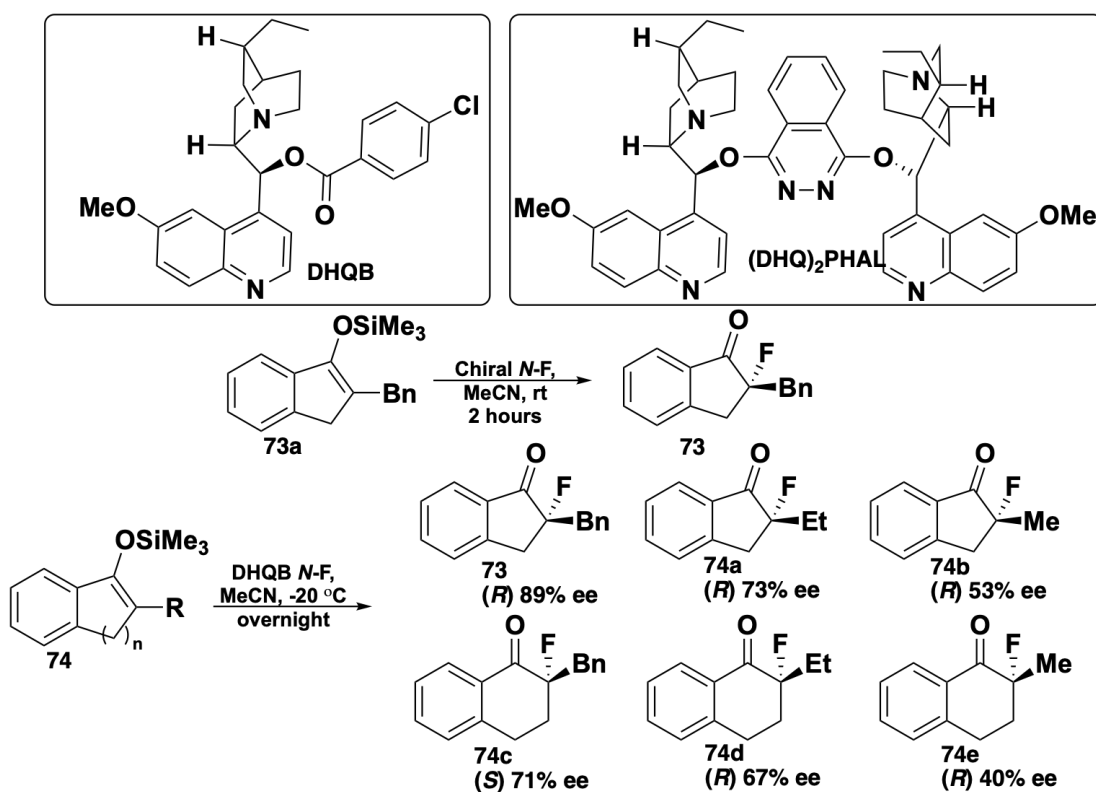
Scheme 30: Reactions of Chiral N-F Reagents with Silyl Enol Ethers

After screening eleven *N*-F alkaloids as fluorine transfer agents, the dihydroquinine 4-chlorobenzoate (DHQB) based and hydroquinine 1,4-phthalazinediyl diether ((DHQ)$_2$PHAL) derived molecules performed best in the enantioselective fluorination of the trimethyl silyl enol ether of 2-benzyl indanone (**73a**) to give the product with *R* configuration (**73** with *ee*s of 82 and 81% respectively). In light of this, due to reagent cost, the DHQB based molecule was selected for further study. When applied in further fluorinations of trimethyl silyl enol ethers of indanone and tetralone at -20ºC a range of *ee*s were obtained, from 40-91%. The larger the substituent the

higher the *ee*, whilst the benzyl substituted tetralone alone gave the product with *S* configuration.[158]

Shibata then moved on to the enantioselective fluorination of bioactive molecule, MaxiPost (**75**, *Scheme 31*). MaxiPost was developed by Bristol-Myers-Squibb, as a potential treatment for stroke; up until Shibata's publication in 2002, an enantioselective synthesis of this molecule had not been developed. A number of alkaloid skeletons were screened as potential fluorine transfer agents. The DHQB and (DHQ)₂PHAL based *N*-F compounds that had been found to be successful in the previous work both provided the desired *S* configuration in the product with 18 and 53% *ee* respectively. Higher *ee* values were found when the alkaloid hydroquinine anthraquinone-1,4-diyl diether ((DHQ)AQN) was employed in acetonitrile at 0°C, giving an *ee* of 74%. Altering the solvent to ethanol reduced the *ee* to 8% under these conditions. The highest *ee* for this reaction was achieved when it was performed at -80°C in a 3:4 mixture of acetonitrile and dichloromethane. The yield under these conditions was 94% with an *ee* of 84%.[159] There are a number of other examples of these types of chiral amines being applied as fluorine transfer agents in electrophilic fluorination.[160–165]

Scheme 31: Synthesis of Maxipost with a Chiral N-F Reagent
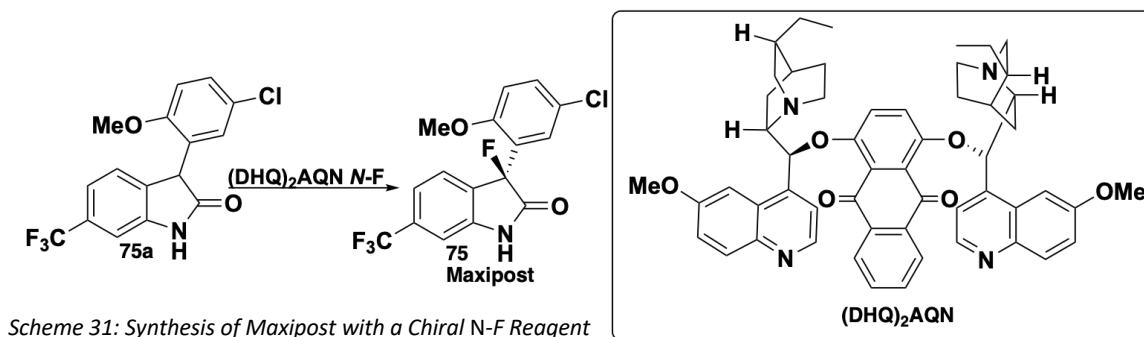
1.2.2.3. Neutral *N*-F Reagents

The final class of electrophilic fluorinating reagents to be discussed are those in which the nitrogen is not positively charged. First reported in 1987 by DesMarteau, novel *N*-F compounds based on sulfonamides were prepared. These were then utilised

in reactions with aromatic compounds to determine their applicability as fluorinating reagents. As with the charged fluorinating reagents, these molecules can be prepared by reaction with fluorine gas (*Scheme 32*).[166]
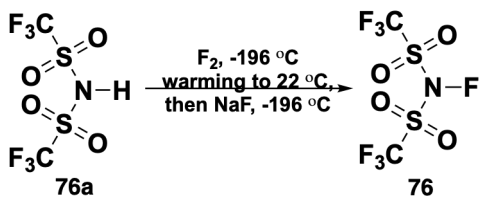
Scheme 32: Synthesis of a Neutral N-F Reagent

Of these types of reagent, the most widely used is *N*-fluorobenzenesulfonimide (NFSI), which has phenyl rings attached to the sulfur atoms. Commercially available at £3,468 per mol, NFSI is a bench stable reagent requiring no special handling.[81] Whilst NFSI is less reactive than positively charged *N*-F reagents discussed above,[13] it has been applied to fluorination reactions with nucleophiles in a similar manner to the aforementioned reagents. Differding and co-workers displayed the use of a neutral *N*-F reagent (**80**) in the fluorination of enolates. Depending on the base employed in the reaction, mono- or di-fluorinated products could be obtained (*Scheme 33*).[167]
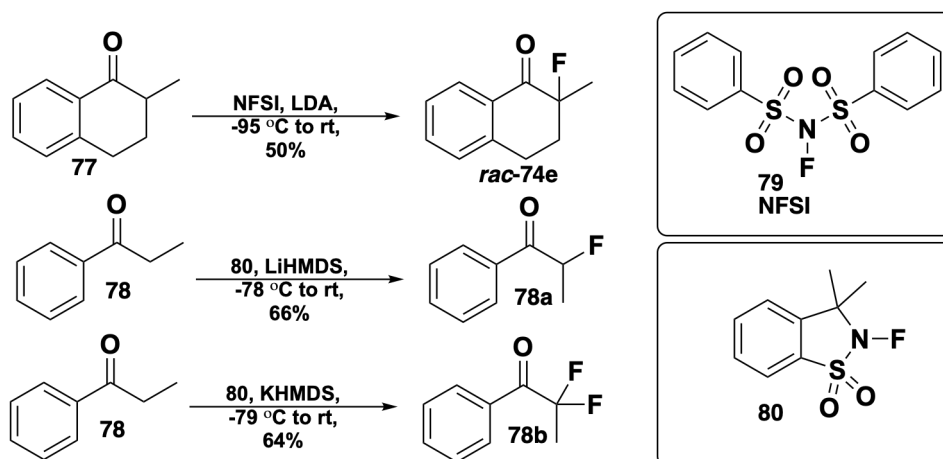
Scheme 33: Fluorination of Metal Enolates using Neutral N-F Reagents

1.2.2.3.1.   Mechanism of Fluorination with Neutral *N*-F Reagents

In an effort to determine the mechanism of fluorinations with neutral *N*-F reagents some experiments were performed with the inclusion of a radical clock substrate (of the type **81**, *Scheme 34*). It was predicted that should the mechanism proceed *via* SET a radical intermediate would be formed resulting in the rapid cyclisation to form the five membered ring leading to products **81b** and **81c**. If the mechanism was S$_N$2 attack of the nucleophile at fluorine then the open chain product (**81a**) would be observed.[168]
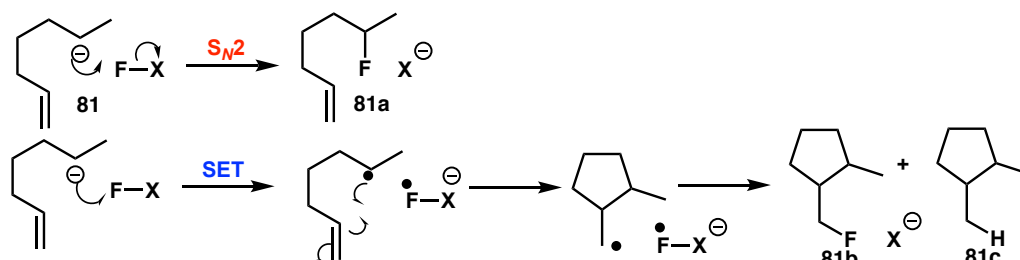
*Scheme 34: Possible reaction pathways for **81** with neutral* N-F *reagents*

When NFSI and **80** were employed, the mono- and di-fluorinated products associated with an S$_N$2 mechanism were observed along with starting material. This work appears to provide evidence for a two electron process although it does not rule out electron transfer followed by rapid recombination with the fluorinating reagent which would yield the same products.[168] Following this work, Differding and colleagues continued to investigate the mechanism of fluorination with these reagents. It was identified that the observed products could be the result of an S$_N$2 type reaction or that the radical could be formed as in the SET pathway (*Scheme 34*) as part of a radical-radical anion pair with the fluorinating reagent; this could then allow the rapid transfer of a fluorine radical. In order to distinguish between the two pathways, the rate constant of the reaction of reagent **80** with a number of nucleophiles was measured.

These values were then compared to a calculated value of the rate constant for an electron transfer reaction. When following the reactions to obtain kinetic data samples of the reactions were taken and quenched using 0.1 N aqueous HCl or saturated

aqueous ammonium chloride solution. The observed rates of reaction with enolates **78a**

and **79a** were much faster than those predicted for an electron transfer mechanism. It

was surmised from these results that these reactions proceeded *via* S_N2. From the

reaction with *N,N,N',N'*-tetramethyl-*p*-phenylenediamine (TMPDA, **80a**) the rate

matched that predicted for electron transfer and no fluorinated products were isolated.

The only observed product was the TMPDA[+.] radical cation (**80**, *scheme 35*).[169] This work

appears to show that the neutral *N*-F reagents can participate in both S_N2 reactions and

in reactions with a SET mechanism. Which path the reaction proceeds down appears to

be dependent on the substrate.
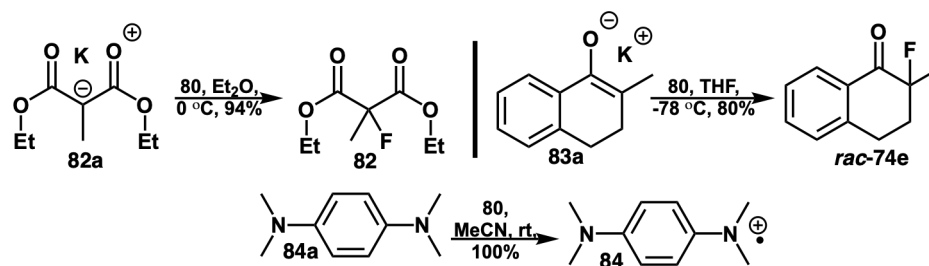
*Scheme 35: Apparent S_N2 and SET Behaviour of Compound **72** with Different Substrates*

1.2.3. Electrophilic Fluorination of Steroids in the 6α-position

Given the high proportion of steroidal drugs that incorporate fluorine into the 6-

position (*vide supra*), efficient methods of fluorine introduction are desirable.   As

discussed above, perchoryl fluoride was initially used for this purpose but the properties

of the reagent make its use impractical.   With the advent of safer, more stable

electrophilic fluorinating reagents, a wider range of syntheses are accessible. Poss *et al.*

applied *N*-fluoropyridinium tetrafluoroborate (*N*-FPy) to the fluorination of dienol ester

derivatives of steroid molecules. Given that commercially available drugs are usually the

6α –fluorides, in which the fluorine adopts an equatorial position, the ratio of α:β

products under different reaction conditions is of great interest. The reaction of steroid

dienol acetate (**81a**) with *N*-FPy at 80˚C for 5 hours afforded a mixture of regioisomeric

products in 39% yield (*Scheme 36*). This reaction yielded only the 6α- and 16α- products

in a 3:1 ratio. However, when the temperature was lowered to 50˚C and reaction time

extended to 2 days, the 6β-product was also observed in addition to the 6α- and 16α-products in a ratio of 4:4:1 (6α:6β:16α). Similar reactivity was observed for the related compound (**82a**); when it was heated to reflux in acetonitrile with *N*-FPy, a 3:1 mixture of 6α- and 17α-products was observed. The overall yield was 87%, but when the temperature was lowered to 40°C, the outcome changed to a 2:2:1 mixture of 6α-, 6β- and 17α-products in 99% yield.[170]
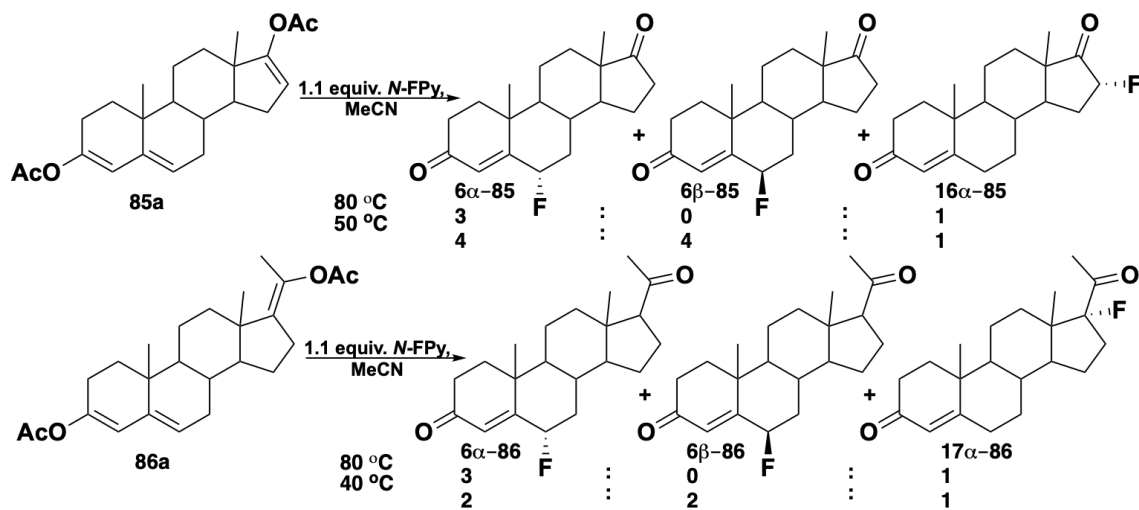
Scheme 36: Fluorination of steroidal compounds with N-*FPy*

Three additional steroidal enol ester derivatives were fluorinated at both 80˚C and 40˚C; these molecules could only be fluorinated in the 6-position (*Scheme 37*). The α/β ratios of products were examined for each reaction; generally, the reactions at higher temperature tended to yield a higher proportion of the α-stereoisomer. At the lower temperature of 40˚C the reaction showed less selectivity, forming either both products in equal amounts or slightly more of the undesired β-isomer. A silyl enol ether derivative (**90a**) was also tested at 25˚C as an alternative to the acetate. This reaction showed a preference for the formation of the β-isomer in a ratio of 1:3 α:β.[170]
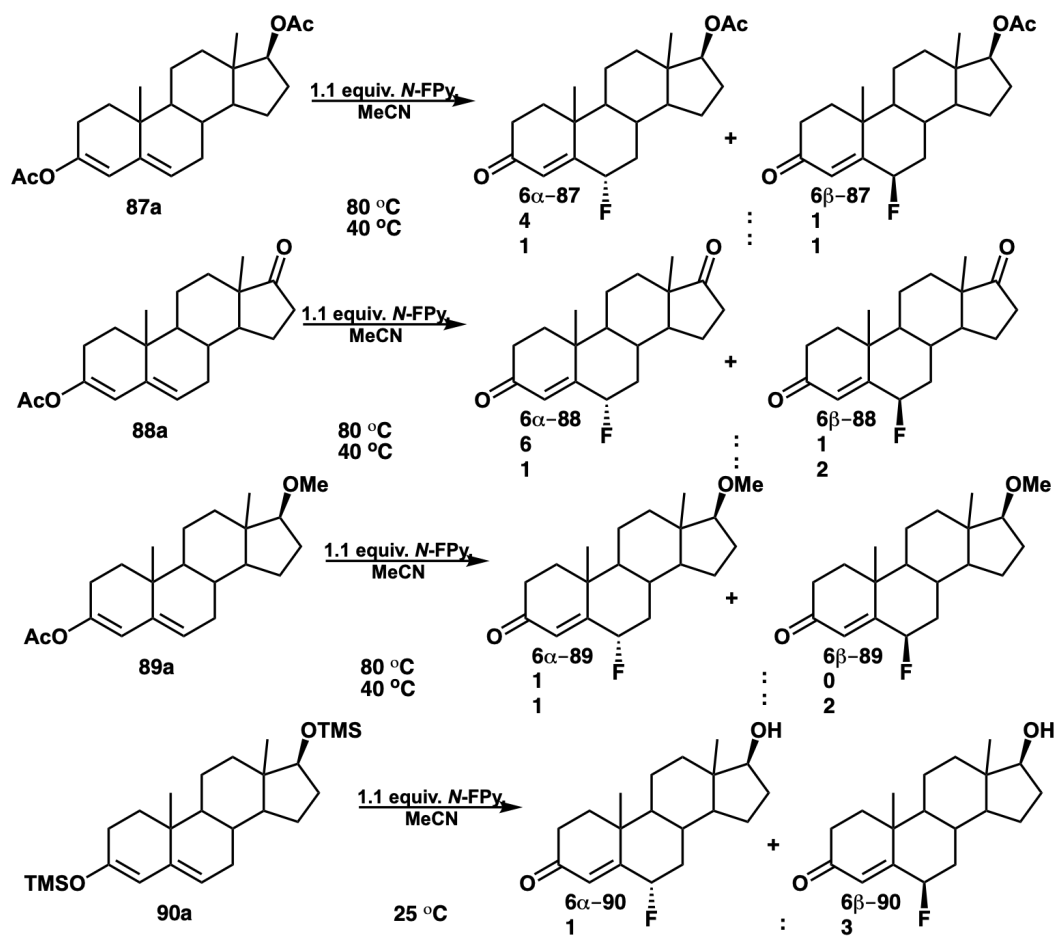
Scheme 37: Fluorination of Steroidal Enol Esters and Silyl Enol Ether with N-*FPy*

Lal then published electrophilic steroidal fluorinations with SelectFluor (*Scheme 38*). Four different steroidal substrates were examined in the fluorination reaction. After reaction with SelectFluor at room temperature for 15 minutes the only products observed were the α- and β-stereoisomers. The ratio of products appears to depend on the substrate, however generally no clear preference for a particular product was observed.[171]
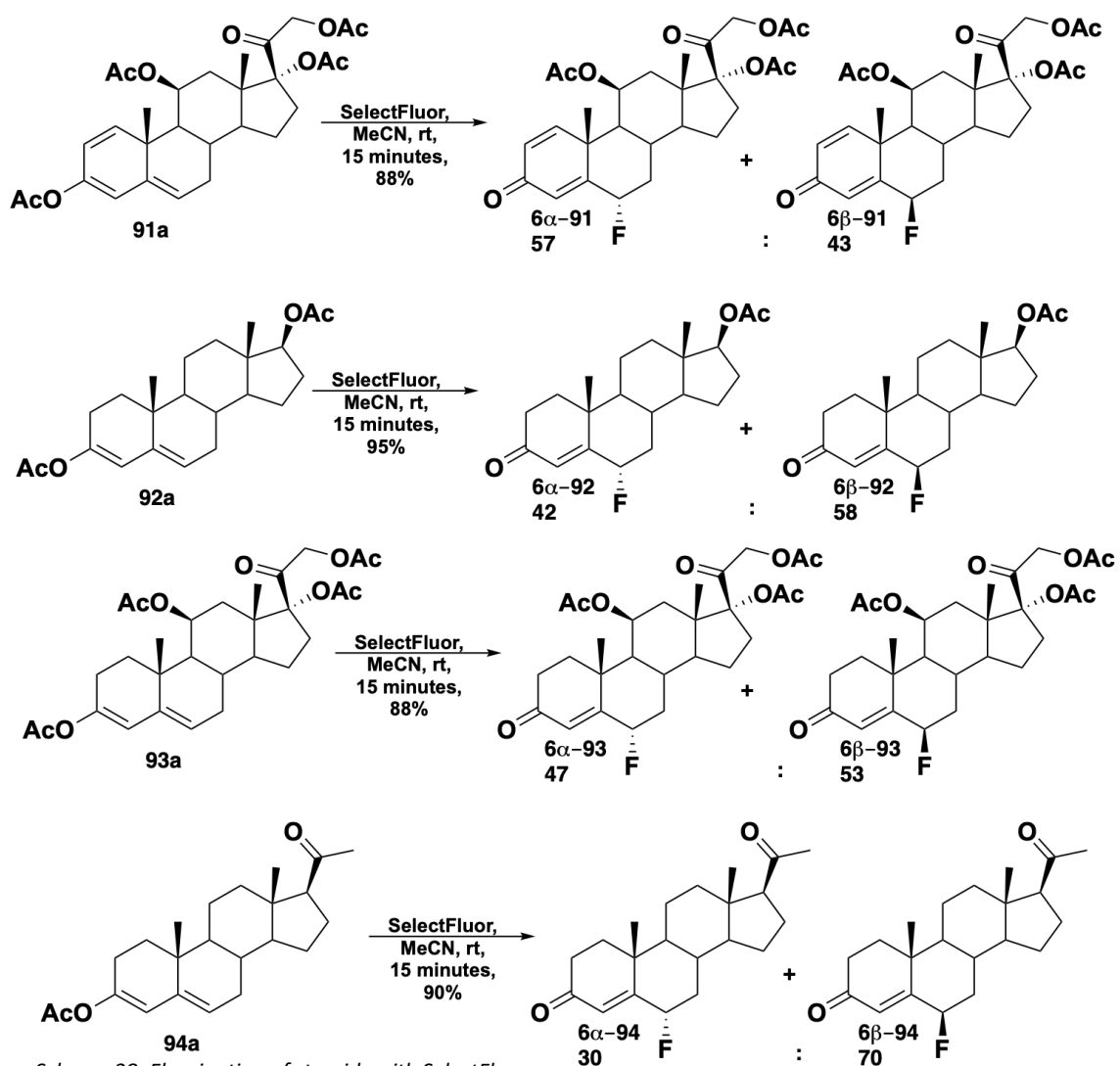
Scheme 38: Fluorination of steroids with SelectFluor

In 1997, Herrinton and co-workers published work in which the electrophilic fluorination of dienol ester derivatives of steroids were fluorinated by three different electrophilic fluorinating reagents. The fluorination of dienol acetate derivatives of three different steroids was attempted with *N*-FPy, NFSI and SelectFluor in by far the most rigorous study of steroidal fluorination to be published in the primary literature. In the initial reaction of testosterone derivative **92a** with NFSI a mixture of products was obtained (*Scheme 39*). A 5:95 mixture of the α:β products was isolated in 55-60% yield was isolated after heating the dienol acetate with 1.5 equivalents NFSI in THF at 40°C. This result was surprising, given that virtually no facial selectivity was observed either in Poss

and Lal's previous studies of steroidal fluorinations for the other reagents, or in the initial studies by Herrinton. NFSI was used no further and the cause of the selectivity was not investigated, as the purpose of the work was to form the 6α-isomer selectively.[172]
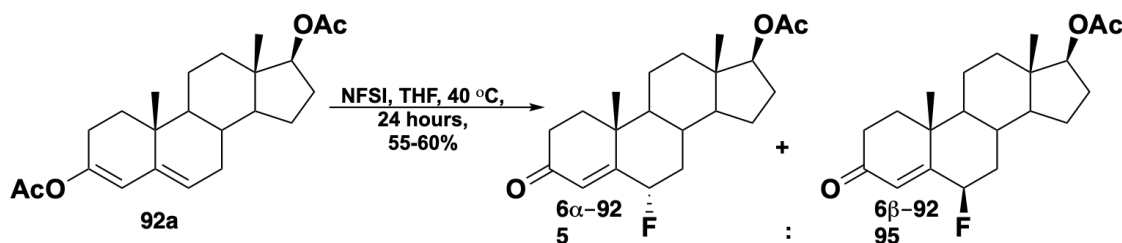
*Scheme 39: Fluorination of **92a** with NFSI*

Herrinton and co-workers investigated the effect of temperature on the α-selectivity on steroidal fluorinations with 1.2 equivalents of *N*-FPy or SelectFluor. At 40˚C, the reaction with *N*-FPy was found to be incomplete (15-20% conversion) in the designated three hour reaction time, so it was decided that at this temperature reactions with *N*-FPy should be monitored after 120 hours (*Scheme 40*). In the study of these reactions, a third product in addition to the 6-fluorinated isomers was detected.
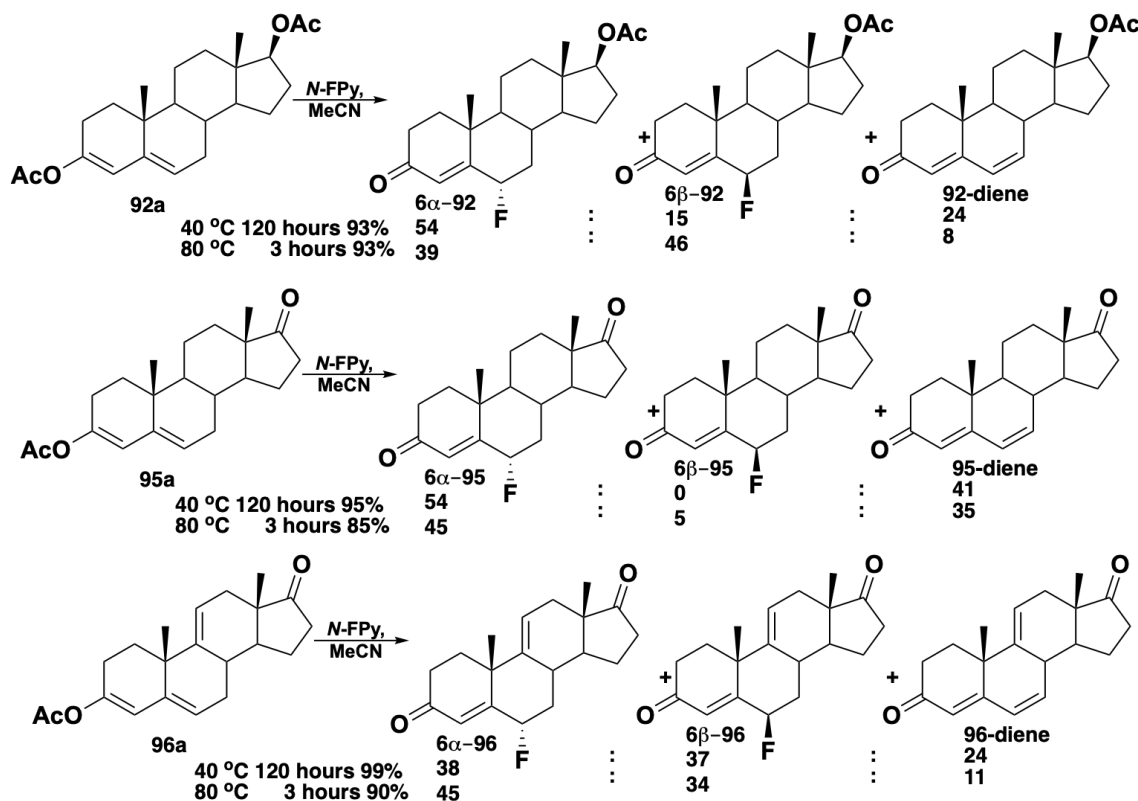
Scheme 40: Fluorinations of Steroidal Enol Esters with N-*FPy*

This product was identified as non-fluorinated dienone (**92-diene**, **95-diene** and **96-diene**). These products were more favoured in the reactions with *N*-FPy at 40˚C. Increasing the temperature to 80˚C with *N*-FPy as the fluorinating reagent generally produced slightly more of the 6α-product, but the selectivity was still poor.

The reactions with SelectFluor were carried out at 0˚C and 80˚C (*Scheme 41*). Unlike those with *N*-FPy, the reactions at the lower temperature were complete after 3 hours. Again, dienone products were observed with steroids **92a** and **95a**. However only in the reaction with steroid **92a** at 80˚C was this side product observed in significant amounts. None of the reactions with SelectFluor at the lower temperature of 0˚C produced dienone side products. No significant α/β selectivity with SelectFluor was observed despite the improved apparent selectivity for fluorinated products over the non-fluorinated dienones. The α- and β-products were present in a roughly 1:1 ratio early stage in the reaction; however, as the reaction progressed, the amount of β-product decreased whilst the dienone product increased. It was therefore thought that the β-product it was more susceptible to elimination to give the dienone product along with HF due to the axial orientation of the C-F bond. This hypothesis is supported by the fact that the experiments with the longest reaction times (120h at 40˚C with *N*-FPy) yielded higher proportions of dienone. At both temperatures, the reaction with *N*-FPy appeared to give more of the dienone product than the reaction with SelectFluor. It was assumed that this was due to the formation of pyridine in the reaction mixture, and through its action as a base the elimination of HF was promoted.
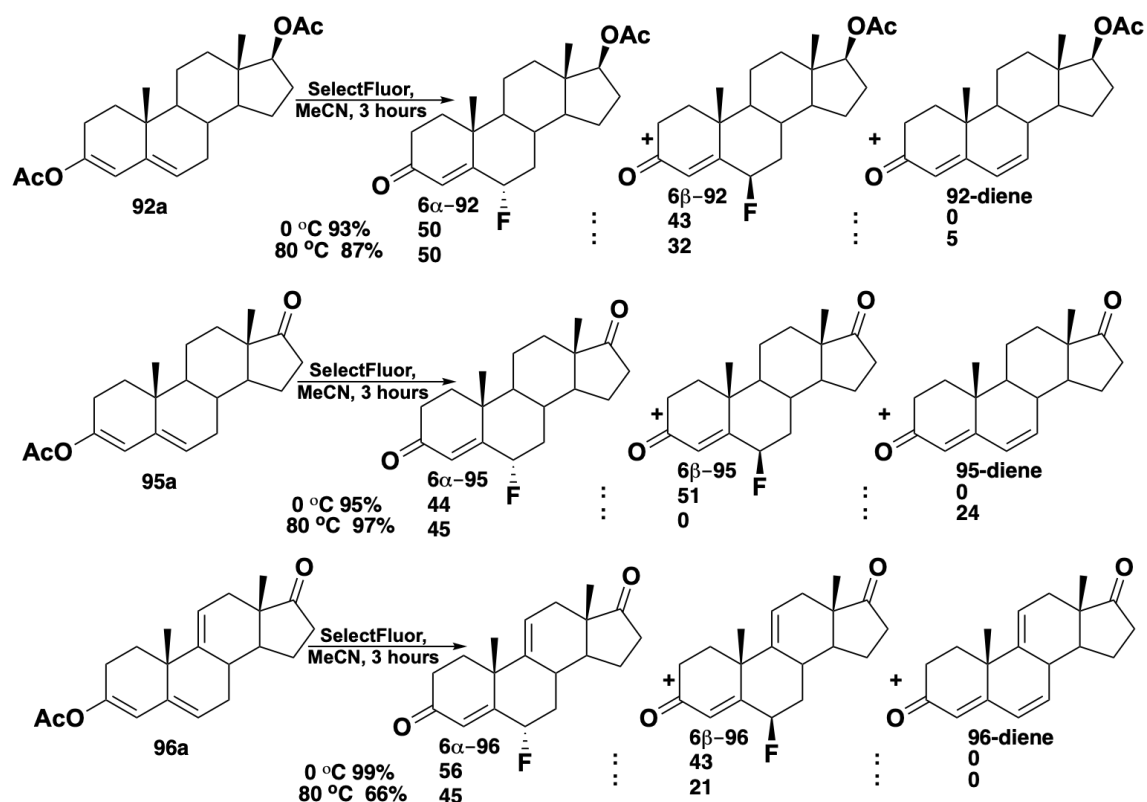
*Scheme 41: Reaction of **92a**, **95a** and **96a** with SelectFluor*

When steroid **96a** was reacted at 80°C with SelectFluor the yield of the reaction was significantly diminished. It was found that this was due to excess reagent reacting with the 9,11-double bond in the 6-fluoro products, generating phenolic products (*Scheme 42*). Fluorination at this double bond presumably results in the formation of a positive charge on the 9-position of the steroid, this would then facilitate the migration of the methyl group, allowing the A ring to aromatise.
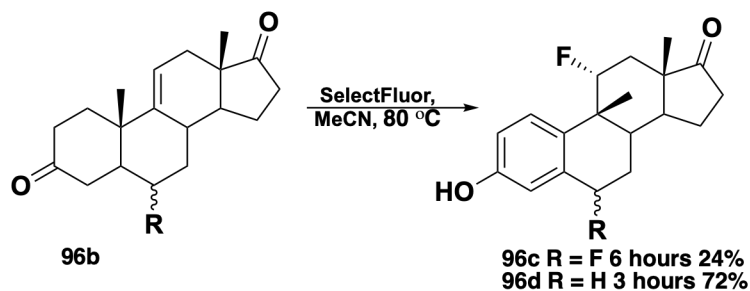
*Scheme 42: Rearrangement of **96b***

57

After 6 hours the phenolic products had been produced (24% yield) when the enol acetate was reacted with SelectFluor at 80˚C. The ratio of 6α/β-fluoro products was not reported, so it is unclear whether the two isomers participate differently in this reaction. The non-fluorinated parent steroid produced the corresponding phenol product in 72% yield after reaction with SelectFluor at 80˚C for 3 hours.

SelectFluor was therefore identified as the best reagent for 6α-product formation in high yield, and the reaction with steroid **96a** was selected for further investigation. Lowering the temperature of the reaction was investigated in order to prevent the unwanted formation of phenol products. It was found that decreasing the temperature below -30°C led to slow reaction and therefore poor conversion (12% after 24h); however, the unwanted reaction with excess SelectFluor was not observed. At 0˚C, the reaction took 30 minutes, and produced a 1.3:1 mixture of α- and β-products in 65-70% isolated yield. Though it was claimed that the yield of products was highest at -25°C, no percentage was reported. The number of equivalents SelectFluor required was then examined, and it was found that a minimum of 1.1 equivalents was required to allow the reaction to reach complete conversion. With 1.1 equivalents of SelectFluor, 95% conversion of the starting material was observed at -25°C with full consumption achieved by warming the reaction mixture to 0-5°C from -25°C. The isolated yields achieved for these conditions were 80-85% but the ratio of products was unchanged from that observed at 0˚C.

Herrinton and co-workers had been unable to install fluorine in the 6α-position of the steroid directly. An attempt was therefore made to convert the mixture to one which predominantly contained the desired 6α-product. It was discovered that the α-product was favoured by a 83:17 ratio over the β-diastereoisomer under acidic conditions. The α-product was found to crystallise more readily, leading to crystals enriched in the α-isomer whilst the mother liquor contained more of the β-diastereoisomer. It proved possible to equilibrate the mixture so that the α-

diastereoisomer crystallised out, leaving the β-diastereoisomer in acidic solution where it isomerised to the desired α-product. The solvent and acid used were optimised in order to make this process as efficient as possible. The best results were obtained when 2-propanol or ethyl acetate were used as reaction solvents, while the best acid was HCl (*Scheme 43*). Equilibration was not observed in the presence of strong acids with non-nucleophilic counterions (methanesulfonic acid, sulfuric acid, perchloric acid). The number of equivalents of HCl proved critical, if more than one equivalent HCl was used 6-chloro products were observed. The 6α-product was isolated in 83% yield from the equilibration of a mixture containing a 57:43 ratio of α- and β-fluorides. The desired α-isomer crystallised out, pushing the equilibrium towards the formation of more of the α in the mother liquor. Once the solid had been removed by filtration and recrystallised, the resulting product contained >99% of the desired 6α-fluorosteroid.

Scheme 43: Equilibration of **96**
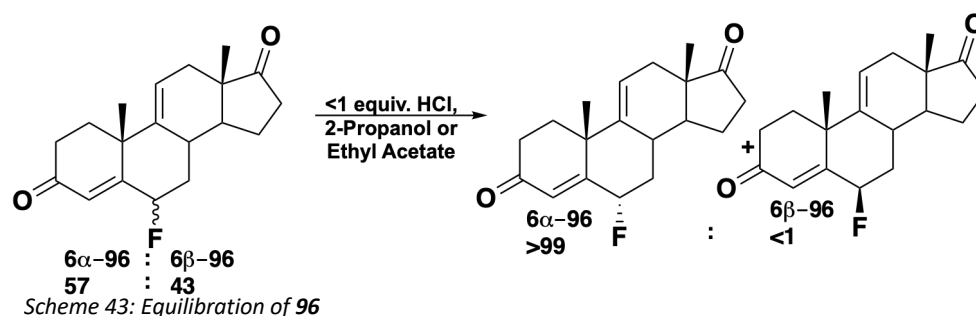
Equilibration of a mixture of 6α- and 6β-fluorosteroids to predominantly the 6α-product is not a novel concept. A patent filed in 1960 by Pfizer illustrated the conversion of a 6β-fluorosteroid to the corresponding 6α-isomer. The 6β-fluoro intermediate was treated with HCl in acetic acid in order to achieve the equilibration to the desired product.[173] In 1975 the Upjohn company filed a patent on the synthesis of a 6α-fluorosteroid which involved the treatment of a mixture of the α- and β-fluorides with HCl or a HCl-DMF complex in chloroform to yield predominantly the 6α-product.[174] More recently (in 2002), a process was patented for the equilibration of a mixture of 6α and 6β-fluorosteroids to the desired 6α-isomer. On this occasion, organic bases were used instead of acidic conditions. It is claimed that fluoroproducts can be isolated in 65-88% yield with a minimum α/β ratio of 95:5 through this process. One example details the

equilibration of steroid **94a** from a 38:62 α/β mixture in acetone using 1.3 equivalents of DBN (*Scheme 44*). The equilibration was complete after stirring at room temperature for 48 hours and the resultant residue from concentrating the reaction mixture was dissolved in DMF. This solution was then added dropwise to acidified cold water, resulting in precipitation of the product which was then collected by vacuum filtration. The inventors stated that DBU could be used interchangeably with DBN as the base.[175]

6α-97 : 6β-97
38 : 62

Scheme 44: Equilibration of 97
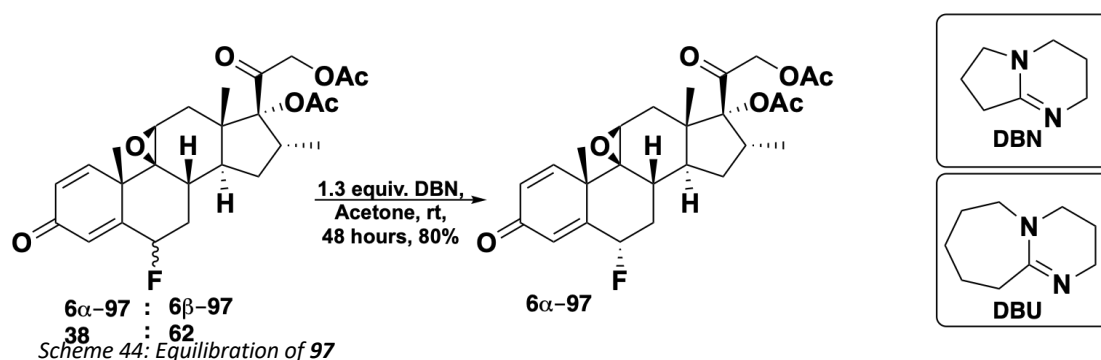
A number of patents detail diastereoselective syntheses of 6α-fluorosteroids as alternatives to the equilibration methods described above. One patent filed in 2001 by Italian company Farmabios[176] outlines the synthesis of a number of 6α-fluorosteroids from starting materials which all contain a free 17α-hydroxyl group. The reactions described in the patent involved the fluorination of dienol acetate esters of steroid derivatives with AccuFluor or SelectFluor resulting in very high α/β ratios of products in the range 94.4:5.6 to 96:4. The dienol esters were synthesised from the parent ketones and isopropenyl acetate with catalytic *p*-toluenesulfonic acid at 80˚C for 1 hour before cooling to 50˚C. Triethylamine was then added to control pH, along with acetonitrile. This solution was then concentrated and cooled to 0˚C; at this point the fluorinating reagent (either SelectFluor or AccuFluor) was added and the reaction continued at 0˚C for 12 hours. After this time the product precipitated out of solution and could be collected by filtration and isolated following washing with aqueous ammonia solution.

An interesting patent filed in 2003 detailed the diastereoselective synthesis of five 6α-fluorosteroid compounds from their respective dienol ester benzoates or 4-methyl benzoates (eg. **98a**, *Scheme 45*).[177] The lowest reported α/β ratio reported was

98.3:1.7 and the highest 99:1. On this occasion, SelectFluor was the fluorinating reagent of choice. The dienol ester was dissolved in acetonitrile; pyridine (1.05 equivalents) and methanesulfonic acid (1 equivalent) were then added to this solution followed by SelectFluor (1.02 equivalents). The reaction mixture was maintained at 0-5˚C during the addition of reagents; it was then allowed to warm to room temperature and left to react until HPLC analysis showed the mixture of products to contain only 1% of the undesired 6β-isomer. It is unclear from the patent whether higher proportions of the 6β-isomer are observed earlier in the reaction, or indeed how long the reaction times are, but the results are intriguing nonetheless.

Scheme 45: Fluorination Procedure Using MsOH and Pyridine as Additives
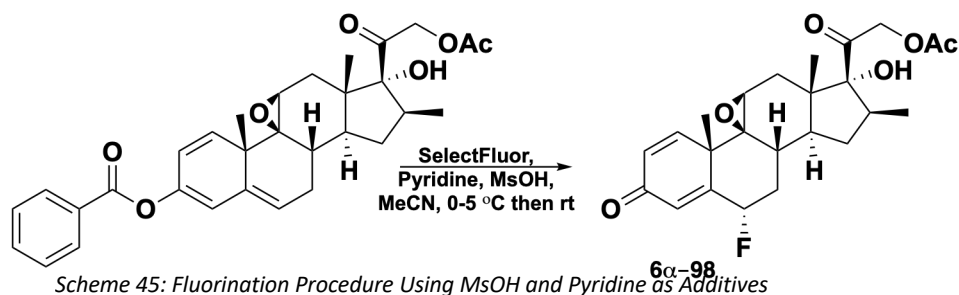
Stereoselective syntheses of 6α-fluorosteroids have also been claimed from different dienol esters. The patent for the use of 4-nitrobenzoate dienol esters was filed in 2013 by Trifarma;[178] the claim outlined the synthesis and subsequent fluorination of a dienol ester of the type **98b** shown in *Scheme 46*. The diastereoselectivities quoted were high, with the lowest an α/β ratio in the product of 99.4:0.6. In order to obtain the 6α-fluorosteroid, 0.65 equivalents pyridine were dissolved in acetonitrile and the 4-nitrobenzoate enol ester was added, followed by 1 equivalent SelectFluor, and the mixture was allowed to react for 1 hour. No details were given on the temperature of the reaction.

Scheme 46: Fluorination of 4-Nitrobenzoate 95b with Selectfluor
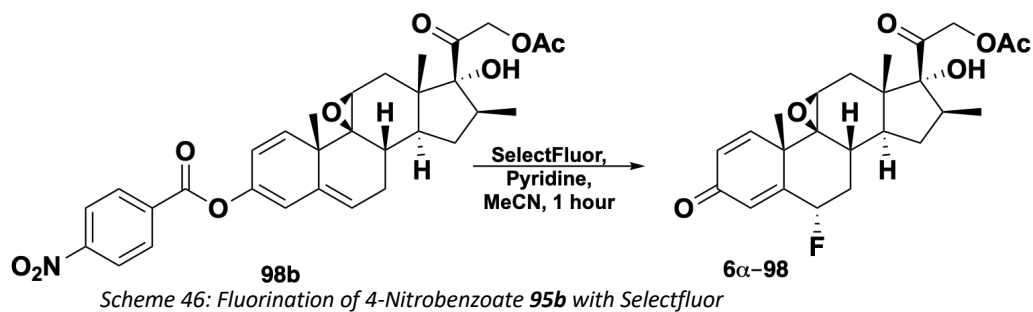
1.2.3.1. Electrophilic Fluorination of Steroids as Precursors to Fluticasone Propionate and Fluticasone Furoate

Given the high demand for fluticasone propionate and fluticasone furoate a cost efficient and high yielding synthesis is required. The current synthesis employed by GSK involves early incorporation of the 6α-fluorine (*Scheme 47*). This is achieved *via* electrophilic fluorination of dienol ester **96b** using Selectfluor. The current optimised conditions involve the addition of 1.2 equivalents methanesulfonic acid and at least 2 equivalents pyridine as additives and a mixture of acetonitrile and 2-methyl THF. The reaction mixture was maintained at 0-5°C for 5 hours before warming to 20°C. Development of the process resulted in the discovery that higher α/β selectivity could be achieved under anhydrous conditions; however, side products were also observed. The reaction proceeded more cleanly when water was added but the α/β selectivity was lower. The isolated dienol benzoate was unstable to air, undergoing oxidation at the 6 position, so the crude benzoylation product was taken on directly without purification. This has the added advantage of utilising left-over pyridine from the reaction mixture of the benzoylation step in the fluorination. Investigations into the use of additives found methanesulfonic acid addition to be critical to high diastereoselectivity, affording α/β ratios of 30:1 whereas the ratio is 10:1 in the absence of the additive. The current process affords **6α-99** in 74-82% yield and only 4% of the undesired **6β-99**. Whilst this selectivity is high, the role of the additives is poorly understood and the origin of the diastereoselectivity is unknown. There is scope to improve the efficiency of the process by improving the overall yield of the reaction or the diastereoselectivity.
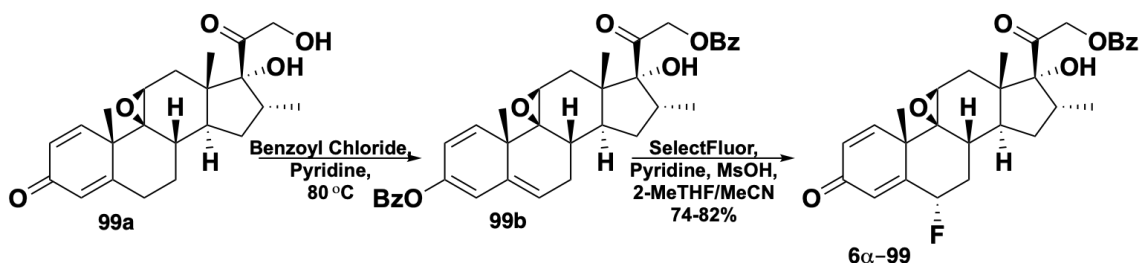
Scheme 47: GSK Fluorination Procedure in the Synthesis of Fluticasone Esters

2.   Aims

The mechanism of electrophilic fluorination using SelectFluor is currently not well understood, particularly *via* enol ester nucleophiles that have proven so useful in the generation of 6-fluorinated steroids. This makes the design of synthetic routes to bioactive 6α-fluorosteroids with high yields and high selectivities difficult. In order to design a successful high yielding fluorination process it is proposed that developing an understanding of the fluorination mechanism of simple enol esters would be of importance.

The work described herein is concerned with generating an understanding of the mechanism in operation in the electrophilic fluorination of tetralone derivatives as a simple model which can be readily modified to elucidate the reaction mechanism. This was achieved *via* the design and synthesis of structurally related but electronically diverse sets of substrates which can then be applied to kinetic and computational DFT studies. Once the mechanism of fluorination of tetralone derivatives was established attention was turned to determining whether the mechanism in operation for these small molecules is conserved in the fluorination reactions of both small steroidal models and analogues of **99b** (*Scheme 47,* above) itself.

The role of the methanesulfonic acid and pyridine additives was also interrogated to determine whether they play any significant role in the fluorination step or are present in order to equilibrate the undesired β-steroid to the desired α-isomer. This information in combination with the knowledge gained from kinetic studies should allow a better understanding of the industrial fluorination process, allowing the potential for a more efficient route to the 6α-fluorosteroid to be designed.

3. Results and Discussion

3.1. Fluorination of Tetralone Derivatives with SelectFluor

The objective of the project was to determine whether the current electrophilic fluorination process in the synthesis of fluticasone propionate (**29**, shown in *Figure 23* on page 23) and fluticasone furoate (**36**, shown in *Figure 24* on page 24) could be improved upon. However, the direct observation of this reaction had limited potential. The physical properties of this steroidal dienol benzoate renders the material only sparingly soluble in the solvent systems that are necessary to dissolve SelectFluor. In addition, this complex molecule has few possible vectors around the reacting centre for the synthesis of related compounds whose reactivity could shed light on the reaction mechanism with SelectFluor. It was therefore important to develop a series of model compounds for the study of the mechanism of the reaction with SelectFluor. These compounds had to fulfil key criteria in order to make them useful in this study. It was important that the substrates under investigation should be:

- Synthetically accessible in a few steps
- Access to a series of analogous compounds functionalised at different sites
- Synthesised from inexpensive commercially available materials
- Highly soluble in possible fluorination reaction media
- Easily distinguishable from SelectFluor and any reaction products *via* analytical techniques

Commercially available cyclic ketone 1-tetralone (*Figure 28*) was selected as a candidate that fulfils these criteria. It was envisioned that this ketone could be readily converted into enol ester derivatives and that the fluorination could be studied by ^{1}H NMR spectroscopy to determine the reaction rates. This versatile small ketone also had

opportunities for further functionalisation in order to gain insight in to the relationship between structure and reactivity with SelectFluor.
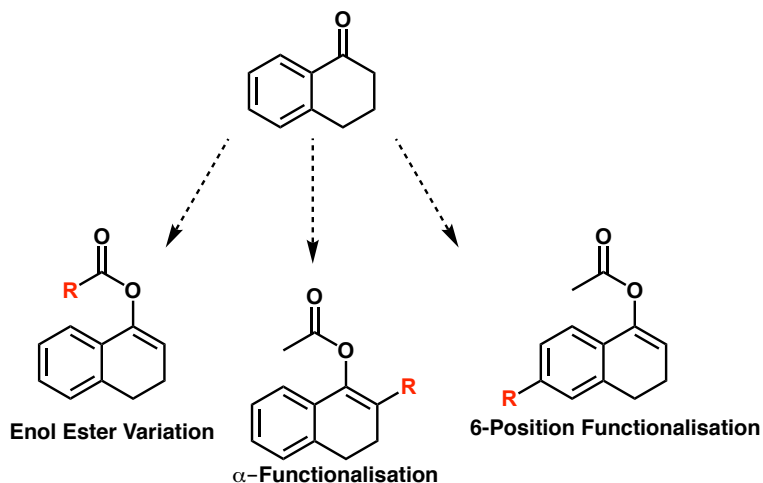
Figure 28: Tetralone Functionalisation Vectors

3.1.1. Possible Mechanistic Pathways

Debate surrounds whether fluorination with SelectFluor operates *via* a one electron radical mechanism or a two electron polar mechanism. There is only one possibility for fluorination *via* a polar mechanism (*Scheme 48*), however the radical question throws up three possible related pathways which differ subtly. The possible polar mechanism involves nucleophilic attack by the enol ester alkene, resulting in the generation of a carbenium ion which is then hydrolysed to form a fluoroketone and carboxylic acid.

Scheme 48: Polar Pathway
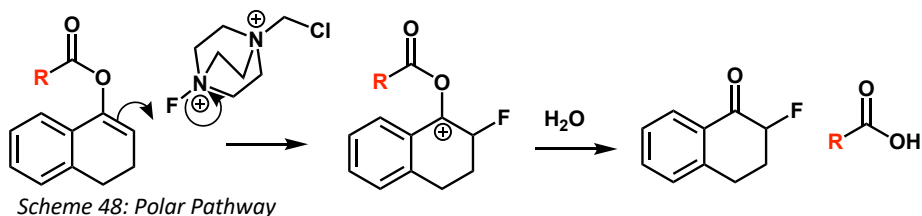
Another possibility is that single electron transfer is possible from the enol ester alkene to SelectFluor. This single electron transfer could result in the formation of a radical cation on the substrate and cleavage of the N-F bond resulting in the formation of a fluorine radical species (*Scheme 49*, A). These would then recombine, forming the

carbenium intermediate postulated in the polar mechanism. It is also possible that the N-F bond remains intact and that it is this radical species that combines with the radical cation (*Scheme 49*, B).
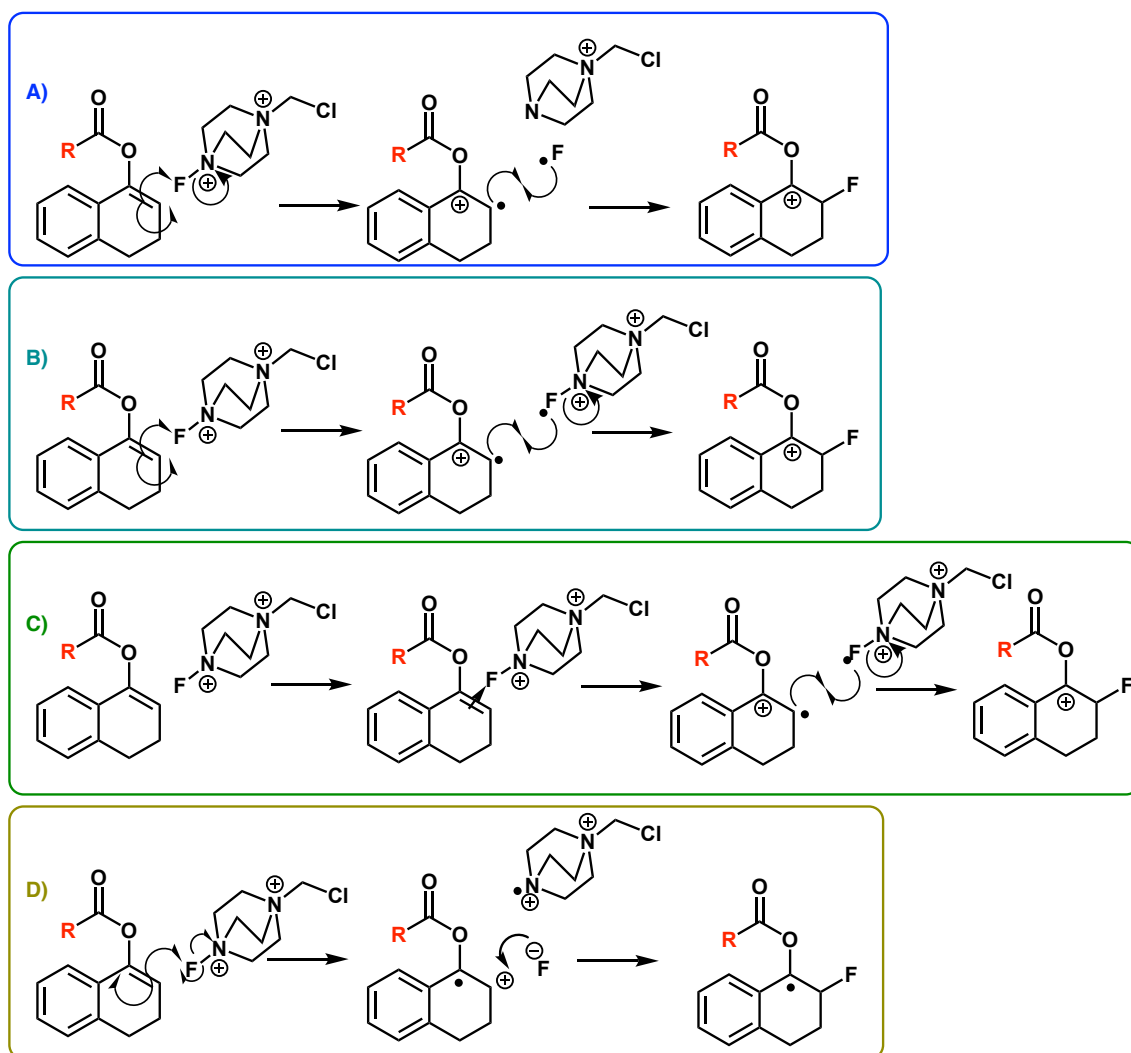
Scheme 49: Possible Radical Pathways

A third possibility is that charge transfer from the enol ester to SelectFluor results in the formation of a charge-transfer complex which can then reorganise to yield once again the carbenium intermediate and SelectFluor-byproduct (*Scheme 49*, C). The final possible mechanism considered is that single electron transfer from the enol ester results in again, formation of a radical cation however in this instance the positive charge would reside on the alpha-carbon (*Scheme 49*, D). Single electron transfer in this case

would result in the cleavage of the N-F bond, generating fluoride. This would then react with the radical cation intermediate generating a ketyl radical. Reorganisation and hydrolysis would then yield the fluoroketone product.

In support of the polar mechanism are the studies conducted by Aggarwal,[179] Mayr[150] and Hodgson[153] in which evidence for this type of reactivity with their substrates is observed. In particular, the work using enamines is promising for this type of reactivity given that both enol esters and enamines are related structurally as enol equivalents. The research by Liu using vinyl azides implicates radicals in the mechanism,[147,149] indicating that both the generation of the SelectFluor-centred radical and the formation of the charge transfer complex are possible. Reaction of a fluoride anion with the radical cation of tetralone enol acetate has been shown to be possible by Thiebault *et al.*[180] In this study the enol ester was electrochemically oxidised in the presence of fluoride in the form of TREAT-HF (*Scheme 50*). This resulted in the formation of the desired alpha-fluoroketone along with 1-acetoxynaphthalene, therefore if this type of mechanism is in operation it may be expected that these side products would also be observed in the reaction with SelectFluor. The formation of a radical centred on a free fluorine atom is unlikely due to the instability of such a species, nonetheless its involvement cannot be ruled out.
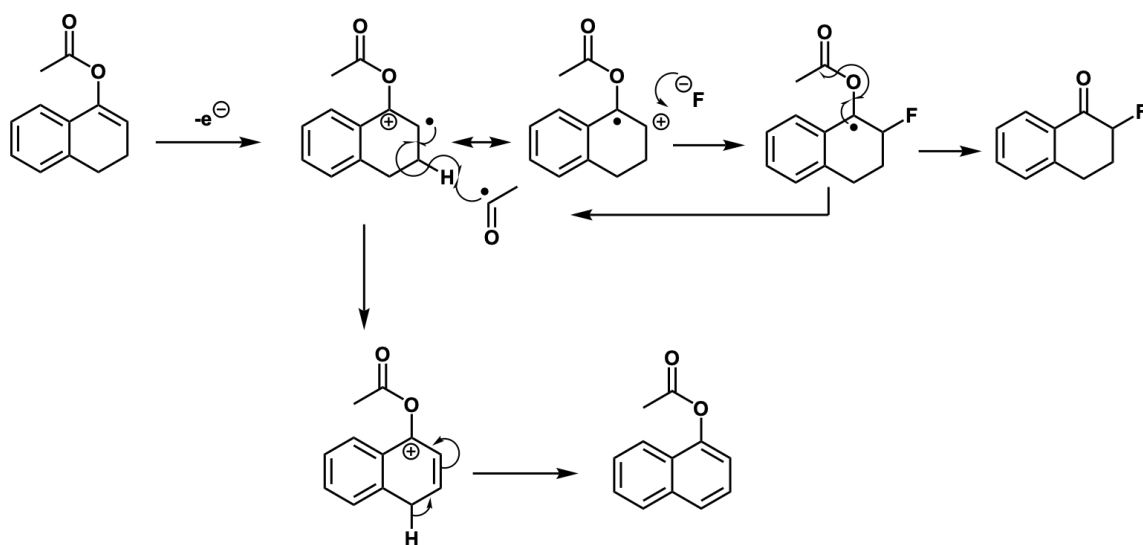
Scheme 50: Electrochemical Oxidation and Fluorination of Tetralone Enol Acetate

3.1.2. Synthesis of Enol Acetates of Tetralone and Indanone

Now that a reasonable strategy had been selected for the mechanistic studies it was necessary to find a synthetic route to the enol esters to be studied. In order to develop a robust means of studying this fluorination reaction a simple enol ester was desired which could be accessed in large quantities with minimal synthetic effort. Known enol acetate **100** was therefore selected as an ideal candidate. It was accessed synthetically in two ways. Deprotonation of 1-tetralone with LDA, followed by acetylation using acetic anhydride at -78 °C, afforded the desired compound in moderate (65%) yield after work-up and vacuum distillation. Whilst this route yielded sufficient compound to begin monitoring the fluorination reaction, an alternative route which did not require cryogenic conditions was identified. The reaction of 1-tetralone with isopropenyl acetate using catalytic toluene sulfonic acid afforded the desired compound in good (90%) yield (*Scheme 51*). This route was an improvement on the LDA conditions as not only did it provide the compound in higher yield but also allowed the isolation of the product without laborious purification.
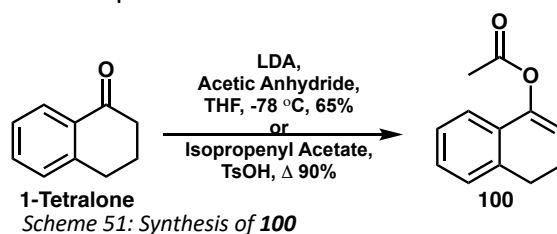
*Scheme 51: Synthesis of **100***

As a complementary substrate to the six-membered ketone 1-tetralone it was proposed that five-membered 1-indanone derivative **101** would also be useful. The potential for the release of strain in the smaller indanone enol acetate should result in a rate acceleration compared to the tetralone compound, allowing a wider range of reaction times to be available which would aid in the selection of the correct analytical technique for the study of the reaction. Indanone substrate **101** was synthesised *via* deprotonation of 1-indanone with sodium hydride followed by acetylation of the enolate with acetyl chloride. This yielded the desired product in poor (12%) yield. This was

disappointing, but the isopropenyl acetate conditions could also be applied to this compound affording **101** in a much improved 78% yield (*Scheme 52*).
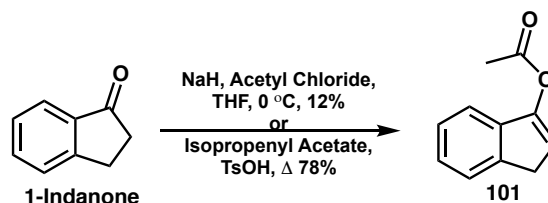
*Scheme 52: Synthesis of Compound **101***

3.1.3. Assay Development

The ideal monitoring method for the fluorination reaction would allow the generation of a high density of data points, direct observation of the bulk reaction mixture (as opposed to a sampling and quenching procedure) and ideally the ability to observe and quantify the concentrations of all of the reaction components. The first possible monitoring techniques investigated were UV/vis spectroscopy and ^{1}H NMR. Whilst it would only be possible to observe the reaction components which have a chromophore with UV/vis it is possible to record many more data points in any given time than with NMR. Despite this, NMR spectroscopy allows direct observation of both reactants and the products of the reaction. For both techniques it is necessary for the reaction mixture to be homogeneous which posed some challenges due to the poor solubility of SelectFluor in most common organic solvents.

3.1.3.1.   Initial NMR Experiments

Firstly, attention was turned to the fluorination of compound **100** in deuterated acetonitrile, following the reaction by ^{1}H NMR. Following the fluorination reaction by ^{1}H NMR is preferential to using ^{19}F NMR as the starting enol ester is not visible by ^{19}F NMR and the signal for the SelectFluor N-F appears at around 50 ppm, whilst the product (compound **102**) appears at around -190 ppm making it difficult to observe both signals simultaneously. In addition to this, the two tetrafluoroborate counterions associated

with the SelectFluor dication contribute a large signal at -150 ppm, which makes small concentrations of other fluorinated species in a similar range difficult to observe and accurately quantify. The products of the fluorination of **100** are shown in *Scheme 53*.

Scheme 53: Fluorination of **100**
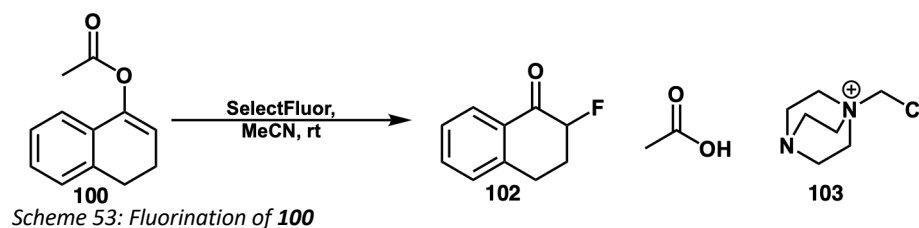
The ^{1}H NMR spectra of the starting material, SelectFluor, the fluoroketone product **102** and SelectFluor-byproduct **103** show very little overlap (*Figure 29*) allowing simple monitoring of the reaction progression and easy identification and quantification of the components present. In the initial NMR study 1.4 equivalents of SelectFluor were used in deuterated acetonitrile at a concentration of 0.21 M in enol ester. Despite the high concentration and excess of fluorinating reagent used, the reaction failed to reach completion after 45 hours. It was thought that this was due to the poor solubility of SelectFluor in acetonitrile at this concentration. In addition to this, whilst the desired product was forming, an unidentifiable by-product was also observed in the spectrum. The equivalent bench scale reaction appeared to be complete by TLC after 6 hours. It was therefore proposed that the likely higher water content in "bench" acetonitrile combined with the ability to stir the reaction was allowing a better outcome whilst the ampules of deuterated solvent were likely to have a negligible aqueous content. In addition to solubilisation of SelectFluor, water plays a key role in this reaction as a nucleophile to hydrolyse the enol ester post-fluorination, yielding compound **102** and the associated carboxylic acid by-product. The poor solubility of SelectFluor in the NMR experiment was the primary concern due to the concentration of fluorinating reagent in solution being effectively unknown. A simple experiment was conducted where a known mass of SelectFluor was suspended in a known volume of acetonitrile and mixed. Water was then added in known quantities until no undissolved SelectFluor could be seen. A 0.2 M solution of SelectFluor was formed in 3% *(v/v)* water in acetonitrile. The original

NMR study was then repeated with this level of water content and the reaction was able to achieve full conversion after 40 minutes. The formation of acetic acid was now observed in the ^{1}H NMR, confirming the role of water as a nucleophile.
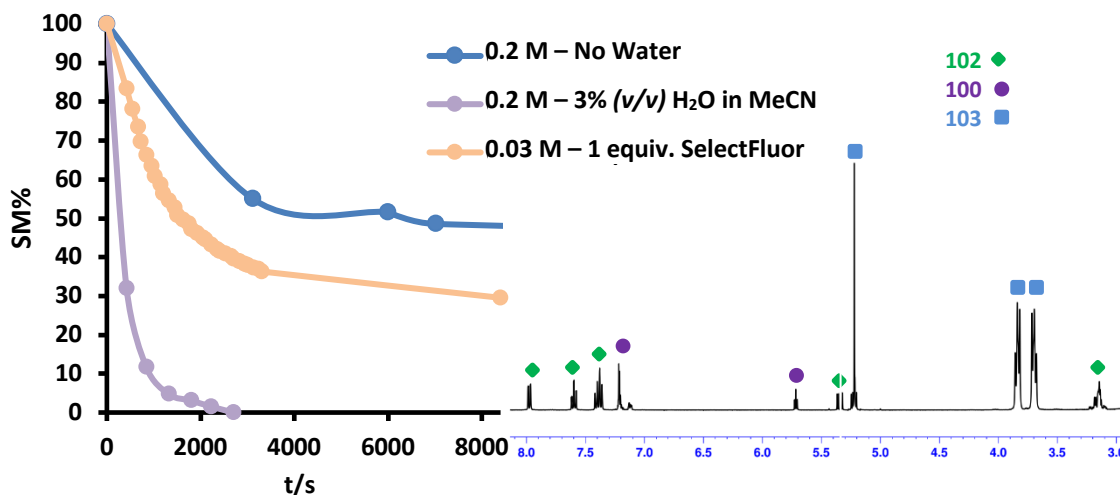
Figure 29: Initial kinetic experiments (left) ^{1}H NMR spectrum from 0.03 M kinetic run (right)

These initial experiments gave confidence in the ability to monitor this fluorination reaction by ^{1}H NMR, however the rate was too high to measure accurately. It was thought that reducing the concentration to 0.03 M and the number of equivalents of SelectFluor to 1 would allow the monitoring of the reaction. However, this experiment failed to reach full conversion. The reaction achieved 75% conversion after 4 hours and appeared to have stopped. This result called into question the purity of the commercial fluorinating reagent; however, when the amount of active fluorinating reagent was determined *via* iodometric titration the reagent was found to be 95% active. It was clear that there was another factor at play.

3.1.3.2.   UV/Vis Experiments

As predicted, changing the structure of the enol ester to the five-membered indanone derivative **101** resulted in an increase in rate. Complete conversion of this compound to its corresponding alpha-fluoroketone was observed by TLC at room temperature after 2 hours in 3% *(v/v)* water in acetonitrile using 1.1 equivalents of

SelectFluor at a concentration of 0.03 M. This makes this compound more amenable to monitoring *via* UV/vis spectroscopy. When the fluorination of tetralone compound **100** was studied by this technique the high dilution required to obtain measurable absorbances meant that the reaction was so slow that it appeared to be incomplete after several days. Both the indanone-derived enol ester **101** and the fluorinated product **101a** (*Figure 30*) have λ_{max} at around 250 nm (presumably from the aromatic ring) which shifts slightly from the starting material. The enol ester has a relatively high absorbance at around 220 nm, the disappearance of which could potentially be monitored by UV/vis (*Figure 30*). The isosbestic points visible in the overlaid spectra of the reaction are indicative of a clean starting material to product conversion for this reaction. The reaction was conducted at a concentration of 1.15×10^{-4} M at 60 °C with 1 equivalent of SelectFluor. However, similar to the NMR experiments, the reaction reached ~70% conversion and progressed no further.   This appeared to be a general problem associated with these fluorination conditions.
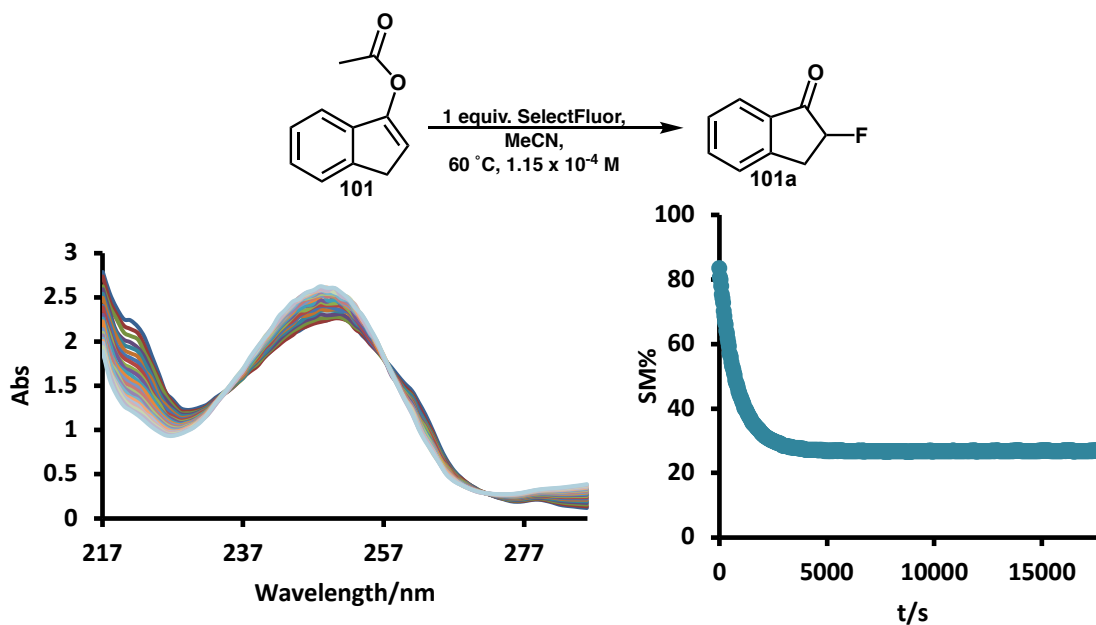
Figure 30: Fluorination of **101** followed by UV/vis

3.1.3.3.   Increasing the Water Content

Using 3% *(v/v)* water in acetonitrile had improved the ability to follow the reaction progression however full conversion of the enol ester substrate could not be obtained unless an excess of SelectFluor was used.   Attention was therefore turned to understanding this issue. The water content was increased to 50% *(v/v)* to ensure that SelectFluor was definitely in solution. NMR was once again selected as a monitoring technique as all of the components of the reaction could readily be observed.   A reference was added to the reaction mixture to calibrate the NMR integrals against. Cyclohexane was chosen as the singlet produced does not overlap with any other signals in the spectra. Unfortunately, cyclohexane is not miscible with this reaction mixture and when it was added a biphase was created. To circumvent this the standard was sealed inside a capillary that could be added to the NMR tube, allowing the reference signals to be observed without the standard interfering with the reaction media. The reaction was conducted at a concentration of 0.076 M. The consumption of both enol ester and SelectFluor were monitored using 1 equivalent of fluorinating reagent. Second order behaviour was observed for both the enol ester and SelectFluor (*Figure 31*).
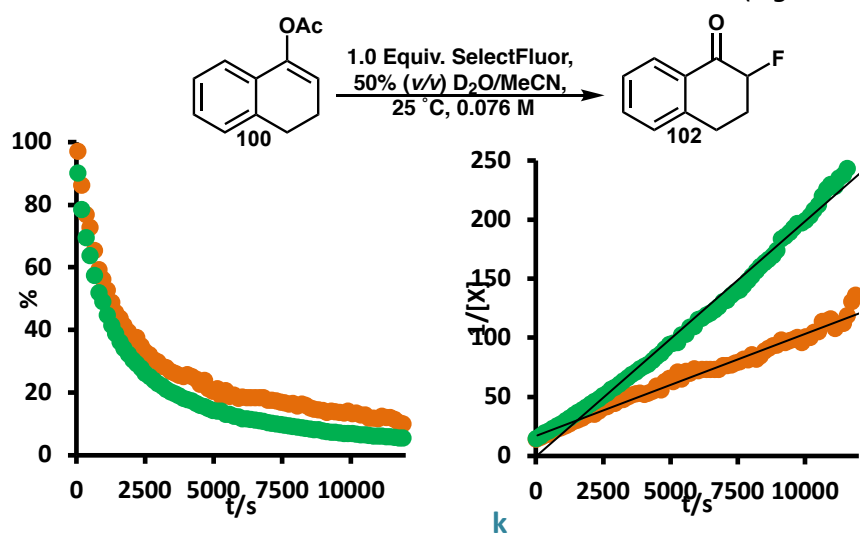
● *SelectFluor*	1.99×10^{-2} M^{-1} s^{-1}
● *Enol Ester* **100**	8.64×10^{-3} M^{-1} s^{-1}

*Figure 31: Fluorination of **100** in 50% (v/v) water, k is an average of two runs*

It was immediately obvious that the rate of SelectFluor consumption was faster than that of the enol ester. Higher overall conversion of enol ester at the end of the reaction was observed, now reaching ~90%. This suggests that the 3% *(v/v)* conditions did not contain enough water to fully solubilise the SelectFluor. The faster rate of reaction for SelectFluor was indicative that it is possible that a side reaction competes with fluorination.

With these promising results in hand, the number of equivalents of SelectFluor was increased to 1.5 in an attempt to obtain full conversion of the starting material. This was the case, and the rate of reaction of enol ester now surpassed that of SelectFluor. This was indicative that there was no substance preventing the enol ester from reacting with SelectFluor. The number of equivalents of SelectFluor was then varied to 0.5 and 2.0 equivalents (*Table 2*). When 0.5 equivalents of SelectFluor were used the order of the reaction in SelectFluor changed to first order and when 2.0 equivalents of SelectFluor were used the order in enol ester became first order. As the order in each of the reacting partners appeared highly sensitive to the concentration of the other the rate constants cannot be directly compared as the first order reaction rate constant has units of s^{-1} whereas the second order rate constant has units of L mol^{-1} s^{-1}. Therefore the half-lives of each component in these reactions were compared instead of comparisons between rates. There was a near linear correlation between the half-life of the enol ester and the SelectFluor concentration.

*Table 2: Effect of Changing Number of SelectFluor Equivalents in 50% (v/v) D$_2$O/MeCN at 25 ˚C (0.076 M initial concentration in enol ester **100**), k is an average of two runs*

No. Equiv. SelectFluor	k (Enol Ester 100)	k (SelectFluor)
0.5	2.17×10^{-3} M^{-1} s^{-1}	7.97×10^{-4} s^{-1}
1.5	2.56×10^{-2} M^{-1} s^{-1}	7.03×10^{-3} M^{-1} s^{-1}
2.0	1.36×10^{-3} s^{-1}	2.28×10^{-3} M^{-1} s^{-1}

The decrease in substrate half-life with increasing SelectFluor concentration would be expected if SelectFluor is involved in the rate determining step however it was important to establish whether factors aside from the fluorination reaction might be at play in the increased consumption of the starting material. Acid-catalysed hydrolysis of the substrate could be a possibility given that the dissolution of SelectFluor in aqueous media has a dramatic effect on the pH. In 50% *(v/v)* aqueous acetonitrile a 0.152 M solution of SelectFluor has a pH of 2.12. There is in fact a linear correlation between the half-life of the enol ester and pH (*Figure 32*). Whilst no hydrolysis of the enol ester to 1-tetralone had been observed during these fluorination reactions it was feared that the high water content in the reaction would allow pH to play a role in the fluorination reaction, complicating the data. The high water content reactions were also plagued by inconsistency issues which could be caused by the delicate balance of solubilising the highly charged fluorinating reagent as well as the hydrophobic enol ester compound. Conditions with as low a water content as possible were sought.
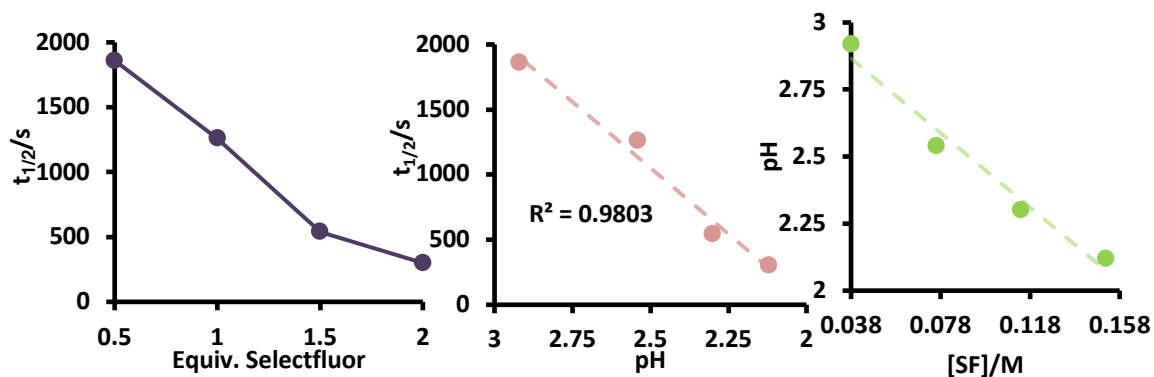
Figure 32: Relationship between pH, SelectFluor Concentration and Enol Ester **100** $t_{1/2}$ in 50% (v/v) D$_2$O/MeCN at 25 °C (0.076 M initial concentration in **100**)

3.1.3.4.   Decreasing the Water Content to 5% *(v/v)*

The water content could be decreased to 5% *(v/v)* in acetonitrile without any detrimental effects on the reaction. At a concentration of 0.076 M using 1 equivalent of SelectFluor, as previously observed, the fluorinating reagent was consumed faster than the enol ester. Complete consumption of SelectFluor was observed after 50 minutes

whilst the enol ester only achieved 75% conversion. The biggest difference between the 50% *(v/v)* water content reactions and the lower aqueous 5% *(v/v)* was the increase in reaction rate. Full SelectFluor consumption with 1 equivalent was observed in 50% *(v/v)* after 200 minutes (at a concentration of 0.076 M), taking four times as long to reach full consumption compared to the reaction in 5% *(v/v)* water in acetonitrile. The change from 50% *(v/v)* water to 5% *(v/v)* represents a change to a less polar reaction medium. The fact that this has the effect of increasing the reaction rate could be indicative of a rate determining step in which charge dispersion occurs, this is consistent with any of the possible mechanisms postulated (*vide supra*).
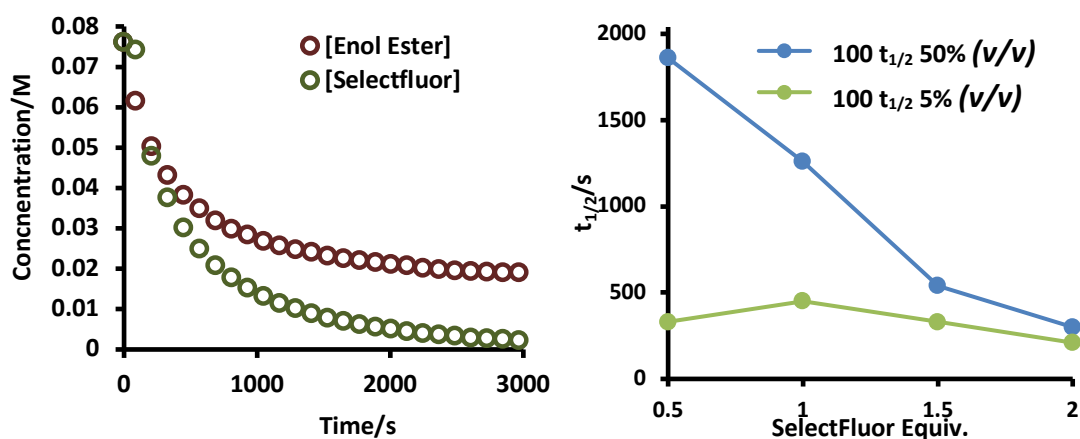
*Figure 33: Left: Comparison of Enol Ester and SelectFluor Consumption using 1 Equivalent of SelectFluor at 0.076 M Initial Concentration in 5% (v/v) D₂O/MeCN at 25 ˚C, Right: Comparison of Effect of Number of SelectFluor Equivalents in 50% D₂O/MeCN and 5% (v/v) D₂O/MeCN on Enol Ester **100** Half-Life at 25 ˚C, 0.076 M Initial Concentration in **100***

Lowering the concentration to 0.038 M in enol ester resulted in a decrease in reaction rate and no change in enol ester conversion. Reactions were again conducted using 0.5, 1.5 and 2.0 equivalents of SelectFluor at enol ester concentrations of 0.076 M and 0.038 M. Once again, the order of reaction in each of the reacting partners was highly dependent on the concentration of the other.   SelectFluor exhibited first order behaviour when reacted with an equimolar amount of enol ester. Given that the order of reaction appears to be highly sensitive to which reagent is present in excess this result supports the hypothesis that there is a background process competing for SelectFluor which results in the concentration available for the fluorination reaction being slightly

lower than that which is added to the reaction. Whilst the excess reagent profiles could broadly be ascribed second order behaviour, for both the enol ester and SelectFluor there is significant curvature in the data. This suggests that this simple treatment of the kinetic data does not tell the full story. In an effort to understand this behaviour the number of equivalents of SelectFluor were varied to 0.5, 1.5 and 2.0 equivalents at the two concentrations (*Figure 34*).

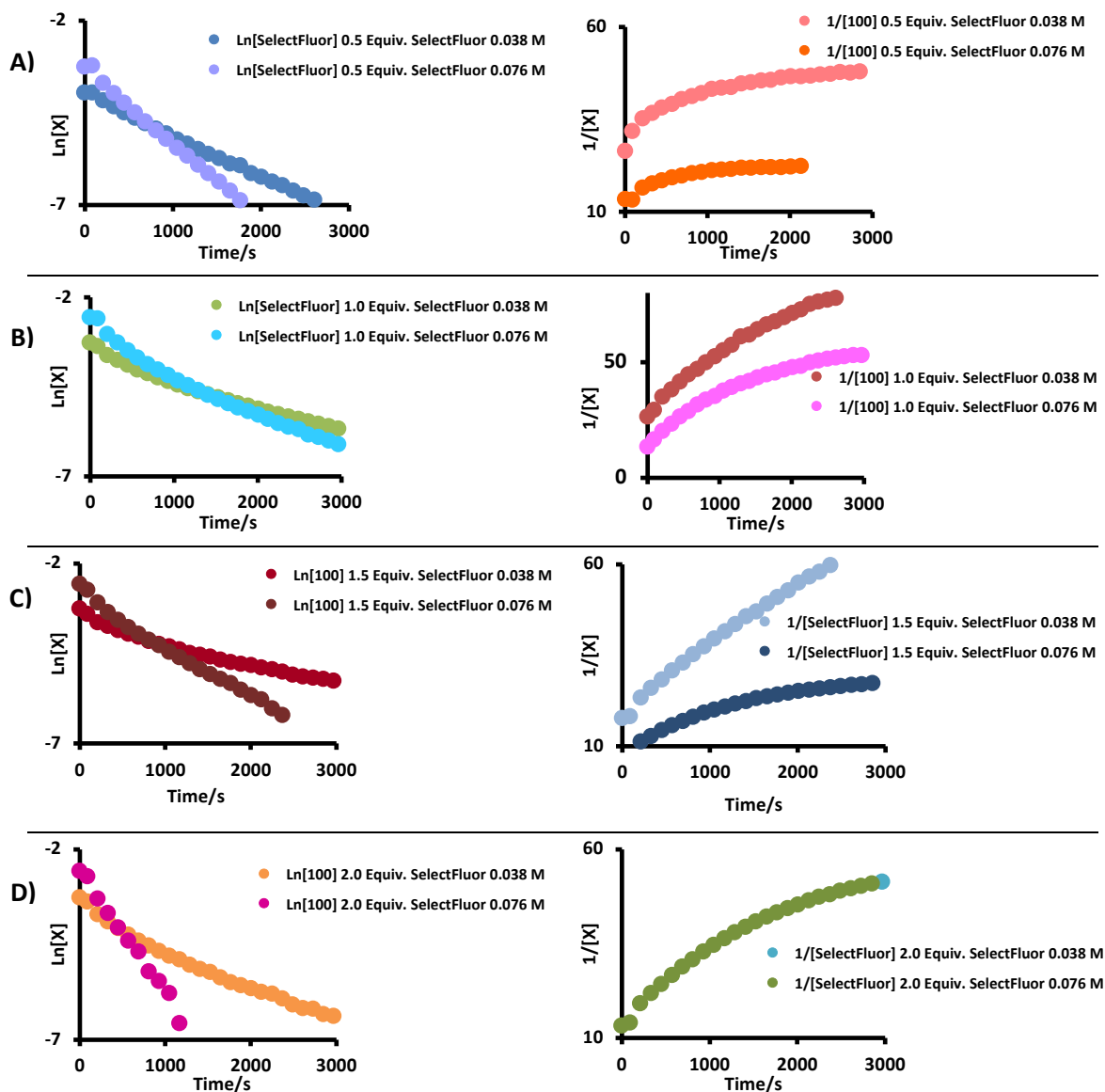*Figure 34: Rate Plots with Different Equivalents of SelectFluor at 25 ˚C in 5% (v/v) D₂O/MeCN (Concentrations Refer to Initial Concentrations of Enol Ester **100**)*

The apparent order of reaction in each substrate fluctuated depending on which species was in excess. At 0.5 equivalents the SelectFluor consumption could be fitted well to first order behaviour at both 0.076 M and 0.038 M. Again, the enol ester behaviour appeared to be more complex, fitting poorly to second order (*Figure 34*, A). When 1.5 equivalents of SelectFluor were utilised the enol ester consumption appeared to be characteristically first order and full consumption of the substrate was observed. The consumption of SelectFluor appeared to be more complex, and poorly fitted to second order kinetic behaviour in this instance (*Figure 34*, C). At 2.0 equivalents the behaviour was similar to that observed with 1.5 equivalents of SelectFluor (*Figure 34*, D).

The relationship between concentration and reaction rate at the different equivalents is not obvious (*Table 3*). With 0.5 equivalents of SelectFluor, the rate doubles when the concentration is doubled however the rate of enol ester consumption decreases by a factor of 1.5 (entries 1 and 5). For 1.0 equivalents (entries 2 and 6) the rate of SelectFluor reaction increases by a factor of 1.7 when the concentration is increased from 0.038 M to 0.076 M. The enol ester is consumed at approximately the same rate at both of the concentrations examined. Using 1.5 equivalents of SelectFluor (entries 3 and 7) results in a rate decrease with increasing concentration by a factor of 1.6 for SelectFluor and a rate increase of a factor of 3 for enol ester. With 2.0 equivalents of SelectFluor (entries 4 and 8) the rate remains constant when the concentration is doubled whilst the rate of enol ester consumption is 3 times higher at the higher concentration. Given the changes in reaction order, direct comparisons of the reaction rates of the two species are difficult therefore the comparison of half-lives is necessary. In this case, as the concentrations of each species are varied independently, the half-life is defined as the time taken for the concentration to decrease by half the concentration of the minor reaction component. For example, in entry 1, the initial concentration of SelectFluor is 0.019 M, therefore the half-life is the time at which the concentration has decreased by 0.0095 M.

*Table 3: Rate of Reaction of Enol Ester **100** and SelectFluor in 5% (v/v) D_2O in MeCN at 25 ˚C, k is an average of two runs*

	SelectFluor				**Enol Ester 100**			
Entry	**Conc/M**	**k**	**R^2**	**$t_{1/2}$***	**Conc/M**	**k**	**R^2**	**$t_{1/2}$***
1	0.019	1.11×10^{-3} s^{-1}	0.997	570	0.038	5.58×10^{-3} M^{-1} s^{-1}	0.807	210
2	0.038	6.77×10^{-4} s^{-1}	0.978	450	0.038	1.50×10^{-2} M^{-1} s^{-1}	0.951	930
3	0.057	1.02×10^{-2} M^{-1} s^{-1}	0.934	330	0.038	4.11×10^{-4} s^{-1}	0.962	570
4	0.076	1.25×10^{-2} M^{-1} s^{-1}	0.945	210	0.038	1.00×10^{-3} s^{-1}	0.978	330
5	0.038	2.06×10^{-3} s^{-1}	0.998	330	0.076	3.73×10^{-3} M^{-1} s^{-1}	0.773	330
6	0.076	1.14×10^{-3} s^{-1}	0.972	330	0.076	1.26×10^{-2} M^{-1} s^{-1}	0.928	450
7	0.114	6.44×10^{-3} M^{-1} s^{-1}	0.919	330	0.076	1.46×10^{-3} s^{-1}	0.992	330
8	0.152	8.85×10^{-3} M^{-1} s^{-1}	0.907	210	0.076	3.26×10^{-3} s^{-1}	0.992	210

For the experiments where the initial concentration of enol ester was 0.038 M (entries 1-4), the SelectFluor half-lives steadily decrease as the number of equivalents of SelectFluor (i.e. SelectFluor concentration) is increased. When the concentration of enol ester was 0.076 M (entries 5-8), the SelectFluor half-life remained constant at 330 seconds for all equivalents except 2.0 equivalents of SelectFluor where it decreased to 210 seconds. When the enol ester is in excess (entries 1 and 5) the half-life of the enol ester is shorter than that observed for SelectFluor however for all other instances the half-life of the enol ester is either longer or the same as the SelectFluor half-life. From these data it is evident that the relationship between reaction rate and concentration is complex in this instance.

When an excess of SelectFluor is used, pseudo-first order behaviour is observed in the enol ester and a first order rate constant can be measured. This is indicative that the reaction is first order in substrate. When the concentration of SelectFluor in the reaction is increased (maintaining a substrate concentration of 0.076), the rate of reaction increases. In fact, the relationship between SelectFluor concentration and the

rate of enol ester consumption is linear (*Figure 35*). This is indicative that the reaction is also first order in SelectFluor. This indicates that both reactants are involved in the rate determining step and that the reaction is second order overall, suggesting a bimolecular transition state.

$y = 0.0302x - 0.0012$
$R^2 = 0.9764$
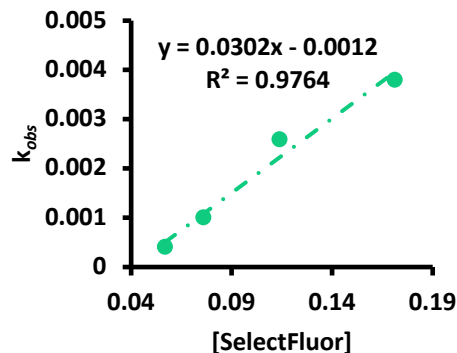
*Figure 35: Relationship Between SelectFluor Concentration and Reaction Rate of **100** in 5%(v/v) D$_2$O/MeCN at 25 ˚C Initial **100** Concentration of 0.076 M, k is an average of two runs*

Whilst the behaviour in these fluorination reactions was not fully understood, a method where good-quality, reproducible, and consistent data could be obtained had now been developed. Based on this dataset it was possible to select 0.038 M initial substrate concentration, 1.5 equivalents of SelectFluor in 5% *(v/v)* D$_2$O in MeCN at 25 ˚C as conditions to be used for further studies of these fluorination reactions.

*Figure 36: ^{1}H NMR of Reaction Mixture over time at 0.038 M initial **100** Concentration in 5% (v/v) D$_2$O/MeCN*

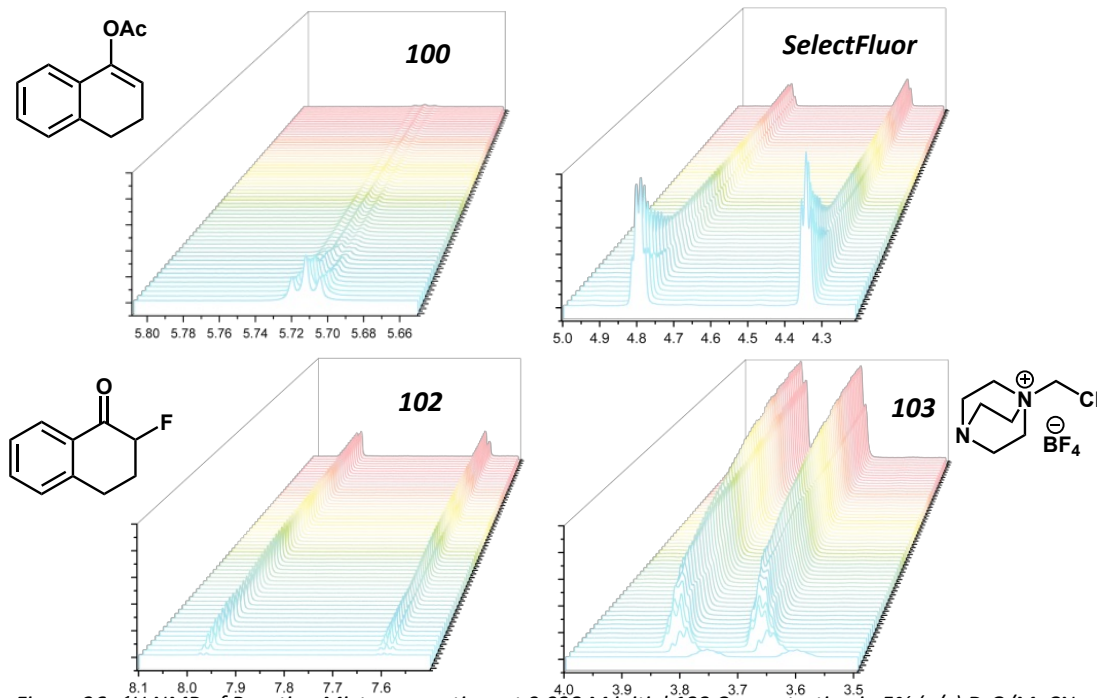Using 1.5 equivalents of SelectFluor produced easy to interpret first order kinetic behaviour in the enol ester substrate whilst the reaction time at 0.038 M was a manageable length such that moderate increases or decreases in rate at this concentration would still be practical to measure using NMR spectroscopic experiments.

3.1.3.5.   Determining the Free Energy Barrier to Reaction

Now that a robust methodology for the study of the kinetics of this fluorination reaction had been developed further information about the nature of this fluorination reaction could be obtained. Measurement of the energy barriers to the fluorination reaction of simple tetralone substrate **100** is of use in understanding the details of this reaction. It is possible to obtain this information by carrying out the reaction at different temperatures. The relationship between rate and temperature can then be converted into numerical values for the enthalpy and entropy of the rate determining step using the Eyring equation (e*quation 1*, below). These values can then be used to calculate the Gibbs Free Energy of the rate determining step.

Equation 1: The Eyring Equation

$$k = \frac{k_B T}{h} \, e^{\frac{\Delta H}{RT}} \, e^{\frac{\Delta S}{R}}$$

To this end, the reaction was carried out at 5 °C, 15 °C, 25 °C, 35 °C and 45 °C, followed by ^{1}H NMR in each case, and the reaction rates were determined. The natural log of the rate divided by the temperature is plotted against 1/T. This yields a linear plot in which the slope is $\Delta H^{\ddagger}$ divided by the physical constant R and the y-intercept is $\Delta S^{\ddagger}$ divided by R plus the natural log of Boltzmann's constant divided by Planck's constant. This treatment of the data delivered an entropy of activation of -24 cal mol^{-1} K^{-1}, and an enthalpy of activation of 14.2 kcal mol^{-1}. Applying the equation for calculating Gibbs Free Energy (*Equation 2*), at 25 °C the energy barrier to this fluorination reaction is 22.0 kcal mol^{-1} (*Figure 37*). The entropic penalty to the reaction is consistent with a bimolecular reaction in which the two molecules come together in the transition state.[181]

$$\Delta G = \Delta H - T\Delta S$$

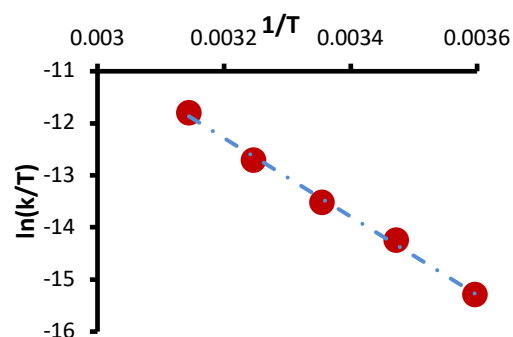| Equation: y = -7533.5x + 11.824		
ΔG/kcal mol^{-1}	ΔH/kcal mol^{-1}	ΔS/cal mol^{-1} K^{-1}
22.0	14.2	-24

Figure 37: Eyring Analysis and Gibbs Free Energy

This is consistent with the earlier kinetic data which predicts that these two molecules are SelectFluor and the substrate, based on the observed reaction orders. The Eyring data from the reaction indicates that the reaction is endothermic to the rate determining step however a large exotherm is observed with large scale reactions giving out a lot of heat. This indicates that there is a large energy difference between the transition state of the rate determining step and the intermediates formed from this state, indicating a low chance of reversibility of the reaction.

3.1.3.6.   Natural Abundance Kinetic Isotope Effect

Reaction pathways can be affected by an atom being substituted for one of its isotopes, and this phenomenon is known as a kinetic isotope effect. Substitution of, for example, a highly abundant carbon-12 atom with carbon-13 will have no effect on a molecule. Now that this position contains a slightly heavier atom it will take more energy to involve it in vibrational processes such as bond breaking or bond forming processes in a transition state. If a compound is enriched with an isotope at a position directly involved in a rate determining pathway less of the isotope will appear in the product of the reaction as slightly more energy is required to get it to react and so this reaction is slightly disfavoured relative to the unlabelled position.

Substitution of a highly abundant carbon-12 with NMR-active carbon-13 is highly desirable as the content of this isotope in the product or in recovered starting material
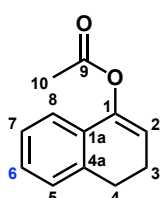
of the reaction can be directly measured. Unfortunately given the low natural abundance of carbon-13, incorporation of this isotope into a molecule can be difficult and expensive. In the mid 1990's Singleton and Thomas devised a practical solution to this problem.[182] Whilst the abundance of carbon-13 is only 1.1% it is sufficiently abundant that it can be detected by NMR spectroscopy. They postulated that it would be possible to measure the amount of carbon-13 conserved in a given position by allowing a reaction to proceed to not quite complete conversion and recovering the remaining starting material and measuring the relative carbon-13 remaining in each position with respect to an internal standard – this being a carbon in the molecule that does not participate in the reaction. Using this technique, the kinetic isotope effect can be calculated from the conversion, and the integral of a given position in the carbon-13 spectrum of the recovered starting material relative to the integral in the starting material before it was subjected to the reaction conditions using *Equation 3*. F is the fractional conversion, R is the integral in the recovered starting material and R_0 is the integral before the compound has been subjected to the reaction conditions. In order to obtain this information it is necessary to run an inverse gated ^{1}H-decoupling carbon-^{13}C NMR programme with a high number of scans so that the signal to noise ratio is large and the spectrum can be integrated accurately. Each carbon-13 atom must fully relax between pulses to obtain accurate integrals and therefore the paramagnetic relaxation agent [Cr(acac)$_3$] is added.

Equation 3: Calculating KIE

$$KIE = \frac{\ln{(1 - F)}}{\ln{[(1 - F)\frac{R}{R_0}]}}$$

To this end, the carbon-13 spectrum of **100** was acquired in a 0.1 M solution of [Cr(acac)$_3$] in chloroform as the relaxation agent, and the methyl group of the acetate was used as a reference. Compound **100** was then subjected to the reaction conditions using 0.8 equivalents of SelectFluor to ensure that the reaction did not go to completion. The reaction was determined to have reached 78% conversion (F = 0.78) and the remaining starting material was isolated *via* column chromatography. Upon analysis of

the $^{13}C\{^1H\}$ NMR spectrum, once again with [Cr(acac)$_3$] as relaxation agent, it somewhat surprisingly transpired that the carbon with the largest kinetic isotope effect was aromatic carbon 6 (*Figure 38*). This result is indicative that the aryl ring of the tetralone plays a role in the rate determining step, potentially stabilising a (partial) positive charge in position 1.


Carbon	KIE	Carbon	KIE
1	0.997	5	0.993
1a	0.994	**6**	**1.031**
2	0.998	7	0.993
3	0.995	8	0.995
4	0.993	9	0.992
4a	0.992	**10**	**1.000†**

Figure 38: Natural Abundance KIE †Used as Internal Standard Reference Integral

3.1.3.7.   Cyclohexanone Analogues

In order to test the hypothesis that the aromatic ring of tetralone makes a favourable contribution to the rate of reaction, two cyclohexanone-based enol acetates were synthesised. The direct comparator for tetralone **104** was synthesised using isopropenyl acetate under acidic conditions. After aqueous work up the desired compound could then be isolated *via* vacuum distillation in 53% yield (*Scheme 54*). The comparatively lower yield with respect to the tetralone and indanone derivatives was attributed to the volatility of the compound, and it is likely that some was lost during *in vacuo* concentration of the organic phase after work up. The 4-*tert*-butyl analogue **105** could be synthesised in an identical manner, this time in good 74% yield.

*Scheme 54: Synthesis of **104** and **105***
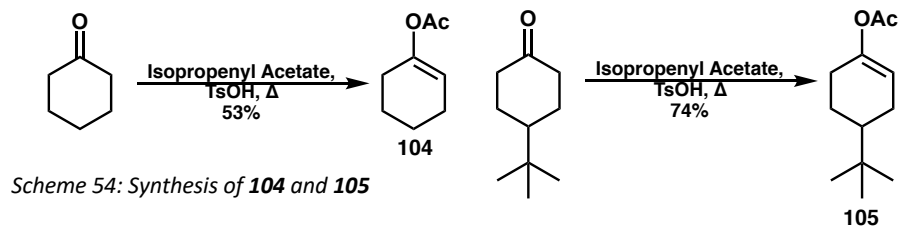
When these compounds were subjected to the standard fluorination conditions the rate of reaction could be measured (*Figure 39*). As expected, a decrease in reaction rate relative to the tetralone compound was observed for both compounds. The 4-*tert*-butyl compound reacted at a slightly faster rate than the unsubstituted cyclohexanone derivative. These results were consistent with previous observations that the aryl ring of the tetralone provides some degree of stabilisation to the transition state, implicating charged intermediates in the reaction.

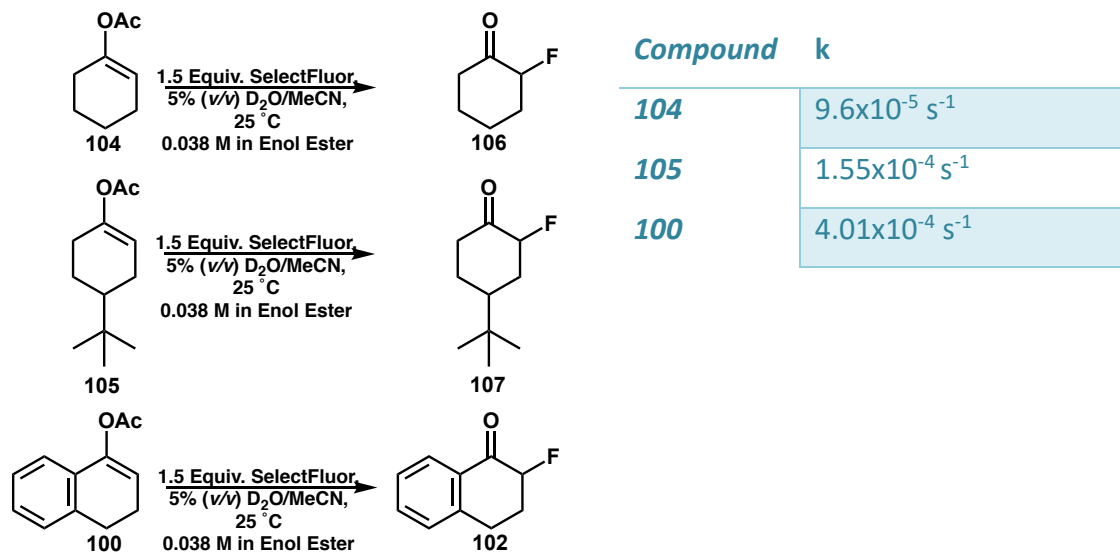| *Compound*	k
104	9.6×10^{-5} s^{-1}
105	1.55×10^{-4} s^{-1}
100	4.01×10^{-4} s^{-1}

Figure 39: Comparison of rates of Fluorination

The fluorination of compound **105** generates a 2:1 mixture of diastereoisomers, with the major product being the axial fluoride. The equatorial geometry can be readily assigned to compounds **102** and **106** based on the NMR spectra (*Figure 40*). For compound **102** the geminal proton to the fluorine appears as a doublet of doublet of doublets with coupling of 47.9 Hz (geminal HF coupling), 12.7 Hz (coupling to the axial proton in position 3) and 5.1 Hz (coupling to the equatorial proton in position 3) whilst the fluorine signal in the ^{19}F NMR appears as a doublet of triplets, with large 47.9 Hz geminal coupling and equivalent coupling to the two protons on carbon 3. Were the fluorine in the axial position a greater overlap between the C-H σ orbitals and the C-F σ*

orbital would be expected, leading to more complex splitting and differentiation between the axial and equatorial protons. Indeed, the axial fluoride product (**107-ax**) of the fluorination of **105** exhibits a distinctive coupling pattern in the fluorine and proton NMR spectra whilst the signals recorded for the equatorial product (**107-eq**) are more analogous to those produced in the spectrum of tetralone compound **102**. In equatorial compound **107-eq** the geminal proton at position 2 appears as a doublet of doublet of doublet of doublets. It has large HF coupling of 48.6 Hz, coupling to the axial proton on carbon 3 of magnitude 12.0 Hz, coupling to the equatorial proton on carbon 3 of 6.7 Hz and coupling to the proton on carbon 4 of 1.1 Hz. The fluorine NMR signal is poorly resolved, with only the geminal 48.6 Hz coupling evident. In axial fluoride **107-ax** the coupling pattern for the geminal proton is less pronounced. It retains the large geminal HF coupling (50.3 Hz), as well as coupling to both protons on carbon 3 as well as the one on carbon 4. The fluorine NMR spectrum is more elaborate. The signal appears as a doublet of doublet of doublet of doublets. The large coupling being HF coupling, it then couples to the axial proton on carbon 3 with a magnitude of 43.8 Hz, to the equatorial proton on carbon 3 with a magnitude of 13.0 Hz and to the proton on carbon 4 with a magnitude of 5.9 Hz.
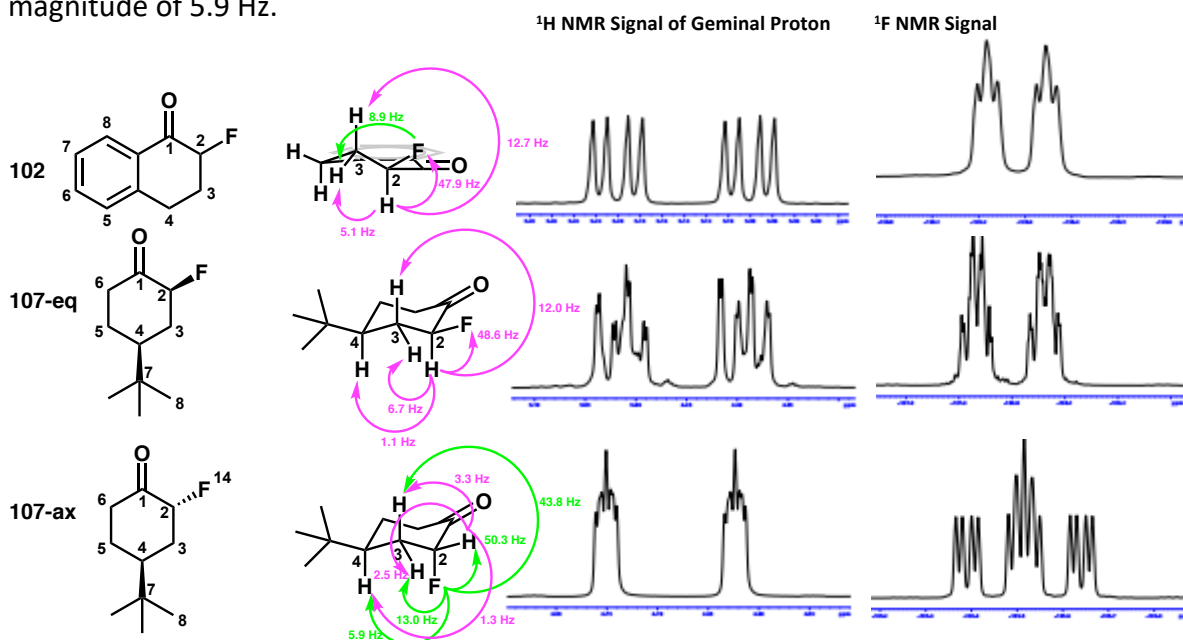

Figure 40: NMR Spectra of **102**, **107-eq** and **107-ax**

3.1.4. Fluorination of Enol Benzoates of Tetralone

The initial studies of enol acetates had provided some insight; attention was now turned to modulation of the electronic properties of enol esters of tetralone. The variation of the ester component was proposed as a straightforward means of doing this.

3.1.4.1. Synthesis of Enol Benzoates

The synthesis of a suite of compounds of the type **108-X** (shown in *Figure 41*) was sought. It was envisioned that variation of the substituent in the *para*-position would allow the electronic properties of the molecule to be tuned and the effect of these properties measured through their rate of reaction with SelectFluor. Despite their apparent structural simplicity, only the parent 1-tetralone enol benzoate is known in the literature. The first reported synthesis is from a publication by Goldblum and Mechoulam in 1977.[183]
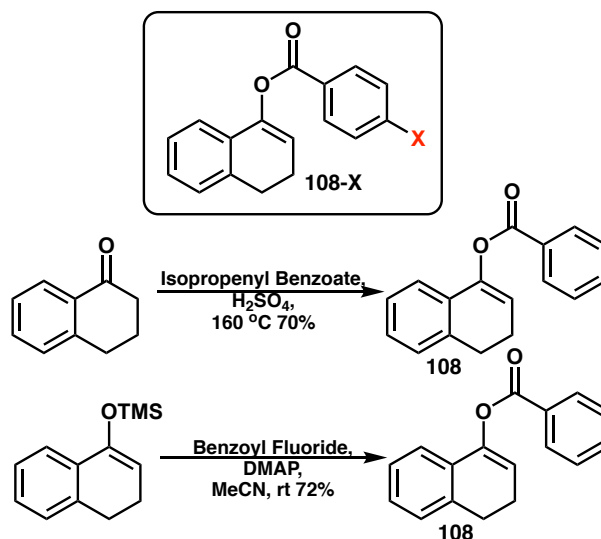


Figure 41: Reported syntheses of Compound *108*

Goldblum and Mechoulam were able to isolate compound **108** in 70% yield as an oil after heating a mixture of 1-tetralone and a few drops of concentrated sulfuric acid in isopropenyl benzoate at 160 °C for 20 hours.[183] The only other published preparation of compound **108** was the conversion of the silyl enol ether to enol benzoate using benzoyl

fluoride as reported by Levacher *et al.* where the compound was isolated in 72% yield, although unfortunately no characterisation data were reported.[184]

Neither isopropenyl benzoate or benzoyl fluoride are commercially available therefore the development of an alternative synthesis was sought. Initially, the analogous synthesis to the LDA conditions used to generate enol acetate **100** were trialled. The ketone was deprotonated with LDA at -78 °C and a solution of benzoic anhydride in THF was added. The ^{1}H NMR of the crude product indicated the presence of the desired product, however upon work-up a red gum was produced from which no product could be isolated. Conditions using commercially available benzoyl chloride were attempted both with formal deprotonation of the ketone and under Lewis and Brønsted acid catalysis. These proved unsuccessful in producing the desired compound. Somewhat inspired by the work of Levacher *et al.* converting an enol ether to an enol benzoate, conversion of the enol acetate **100** using benzoyl chloride and catalytic *para*-toluenesulfonic acid was attempted. This procedure allowed the production of compound **108** in modest 11% yield (*Scheme 55*). Whilst the yield for this reaction was low, the product was isolated as a white solid with minimal purification. Further development of this route allowed enol benzoates to be synthesised in one pot from the ketone. 1-Tetralone was suspended in isopropenyl acetate with *para*-toluenesulfonic acid and the required benzoyl chloride analogue with distillation apparatus fitted. The mixture was then heated to 100 °C for 1-2 hours in order to form the enol acetate. The temperature was then increased to 170 °C which allowed conversion to the benzoate. Whilst the yields obtained *via* this technique were poor, the direct isolation of enol benzoates in high purity for kinetic experiments was the primary concern and this methodology was sufficient to serve this purpose.

Scheme 55: Synthesis of Enol Benzoates of Tetralone
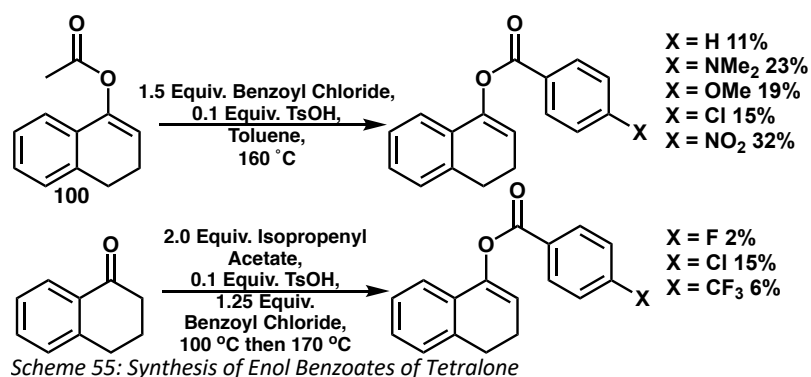
It was unclear how this benzoylation mechanism operates. The reaction does not work directly on the ketone and that the acetate must be formed first. A mechanistic rationale is postulated in *Scheme 56*. In this proposed mechanism, the oxygen attacks the benzoyl chloride to form positively charged intermediate **108a** from which **108b** is formed upon loss of HCl. The chloride counterion then acts as a nucleophile to attack at the acetate, generating acetyl chloride and the enol benzoate **108-X**. The reasoning as to why the benzoate is that acetyl chloride is the more volatile of the two acyl chlorides, and the reaction is an equilibrium, the removal of the acetyl chloride drives the reaction towards the benzoylated product. To provide evidence for this hypothesis a sample of the benzoate compound **108** was dissolved in deuterated chloroform and acetyl chloride was added. The mixture was then heated to 60 °C. After 8 hours 5% of the enol acetate was detected by ^{1}H NMR spectroscopy, showing that this reaction is reversible.

Scheme 56: Proposed Mechanism for the Formation of Enol Benzoates
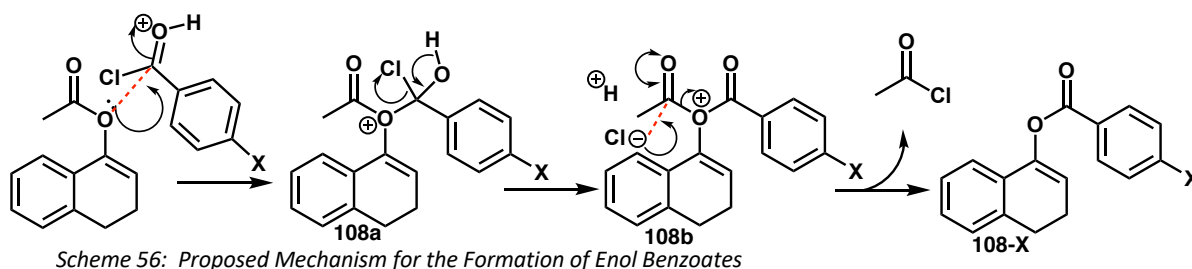
A number of substrates with a broad range of electronic properties were synthesised using this method (*Figure 42*). Substrates that could donate electron density into the aryl ring through resonance such as dimethylamino compound **109** and methoxy compound **110** and to a lesser extent fluoro compound **111** were of interest, as well as

compounds containing inductively withdrawing substituents, such as nitro compound **115**, CF₃ compound **114** and ester compound **113**.
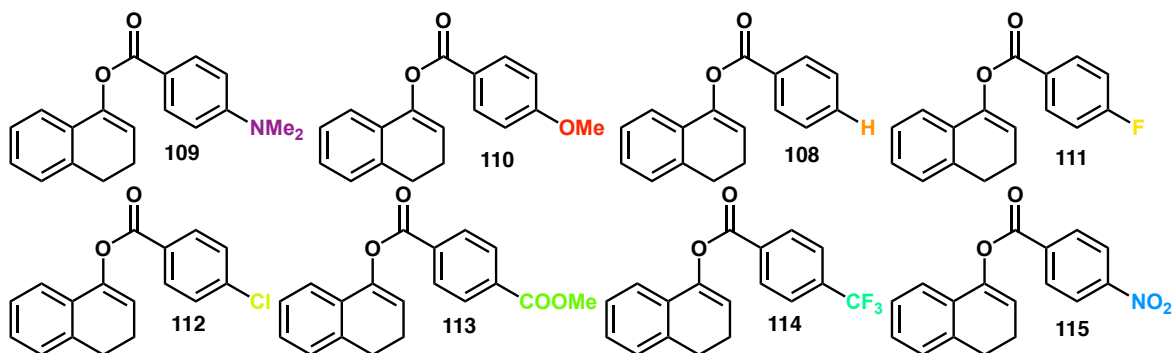


Figure 42: Substituted Benzoates

3.1.4.2. Hammett Study

These enol benzoate substrates were subjected to the fluorination reaction conditions and the rate of fluorination was determined for each (*Scheme 57*). Hammett noticed that the same trend was observed for benzoic acid pK_a and the rate of methyl benzoate hydrolysis depending on the *meta* or *para* substituent, it was therefore surmised that the substituent effects on both situations must be related. Using this information the Hammett σ constants were defined. A plot of the log of the equilibrium constant for a given X-substituted benzoic acid divided by the equilibrium constant for benzoic acid yields a straight line with gradient (ρ) equal to 1.

Scheme 57: Fluorination of Enol Benzoates
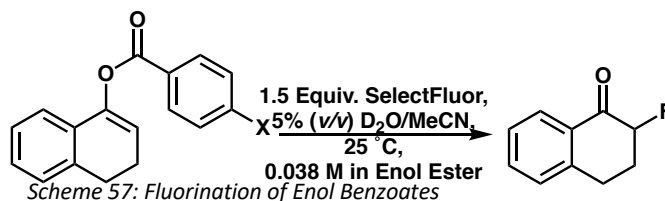
The X-axis then informs on the σ value for each of the substituents. Plotting rate data obtained from reactions of compounds bearing a substituent for which the value of σ is known can yield valuable information about the reaction mechanism. Variations on σ exist and can be used to determine mechanistic information. For instance, the σ^- constants were determined based on the ionisation of substituted phenols, whilst the σ^+ constants were determined from the reactivity of a number of cumaryl chlorides in an

S_N1 reaction. Therefore if the trend in reaction rates correlates to σ it is likely that the reactivity is similar to that observed in the ionisation of benzoic acids, if it correlates to σ^- it is likely that a negative charge is developed during the rate determining step, and if it correlates to σ^+ it implicates a mechanism in which a positive charge is generated. If the rate data is plotted against these constants and no correlation to any of the three constants is observed, then it is likely that the mechanism in operation is unrelated to the reactions that the constants are derived from. The σ, σ_p^+ and σ_p^- constants are all defined based on polar reactivity, therefore a lack of correlation could be indicative of radical reactivity. Both methoxy and nitro groups are known to stabilise radicals however these substituents have very different σ, σ_p^+ and σ_p^- parameters.[185] With this in mind, the rate of reaction of each compound within the 1-tetralone enol benzoate series with SelectFluor was determined and the data were plotted against the Hammett σ_p values (*Figure 43*).

$$y = -0.5283x + 0.0686$$
$$R^2 = 0.9593$$
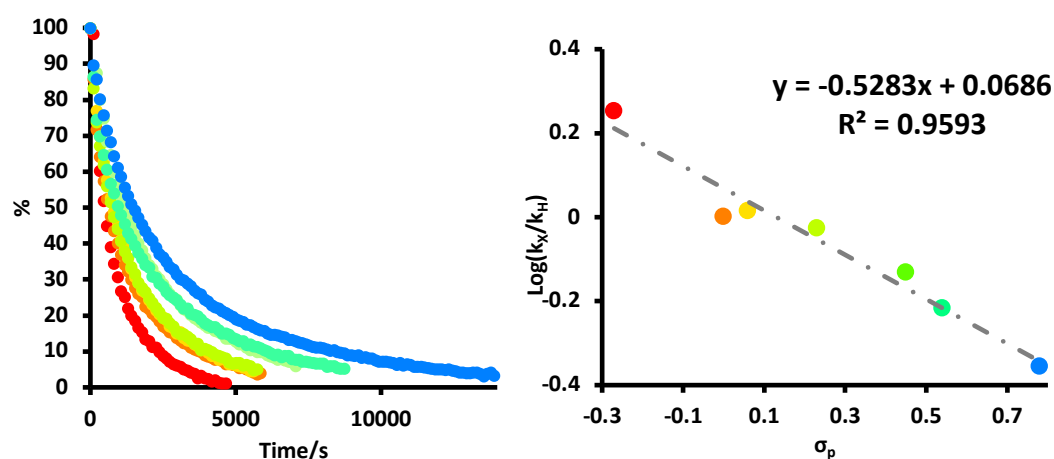
X		σ_p	σ_p^+	k (enol ester)
●	OMe	-0.27	-0.78	8.89×10^{-4} s^{-1}
●	H	0.00	0.00	4.97×10^{-4} s^{-1}
●	F	0.06	-0.07	5.13×10^{-4} s^{-1}
●	Cl	0.23	0.11	4.68×10^{-4} s^{-1}
●	COOMe	0.45	0.49	3.78×10^{-4} s^{-1}
●	CF$_3$	0.54	0.61	3.01×10^{-4} s^{-1}
●	NO$_2$	0.78	0.78	2.19×10^{-4} s^{-1}

Figure 43: Hammett Study of Enol Benzoates, 1.5 Equiv. SelectFluor, 5% (v/v) D$_2$O/MeCN, 25 ˚C, 0.038 M initial Enol Ester Concentration, k is an average of two runs

When the data is analysed, it is apparent that there is an imperfect linear correlation between the Hammett σ_p values and the rate data. The value of ρ is less than one, indicating that the substituents in this reaction are having less of a pronounced effect on the reaction than in the dissociation of benzoic acids. The sign of ρ is negative, indicating that electron donating substituents increase the rate of the reaction whilst electron withdrawing substituents slow the reaction. This result is potentially indicative of the development of a (partial) positive charge. Further evidence for the development of positively charged species was the better correlation observed when the rate data were plotted against the σ_p^+ constants (*Figure 44*). Again, a negative value of ρ was obtained. The slope was not very steep, and generally for reactions in which a positive charge is formed ρ can be very large and negative.[186–188] It was clear from these data that whilst the substituent was definitely having an effect on the progress of the reaction, it was not a large influence. Another intriguing aspect of these data is the apparent break in the Hammett plot against σ_p^+ (*Figure 44*). Breaks such as this, where there appear to be two correlations and the value of ρ changes for some of the substituents but the sign of ρ remains the same can be indicative of a change in the rate determining step of a reaction but not an overall change in the reaction mechanism.
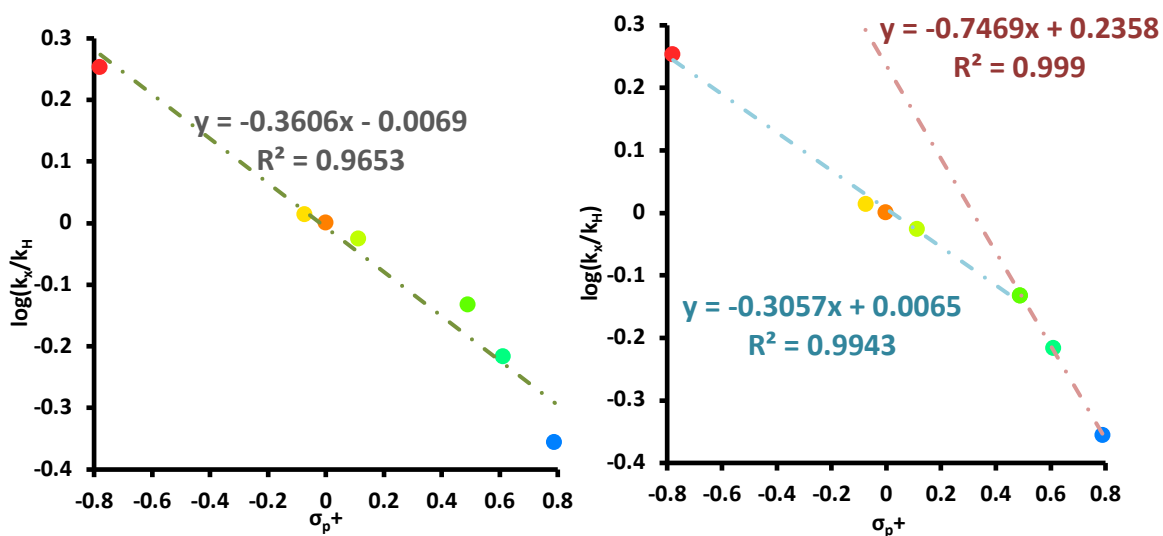

Figure 44: σ_p^+ plots

The change in rate determining step could be in the formation of some kind of pre-reaction complex or in a change in the hydrolysis behaviour. In order to determine whether either of these are likely or whether the break is an artefact of plotting experimental data it was decided that gaining insight into the activation barriers to the reactions of some of these compounds would be of use. Eyring analyses were once again performed on methoxy compound **110**, parent benzoate **108** and nitro compound **115** to find out if there was any change in behaviour. Once again the reactions were carried out at 5, 15, 25, 35 and 45 °C and the Eyring equation applied to find the $\Delta H^{\ddagger}$, $\Delta S^{\ddagger}$ and $\Delta G^{\ddagger}$ values for each of these substrates (*Figure 45*).
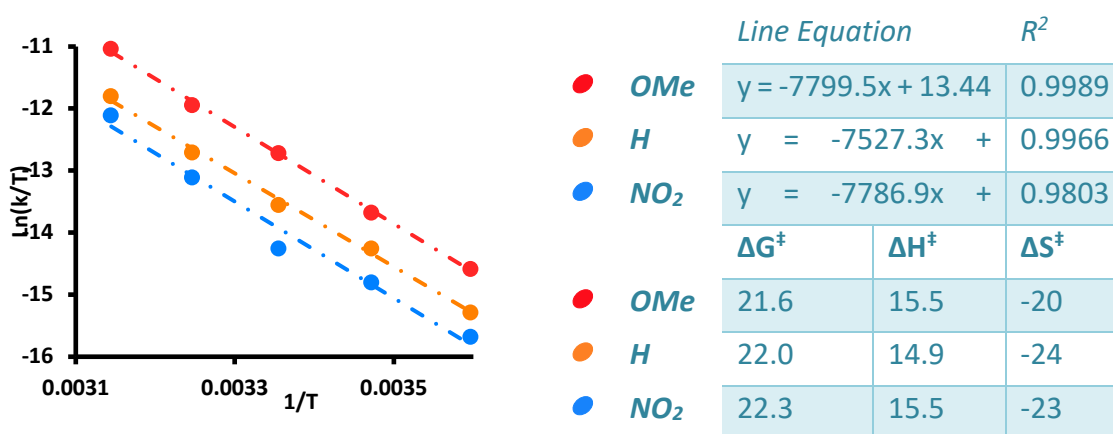

	Line Equation	R^2
OMe	y = -7799.5x + 13.44	0.9989
H	y = -7527.3x +	0.9966
NO₂	y = -7786.9x +	0.9803

	$\Delta G^{\ddagger}$	$\Delta H^{\ddagger}$	$\Delta S^{\ddagger}$
OMe	21.6	15.5	-20
H	22.0	14.9	-24
NO₂	22.3	15.5	-23

*Figure 45: Eyring Analysis of Compounds **108**, **110** and **115** (G and H in kcal mol^{-1}, S in cal mol^{-1} K^{-1})*

This analysis produced similar values to those observed with the enol acetate (page 82), with $\Delta G^{\ddagger}$ increasing from the lowest energy methoxy to the higher energy, slow to react nitro compound. The values of $\Delta S^{\ddagger}$ were within experimental error of each other suggesting a similar entropic environment for the transition states of the reactions of all the benzoates analysed as well as the enol acetate. These results are consistent with a similar rate determining step for all three of the enol benzoates, indicating that the break in the Hammett plot is an artefact of the experimental data rather than evidence of a change in the rate determining step of the fluorination reaction.

3.1.4.3. Effect of Substituting Methanol for Water

In order to gain further information about the reaction, the 5% *(v/v)* water/acetonitrile mixture was exchanged for a 5% *(v/v)* methanol/acetonitrile solvent system. Given that methanol is more nucleophilic than water,[189] a rate increase should be observed were hydrolysis of the enol ester the rate determining step.

The conditions used were identical to those used for the aqueous fluorination other than the change in solvent system. The fluorination proceeded smoothly, producing fluoroketone product **102**, consumed SelectFluor **103** and methyl benzoate as the only products. The rate of reaction was slightly higher (*Scheme 58*), however not appreciably, indicating that hydrolysis of the enol ester is not the rate determining step and that water is not involved in the rate determining step. The rate increase was in keeping with the increase observed in rate when the water content was decreased and follows the same trend. Decreasing the solvent polarity has a positive effect on the reaction rate.

5% (v/v) XOH in MeCN	k (enol ester)
XOH = H_2O	4.97×10^{-4} s^{-1}
XOH = MeOH	6.21×10^{-4} s^{-1}
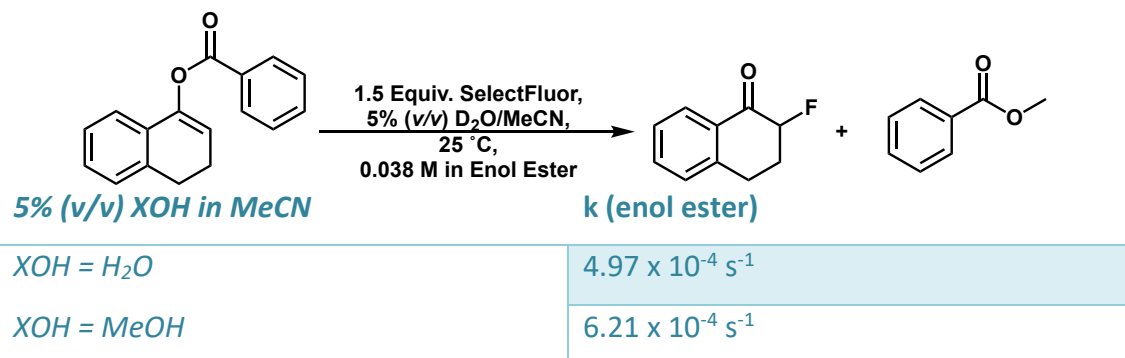
Scheme 58: Use of Methanol instead of Water, k is an average of two runs

3.1.4.4. Reaction of Compound 109 with SelectFluor

The only compound in the enol benzoate series that was synthesised that reacted with SelectFluor and did not produce the alpha-fluoroketone as the product was the 4-NMe$_2$ substituted compound **109**. When SelectFluor was added to the solution of compound **109** in 5% *(v/v)* water/acetonitrile a deep purple colour developed. During

all of the other fluorinations discussed the reactions remained colourless throughout therefore this was immediately identified as divergent behaviour. When the mixture was analysed by ^{1}H NMR spectroscopy, neither the SelectFluor signals or the signals for the dimethylamino substituted ring were observed. It was postulated that this behaviour was likely to be the formation of a charge transfer complex (*Scheme 59*).
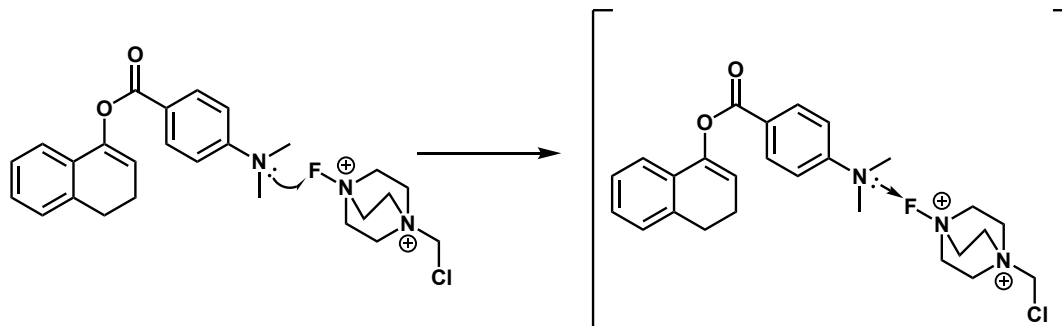

*Scheme 59: Formation of Charge Transfer Complex of SelectFluor and **109***

In order to determine whether it was likely that the alkene of the enol ester was forming the charge transfer complex or the dimethylamino containing aryl ring was the electron donor SelectFluor was mixed with *N,N*-dimethylaminobenzene. When SelectFluor was added to a solution of the amine in 5% *(v/v)* aqueous acetonitrile again a deep colour developed. On this occasion the colour was green. This result indicated that the charge transfer complex was formed as a result of the presence of a dimethylamino-aryl moiety in the molecule, rather than charge transfer from the enol ester alkene. This behaviour is analogous to the reactivity observed by Differding[169] and Kochi[108] described above for neutral *N*-F and *N*-Fluoropyridinium reagents respectively.

3.1.5. Alpha-Substituted Enol Esters

Attention was then turned to the design and synthesis of alpha-substituted tetralone derivatives. The substituents on the enol benzoates had some effect on the rate of reaction however given their distal position from the reacting centre it was unclear as to whether the effect observed was the result of the formation of an intermediate carbenium or a radical cation-type species.

3.1.5.1.   Synthesis of Alpha-Substituted Compounds

Compounds which were substituted with aromatic rings in the alpha-position were sought so that the Hammett treatment could be applied to the kinetic data. The simplest means of installing this type of functionality is *via* cross coupling chemistry. It was proposed that if a bromine could be installed in the alpha-position to the ketone, followed by formation of the enol ester, a vinyl bromide suitable for Suzuki-Miyaura cross coupling could be generated. The bromine was installed through reaction of tetralone with *N*-bromosuccinimide under acidic conditions. The synthesis of the enol acetate was then attempted *via* the previously successful isopropenyl acetate conditions. On this occasion, the reaction was not successful and none of the desired product **116** was formed. Formal deprotonation conditions were then investigated. It was found that the enol acetate could readily be formed *via* deprotonation of the crude alpha-bromoketone at -78 ˚C with either LDA or NaHMDS in THF followed by treatment of the mixture with acetic anhydride (*Scheme 60*). The addition of the electrophile resulted in the formation of a thick slurry which mobilised on warming of the reaction mixture to room temperature. This procedure allowed the desired product (**116**) to be formed in 52-70% yield. The alpha-bromoketone was not purified and was used directly after synthesis to avoid prolonged exposure to the compound due to its lachrymatory properties.

Scheme 60: Synthesis of Compound **116**
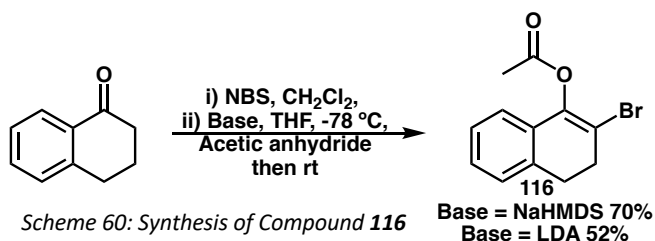
Although predominantly an intermediate on the way to alpha-aryl substituted compounds, the alpha-bromo compound could also be employed in a fluorination reaction (*Scheme 61*). The rate of reaction with this compound, which contains an electron withdrawing substituent in the alpha-position, could also provide information about the nature of the transition state. Consistent with the results obtained from the

benzoate series the introduction of electron-withdrawing bromine in the alpha position resulted in a decrease in the reaction rate. The reaction took 90 hours to reach completion, too slow to be conveniently monitored by ^{1}H NMR spectroscopy. The reaction produced compound **117** in 65% yield.
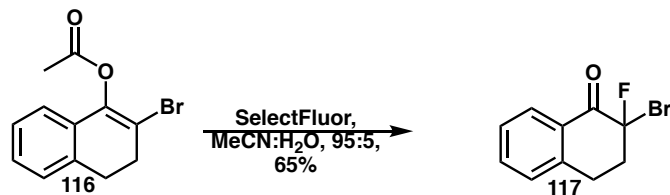
*Scheme 61: Synthesis of Compound **117***

A crystal structure was obtained for this compound, in which the bromine occupies the axial position (*Figure 46*). This behaviour is known for alpha-bromoketones and occurs as a result of the large electron cloud of bromine forming a repulsive interaction with the carbonyl.[190] The ^{1}H and ^{19}F NMR spectra suggest that this behaviour also occurs in the solution phase as well as in the solid phase. The ^{19}F NMR signal appears as a doublet of doublet of triplets with relatively small coupling to the protons on the adjacent carbon 3 of 7.0 Hz and 3.7 Hz for the axial and equatorial protons respectively, and couples to both protons on carbon 4 with a magnitude of 1.3 Hz. This coupling is consistent with an equatorial fluoride compound and the spectrum bears a resemblance to those of equatorial fluorides **102** and **107eq** were the ^2J HF coupling absent.
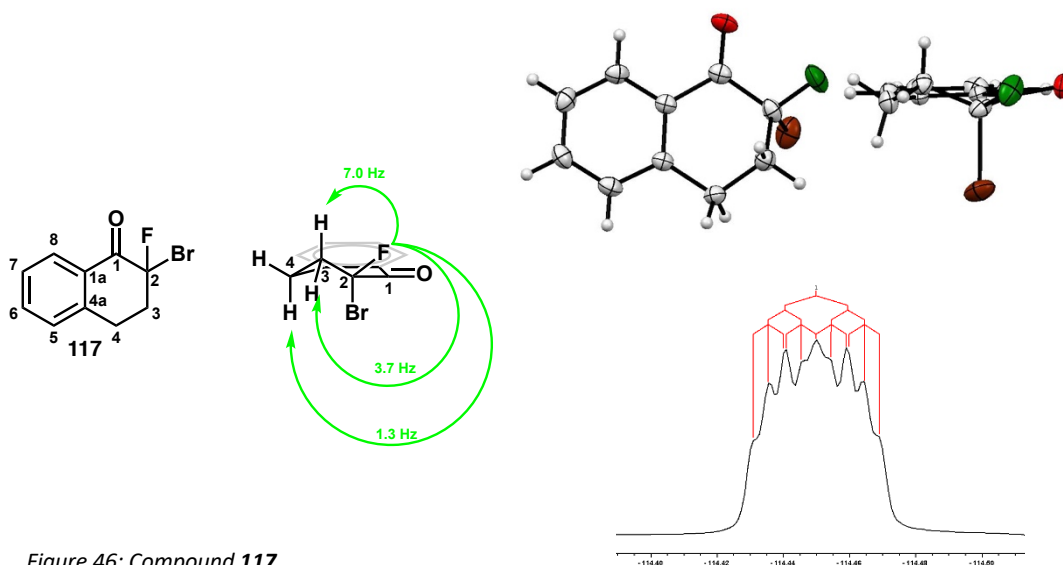
*Figure 46: Compound **117***

The vinyl bromide was utilised in Suzuki-Miyaura cross coupling reactions with a range of boronic acids in the presence of 5 mol% of a palladium catalyst. The reactions proceeded smoothly, allowing moderate to high yields of the desired compounds to be isolated upon filtration of the reaction mixtures through silica in 10% ethyl acetate/hexane solution. A range of substrates for the fluorination was sought, containing both electron donating and electron withdrawing functionality (*Scheme 62*).


118 X = OMe 66%
119 X = Me 63%
120 X = H 87%
121 X = COOMe 69%
122 X = C(O)Me 93%
123 X = CF$_3$ 76%

ArB(OH)$_2$, Pd(dppf)Cl$_2$, K$_3$PO$_4$, Toluene, H$_2$O, 80 °C
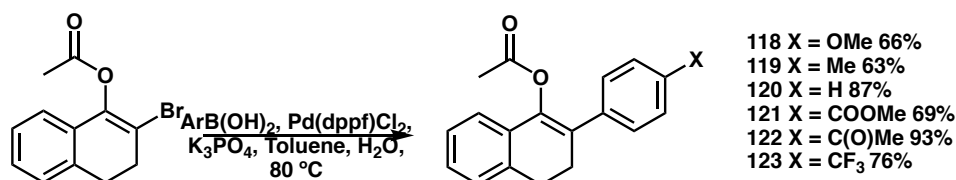
*Scheme 62: Synthesis of Compounds **118-123***

Compounds containing carbonyl functionality in the 4-position were desired as these compounds offer an opportunity to differentiate between radical intermediates and polar intermediates. Were a radical formed, resonance forms could be envisioned in which the radical resides at the carbonyl carbon in the form of a ketyl radical, and this would result in a decrease in the activation energy of the reaction and a deviation from the Hammett plot against either σ_p or σ_p^+. Conversely, if a cationic intermediate were formed, the carbonyl containing substituents of **121** and **122** would be destabilising and increase the energy barrier resulting in good agreement with the behaviour predicted by Hammett parameters.

3.1.5.2.　　Hammett Study

Compounds **118**-**123** were then subjected to the fluorination conditions and the rates of each reaction were determined. As observed previously, a smooth pseudo-first order reaction was observed during the reaction of all of these compounds with 1.5 equivalents of SelectFluor in 5% *(v/v)* water in acetonitrile solution at 25 ˚C with initial substrate concentration of 0.038 to yield the expected alpha-fluoroketone and a non-fluorinated side product (*Scheme 63*).

Scheme 63: Fluorination of Compounds **118-123**
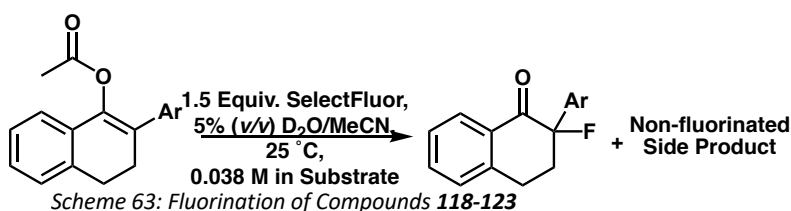
The data was again fitted to the Hammett σ_p and σ_p^+ parameters and a reasonable correlation was observed, with the data again fitting better to the σ_p^+ parameters rather than the σ_p parameters (*Figure 47*). As observed with the enol benzoate compounds the value of ρ was negative, consistent again with the generation of a (partial) positive charge in the transition state. The value of ρ was larger than that observed for the benzoate series, suggesting that the substituents were imparting a greater effect on the reaction than when they are situated on the enol benzoate.
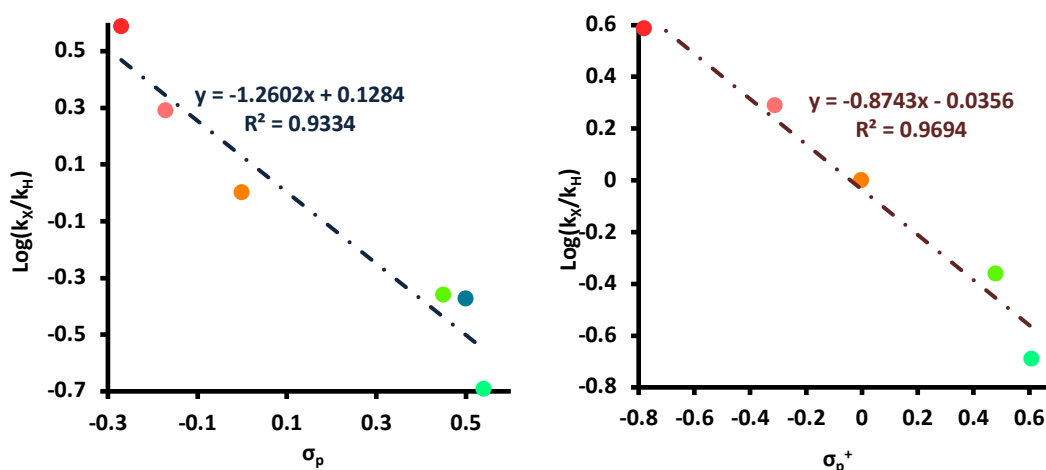
X		σ_p	σ_p^+	k (enol ester)
●	**OMe**	-0.27	-0.78	2.37×10^{-3} s^{-1}
●	**Me**	-0.17	-0.31	1.19×10^{-3} s^{-1}
●	**H**	0.00	0.00	6.15×10^{-4} s^{-1}
●	**COOMe**	0.45	0.49	2.59×10^{-4} s^{-1}
●	**C(O)Me**	0.50	-	1.25×10^{-4} s^{-1}
●	**CF$_3$**	0.54	0.61	2.67×10^{-4} s^{-1}

*Figure 47: Hammett Plots of Compounds **118-123**, with 1.5 equivalents of SelectFluor in 5% (v/v) D$_2$O/MeCN at 25 ˚C, initial substrate concentration of 0.038 M, k is an average of two runs*

No deviation from the expected behaviour was observed when compound **122** or compound **121** was applied in the fluorination reaction. There was no deviation from the

behaviour observed for the other substrates which may have been expected were the reaction to result in the formation of radical intermediates.

Whilst the fit was satisfactory against the σ_p^+ parameters, the data was also treated according to the Swain-Lupton protocol, resulting in a resonance contribution (R) of 64% and an inductive contribution (F) of 36%. This yielded an almost identical fit to that observed for the σ_p^+ parameters and indicated that resonance effects have a strong influence on the course of the reaction suggesting that substituents that are able to contribute electron density to the aryl ring through resonance result in a rate enhancement.

3.1.5.3.   Eyring Analysis on Alpha-Phenyl Compound 120

Alpha-aryl substituted compounds appeared to be behaving in a related manner to the other compounds thus far discussed, however in order to gather further evidence that the reaction mechanism is shared across the different compound series the energy barriers to reaction were obtained for compound **120** (*Figure 48*). The reaction was again conducted at five temperatures differing by 10 degree increments. The data was plotted as previously described and the values of $\Delta G^{\ddagger}$, $\Delta H^{\ddagger}$ and $\Delta S^{\ddagger}$ calculated.

Equation: y = -7811.8x + 12.988

ΔG/kcal mol^{-1}	ΔH/kcal mol^{-1}	ΔS/cal mol^{-1} K^{-1}
21.9	15.5	-21
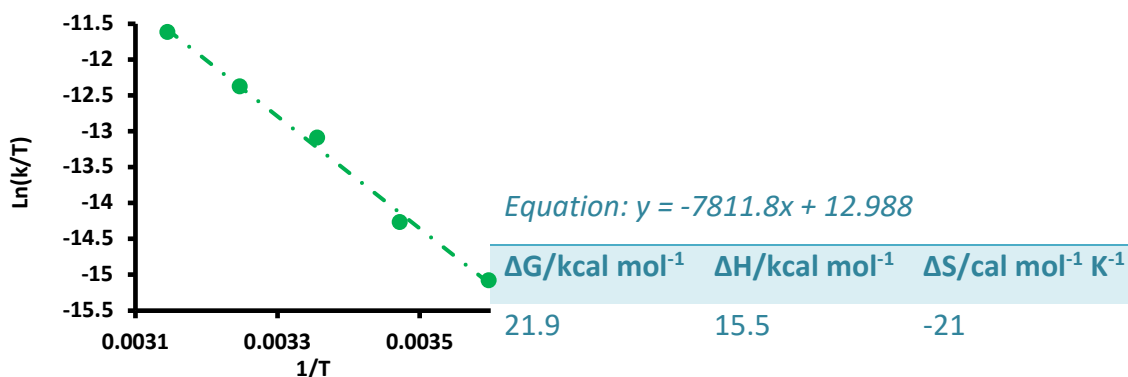
*Figure 48: Eyring Analysis of Compound **120***

Pleasingly, the data were in good agreement with the values obtained for the other compounds studied. The energy barrier $\Delta G^{\ddagger}$ was slightly lower, consistent with the fact that at room temperature the rate of reaction for this compound is slightly faster

than that observed for parent acetate **100**. The value of $\Delta S^{\ddagger}$ is again consistent with a bimolecular reaction, likely due to enol ester and SelectFluor coming together in the transition state. These data indicate that the rate determining step of the reaction of this series of compounds is related to that of the tetralone enol acetate and the enol benzoates.

3.1.5.4.   Identification of the Side Product

Whilst these compounds exhibit smooth first order reaction under the standard fluorination conditions and the kinetic data gathered indicates that the rate determining steps of the reaction of these compounds and compounds **109**-**115** are related, an additional complication was experienced in the analysis of these reactions. It quickly became apparent that although smooth consumption of the starting enol ester was observed two different products were forming in the reaction. Only one of the products was fluorinated – this being the expected alpha-fluoroketone. The non-fluorinated product was identified upon isolation and analysis of the NMR and IR spectra as the GC/MS was inconclusive. Independent synthesis of the postulated compound confirmed its identity to be alpha-ester compound **120b**. In order to synthesise the proposed side product, the epoxide (**125**) was formed from compound **120** and mCPBA in 81% yield (*Scheme 64*). Upon heating this underwent a rearrangement to form the alpha-ester product. The ^{1}H NMR of the isolated material from the fluorination could be compared to the rearrangement product and was found to be an exact match.

*Scheme 64: Synthesis of **120b***
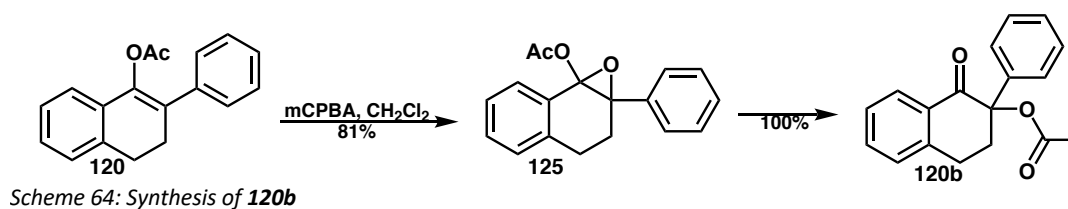
This type of side product was observed in the fluorination of all of the alpha-aryl compounds however the proportion of it that was produced varied markedly depending

on the electronics of the alpha-aryl substituent with more electron donating substituents leading to higher amounts of side product being formed. The amount observed for each compound is shown in *Table 4*.

Table 4: Quantities of Side Product Formed, Ratio Determined by ¹H NMR Referenced to Cyclohexane Internal Standard

Compound	Side Product	% Formed
118	118b	40
119	119b	27
120	120b	16
121	121b	15
122	122b	10
123	123b	13

Given the smooth kinetic behaviour observed it is unlikely that the side product was forming independently from the fluorination reaction. The ester might be forming as a result of the fluoroketone (**120a**) reacting with the acetic acid produced in the reaction, producing this unusual product. The fluoroketone product was therefore heated with acetic acid in acetonitrile to discern whether the side product would form under these conditions (*Scheme 65*). There was no sign of this being formed after 8 hours, making it unlikely that this is the pathway by which it forms.
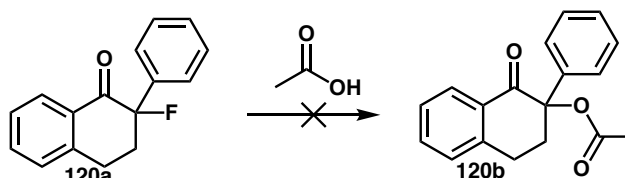
Scheme 65: Attempted formation of **120b** from **120a**

The alpha-fluorocarbenium ion is postulated as an intermediate in all but one of the proposed possible mechanisms. It was therefore proposed that the side product could have formed *via* further reaction of this intermediate. Three possible routes from the alpha-fluorocarbenium to the side products were envisioned: (i) migration of the alpha substituent; (ii) 1,2-alkyl shift yielding a ring contracted intermediate; or (iii) a 1,2-fluoride shift. The transference of fluoride to a sterically adjacent positive charge is

known to be possible *via* a fluoronium intermediate[191–195] (*Scheme 66*, **B**) however fluorine is not known to form 3-membered halonium intermediates which are well defined for the other halogens. In fact, seminal NMR spectroscopy studies by George Olah uncovered that the isomerisation observed in alpha-fluorocarbeniums occurs solely through 1,2-alkyl shifts rather than the formation of a halonium (*Scheme 66*, **A**).
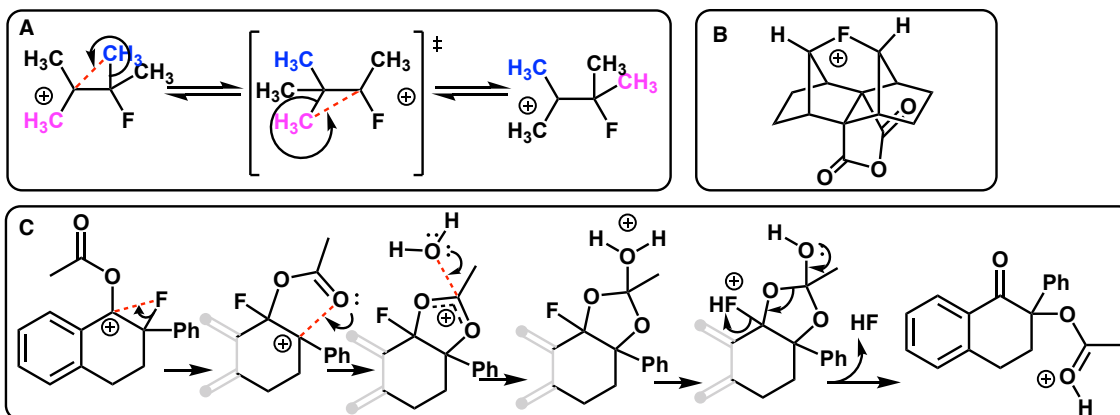

Scheme 66: Fluorocarbenium compounds

It was therefore surmised that the side product formation was more likely to occur *via* a carbon shift. The possible carbon shift pathways are depicted in *Scheme 67*. The dependence of the electronic properties of the alpha-aryl substituent on the quantity of side product formed indicates that not only do electron donating substituents increase the likelihood of its occurrence but also that structural differences can impact this process.
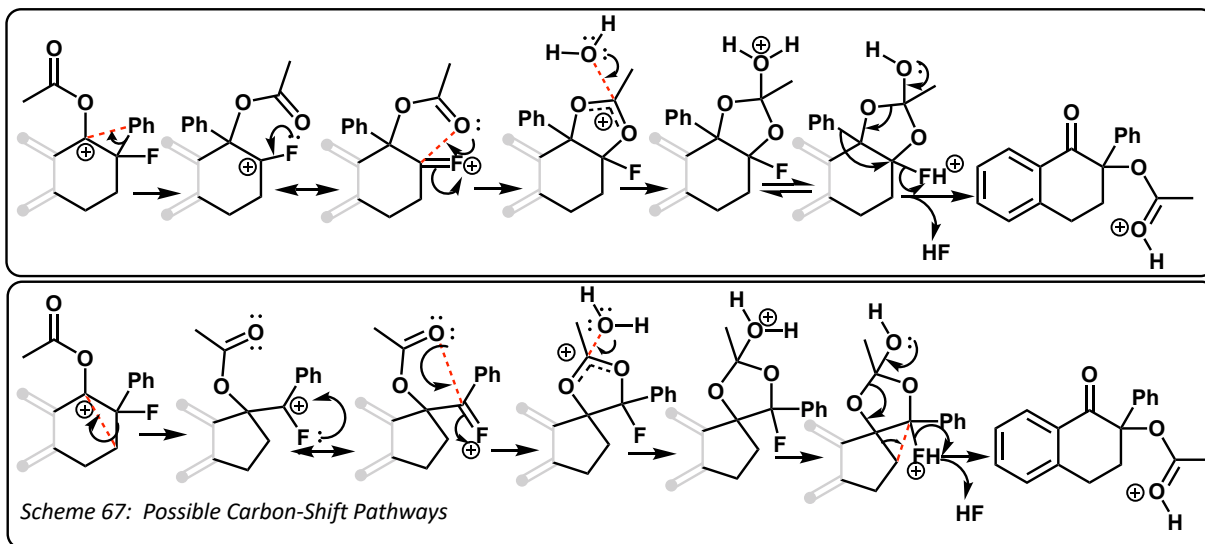
Scheme 67: Possible Carbon-Shift Pathways

In order to differentiate between the aryl-shift process or ring contraction process, the 1-indanone analogue of compound **127** was synthesised (*Scheme 68*). It was expected that the 5-membered indanone compound would disfavour the ring-contraction pathway as this would result in the formation of a highly strained 4-membered intermediate. Compound **127** was accessed *via* a similar route to compounds **118**-**123** albeit in diminished isolated yield. When this compound was subjected to the fluorination conditions the formation of side product **127b** was observed in identical proportions to the corresponding product from 1-tetralone compound **120**, suggesting that this may be forming *via* a 1,2-shift of the aryl substituent. Computational investigations of these pathways will be discussed later.
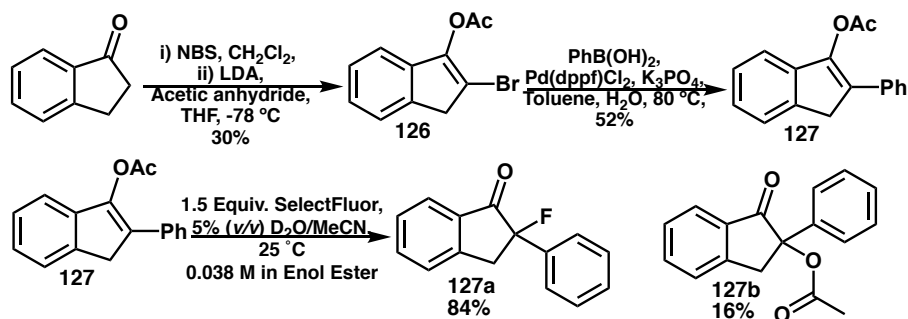
Scheme 68: Synthesis of Compound **127** and Fluorination

3.1.6. 6-Substituted Tetralones

The kinetic isotope effect on compound **100** uncovered evidence of participation of the aryl ring of tetralone in stabilising the transition state of the rate determining step of this fluorination reaction, with the highest kinetic isotope effect observed for the 6-carbon. Introducing substituents with differing electronic properties in this position should then have an impact on the reaction rate (*Scheme 69*). It was essential to incorporate substrates which had differing σ_p and σ_p^+ parameters in order to determine whether a carbenium is generated at the carbonyl carbon of tetralone.
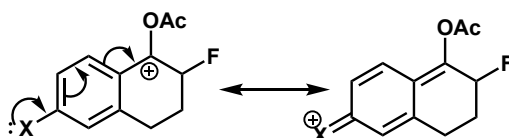
Scheme 69: 6-Substituted Compounds

Therefore compounds bearing substituents which would be able to interact with a carbenium through resonance were desirable.

3.1.6.1. Substrate Synthesis

Unlike the previous series, it is not possible to access all of the desired 6-substituted compounds *via* a common intermediate. Compounds **128**, **129** and **130** are commercially available and therefore became the feedstocks for synthesis of 6-substituted compounds. Direct acetylation of **128** with isopropenyl acetate yielded compound **131** in 40% yield (*Scheme 70*). The generation of the other substrates required more synthetic manipulations. Compound **128** was demethylated by refluxing in aqueous HBr and this crude material was then acetylated on the phenolic hydroxyl as well as at the ketone to form diacetyl compound **132** in 36% yield over the two steps (*Scheme 70*). The 6-aminoketone **129** can be transformed into a diazonium using sodium nitrite and aqueous HCl at 0 ˚C; with the addition of copper (I) chloride and warming to room temperature this decomposes with the extrusion of nitrogen to form the 6-chloro-1-tetralone. This crude material was then directly acetylated with isopropenyl acetate to form compound **133** in 17% yield over two steps (*Scheme 70*). Compound **130** can be methylated under acidic conditions by refluxing in methanolic HCl generated *in situ* from the reaction between trimethylsilyl chloride and methanol (*Scheme 70*). The crude material from this reaction was then subjected to acetylation conditions using isopropenyl acetate to yield compound **134** in 20% yield over two steps (*Scheme 70*).
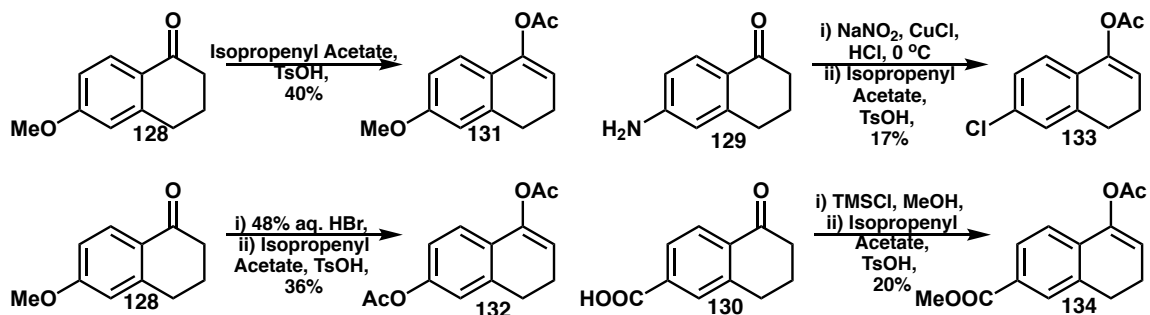
Scheme 70: Synthesis of Compounds **131-134**

3.1.6.2. Hammett Study

This series of substrates was subjected to the standard fluorination conditions and the reaction rates were measured by monitoring reactions using ^{1}H NMR spectroscopy as before. In good agreement with the previous series, the electron donating methoxy substituent had the effect of increasing the rate of reaction with SelectFluor whilst the electron withdrawing ester substituent on compound **134** slowed the reaction. The data was once more plotted against both the σ_p and σ_p^+ parameters. On this occasion a poor correlation was observed between the rate data for these compounds and σ_p whilst the correlation was much improved against σ_p^+. The resonance-donating ability of substituents appeared to be particularly dominant. Compound **132** offers an illustration of this as it has a σ_p^+ of -0.19 which reflects its resonance donating-ability (*Table 5*). The positive σ_p value of 0.31 reflects its inductive-withdrawing properties, but the substituent exhibits a rate enhancement in the reaction compared to unsubstituted compound **100**. This clearly indicates that resonance donating ability is a more significant factor in the reaction.

*Table 5: Hammett Parameters and Reaction Rates for Compounds **131-134** and **100** using 1.5 Equivalents of SelectFluor in 5% (v/v) D$_2$O/MeCN at 25 ˚C with initial substrate concentration of 0.038 M, k is an average of two runs*

X			σ_p	σ_p^+	k (enol ester)
🔴	**OMe**	**131**	-0.27	-0.78	8.76×10^{-3} s^{-1}
🟤	**OCOMe**	**132**	0.31	-0.19	6.17×10^{-3} s^{-1}
🟠	**H**	**100**	0.00	0.00	4.01×10^{-4} s^{-1}
🟢	**Cl**	**133**	0.23	0.11	4.23×10^{-4} s^{-1}
🟢	**COOMe**	**134**	0.45	0.49	1.71×10^{-4} s^{-1}

The value of ρ for the plot of $\log(k_x/k_H)$ against σ_p^+ was once again negative, indicating the generation of positive charge (*Figure 49*). It was also larger in magnitude than the values obtained for compounds **110**-**115** and compounds **118**-**123** indicating that the substituents in this instance are having a greater impact on the rate of reaction. This is consistent with the build-up of charge being at the tetralone carbonyl position, which is directly in conjugation with the aryl ring of the tetralone scaffold.

Figure 49: Hammett Plots for Compounds **131-134** and **100**
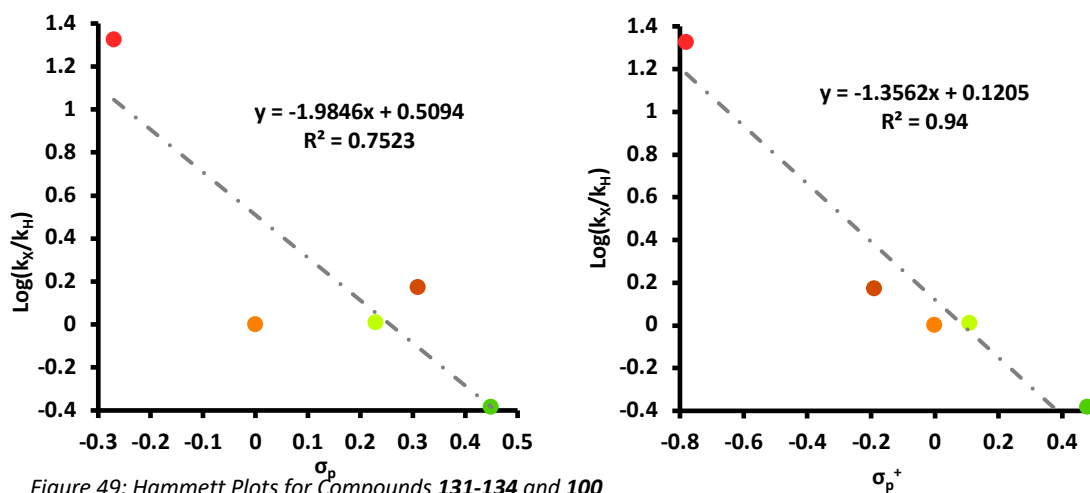
3.1.7. Attempts at Radical Detection

Whilst the evidence discussed thus far appears to provide compelling evidence for the formation of a carbenium, it is also conceivable that these substrates would behave in this manner during the formation of a radical cation. It was therefore necessary to identify whether any radical intermediates could be detected either by direct observation or during radical trapping experiments.

3.1.7.1. EPR Experiment

The first attempt at detecting radical intermediates was *via* direct observation through EPR spectroscopy. SelectFluor and enol ester substrate **100** were combined in acetonitrile/water and the mixture was analysed by EPR. This analysis did not detect any unpaired electron containing species however this was not conclusive evidence to exclude the presence of such intermediates. It does, however, confirm that if such intermediates exist they are short lived enough to avoid detection. Moreover, were the substrate and SelectFluor likely to form a long-lived radical species this would likely be in the form of a charge transfer complex. Charge transfer complexes of *N*-F reagents are known (*vide supra*) and these species were found to be highly coloured, a common

property of charge transfer complexes. Given that the fluorination reactions discussed remain colourless throughout it is unlikely that such a species would occur.

3.1.7.2. Cyclopropane-Containing Substrates

A common means of determining the presence of radical intermediates on a reaction pathway is the use of radical clocks. These are radical fragmentations or rearrangements for which the rate constant has been determined and are usually very fast radical reactions which compete with the product-forming pathway of the reaction being studied. The rate constants for a vast number of radical clocks have been determined and a common moiety that often finds use in organic chemistry is the cyclopropane ring, given its ability to undergo extremely rapid radical-induced ring opening. The propensity for a cyclopropane to undergo radical-induced ring opening can be enhanced *via* the introduction of aromatic rings on the cyclopropane, which can result in ring opening over five thousand times as fast as the unsubstituted parent molecule (*Scheme 71*).[196–200] For example, Watson *et al.* used the ring opening of cyclopropane containing compound **135** to provide evidence for the presence of a transient alpha-
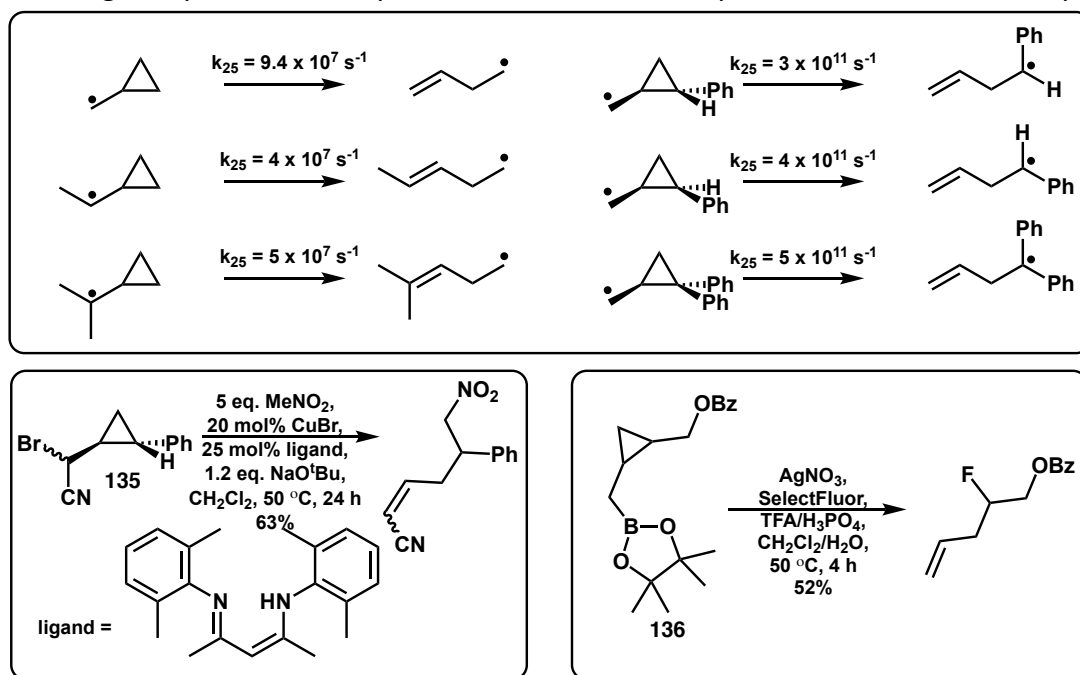
Scheme 71: Radical Probes

cyano radical in the reaction mechanism of their copper-catalysed alkylation reaction (*Scheme 71*).[201] In the field of fluorination chemistry a cyclopropane radical clock has been used by Li and co-workers to elucidate the mechanism of silver catalysed fluorination of alkylboronates. Fluorination of cyclopropane compound **136** yielded only the ring opened fluorinated product, supporting the proposed mechanism involving the generation of an alkyl radical as a result of the loss of the boronate group.[202]

The introduction of cyclopropane containing moieties in the 1-tetralone enol ester class is therefore instructive in deducing whether radicals play a role in the fluorination mechanism of these compounds with SelectFluor. As previously discussed, changing the identity of the ester portion of the enol ester and varying the alpha-substituent next to the carbonyl are synthetically attractive prospects. In light of this both the cyclopropane bearing enol ester (**137**) and alpha substituted cyclopropyl (**138**) compounds were synthesised in the same manner as described previously (*Scheme 72*).

Scheme72: Synthesis of Compounds **137** and **138**
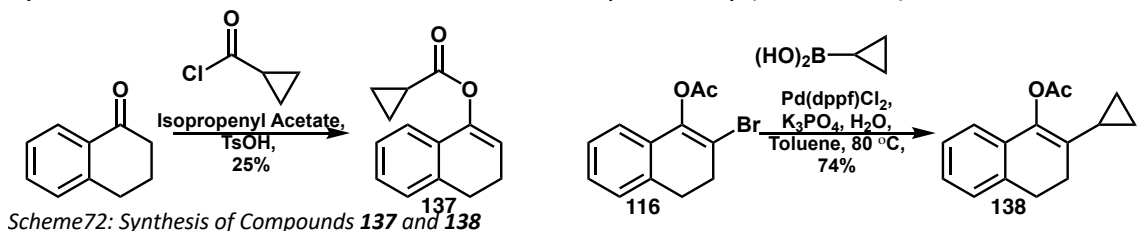
It is possible for ring opened products to be produced from the formation and subsequent intramolecular reaction of a radical intermediate. The most feasible radical reaction mechanisms (*Scheme 73*) result in the formation of a radical cation intermediate with the radical situated either on the alpha-carbon (compound **137a**) or on the carbonyl carbon in the form of a ketyl radical (compound **137b**). For **137a**, attack on the cyclopropyl can be envisioned, resulting in the formation of a six-membered ring and opening of the cyclopropane (**137a-1**). Loss of a hydrogen radical could then facilitate the formation of an alkene (**137a-2**) and hydrolysis of the carbenium ester intermediate (**137a-3**) would then return a tetralone compound with an acid at the end of an alkyl chain on the alpha-carbon (**137a-4**). Were the radical cation formed in which the carbonyl carbon bears the radical (**137b**) it is possible that this radical would attack the

cyclopropane, breaking open the ring and forming a spirocyclic 6,5-ester compound (**137b-1**). As with the previous example loss of a hydrogen would allow the formation of an alkene (**137b-2**), hydration of the carbenium on the tetralone alpha carbon would then yield the final compound **137b-4**.
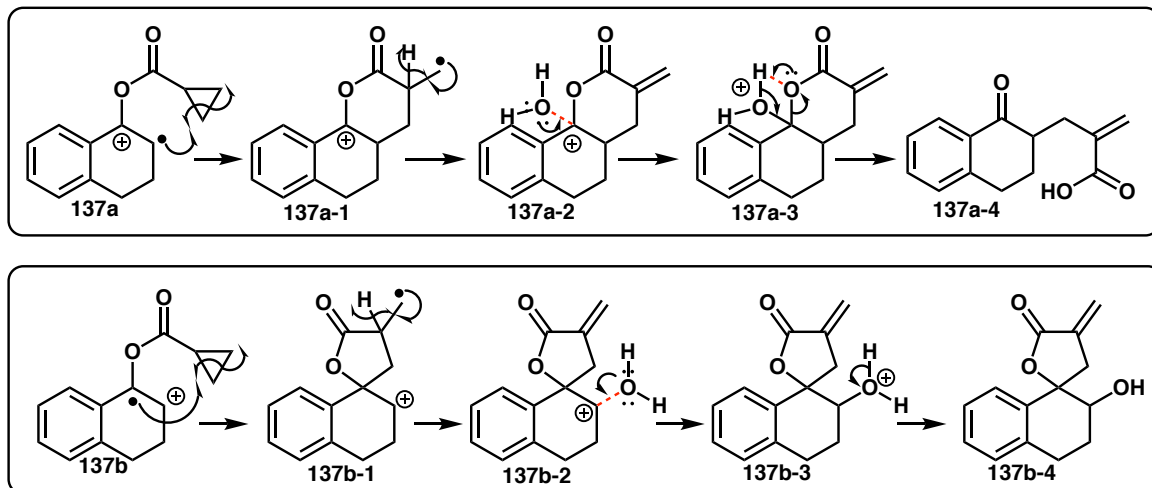
Scheme 73: Possible Radical Ring Opening Pathways of **137**

Whilst it is possible to draw a feasible mechanism for the ring opening of the cyclopropanecarboxylate ester this type of behaviour is not well precedented if at all. In compound **138** the ring is located in direct proximity to the reactive alkene. Moreover, the generation of a radical cation which places the radical on the alpha-carbon (**138c**, *Scheme 74*, proposed in all but one of the possible radical mechanisms above) yields a compound with many more similarities to the radical clocks for which the rate of ring opening has been determined. The possible ring opening mechanism for this compound is shown in *Scheme 74*.   It is immediately apparent that this ring-opening pathway is much more closely related to the radical clock reactions shown in *Scheme 74*. Once the radical ring-opened intermediate **138c-1** has been generated there are possibilities for the formation of multiple products. The first pathway shown involves the loss of a hydrogen radical to form the alkene (**138c-2**), subsequent hydrolysis of the ester carbenium (**138c-3**) would result in the generation of conjugated dienone compound **138c-4**. If the ring opened radical intermediate **138c-1** were to abstract a proton from the solvent followed by hydrolysis, enone compound **138c-7** would be produced. Further reaction of the radical intermediate **138c-1** with the alkene generated from ring

opening would lead to the formation of a spirocyclic 6,4-radical intermediate. Hydrogen abstraction from the solvent and subsequent hydrolysis would then lead to spirocyclic ketone **138c-11**. Other reaction pathways would also be possible after the radical-induced ring opening, suggesting that a complex reaction profile with multiple products could be indicative of radical behaviour.
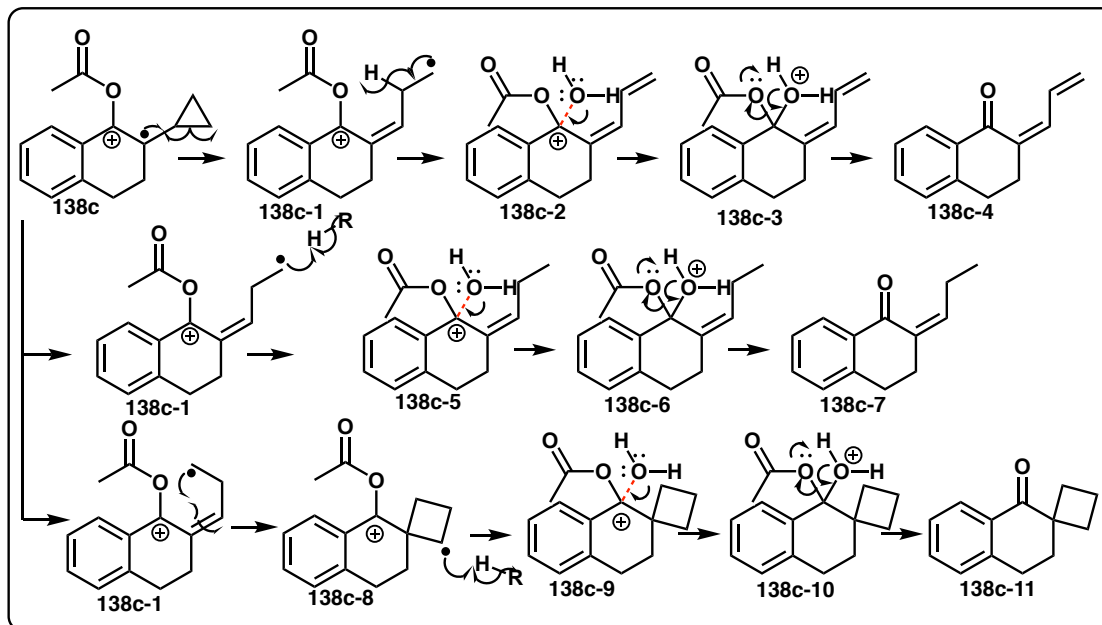
Scheme 74: Possible Radical Ring Opening pathways of Compound 138

When these compounds were subjected to the fluorination conditions smooth conversion to a single product was observed. Ester compound **137** converted entirely to the fluoroketone product and the corresponding cyclopropane carboxylic acid without any evidence of ring opened products being formed (*Scheme 75*).
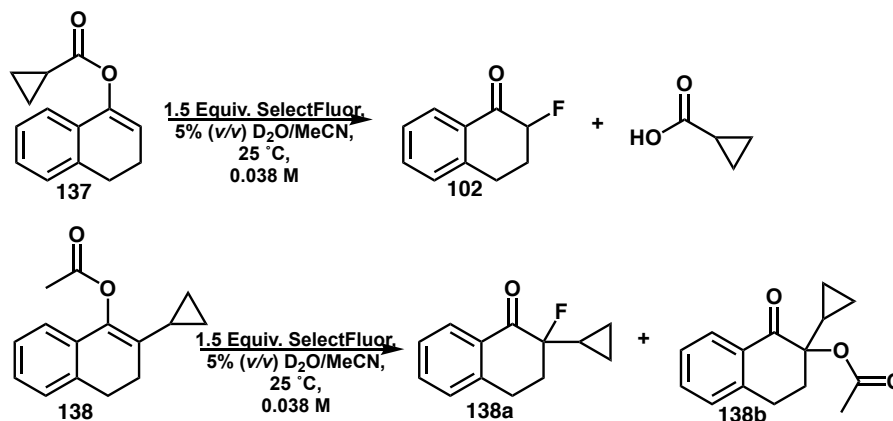
Scheme 75: Fluorination of 137 and 138, determined by ^{1}H NMR

For the alpha-cyclopropane compound **138** there was no evidence of ring opening during the fluorination.

Much like its alpha-aryl counterparts (compounds **118**-**123**), production of the ester side product **138b** was also observed. In this instance a higher proportion of the side product was produced than was observed for the unsubstituted alpha-phenyl compound **120**. Pure samples of the alpha-cyclopropyl fluorinated product **138a** and side product **138b** were obtained by column chromatography on silica gel. Whilst the ester compound **138b** appeared to be completely stable, over time the NMR sample of the fluorinated product **138a** in chloroform-*d* appeared to degrade, changing colour from pale yellow to dark brown. ^{1}H and ^{19}F NMR analyses revealed that the compound had significantly degraded to multiple fluorinated compounds, leaving behind negligible amounts of the original product **138a**. Moreover, several instances of distinctive coupling of *ca.* 50 Hz was observable in both the ^{1}H and ^{19}F NMR, indicative of the presence of geminal ^{2}J HF coupling. It is possible that the Lewis acidic silicon in the glass of the NMR tube was sufficient to remove fluoride from the compound resulting in the generation of a carbenium adjacent to the cyclopropane (*Scheme 76*).
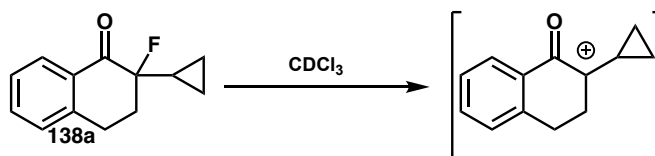
Scheme 76: Decomposition of **138a**

3.1.7.3.   TEMPO as a Radical Trap

The 2,2,6,6-tetramethyl-1-piperidinyloxy free radical (TEMPO) is commonly used as a mechanistic probe in reactions in which a radical mechanism is suspected. Due to the unpaired electron present on oxygen in this molecule it is possible for it to react with a radical generated in a reaction, forming adducts with TEMPO or disrupting the reaction pathway by some other means. The work of Liu *et al.* discussed above utilised TEMPO as a radical probe, forming adducts with their vinyl azide substrates. It was proposed

that the introduction of TEMPO into the reaction mixture of an enol ester fluorination could be informative.

A reaction between the simple enol acetate of tetralone (compound **100**) and SelectFluor in 50% *(v/v)* water in acetonitrile was followed by ^{1}H NMR (*Figure 50*). When the reaction reached 50% conversion 1.0 equivalents of solid TEMPO were introduced to the reaction mixture. Subsequent monitoring of this reaction by ^{1}H NMR revealed the near-immediate consumption of the remaining SelectFluor in the reaction mixture accompanied by no further formation of alpha-fluoroketone product **102** or consumption of the enol ester starting material **100**.
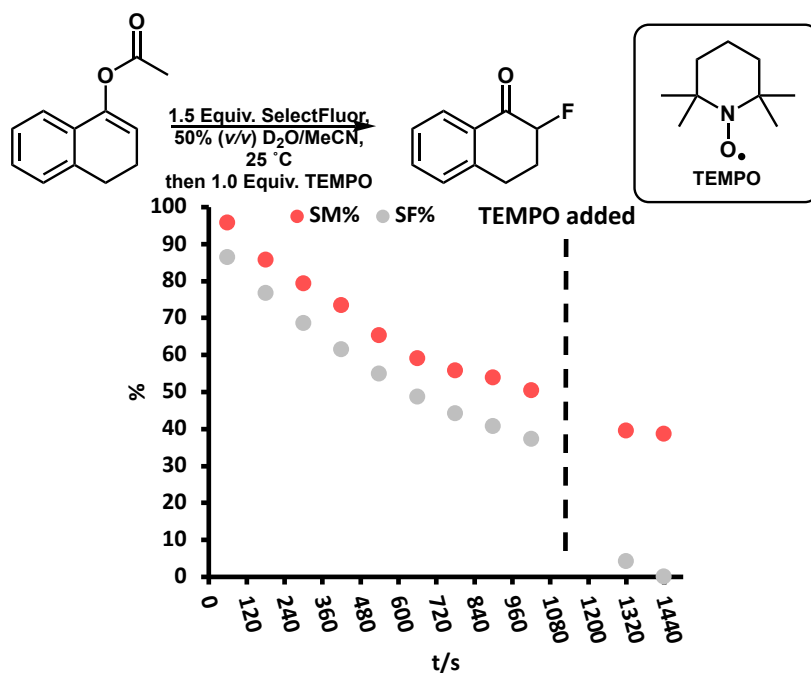
Figure 50: TEMPO Experiment

This was initially thought to be potential evidence of radical processes on the reaction pathway, however given that the enol ester substrate appears to not interact with TEMPO at all the results were not conclusive and did not rule out that a competing reaction pathway could be taking place between SelectFluor and TEMPO. It is known that SelectFluor can behave as an oxidant and is often employed as such for transition metal catalysed reactions.[106] It was therefore possible that the TEMPO was being oxidised in the reaction by SelectFluor, accounting for the complete destruction of the

reagent during the fluorination reaction. The "oxidised TEMPO" oxoammonium salts are known and the tetrafluoroborate is easily prepared *via* reaction of TEMPO with bleach in aqueous tetrafluoroboric acid (*Scheme 77*). The oxoammonium salt **139** is distinctively yellow in colour, compared to the bright orange of TEMPO. The mixing of SelectFluor with TEMPO in 5% *(v/v)* water in acetonitrile results in the formation of a yellow compound, which can be characterised as **139** by IR and UV/vis spectroscopy.
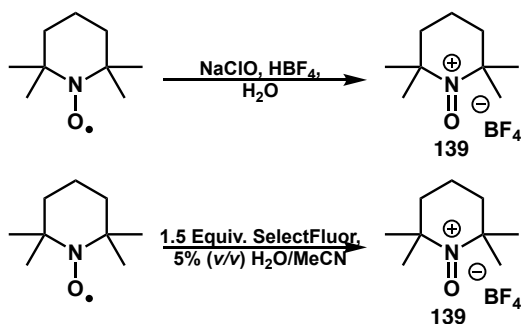
*Scheme 77: Synthesis of Oxoammonium Compound **139***

Attention was then turned to how this oxoammonium compound would react with the enol ester substrates (*Scheme 78*). In particular, the alpha substituted compounds given that they produce side products of unknown origin. If the first step in the fluorination reaction was single electron oxidation of the enol ester by SelectFluor similar behaviour would be observed in the reaction of the enol ester substrates with oxoammonium **139**. When compounds **120** and **138** were combined with 1.5 equivalents of **139** in 5% *(v/v)* water in acetonitrile the formation of aromatised products **140** and **141** were observed instead. There was no evidence for the formation of TEMPO adducts or side products.

120 R = Ph
138 R = Cyclopropyl

140 R = Ph
141 R = Cyclopropyl
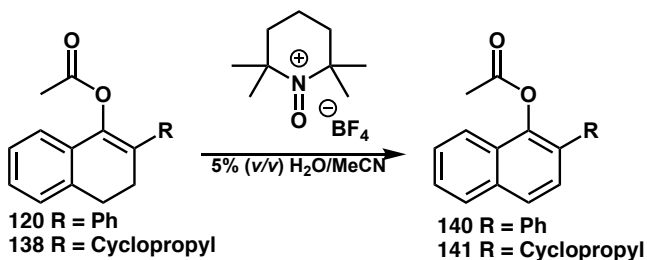
*Scheme 78: Reaction of **120** and **138** with **139***

A possible mechanism for the formation of aromatised products **140** and **141** is proposed in *Scheme 79*. Analogous to the accepted mechanism for the oxidation of alcohols with catalytic TEMPO in bleach (forming an oxoammonium species *in situ*), the

nucleophilic enol ester would attack the oxoammonium species at nitrogen, generating an ylide intermediate which can deprotonate the adjacent carbon resulting in the formation of an alkene and the release of TEMPOH. Loss of a further proton allows the formation of the naphthalene product, driven by the generation of aromaticity.
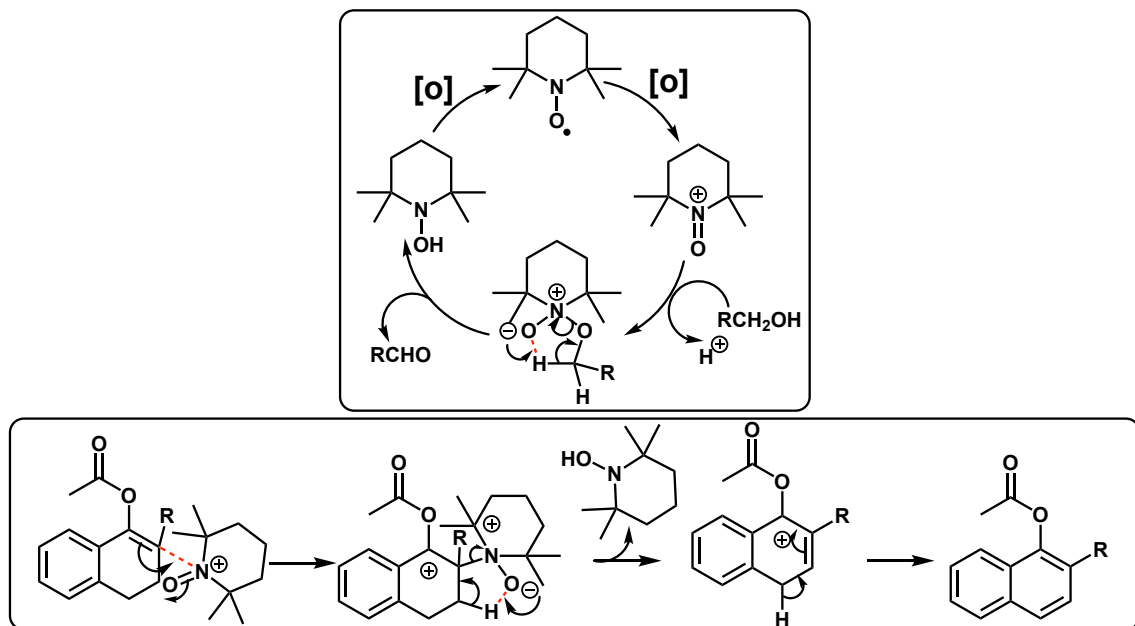
*Scheme 79: Mechanism of TEMPO Oxidation of Alcohols and Proposed Mechanism for the Oxidation of **120** and **138***

3.1.8. ^{18}Oxygen Labelling Experiments

Given the strange behaviour observed when alpha-substituted compounds **118**-**123** and **138** were subjected to the fluorination reaction conditions it was necessary to gain some insight into further steps along the reaction pathway, namely the hydrolysis of the enol ester. In order to achieve this the water used in the solvent mixture was substituted for that which contained an ^{18}oxgen atom. Whether or not the oxygen form water is incorporated into the product molecule gives useful information about the nature of the hydrolysis step. It was also important to determine whether the hydrolysis behaviour was consistent throughout the enol ester series or whether different enol esters would hydrolyse *via* different mechanisms.

Parent compound **100** was subjected to the fluorination conditions with $H_2^{18}O$ and the crude material was analysed by GC/MS to determine whether incorporation had occurred. Surprisingly the only product from the reaction was the [^{18}O]-labelled alpha-fluoroketone **[^{18}O]-102** (*Scheme 80*). Next, three of the enol benzoates **110, 108** and **115** were examined. Given the ambiguity in the Hammett plot it was thought that a change in hydrolysis behaviour could be responsible for the apparent break in the plot against σ_p^+ therefore 4-methoxybenzoate **110**, unsubstituted benzoate **108** and 4-nitrobenzoate **115** were subjected to the fluorination conditions in the presence of $H_2^{18}O$. In these instances, the only product formed was again **[^{18}O]-102**.
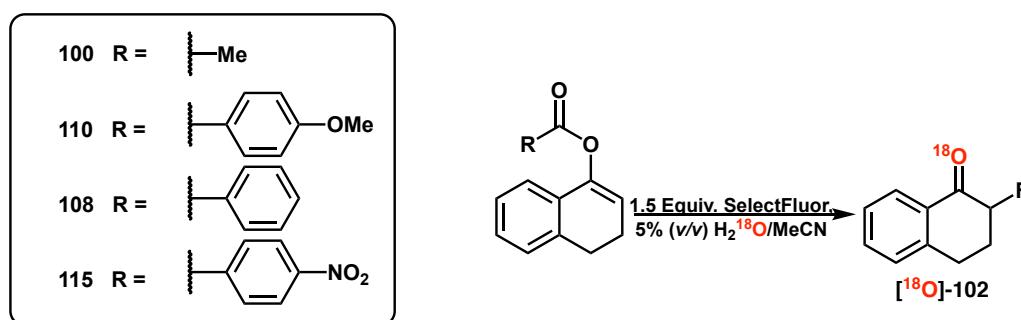
Scheme 80: ^{18}Oxygen-Labelling of **100, 110, 108** and **115**

The alpha-substituted compounds **120** and **138** were next subjected to the conditions. Interestingly, the alpha-cyclopropyl compound **138** again exhibited complete incorporation of ^{18}O in the fluorinated product (*Scheme 81*). The side product, however, gave different results. The molecular ion of the side product was not observed in the GC/MS trace; instead fragmentation of the ester group resulted in the detection of the mass minus $CH_3C=O$.
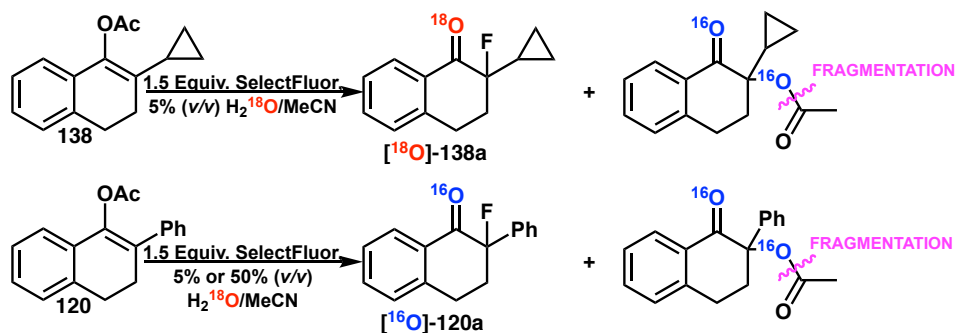
Scheme 81: ^{18}Oxygen-Labelling of **120** and **138**

The fragment that was detected appeared to only contain ^{16}O, indicating that the formation of the side product was an intramolecular process given that the only source of ^{16}O in the reaction mixture was in the starting material enol acetate.

In contrast to the other substrates tested, the alpha-phenyl compound **120** resulted in the formation of a ^{16}O-containing fluorinated product, indicating that this compound undergoes hydrolysis through a different mechanism to the others examined. The formation of the side product appeared to follow the same pattern as the cyclopropyl, again showing only the mass minus $CH_3C=O$ and appearing to have the same ^{16}O substitution pattern. In order to confirm that the carbonyl oxygen in the side products contained ^{18}O, IR spectra of the reaction mixtures were recorded. The IR stretching frequency of the ester carbonyl will move to a lower wavenumber if the ^{16}O isotope has been substituted for ^{18}O. When the reaction mixtures of the alpha-cyclopropyl and alpha-phenyl are compared to the products under "normal" fluorination conditions, the disappearance of the ester carbonyl signal can be observed (*Figure 51*). For the alpha-phenyl compound the ester and ketone carbonyl stretches appear at 1732 cm^{-1} and 1693 cm^{-1} respectively.
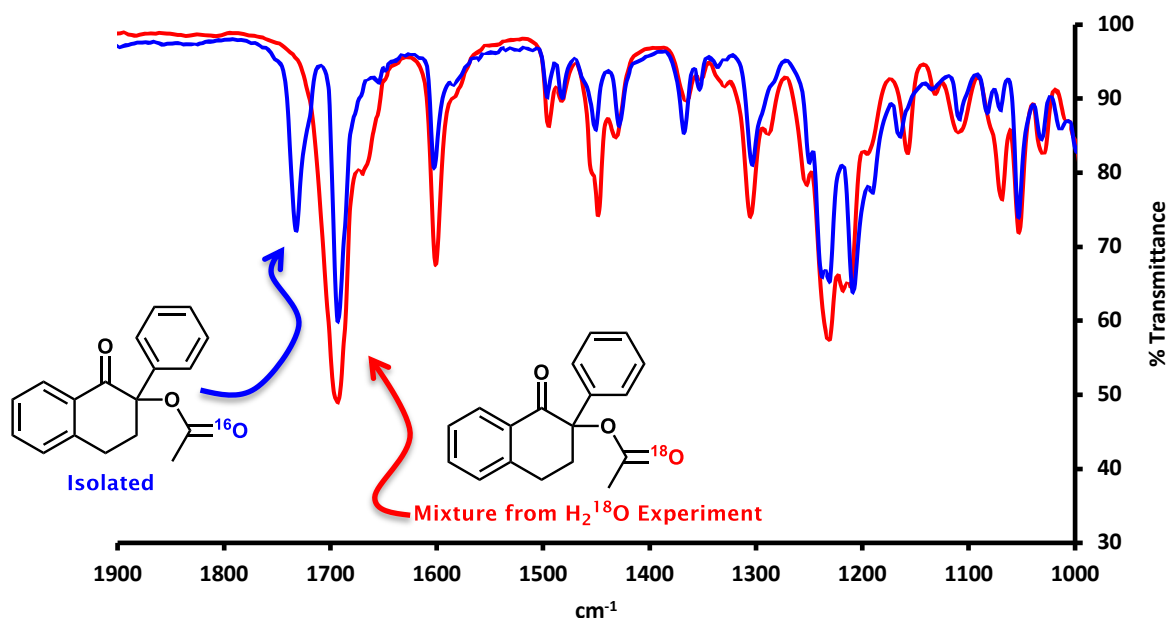
Figure 51: IR Spectrum from ^{18}Oxygen-Labelling Experiment

The ester carbonyl signal has been shifted such that they now coincide with those observed for the ketone, confirming the incorporation of ^{18}oxygen in this position.

3.1.9. Proposed Mechanism

With the evidence gathered during the various studies discussed above it is now possible to propose a mechanism for the fluorination reaction of SelectFluor with enol esters. The dependence of reaction rate on the concentrations of both SelectFluor and enol ester substrate combined with the values of $\Delta S^{\ddagger}$ that have been determined for a representative selection of compounds confirm that this reaction has a bimolecular rate determining step involving both reaction partners. The increased rates of reaction observed for the reactions of enol esters of tetralone compared to the rates observed for cyclohexanone and 4-*tert*butylcyclohexanone derivatives indicate that the presence of the aryl ring has a stabilising effect on the transition state, lowering the energy barrier. The KIE observed at the 6-carbon of compound **100** corroborates this, showing that the aryl ring may be stabilising reaction intermediates through resonance (*Figure 52*). The rate enhancement produced by resonance donating substituents in the 6-position provides further evidence for this. Insight into the nature of the intermediates produced is revealed by the Hammett plots that have been generated. The negative slopes produced in combination with the high degree of correlation observed in the plots against σ_p^+ indicate the build-up of positive charge in the transition state.
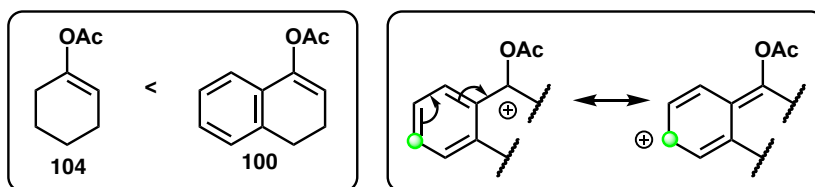
*Figure 52: Comparison of Reactivity of **100** and **104***

Insight into the nature of this positive charge is provided by the fact that no radical intermediates can be detected either directly or indirectly. This in combination with the hydrolysis mode observed for all but the alpha-phenyl compound **120** strongly suggests the presence of a carbenium at the tetralone carbonyl position. When taken together,

this evidence paints a picture of a polar reaction mechanism in which the rate determining step is electrophilic fluorine atom transfer to the enol ester, resulting in the formation of a carbenium. In the case of compounds **100**, **108**, **110**, **115** and **138** this carbenium is intercepted by water in the reaction mixture, resulting in the expulsion of acetate and the generation of the fluoroketone product. In the case of compound **120**, it is likely that the water attacks at the carbonyl carbon of the ester group, resulting in the formation of the ketone *via* this means. The reason for the change in hydrolysis mechanism has been examined computationally and will be interrogated in more detail in a later section. *Scheme 82* depicts the proposed mechanism, based on the evidence that has been gathered and discussed above.
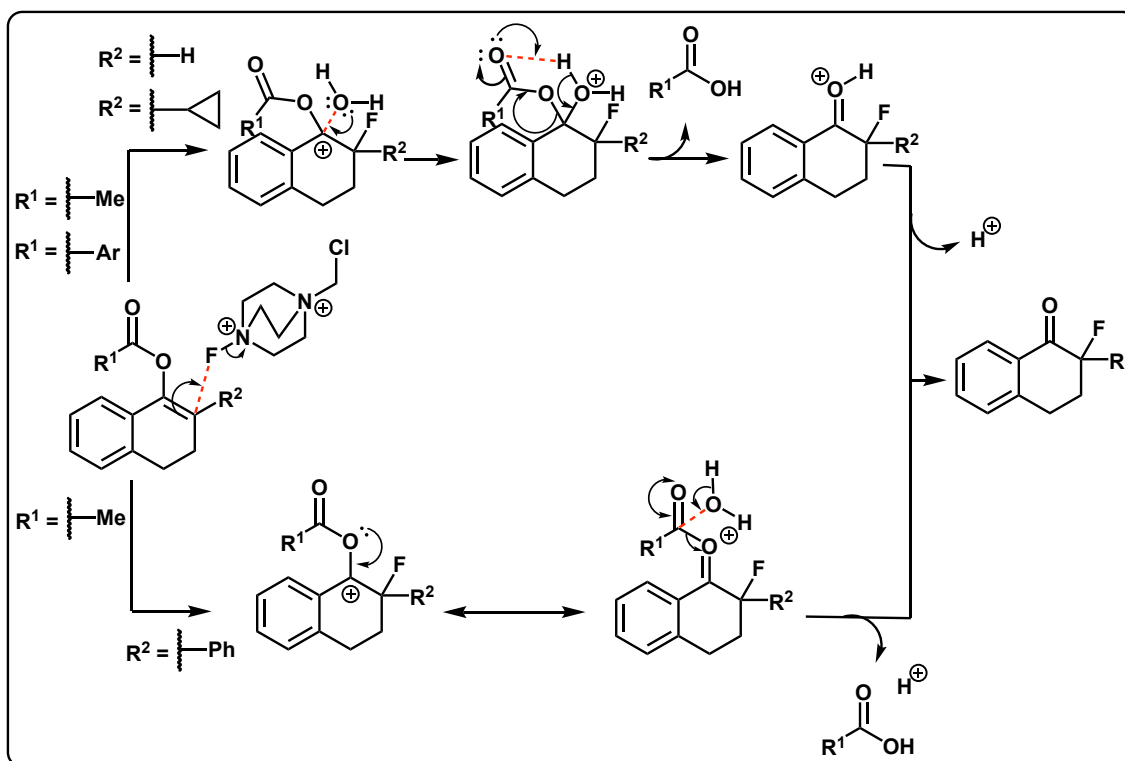
Scheme 82: Proposed Mechanism for the Fluorination of Enol Esters of Tetralone with SelectFluor

3.2. Model Compounds for the Steroid

With a plausible mechanism for the fluorination of simple tetralone/cyclohexanone enol esters established it was important to attempt to discover the generality of this mechanism and most significantly whether it could be applied to

the steroidal molecules of interest. Given the poor solubility properties of the steroid a more closely structurally related model was sought. It was thought that through synthesis of smaller, more soluble analogues insight into the behaviour of steroids could be gained without having to deal with the poor solubility and challenging NMR spectra of the full molecule. The design of model compounds focussed on attempting to replicate the A and B rings of the steroidal system, given that this is the locus for reaction on the steroid (*Figure 53*). It was thought particularly important to replicate the conjugated dienol ester moiety which is present in the steroidal substrate for fluorination in order to be able to identify any differences in reactivity between these types of substrate and the simple enol esters previously studied. The potential ability for the steroid type substrates to allow delocalisation of any charges generated during the reaction could make it possible for these substrates to behave in a different manner to the tetralone-based compounds.
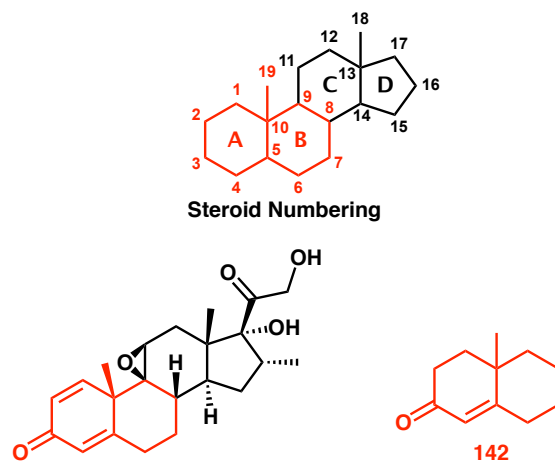
*Figure 53: Steroid Numbering and Model Compound **142***

3.2.1. Synthesis of Bicyclic Enone Model Compound

The first compound targeted as a possible model for the steroid was bicyclic enone compound **142**. It was selected as a robust synthetic route has been published by Pfau and Revial utilising cheap, commercially available starting materials (*Scheme 83*).[203] Formation of an imine (**144**) with 2-methylcyclohexanone and chiral amine **143** allows the reaction of the enamine tautomer (**145**) with methyl vinyl ketone. Hydrolysis of the

intermediate imine (**146**) followed by Robinson annulation of the diketone intermediate (**147**) affords the desired enone product.
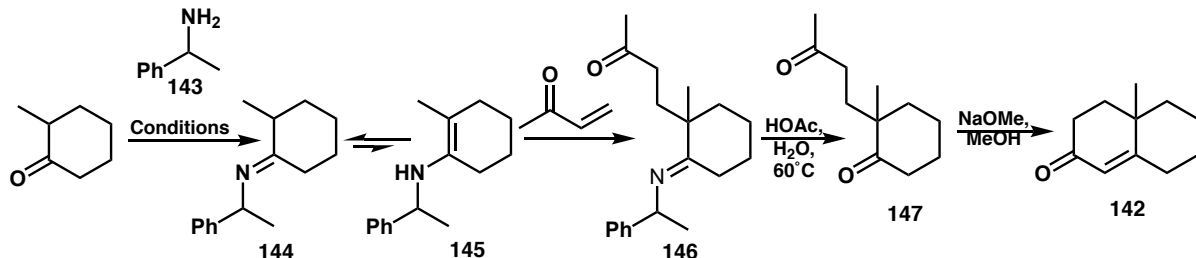
Scheme 83: Route to compound 142

When the synthesis was attempted the initial imine formation step proved to be problematic; the procedure calls for azeotropic removal of water *via* a Dean-Stark trap however in practice this was found to be inefficient, resulting in extended reaction times. Nevertheless the product **142** was reached in a very modest 13% yield after a total of fourteen days to complete the synthetic route (*Table 6*, entry 1). It was found that the rate of imine formation could be increased *via* the addition of *p*-toluenesulfonic acid (*Table 6,* entry 2). This led to an improved overall reaction time of eleven days and increased the yield to 22%. Further improvements on the reaction time could be made by changing the water removal method. Using magnesium sulfate as a drying agent the imine formation step appeared to progress at a lower temperature of 40 ˚C, preventing discolouration of the reaction mixture (*Table 6*, entry 3). NMR monitoring of the crude reaction mixture also appeared to indicate that the formation of the imine was progressing faster than when water was removed from the reaction mixture with the Dean-Stark trap, this allowed the time taken to complete the synthetic route to be truncated to 5 days. The yield under these conditions was slightly diminished to 15%, potentially due to loss of material in the first step due to the ability for magnesium to coordinate ketone compounds resulting in the intermediate not being removed from the mass of magnesium sulfate efficiently. Instead, using 3 Å molecular sieves as a desiccant in the first step allowed for the formation of the product in four days in 23% yield (*Table 6*, entry 4).

*Table 6: Conditions Used in the Imine Formation Step of the Synthesis of **142***

Entry	TsOH	Water Removal	Temperature	Total Reaction Time	Yield
1	None	Dean-Stark	150 ˚C	14 days	13%
2	0.01 equiv.	Dean-Stark	150 ˚C	11 days	22%
3	0.05 equiv.	MgSO₄	40 ˚C	5 days	15%
4	0.05 equiv.	3 Å Mol. Sieves	40 ˚C	4 days	23%

3.2.1.1.   Formation of Dienol Esters of Compound 142

With the conjugated ketone precursor **142** in hand, attention could then be turned to the formation of the dienol ester compounds necessary to participate in the fluorination reaction. The dienol benzoate was the most sought after as it had been identified as the closest analogue to the compound utilised in the steroidal fluorination. Benzoylation was attempted under the conditions used for the synthesis of the steroidal benzoate. Unfortunately, treatment of the ketone with pyridine and benzoyl chloride resulted in the formation of two inseparable regioisomers (**148** and **149**) as identified by their alkenyl proton chemical shifts in the ^{1}H NMR spectrum (*Scheme 84*). The reaction was attempted a number of times, altering the number of equivalents of pyridine used, the atmosphere the reaction was conducted under, the reaction vessel, the scale and the reaction time (Experimental Section, *Table 14*), however the results were inconsistent and it was not possible to find a version of these conditions that would yield the desired regioisomer exclusively. An alternative route was pursued following the procedure of Vandenheuvel and Wallis in which the ketone and benzoyl chloride were heated to reflux in hexane.[204] This procedure allowed the product to be isolated as a white solid in 17% yield. An improvement on this yield to 28% could be achieved by forgoing the solvent and simply heating the ketone in neat benzoyl chloride.
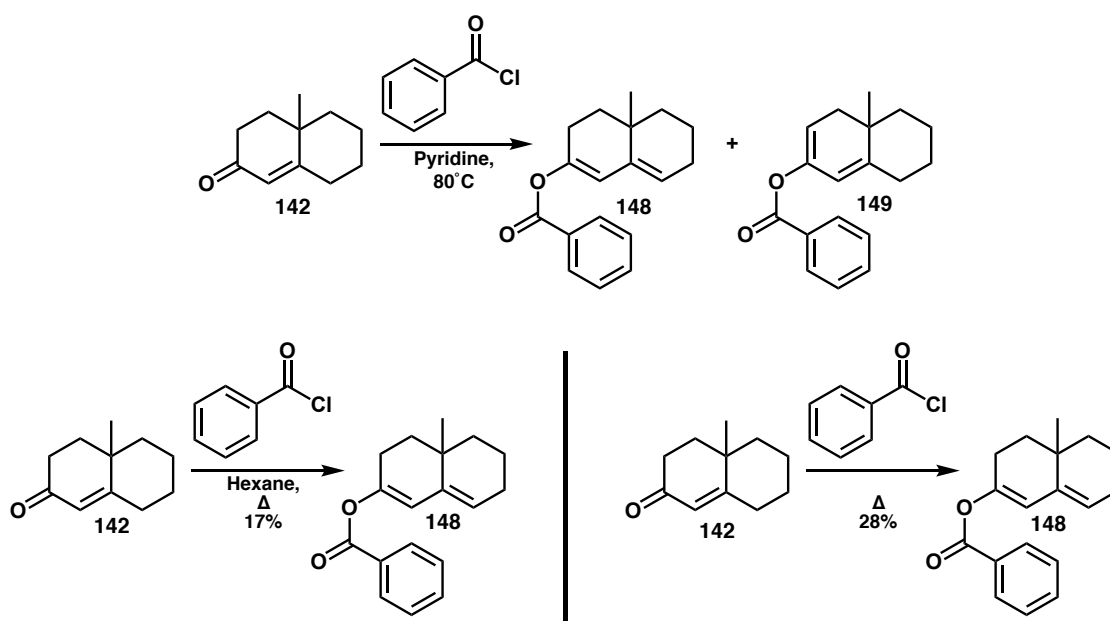
Scheme 84: Synthesis of Compound *148*

Synthesis of the acetate **150** required less optimisation as the desired compound **150** could readily be accessed *via* acetylation with acetic anhydride in pyridine with trimethylsilyl chloride and sodium iodide. Column chromatography of the crude material afforded compound **150** as a pale yellow oil in 74% yield (*Scheme 85*). Unfortunately, this compound appeared to be particularly sensitive to oxidation by atmospheric oxygen as the isolated oil rapidly changes colour from pale yellow to black in a matter of minutes if left to stand in air. ^{1}H NMR analysis of this substance confirmed that the desired compound was no longer present. It was therefore necessary to use the compound immediately after synthesis, making it an unsuitable substrate for kinetic studies.
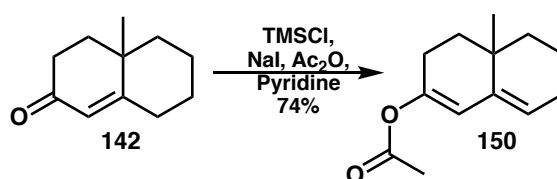
Scheme 85: Synthesis of Compound *150*

3.2.2. Fluorination of Dienol Esters 148 and 150

The highly unstable compound **150** was used to synthesise reference samples of the diastereomeric products α-**151** and β-**151**. Fluorination of **150** was performed in

123

acetonitrile at room temperature overnight (*Scheme 86*). Analysis of the crude reaction mixture by NMR indicated that the two diastereomeric fluorination products had been formed in a ratio of 68:32. Interestingly, in contrast to the behaviour observed in the full steroid, the fluorination of this smaller model compound favours fluorination on the face which bears the methyl group as opposed to in the steroid in which the opposite stereochemistry is preferred.

*Scheme 86: Fluorination of **150***
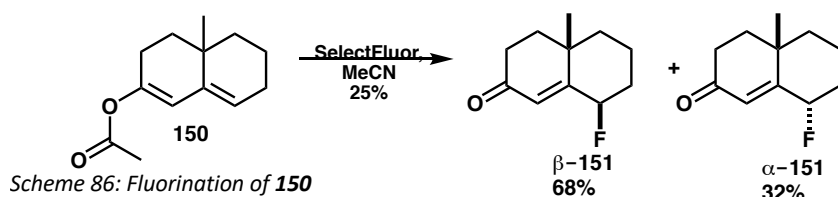
The diastereoisomers were separated by column chromatography, resulting in 25% overall yield. The two compounds exhibit significantly different chemical shifts in the ^{19}F NMR spectrum. One diastereoisomer appears at -168 ppm, whilst the other appears at -187 ppm. Identification of which compound bears an axial fluoride and which bears an equatorial fluoride was easily deduced from the ^{19}F and ^{1}H NMR spectra. The compound with the resonance at -168 ppm was the beta (axial) fluoride (compound **β-151**) whilst the resonance at -187 ppm corresponded to the alpha (equatorial) diastereoisomer (compound **α-151**). On compound **β-151** the proton on carbon 6 appears as a doublet of triplets, exhibiting characteristic geminal coupling to the fluorine atom of 48.9 Hz and a smaller coupling of 2.4 Hz, presumably to the protons on the adjacent carbon 7; however, the corresponding signal for these protons does not exhibit well defined coupling due to the complex nature of the spectra and overlapping signals. In the ^{19}F NMR spectrum the fluorine signal appears as a triplet of doublet of doublets. The large coupling of 48.9 Hz corresponds to geminal coupling to the proton on carbon 6 and coupling of the same magnitude to a proton on carbon 7. This is most likely the axial proton on carbon 7 due to efficient orbital overlap. Once again the signal for the axial proton on carbon 7 is not well resolved and therefore the associated coupling in the ^{1}H NMR spectrum cannot be identified. Coupling of 5.0 Hz can be observed in both the ^{19}F and ^{1}H spectra, corresponding to an interaction between the fluorine and the alkenyl

proton, which is split into a doublet. For compound **α-151** the geminal proton on carbon 6 appears as a doublet of doublet of doublet of doublets with large coupling to the fluorine atom of 47.8 Hz. This type of coupling pattern is consistent with the spectra of the other equatorial fluoride compounds discussed (*vide supra*). The ^{19}F NMR spectrum is poorly resolved, with only the 47.8 Hz geminal coupling apparent.

The dienol benzoate was fluorinated using 1.5 equivalents of SelectFluor in 5% *(v/v)* water in acetonitrile (*Scheme 87*). The reaction resulted in smooth conversion of compound **148** to the two diastereoisomers isolated as a result of the reaction with the dienol acetate. In agreement with the result obtained with **150**, the beta fluoride was favoured in the reaction resulting in a ratio of 63:37 beta:alpha fluorides.
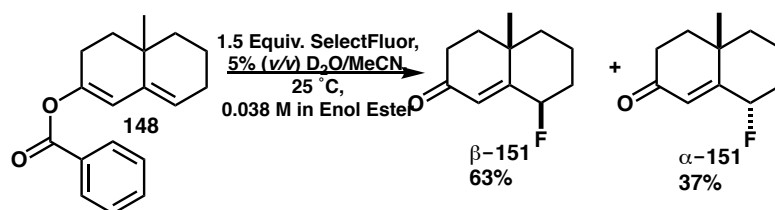
*Scheme 87: Fluorination of **148**, ratio determined by ^{19}F NMR*

3.2.3. Attempted Kinetic Studies

The unstable nature of dienol acetate compound **150** would make it difficult to apply to kinetic experiments; however, the isolation of the dienol benzoate **148** as a solid and the fact that it was possible to store the compound in the fridge for a number of days allowed this compound to be a viable candidate for live reaction monitoring. ^{1}H NMR spectroscopy was selected as a means of obtaining kinetic data as the procedure developed for the tetralone-derived fluorinations could be utilised.

3.2.3.1. Monitoring of the Reaction between 148 and SelectFluor by ^{1}H NMR Spectroscopy

An Eyring analysis of the fluorination reaction of this compound was desired. A kinetic experiment was attempted at 318 K to obtain what had been envisioned to be the highest temperature data point for this study. SelectFluor was added to the sample

which was at 318 K after being locked, shimmed and the initial spectrum acquired. When the first spectrum after the addition of SelectFluor was acquired the reaction had already gone to completion.

Cooling the instrument to 298 K and attempting to obtain kinetic data at this lower temperature was also unsuccessful as the reaction was also very fast at this lower temperature. It was only when the instrument was cooled to 278 K that kinetic data of sufficient quality and density could be obtained. When the data was analysed, first order kinetic behaviour was observed; the same behaviour was observed for the tetralone derived substrates. Comparison of these data to the rate constants obtained for the analogous fluorination reaction of the enol benzoate of tetralone **108** revealed that the rate of reaction for compound **148** was approximately fifty times faster (*Figure 54*). In the time taken for the reaction between compound **148** and SelectFluor to reach completion, the equivalent reaction using **108** had only reached 5% conversion.

Compound	k
108	6.40×10^{-5} s^{-1}
148	3.35×10^{-3} s^{-1}
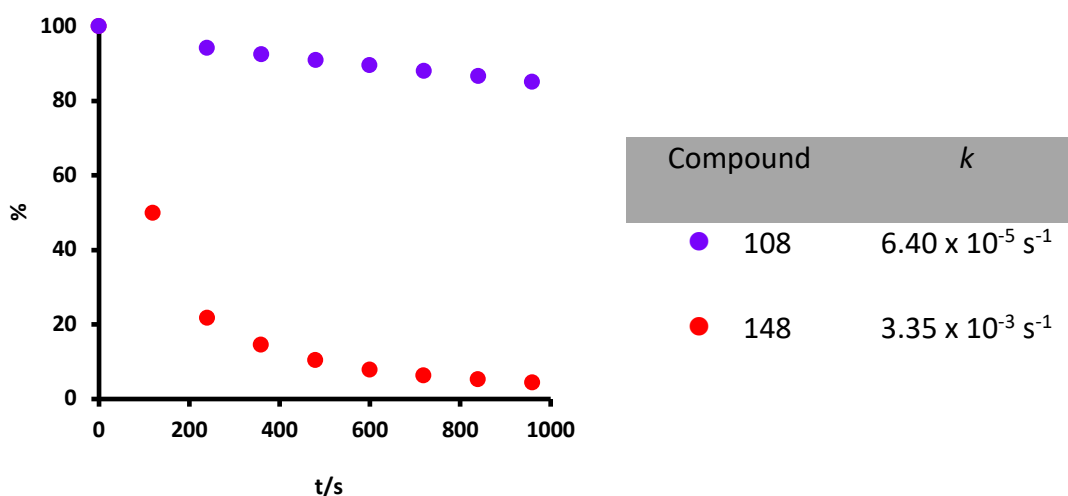
*Figure 54: Comparison of the Fluorination of **148** and **108***

3.2.3.2. Synthesis and Fluorination of Trifluoromethyl Benzoate 152

The dienol 4-trifluoromethylbenzoate **152** was synthesised in an attempt to reduce the reaction rate to something which would be more readily monitored. In a similar manner to the technique which had been applied successfully in the synthesis of dienol benzoate **148**, 4-trifluoromethylbenzoyl chloride was heated with enone **142**

under nitrogen (*Scheme 88*). This allowed the isolation of compound **152** in 32% yield as a white solid.

*Scheme 88: Synthesis of **152***
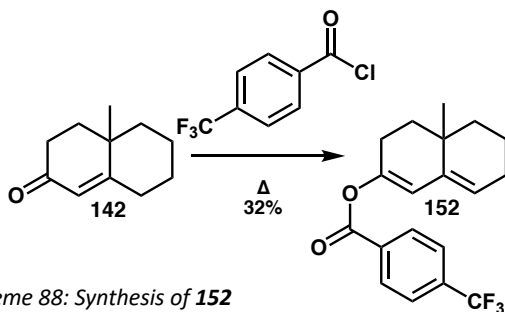
Compound **152** was subjected to the fluorination conditions at 278 K and the reaction was followed by ^{1}H NMR spectroscopy. Changing the identity of the enol ester had no effect on the alpha/beta ratio and this reaction produced compounds β-**151** and α-**151** in a ratio of 64:36. As expected, the rate of reaction was decreased relative to the unsubstituted compound **148**, but the rate of reaction was too high to be able to obtain enough rate measurements at different temperatures for an Eyring analysis. When the relationship between the rate of the 4-trifluoromethyl substituted compound **152** and compound **148** was compared to that of the 4-trifluoromethyl enol benzoate of tetralone **114** and the unsubstituted benzoate of tetralone (**108**) (*Table 7*) it was found that the rate of reaction was decreased by roughly the same factor, suggesting that the 4-substituent in each benzoate compound was exerting a similar level of influence on the rate of reaction. Ideally it would be possible to synthesise and monitor several analogues of these enol benzoates in order to obtain a Hammett plot and determine whether the relationship between the substituent in these benzoates is the same as that found for the tetralone based compounds. The fast nature of the reaction between the benzoylated derivatives of compound **142** would likely make monitoring of reactions of compounds bearing electron donating groups even more difficult to follow than those examined so far.

Compound	k (278 K)	Compound	k (298 K)
148	3.35 x 10^{-3} s^{-1}	**108**	4.97 x 10^{-4} s^{-1}
152	1.84 x 10^{-3} s^{-1}	**114**	3.01 x 10^{-4} s^{-1}

3.2.4. ^{18}Oxygen-Labelling Experiment

Whilst the kinetic experiments had not yielded as much insight into the mechanism of fluorination of these molecules as it was hoped, more information about how these molecules react could be gained from substituting the ^{16}oxygen-containing water for ^{18}oxygen-labelled water. Compound **148** was subjected to the standard fluorination conditions in 5% *(v/v)* H$_2$^{18}O in acetonitrile (*Scheme 89*). When the reaction mixture was analysed by GC/MS the ^{18}oxygen counterparts of both fluorinated diastereoisomers were identified as the only products from the reaction. This provides evidence that a carbenium is generated in the reaction of this compound and that the positive charge resides on the carbonyl carbon.
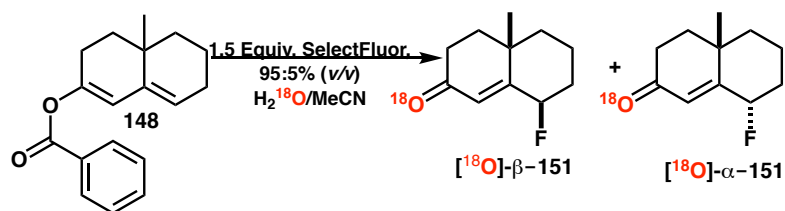
Scheme 89: ^{18}Oxygen-Labelling Experiment with Compound **148**

3.2.5. Synthesis of Bicyclic Dienone 153

Enone **142** did bear some similarity in shape to the A and B rings of the steroidal substrate, but it was missing the additional double bond in the A ring that was present in the steroid. From the results of the mechanistic study into the fluorination of tetralone derivatives it was discovered that adjacent conjugation that can stabilise a positive charge had a large influence on the rate of fluorination. The presence or absence of this

additional olefin may have an influence on the reaction, therefore a model compound which contains this functionality was also targeted (*Figure 55*).
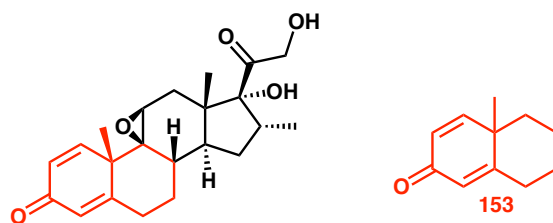
Figure 55: Comparison of Compound 153 with the Steroid

Dienone **153** was synthesised from readily available commercial starting materials. Formylation of cyclohexanone with ethyl formate yields **154**. This was followed by alkylation to install the methyl group to yield the intermediate 1,3-dicarbonyl compound **155**. This was then condensed with acetone and the crude material distilled to afford the desired compound as a yellow oil in 18% yield. This synthetic route was faster and less arduous than the synthesis of enone **142** *(Scheme 90)*. In addition to these advantages it avoided the use of the highly toxic methyl vinyl ketone.
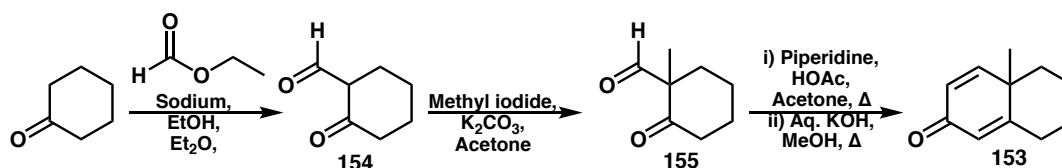
Scheme 90: Synthesis of Compound 153

3.2.6. Attempted Synthesis of Trienol Esters

With the ketone precursor in hand attention was turned to the synthesis of suitable enol esters for fluorination. When the successful conditions for benzoylation which had been found for the synthesis of **148** were applied to this substrate discolouration of the reaction mixture to a deep red colour was observed. This was accompanied by apparent complete decomposition of the starting material (as determined by ^{1}H NMR). Synthesis of the benzoate was then attempted with the addition of pyridine as a base as these compounds are known to undergo rearrangements under acidic conditions to form the corresponding aromatised products;

hydrochloric acid produced by the reaction of the benzoyl chloride may be inducing similar behaviour in either the starting material or product of the reaction leading to the observed degradation. Reactions including pyridine fared better: filtration of the reaction mixture through silica in 10% ethyl acetate in hexane and concentration of the filtrate yielded the desired compound **156** contaminated with a large quantity of benzoyl chloride (*Scheme 91*). Repeated attempts to separate benzoyl chloride from the product *via* chromatography or crystallisation were unsuccessful. Storage of this crude mixture resulted in degradation of the product.
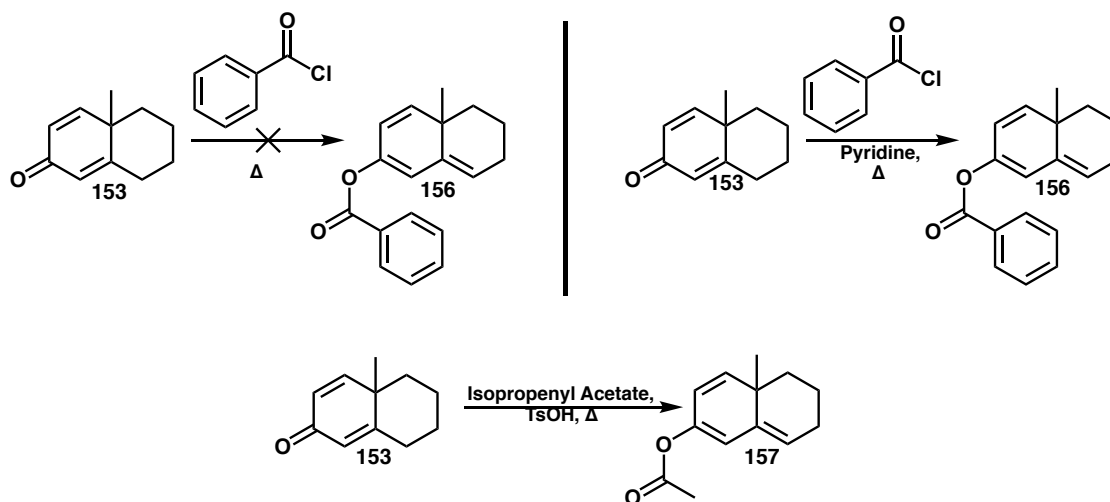
*Scheme 91: Attempted Synthesis of **156** and **157***

Synthesis of the acetate was also attempted under the standard isopropenyl acetate conditions which had been broadly successful for the tetralone compounds. Analysis of the crude reaction mixture by ^{1}H NMR evidenced the apparent formation of the product **157** however this compound was also not isolable by column chromatography or crystallisation (*Scheme 91*). Due to the difficulties in isolation the synthesis of these compounds was abandoned.

3.2.7. Conclusions and Proposed Mechanism for the Fluorination of 148

The fluorination of dienol benzoate **148** proceeded at an accelerated rate compared to tetralone derivative **108**, with the introduction of an electron withdrawing group in the 4-position of the aryl ring resulting in a decrease in reaction rate. This

combined with the incorporation of ^{18}oxygen at the carbonyl position is consistent with the generation of a carbenium in this position. It is therefore postulated that the reason for the increase in reaction rate is the ability for vinylic stabilisation of the positive charge across carbons 3, 4 and 5 (*Scheme 92*). This would allow there to be less of a localisation of positive charge in close proximity to the fluorine atom. The rate enhancement was likely to be so significant due to the fact that whilst delocalisation of the carbenium is possible in the tetralone substrates it comes at the expense of aromaticity, which is a problem not faced by compound **148**.
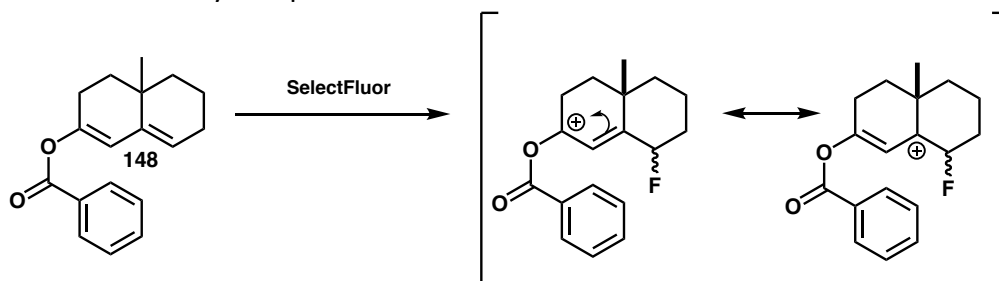
*Scheme 92: Rationale for the Enhanced Rate of Reaction of Compound **148***

It was hoped that compound **156** or **157** would yield further insight into the role of delocalisation in the reaction mechanism, but problems with synthesis and isolation have thus far precluded the study of these compounds in fluorination reactions. If the hypothesis that increased vinylic delocalisation increases the rate of reaction is correct then compounds **156** and **157** would be expected to react at a higher rate than **148** which is already relatively difficult to monitor. When this was taken into consideration along with the knowledge that the steroidal benzoate is the real compound of interest and it was unclear whether the reactivity of these models would be transferable to the steroid the decision was made to proceed to study the steroid directly.

3.3.   Fluorination of Alpha-Methyl Epoxide Derivatives

The bicyclic model compound had allowed a small amount of insight to be gained into the fluorination of more conjugated systems and indicated that it was possible that a related mechanism to the tetralone derivatives was in operation. Attention was then

turned to understanding the fluorination process of the steroidal benzoate **99b** and whether the stereochemical outcome could be tuned during the fluorination step (*Figure 56*).
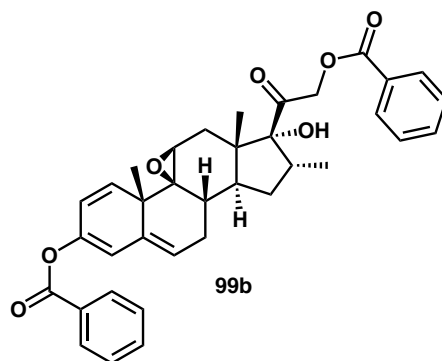
Figure 56: Fluorination Substrate **99b**

3.3.1. Synthesis and Fluorination of Compound 99b

During the industrial process an efficient procedure had been developed in which the crude trienol benzoate was taken crude into the fluorination step without isolation in order to minimise the formation of the 6-hydroxyl side product. For complete interrogation of the reaction mechanism it was necessary to submit clean isolated starting material to the fluorination in order to fully understand the factors at play. Fortunately, an isolation procedure for the synthesis of **99a** had also been developed. Alpha-methyl epoxide **99a** was benzoylated *via* reaction with benzoyl chloride in pyridine at 80 ˚C for 3 hours (*Scheme 93*).
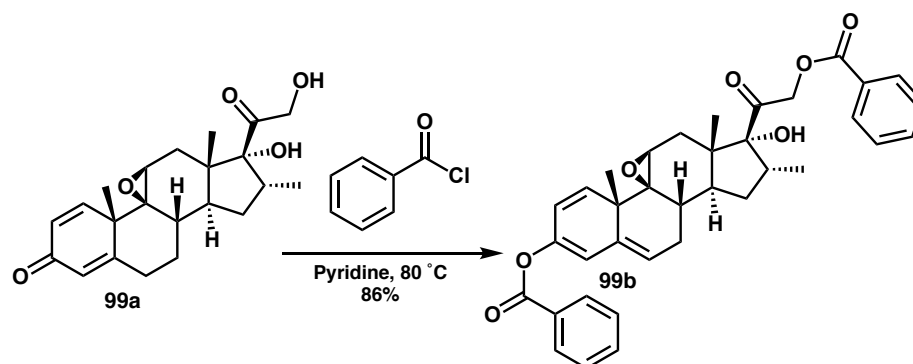
Scheme 93: Synthesis of **99b**

Cooling of the reaction mixture to room temperature followed by the addition of water and acetonitrile resulted the precipitation of benzoyl compound **99b** as an off-white sold. Drying of this solid under vacuum at 40 ˚C overnight yields clean compound in 86% yield ready to be subjected to the fluorination conditions.

When compound **99b** is fluorinated in 5% *(v/v)* water in acetonitrile at a concentration of 0.038 M the formation of two fluorinated products is evidenced by ^{19}F NMR in a ratio of 90:10 (*Scheme 94*). These can readily be identified as the alpha and beta diastereoisomeric products, respectively. When the reaction is conducted at this low concentration both products remain in solution; when reactions are performed at higher concentrations the more polar alpha-product begins to precipitate rapidly from the reaction mixture, leaving the majority of the more soluble beta-product in solution.
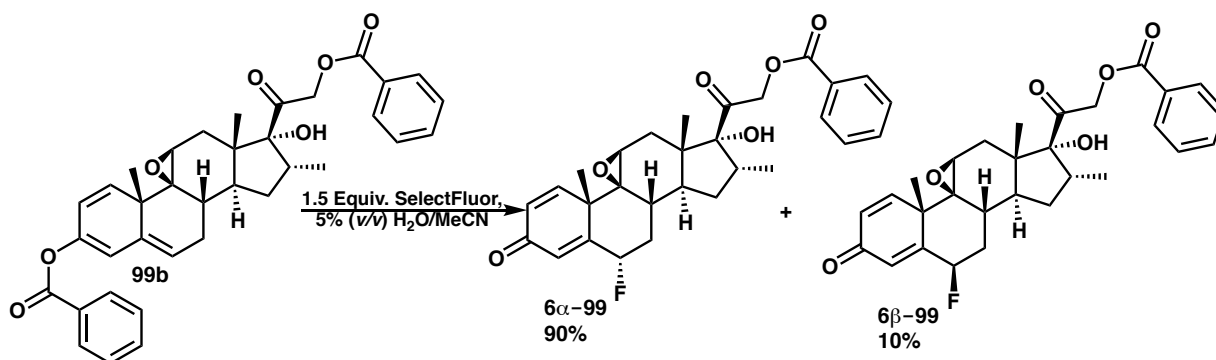
*Scheme 94: Fluorination of **99b***

3.3.2. Synthesis of 4-Substituted Enol Benzoates

With high quality kinetic data for the reactions of 4-substituted enol benzoates of tetralone already in hand, a Hammett series of benzoate compounds of the steroid **99b** was sought. If there were a positive charge generated at the carbonyl position in these compounds during the fluorination reaction, the relationship between the 4-substituent on the benzoate and the charge would be the same as in the tetralone series, therefore a similar relationship between the reaction rate and the Hammett parameters would be expected (i.e. $\rho \approx$ -0.36). To this end, a series of enol benzoates were synthesised using the same conditions as described above, by varying the benzoylating reagent. By these

means the six enol benzoates **158a**-**162a** were synthesised (*Scheme 95*). During isolation of these compounds it immediately became apparent that the solubilities of these compounds varied widely depending on the substituent. The compounds **159a** and **160a** were particularly insoluble, requiring the addition of acetone to the crude aqueous acetonitrile mixture to prevent the compound precipitating as an impure red gum. Once the crude mixture was monophasic water could then be added to facilitate the precipitation of the desired compounds. The compounds **158a** and **162a** appeared to have enhanced solubility in aqueous acetonitrile compared to the parent. This solubility was to the extent that an aqueous extraction in dichloromethane with saturated aqueous copper sulfate was required to remove pyridine from the crude mixture. The crude organic phase was concentrated before the residue was dissolved in acetone and the products were precipitated with water. The extraction protocol lead to significant losses in isolated yield in comparison to the direct precipitation procedure however sufficient material was isolated for the reaction of these compounds to be studied, in appropriate purity for kinetic studies.
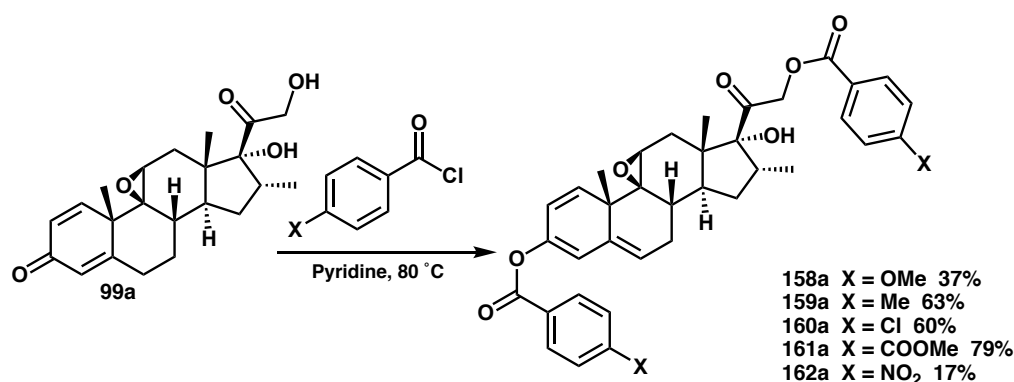
Scheme 95: Synthesis of Compounds **158a-162a**

3.3.3. Assay Development

With a Hammett series of compounds in hand it was then necessary to find an appropriate monitoring technique for the reaction. Whilst ^{1}H NMR spectroscopy has proved fruitful for the study of the smaller model compounds and tetralones, it is unsuitable here due to the poor solubility properties of the steroid. Even at the low

concentration of 0.038 M, complete dissolution of parent compound **99b** does not occur even on heating in 5% *(v/v)* water in acetonitrile. The addition of other solvents to assist dissolution would be desirable however ^{1}H NMR studies limit solvent choice to deuterated solvents and the addition of a third component would only serve to complicate what is already a complex ^{1}H NMR spectrum. In addition to these problems, if the steroid does react analogously to the model compound **148** then the reaction is likely to be too fast to follow by ^{1}H NMR. An alternative technique was therefore sought. React-IR was selected as a possible means of reaction monitoring as it is possible to acquire spectra every fifteen seconds (six times more frequently than by the ^{1}H NMR protocol). The IR-probe was inserted into the reaction which was conducted in an EasyMax reactor (*Figure 57*). The temperature of the reaction mixture was monitored using a temperature probe which measured the reaction mixture directly and a cooling jacket around the vessel maintained the desired temperature. Stirring was accomplished *via* an overhead stirrer. The steroid substrate was dissolved in the solvent mixture and the vessel allowed to reach the desired temperature. Once this temperature had been reached and the IR spectrometer was acquiring spectra the SelectFluor was added and the progress of the reaction was followed until the IR spectra indicated complete consumption of the steroid.
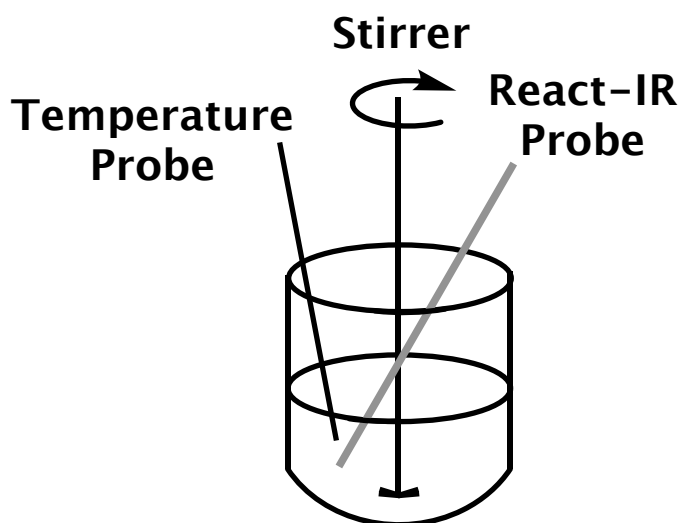
Figure 57: React-IR Set-Up

The reaction between **99b** and 1.5 equivalents SelectFluor was initially attempted under the standard conditions that would be used in ^{1}H NMR experiments (0.038 M at 25 ˚C). The disappearance of a signal at *ca.* 1250 cm^{-1}, assigned to the ester C-O stretch, could be followed (*Figure 58*). At 25 ˚C the reaction appeared to be complete in a matter of seconds. The temperature was lowered to 0 ˚C which allowed more dense kinetic data to be obtained. Reducing the temperature further to -30 ˚C in an attempt to obtain data for an Eyring analysis was unsuccessful as the substrate did not dissolve under these conditions. Attention turned instead to obtaining a Hammett plot. The reaction of 4-methoxy compound **158a** proceeded smoothly at 0 ˚C at 0.038 M in 5% *(v/v)* water in acetonitrile, but when the reactions of the poorly soluble 4-methyl or 4-chloro compounds (**159a** or **160a**) were attempted no dissolution of the substrate was observed and the reaction was therefore not possible to follow. A solvent system that would dissolve all of the Hammett substrates was therefore sought.
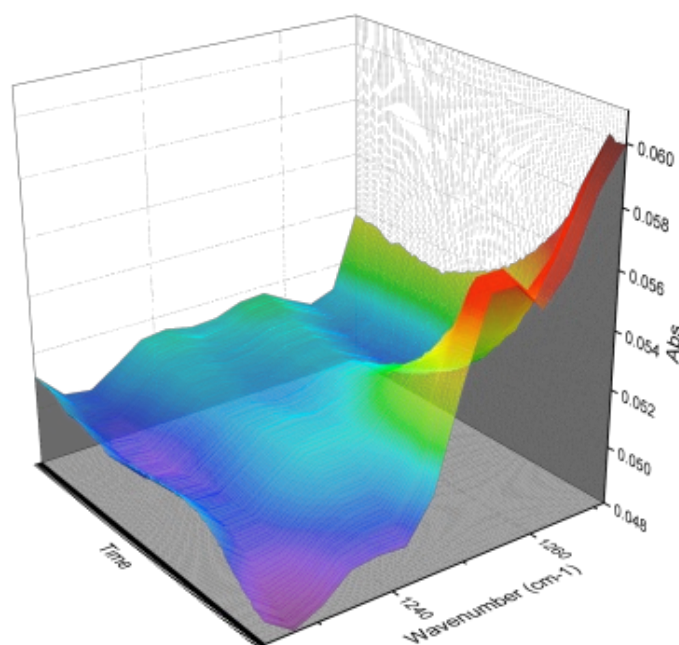
Figure 58: Signal at 1260 cm^{-1} Over Time

A 2:1 mixture of 2-MeTHF and the 5% *(v/v)* water in acetonitrile solvent system appeared to dissolve all of the substrates at 0.038 M, but SelectFluor was insoluble under

these conditions. Given the high aqueous solubility of SelectFluor, the water content of the solvent was increased. The React-IR probe is added to a reaction vessel which is stirred, therefore it may be possible to follow a biphasic mixture. A 2:1 2-MeTHF/water mixture was trialled due to the acceptable solubility of the steroids in 2-MeTHF and high solubility of SelectFluor in water. Unfortunately, the mixture produced noisy spectra under the reaction conditions and it was not possible to obtain a rate constant. A homogeneous mixture was again sought. A 9:1 mixture of THF and water did not result in sufficient SelectFluor dissolution. Using a 2:1 mixture of 2-MeTHF and 5% *(v/v)* water in acetonitrile with the concentration of substrate lowered to 0.019 M allowed for sufficient SelectFluor dissolution for the reaction to be followed. The conditions attempted are summarised in *Table 8*.

*Table 8: Conditions attempted using React-IR. *5% (v/v) indicates 5% (v/v) water in acetonitrile.*

Solvent	X	Concentration	Temperature	Comments
95:5 MeCN:H_2O	H	0.038 M	25 °C	Immediate completion
95:5 MeCN:H_2O	H	0.038 M	0 °C	*k* obtained, n=2
95:5 MeCN:H_2O	H	0.038 M	-30 °C	Substrate insoluble
95:5 MeCN:H_2O	OMe	0.038 M	0 °C	*k* obtained, n=2
95:5 MeCN:H_2O	Me	0.038 M	0 °C	Substrate insoluble
95:5 MeCN:H_2O	Cl	0.038 M	0 °C	Substrate insoluble
2:1 2-MeTHF/5% *(v/v)**	H	0.038 M	0 °C	SelectFluor insoluble
2:1 2-MeTHF:H_2O	H	0.038 M	0 °C	Noisy spectra
90:10 THF:H_2O	H	0.038 M	0 °C	SelectFluor insoluble
2:1 2-MeTHF/5% *(v/v)**	H	0.019 M	0 °C	*k* obtained, n=2

3.3.4. Hammett Study

With suitable conditions obtained to monitor the fluorination the influence of each of the 4-substituents on the rate of reaction could be examined. As has been previously observed in the tetralone series, the addition of an electron donating

substituent in the 4-position results in an increase in the rate of reaction whilst an electron withdrawing substituent decreases the rate of reaction. When $\log_{10}(k_X/k_H)$ is plotted against the Hammett σ_p and σ_p^+ parameters the correlation is stronger to σ_p, in contrast from what was observed for the tetralone series (*Figure 59*). This was somewhat surprising; however, given the enhanced stabilisation afforded by the adjacent alkene in model compound **148** it is possible that this phenomenon is also at play in this instance. The value of ρ for the Hammett plot is still negative, albeit smaller than previously observed, which is still indicative of a build-up of positive charge in the transition state.

X		σ_p	σ_p^+	k
🔴	OMe	-0.27	-0.78	$3.84 \times 10^{-4}\ s^{-1}$
🟠	Me	-0.17	-0.31	$3.61 \times 10^{-4}\ s^{-1}$
🟠	H	0.00	0.00	$3.31 \times 10^{-4}\ s^{-1}$
🟢	Cl	0.23	0.11	$2.55 \times 10^{-4}\ s^{-1}$
🔵	NO$_2$	0.78	0.78	$1.75 \times 10^{-4}\ s^{-1}$
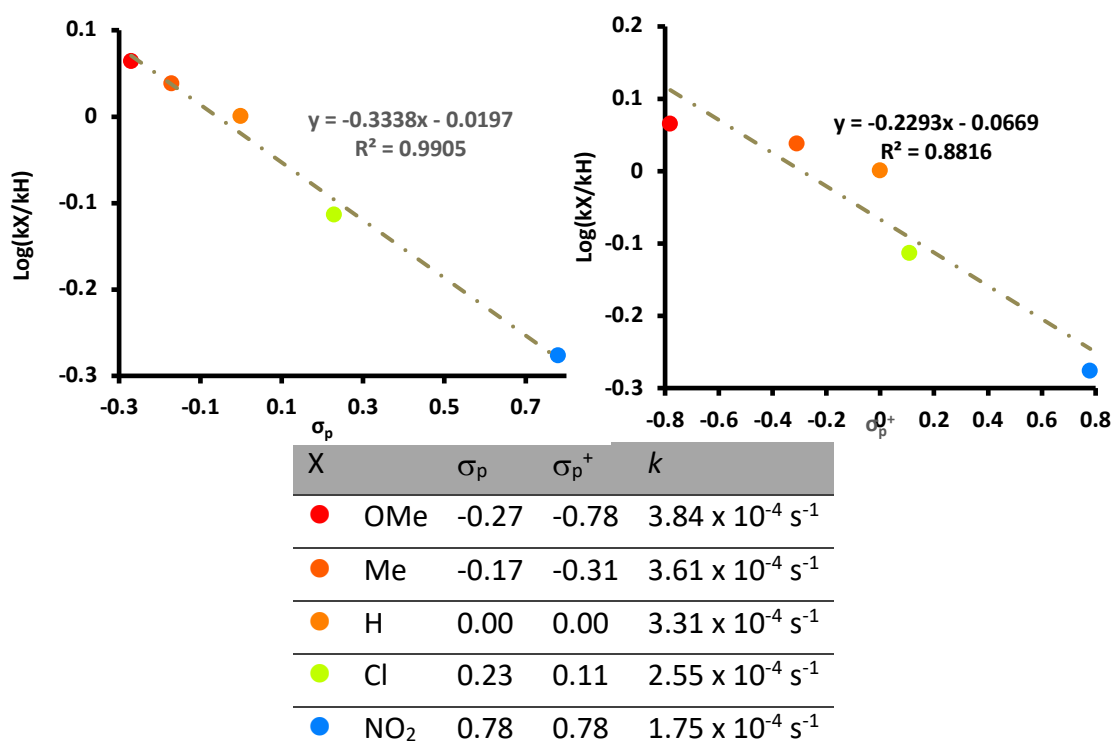
*Figure 59: Hammett Study Using Compounds **158a-163a** and **99b**, 1.5 Equivalents of SelectFluor, 2:1 2-MeTHF/5% (v/v) water/MeCN, 0 ˚C, 0.019 M in substrate, k is an average of two runs*

The rate of reaction at 0 ˚C in 5% *(v/v)* water in acetonitrile of the parent benzoate was again much faster than that observed for the enol benzoate of tetralone at 5 ˚C. Despite the data being collected at a lower temperature the rate of reaction is higher when compared to the rate obtained for the model compound. This adds credence to

the hypothesis that increased vinylic stabilisation of the carbenium leads to an increase in the rate of reaction (*Table 9*).

*Table 9: Comparison of Reaction Rates of **108**, **148** and **99b***

Compound	k	T
108	4.97×10^{-4}	278 K
148	3.35×10^{-3}	278 K
99b	4.35×10^{-3}	273 K

3.3.5. Eyring Analysis

From the Hammett study it is clear that whilst the reaction mechanism is likely to be related to the mechanism in operation for the tetralone substrates there are substantial differences. In order to elucidate this further the reaction of parent benzoate **99b** was conducted at 253 K, 263 K and 283 K in order to obtain the energy barriers to the reaction (*Scheme 96*). Unfortunately, the poor solubility of the reaction components at 243 K and the high rate of reaction at 293 K precluded the access to a fifth data point for the analysis.

*Scheme 96: Conditions for Eyring Experiment on **99b***
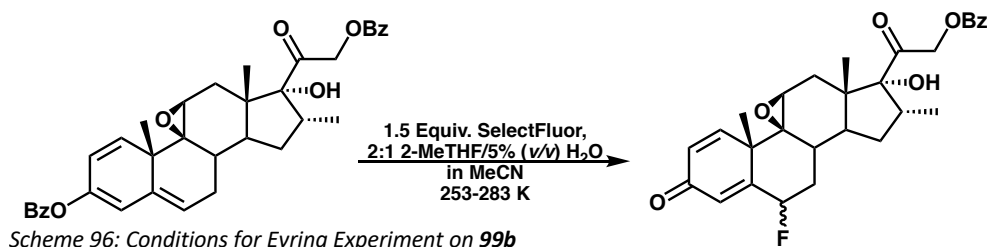
The free energy barrier to reaction at 298 K was found to be 1 kcal mol^{-1} lower than the value obtained for the enol benzoate of tetralone (*Figure 60*). The change in entropy was 11 kcal mol^{-1} K^{-1} larger in magnitude than that observed in the reaction between SelectFluor and the enol benzoate of tetralone. This was indicative that the transition state was more tightly bound than with compound **99b**.

Equation y = -5447.1x + 6.3007

$\Delta G^{\ddagger}/kcal\ mol^{-1}$	$\Delta H^{\ddagger}/kcal\ mol^{-1}$	$\Delta S^{\ddagger}/cal\ mol^{-1}\ K^{-1}$
21.1	10.8	-35
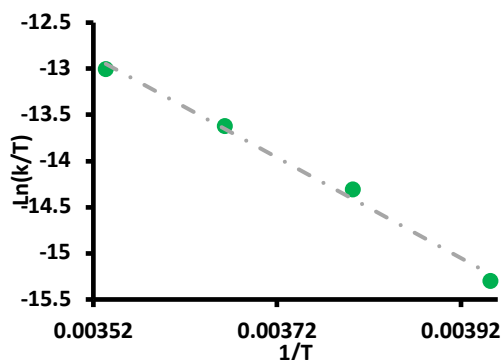
Figure 60: Eyring Analysis of Compound **99b**

3.3.6. Alpha/Beta Ratios of Compounds 99b and 158a-163a

To determine whether the reactions had gone to completion the mixtures were analysed by HPLC at the end of the acquisition period. From this, the diastereomeric ratio could also be obtained. It was of interest to determine whether the ratio could be changed by changing the identity of the enol ester. The outcomes are summarised in *Table 9*. Interestingly, the same alpha/beta ratio was conserved throughout the series and was identical to the ratio obtained when 5% *(v/v)* water in acetonitrile was utilised at the higher concentration of 0.038 M. This indicates that the inherent selectivity of the fluorination reaction is 9:1 alpha/beta.

Table 9: α:β Ratios

X	α	β
OMe	90	10
Me	87	13
H	90	10
Cl	90	10
COOMe	88	12
NO$_2$	89	11

3.3.7. ¹⁸Oxygen Labelling Study

To see if it would be possible to confirm the presence of a carbenium intermediate the reaction between SelectFluor and compound **99b** was performed in 5% *(v/v)* $H_2^{18}O$ in acetonitrile (*Scheme 97*). The reaction mixture was analysed by LC/MS to determine whether ¹⁸oxygen had been incorporated. The mass ion observed corresponded to [M - HF], with the inclusion of ¹⁸oxygen. This provided further evidence that a carbenium was also generated in the reaction of compound **99b** as well as in the reaction of the tetralone derivatives and the reaction of the model compound.
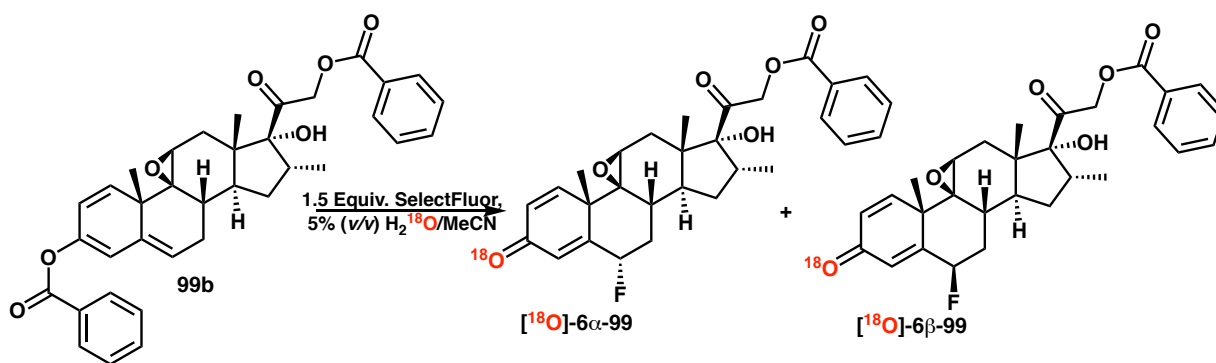
Scheme 97: *¹⁸Oxygen-Labelling Experiment with* **99b**

3.3.8. Conclusions and Proposed Mechanism

Whilst there are apparent differences in the behaviour of the steroidal enol benzoates when compared with enol esters of tetralone clear evidence has been uncovered that implicates the formation of a carbenium in the rate determining step. The ¹⁸oxygen labelling study provides evidence that this carbenium is situated on the carbonyl carbon. The shallow negative slope of the Hammett plot is consistent with delocalisation of the charge such that the substituent effect is not as great as observed with the enol benzoates of tetralone. Stabilising delocalisation is also evidenced by the rate enhancement provided in relation to both the tetralone derived **108** and model compound **148** (*Scheme 98*).
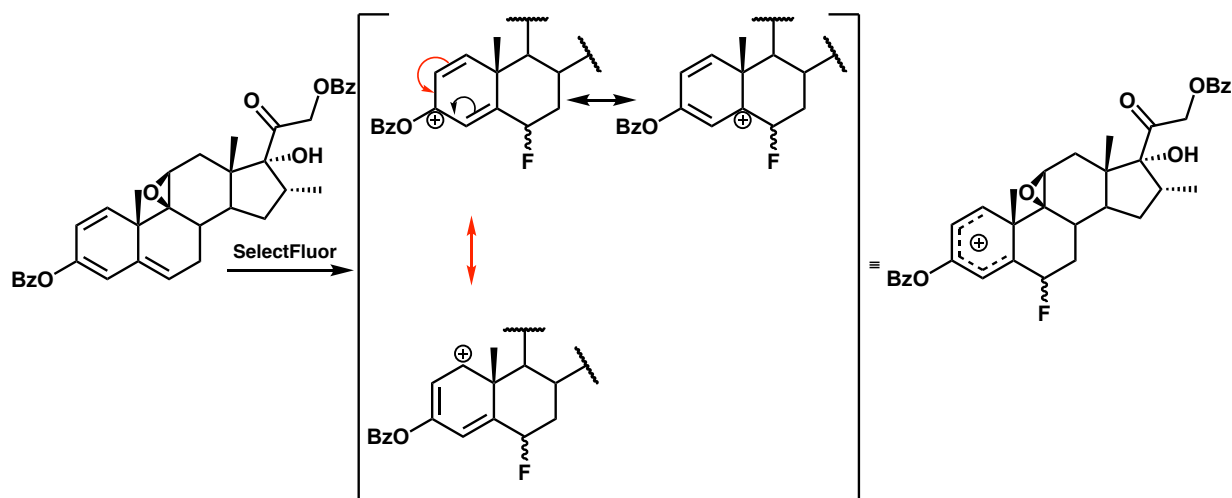
*Scheme 98: Proposed Mechanism for the Fluorination of **99b***

The selectivity of the reaction is independent of solvent, the identity of the benzoate and concentration in the studies that have been conducted. It is likely for that the 9:1 selectivity is intrinsic to the reaction and that the high alpha/beta ratio observed in the industrial process is most likely to be the result of acid-catalysed equilibration of the alpha-fluoride or selective crystallisation of this compound from the reaction mixture.

3.4.   Computational Study

Further understanding into the mechanism of fluorination of enol esters was sought by conducting electronic structure calculations using density functional theory (DFT). The reaction of simple tetralone substrate **100** was examined initially in order to find a methodology that would sufficiently describe the experimental behaviour, providing a model of the reaction mechanism that corroborates the experimental data. This model would then be applied to elucidate the reaction mechanism of side product formation and in future could be used as a predictive model for the behaviour of these types of molecules.

3.4.1. Selection of a Functional and Basis Set

With the experimental values of $\Delta G^{\ddagger}$, $\Delta H^{\ddagger}$, $\Delta S^{\ddagger}$ and a reasonable mechanistic proposal for the rate determining step in hand, a functional and basis set that accurately replicates these values for the energy barriers to fluorine atom transfer was sought. Given the experimental data, a polar transition state was initially investigated for the rate determining fluorine transfer (*Figure 61*). Some common functionals were used with the 6-31G* basis set. The 6-31G* basis set was selected as a compromise between fast calculation time and accuracy in describing the molecules. The 5% *(v/v)* water in acetonitrile solvent system was approximated using the SMD[205] acetonitrile solvation model.
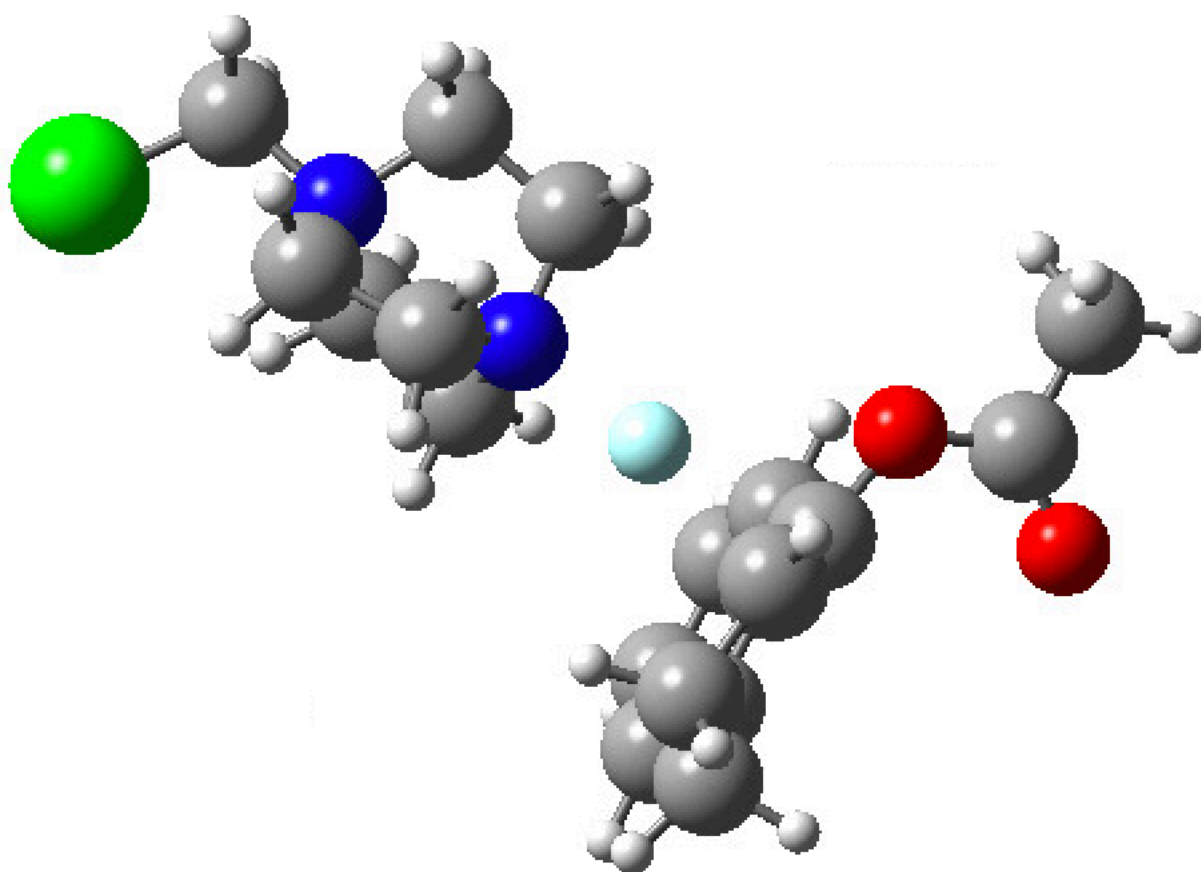
Figure 61: Polar Fluorine Atom Transfer Transition State (ωB97XD, 6-31G SMD solvation MeCN)*

Each of the functionals examined introduced a systematic over-estimation of $\Delta S^{\ddagger}$ and either overestimated or vastly underestimated $\Delta H^{\ddagger}$. The only two functionals which

performed well in estimating $\Delta H^{\ddagger}$ were ωB97XD and CAM-B3LYP, both of which are corrected for long range interactions (*Table 10*). The ωB97XD functional also has Grimme's D2 empirical correction for dispersion interactions and outperforms it's non-dispersion containing counterpart ωB97X. ωB97 contains neither the short range Hartree-Fock exchange denoted by X or the empirical dispersion included in ωB97XD, and this results in a large overestimation of $\Delta G^{\ddagger}$ and $\Delta H^{\ddagger}$. When D3 empirical dispersion is imposed on B3LYP in the B3LYP-D3 functional a very poor approximation of the energy barriers was obtained. The Minnesota functionals that were tested (M06, M06-2X and M06-HF) performed poorly. M06 provided a relatively accurate value for $\Delta G^{\ddagger}$ however the values of $\Delta H^{\ddagger}$ and $\Delta S^{\ddagger}$ were far removed from the experimentally determined results. Despite producing the smallest overestimation of $\Delta S^{\ddagger}$, M06-2X produced a large overestimation of both $\Delta G^{\ddagger}$ and $\Delta H^{\ddagger}$. M06-HF produced large overestimations of all of the energy values. ωB97XD was chosen as giving the best all-round approximation of $\Delta G^{\ddagger}$, $\Delta H^{\ddagger}$ and $\Delta S^{\ddagger}$, compared to the experimental data.

Table 10: Computation of the Polar Transition State Using Different Functionals

Functional	ΔG/ kcal mol^{-1}	ΔH/ kcal mol^{-1}	ΔS/ kcal mol^{-1} K^{-1}	$\Delta\Delta$G$_{(Exp)}$	$\Delta\Delta$H$_{(Exp)}$	$\Delta\Delta$S$_{(Exp)}$
Experimental	22.0	15.0	-24	-	-	-
B3LYP	18.1	6.4	-39.2	-3.9	-8.6	-15.2
B3LYP-D3	16.5	5.0	-38.8	-5.5	-10.0	-14.8
CAM-B3LYP	27.6	15.5	-40.6	+5.6	+0.5	-16.6
ωB97	36.1	24.8	-38.2	+14.1	+9.8	-14.2
ωB97X	33.4	22.4	-36.7	+11.4	+7.4	-12.7
ωB97XD	**27.6**	**16.3**	**-37.7**	**+5.6**	**+1.3**	**-13.7**
M06	21.0	8.5	-42.2	-1.0	-6.5	-18.2
M06-2X	33.9	23.1	-36.3	+11.9	+8.1	-12.3
M06-HF	52.3	40.9	-40.0	+30.3	+25.9	-16.0
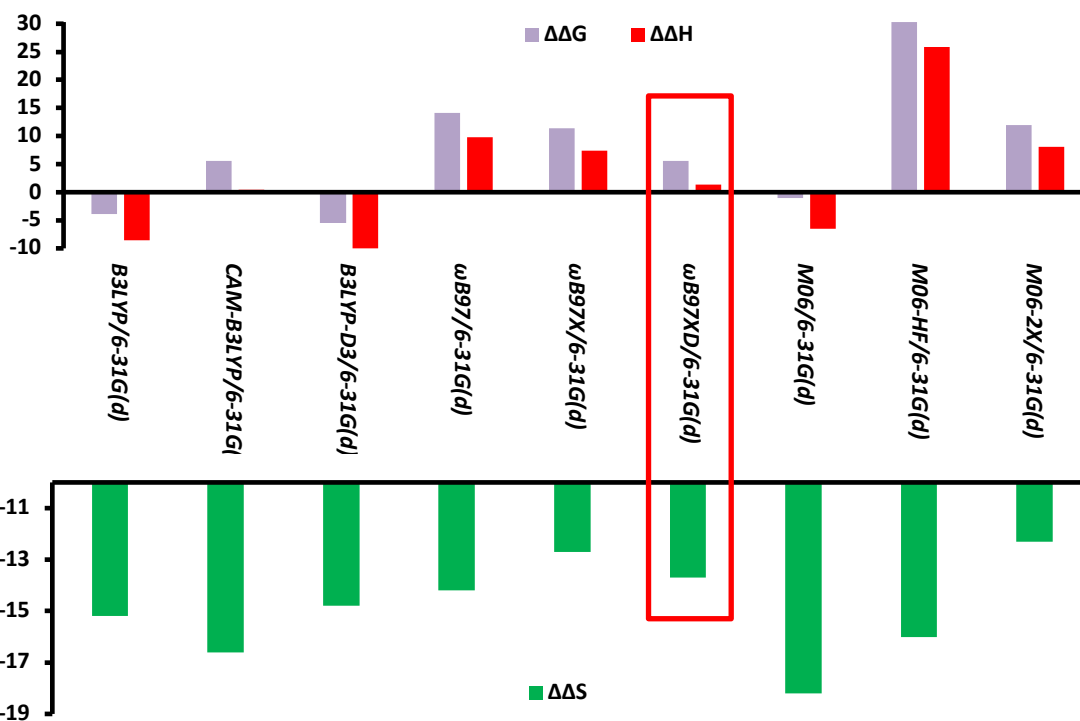
Figure 62: Graphical Comparison of Functional Performance

3.4.2. Computation of Full Polar Pathway for Compound 100

The experimental results provide strong evidence for the generation of a positively charged intermediate in the 1 position next to the carbonyl. A full pathway from enol ester and SelectFluor to the fluoroketone product was therefore computed (*Figure 63*). In good agreement with the experimental data, this pathway indicates fluorine atom transfer (TS1) to be rate determining and irreversible. The energy barrier to the transition state for hydrolysis through the carbenium (TS2) is low, forming a tetrahedral intermediate. The transfer of a proton from the hydrolysing water in P2 to the carbonyl of the ester in P3 lowers the energy further. There is a small barrier (TS3) to the formation of the ketone carbonyl and loss of acetic acid to form protonated ketone product P4.
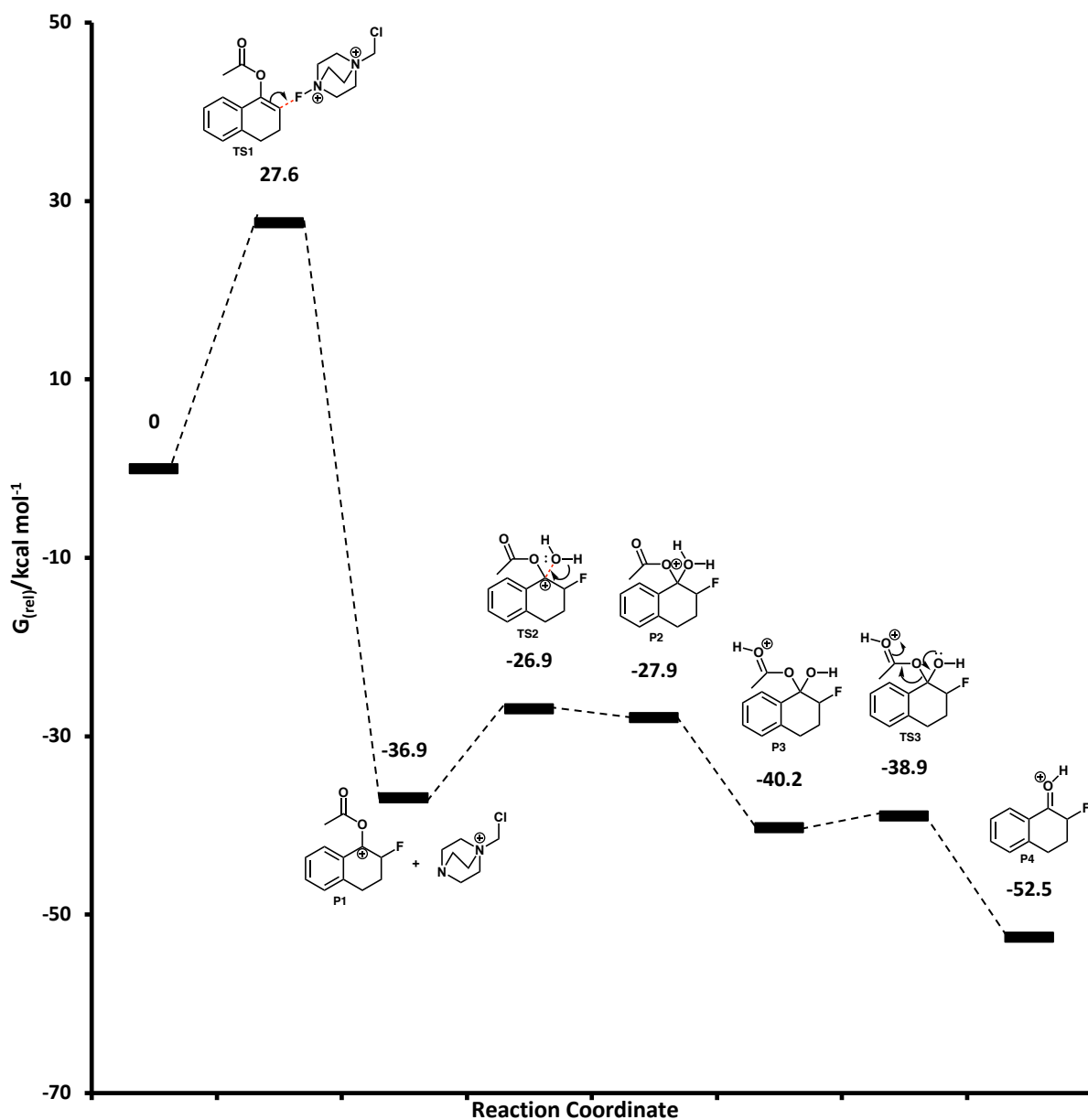
*Figure 63: Polar Pathway for the Fluorination of **100***

3.4.3. Computation of Radical Pathway for Compound 100

Whilst the experimental evidence for a polar pathway is compelling, a radical reaction mechanism could not be entirely discarded. However, the experimental evidence is conclusive in that the transition state for the rate determining step involves the generation of a (partial) positive charge and that the carbenium intermediate **P1** is highly likely to be present along the pathway resulting in the full incorporation of a

solvent oxygen atom in the final product. If a SET mechanism is in operation, it will involve the formation of a radical cation in which the cation resides on the carbonyl carbon. It is therefore necessary to compute the single electron oxidation of the enol ester by SelectFluor.

It is possible to estimate the activation energy to single electron transfer using Marcus theory. This is based on the assumption that the largest barrier to single electron transfer will be the energy required for structural reorganisation resulting from the loss or gain of an electron. The activation energy in this case is described by *equation 4*, which relates the barrier to electron transfer to the internal reorganisation energy and ΔG for the overall reaction.

Equation 4: Calculation of ΔG using Marcus Theory

$$\Delta G^{\ddagger} = \frac{\lambda_i}{4}\left(1 + \frac{\Delta G}{\lambda_i}\right)^2$$

Where λ_I is the internal reorganisation energy which is defined by *equation 5*, below.

Equation 5: Definition of Internal Reorganisation Energy

$$\lambda_i = \frac{1}{2}(\lambda_{i\ enol\ ester\ radical\ cation} + \lambda_{i\ SelectFluor\ radical\ anion})$$

The reorganisation energy λ_I for each species is defined by the following equation (*Equation 6*, below).

Equation 6: Calculation of Reorganisation Energy

$$\lambda_i = \left(E_s(R_R) - E_S(R_s)\right) + \left(E_R(R_S) - E_R(R_R)\right)$$

Where $E_S(R_R)$ is the energy of the neutral species with the geometry of the radical species, $E_S(R_S)$ is the energy of the neutral species in its optimised geometry, $E_R(R_S)$ is the energy of the radical species in the geometry of the neutral species and $E_R(R_R)$ is the energy of the radical in its optimised geometry.

The use of this methodology with ωB97XD, 6-31G* and SMD acetonitrile solvation produces an energy barrier *ca.* 5 kcal mol^{-1} higher in energy than the same functional produces for a polar fluorine atom transfer step. Not only this, but the radical intermediates are relatively high in energy (23.5 kcal/mol relative to the starting materials), indicating that this single electron transfer is likely to be reversible. It was also necessary to attempt to find a transition state for the recombination of these two radical species, forming the cationic intermediate **P1** which is implicated by the experimental data. Optimisation of this transition state proved to be challenging, and attempts to find an open shell singlet transition state resulted in the calculation converging as the closed shell (polar) transition state during the optimisation. Running a potential energy surface (PES) scan in which the distance between the fluorine atom and carbon on the enol ester was varied, starting from the optimised radical structures, suggested that at a N-F distance of *ca*. 2 Å and C-F distance of *ca.* 2.4 Å may be close to a stationary point (*Figure 64*).
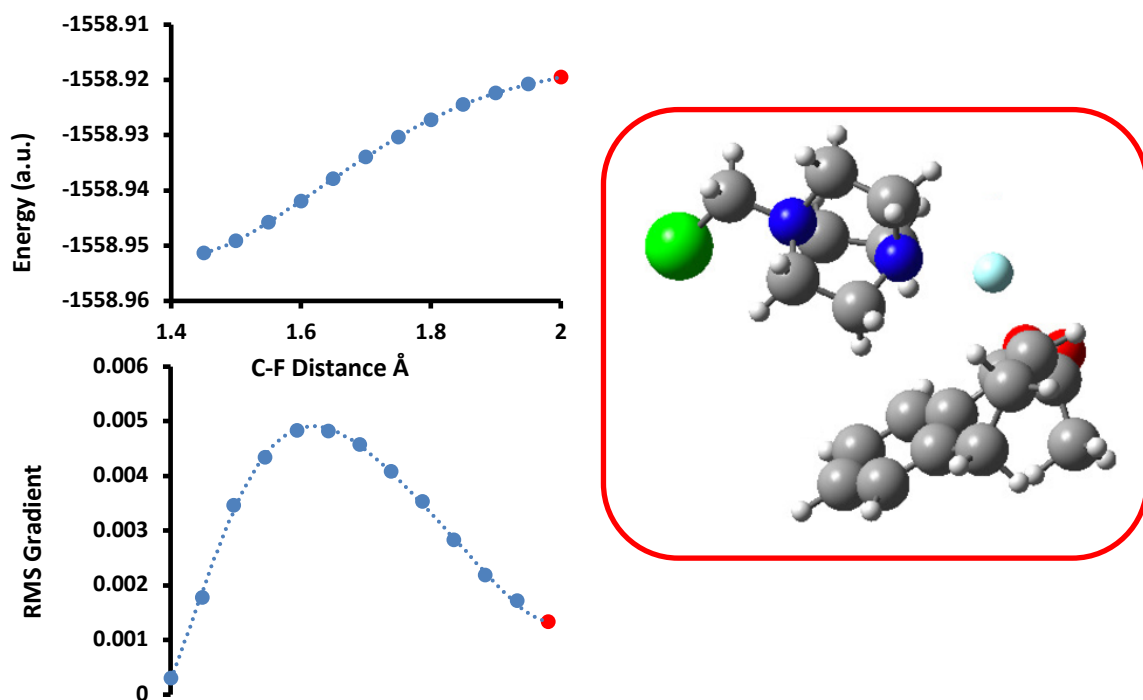
Figure 64: PES Scan Looking for a SET TS

A frequency calculation on this point reveals a single imaginary frequency corresponding to movement of the fluorine towards carbon 2. The energy barrier to this is lower than the reverse reaction yielding starting materials. The reaction coordinate energy diagram is depicted in *figure 65*.
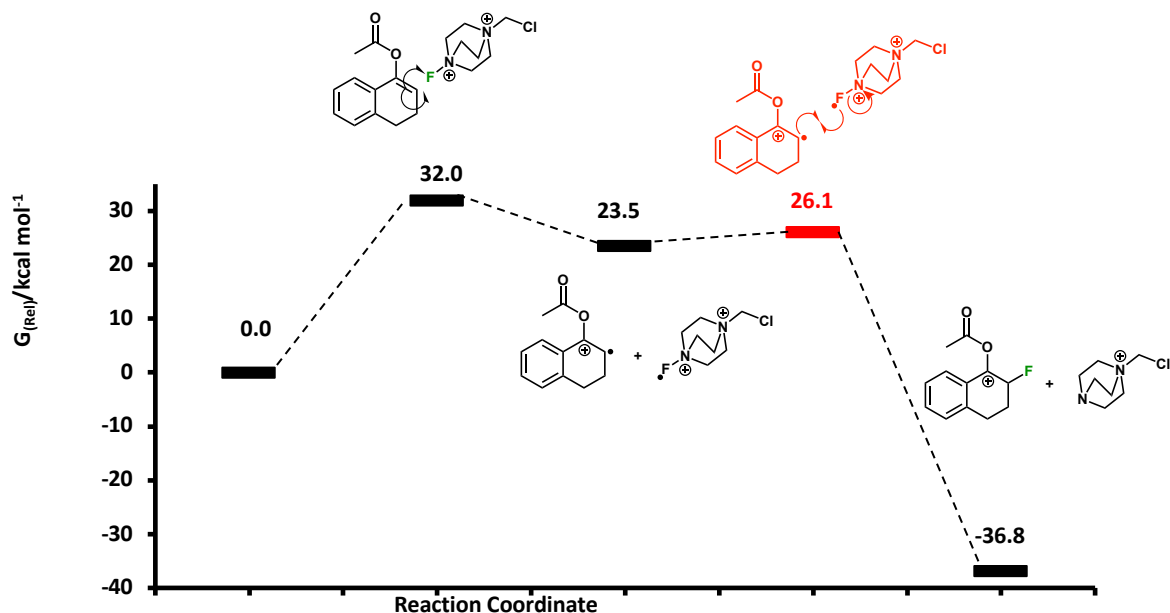
Figure 65: Estimated Reaction Coordinate

Whilst this result adds strength to the hypothesis that the fluorination of the enol acetate of tetralone operates *via* a polar mechanism, due to the calculated energy barrier being slightly lower in relation to the SET mechanism it is possible that this DFT method is biased towards this result therefore it was important to repeat the Marcus calculations using some of the different functionals benchmarked against the experimental data for the polar mechanism, to determine whether different functionals favour different mechanisms.

Table 11 summarises the results from the Marcus theory procedure using the different functionals. The majority of the functionals tested favoured the polar mechanism as having a lower energy barrier, and only three of the nine functionals showed a preference for the SET pathway. However, each functional that supplied SET

as a lower energy pathway overestimated the energy barrier (relative to the experimental value) by at least 10 kcal mol^{-1}. In addition to this, these pathways were only lower in energy than the polar computations by less than 3 kcal mol^{-1}. In stark contrast to the functionals which favoured a polar pathway, the smallest difference in energy for the two processes in this suite of calculations was found to be 3.8 kcal mol^{-1}.

Table 11: Comparison of SET and Polar Energy Barriers

Functional	Marcus SET Pathway		Polar Pathway	
	$\Delta G^{\ddagger}$	ΔG intermediates	$\Delta G^{\ddagger}$	ΔG intermediates
B3LYP	25.9	16.4	18.1	-39.2
B3LYP-D3	42.7	16.8	16.5	-36.9
CAM-B3LYP	31.4	22.6	27.6	-37.5
ωB97	35.5	27.5	36.2	-36.7
ωB97X	33.4	24.6	33.4	-37.3
ωB97XD	32.0	23.6	27.6	-36.9
M06	27.4	17.1	21.0	-45.4
M06-2X	74.4	71.2	33.9	-36.7
M06-HF	49.6	46.1	52.3	-25.0

The DFT calculations that have been carried out indicate that a polar mechanism is more likely than a SET process as generally, the SET pathway is predicted to be much higher energy than the experimental values. Moreover, the methods that come closest to the experimental values (within *ca.* 10 kcal mol^{-1}) for the SET pathway predict the polar pathway to be lower in energy. With this in mind, the use of the ωB97XD functional looking for polar transition states was selected for the rest of the study.

3.4.4. Computational Investigation of Side-Product Formation

With a satisfactory computational methodology for the study of these systems established, attention was next turned to an unanswered question from the experimental data – what is the mechanism in operation for the formation of side-

products with the alpha-substituted compounds? The smooth kinetic behaviour suggests that the side product forms as a result of divergent behaviour *after* fluorine atom transfer. It is likely that this occurs after formation of the carbenium intermediate.

As previously discussed, three possible mechanisms of formation of the side product can be envisioned.

- A 1,2-fluoride shift
- A 1,2-alkyl shift resulting in the formation of a ring contracted intermediate
- A 1,2-alkyl shift resulting in the transfer of the alpha-substituent to the carbonyl carbon.

Based on literature precedent the 1,2-fluoride shift can almost immediately be dismissed (*vide supra*) however this pathway was computed to further establish confidence in the computational methodology. As expected, the transition state for a 1,2-fluoride shift is calculated to be very high in energy: so high in fact that this would become rate determining for this substrate. The energy barrier from the carbenium intermediate to the fluoride shift transition state was calculated to be 81.3 kcal mol^{-1}. The energy barrier calculated would not be consistent with a reaction that occurs at room temperature. This result along with the literature precedent allowed this mechanism to be discounted.

The ring contraction 1,2-alkyl shift was then examined. This mechanism appeared to be more feasible. The energy barrier from the carbenium intermediate was 20.9 kcal mol^{-1} and the transition state was much lower in energy than the fluorination transition state, indicating that once the fluorination has occurred there would be enough energy in the system to overcome this barrier however, the product of the ring contraction was computed to be higher in energy than the starting material which would indicate that this process would likely be reversible. Shifting the phenyl ring proved to be the lowest energy pathway computed in this instance, at 16.6 kcal mol^{-1} higher in energy than the carbenium, suggesting that this could be the mechanism by which the

side product formation operates. Attempts at computation of the carbenium intermediate produced form this alkyl shift pathway resulted in the generation of a 5-membered cyclic intermediate. Such species are known to form and have even been observed experimentally. *Figure 66* shows the reaction coordinate plot for the formation to the second carbenium intermediates *via* all three possible pathways.

Figure 66: Calculated Side Product-Forming Pathways
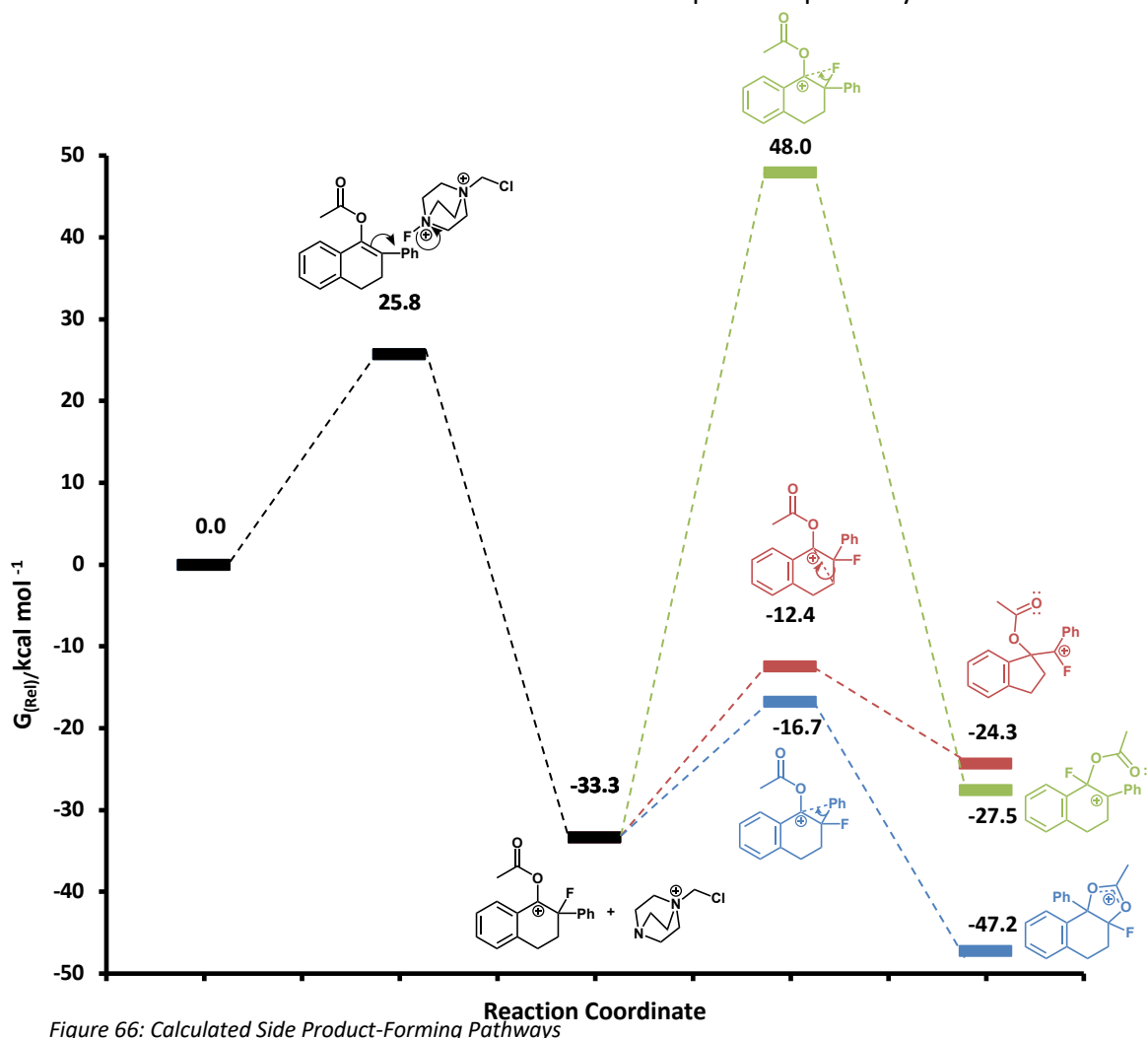
In order to gain further insight into the formation of these products the 1,2-alkyl shifts were computed for the indanone derivative. As predicted, the formation of a 4-membered intermediate on the pathway for the ring contraction was not favourable. The energy barrier from carbenium to ring-contraction transition state was over 20 kcal mol^{-1} higher than that calculated for the tetralone-based compound. Not only this, but

the product of this step was predicted to be a meagre 4.6 kcal mol^{-1} lower in energy than the transition state, suggestive that were this to occur it would be a reversible process (*Figure 67*).
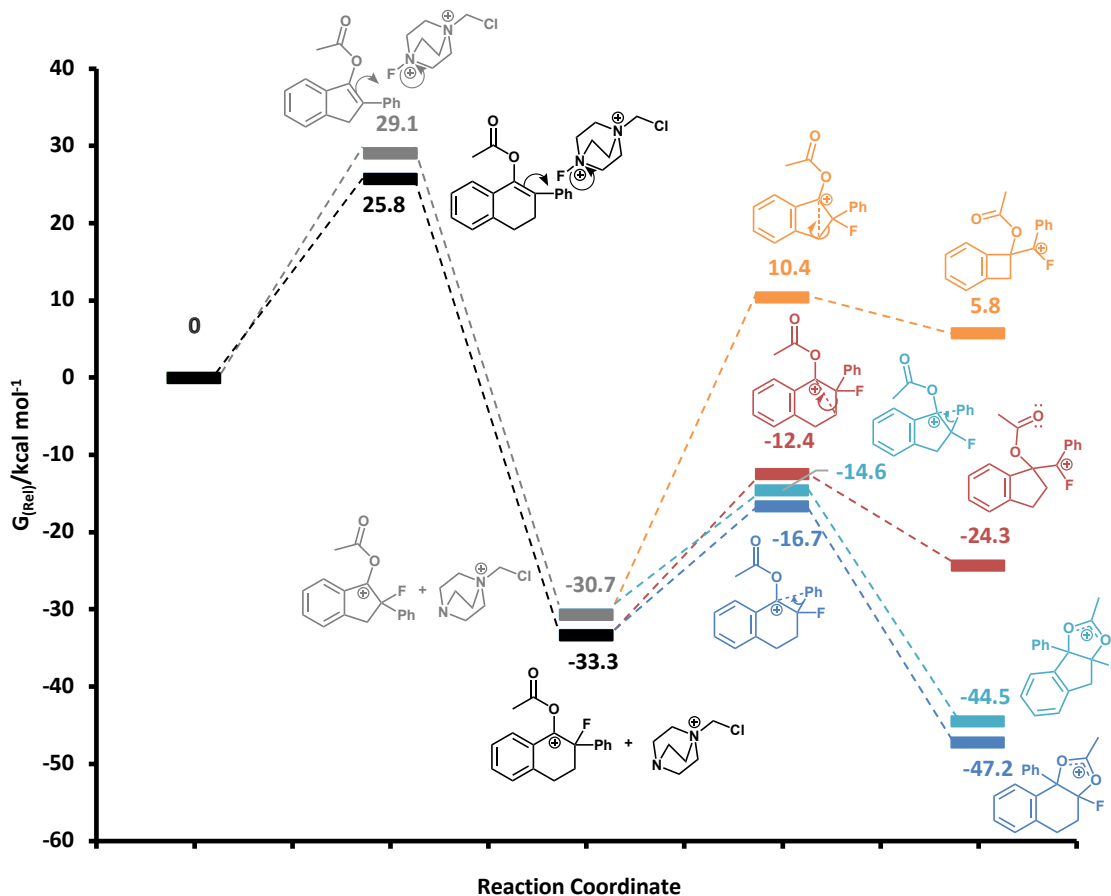
*Figure 67: Reaction Coordinate Comparing 1,2-Shifts For Compound **120** and **127***

Locating a stationary point on the potential energy surface for the phenyl-shift pathway proved to be difficult. From scanning the potential energy surface for different bond distances between the phenyl and the carbon it migrates to it was found that the potential energy surface was very shallow, preventing the location of a transition state. However, it was possible to obtain an estimation of the energy barrier by optimising the geometry with the bond distance fixed at the distance at which the lowest gradient was found during the bond scan. This yielded a single imaginary frequency of the phenyl ring moving towards the carbon in question and resulted in an estimation of a barrier of 16.0 kcal mol^{-1} higher in energy than the carbenium intermediate. If this value is close to the

true value, provided this is the mechanism in operation, this would be in good agreement with the experimental results as both the tetralone and indanone variants yield identical amounts of side product relative to fluorinated product.

*Table 12: Comparison of 1,2-Shifts For Compound **120** and **127***

Compound	**% Side Product**	**ΔG from Carbenium (1,2-Phenyl Shift)**	**ΔG from Carbenium (Ring Contraction)**
120	16	16.6 kcal mol^{-1}	20.9 kcal mol^{-1}
127	16	16.0 kcal mol^{-1}	41.1 kcal mol^{-1}

Possible next steps to the formation of the side product were then computed. Once the 5-membered intermediate is formed, the attack of water at the carbenium would result in the opening of this ring. Locating a transition state for this proved to be highly problematic. Once more it was not possible to identify a stationary point for the transition state; however, from a bond scan a structure was located with a single imaginary frequency which corresponded to the attack of water at the carbenium which had a feasible energy barrier of 14.5 kcal mol^{-1} relative to the previous intermediate. It is possible to obtain a transition state for the hydrolysis if a network or four water molecules is present however this presents issues in quantifying the energetic barrier for this process (*Figure 68*). The imaginary frequency generated from this calculation shows the expected movement of one water towards the positively charged carbon and in addition to this the three other waters move as though in a hydrogen bond network, perhaps sharing the positive charge between them.
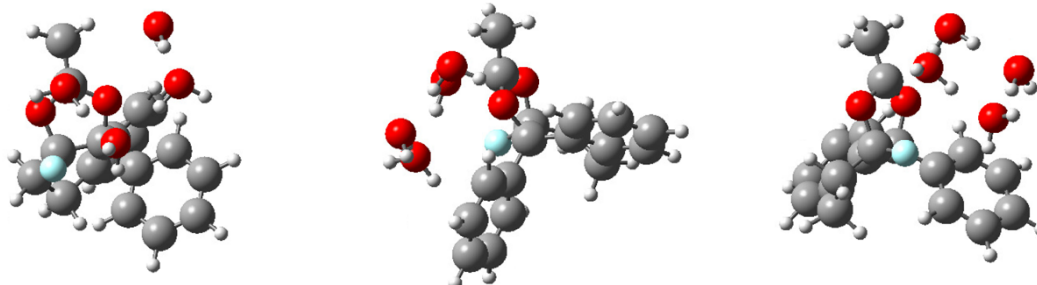
Figure 68: Hydrolysis Transition State with Network of Four Waters

When computing the pathway with only one water (such that the energies can be compared), the product of this step was not possible to compute, likely due to the high energy of the positively charged oxygen of the bound water. It is not possible to know if this structure would ever be formed, as with the high water content and the presence of the des-fluoro SelectFluor it is likely that proton transfers would be able to occur instantaneously and therefore the structures computed are an artificial model to attempt to understand this reaction, rather than an exact reflection of what is occurring in the reaction mixture. With this in mind the result of a proton transfer to the fluorine atom was computed as a possible intermediate. When this structure is minimised loss of HF occurs spontaneously.

Figure 69: Pathway to Side Product

Reaction Coordinate

155
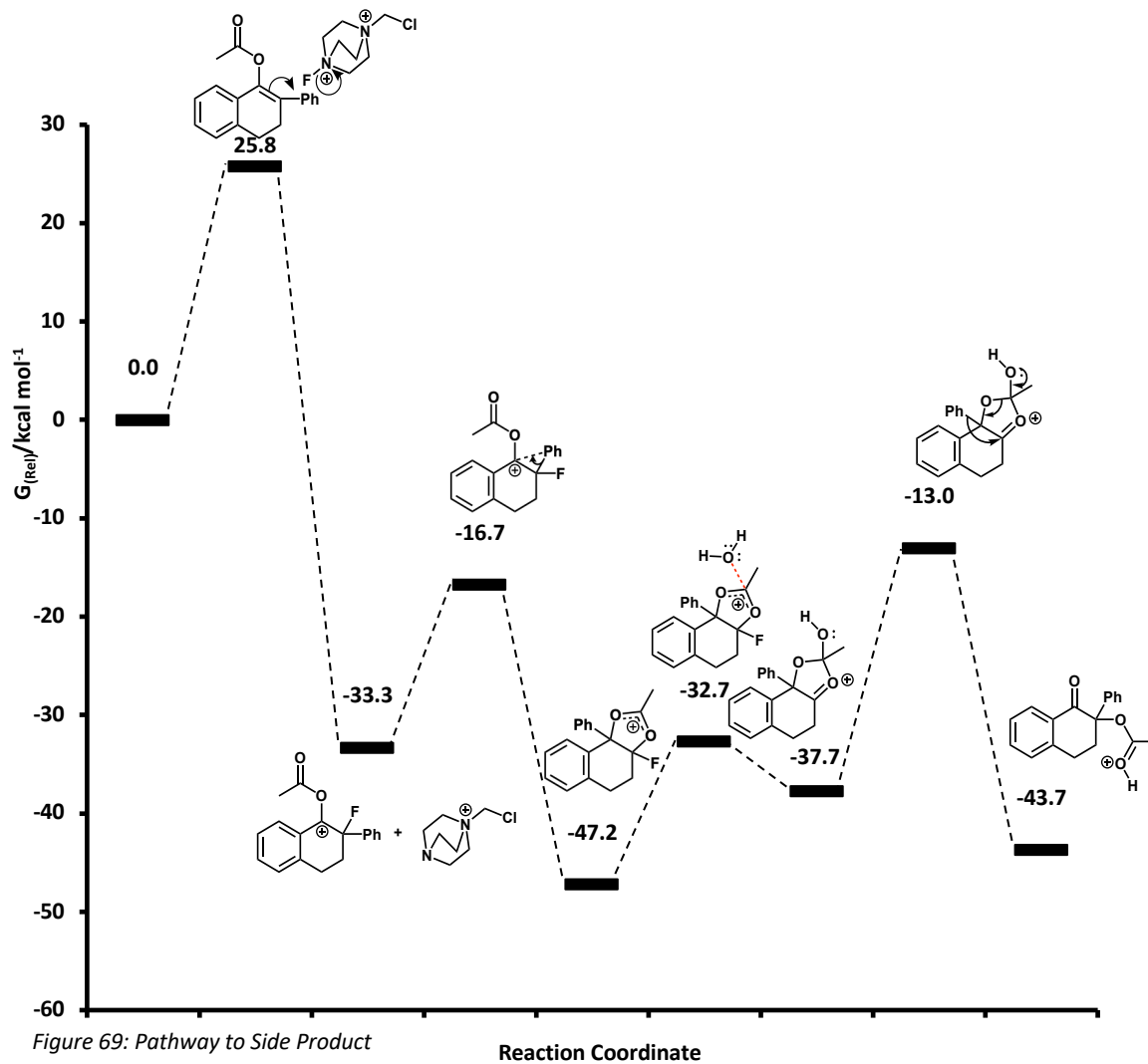
Migration of the phenyl ring to the adjacent carbon results in formation of the side product, all with feasible energy barriers (*Figure 69*).

This pathway was computed for a range of substrates to establish whether the model was consistent with the experimental results. The 4-methoxy substituted substrate **118** was computed first. The barrier to the initial 1,2-phenyl shift is 7.5 kcal mol^{-1} lower than in the unsubstituted compound. The water attack step still appears to be reversible and the barrier to the final phenyl shift is 5.2 kcal mol^{-1} lower than the unsubstituted compound. This is consistent with the observed experimental behaviour and therefore this mechanism is a viable explanation for why these side products are observed. The 4-trifluoromethyl compound **123** was also studied. Consistent with experimental data the energy barrier to the 1,2-aryl shift was higher than the unsubstituted phenyl compound by 3.9 kcal mol^{-1}.
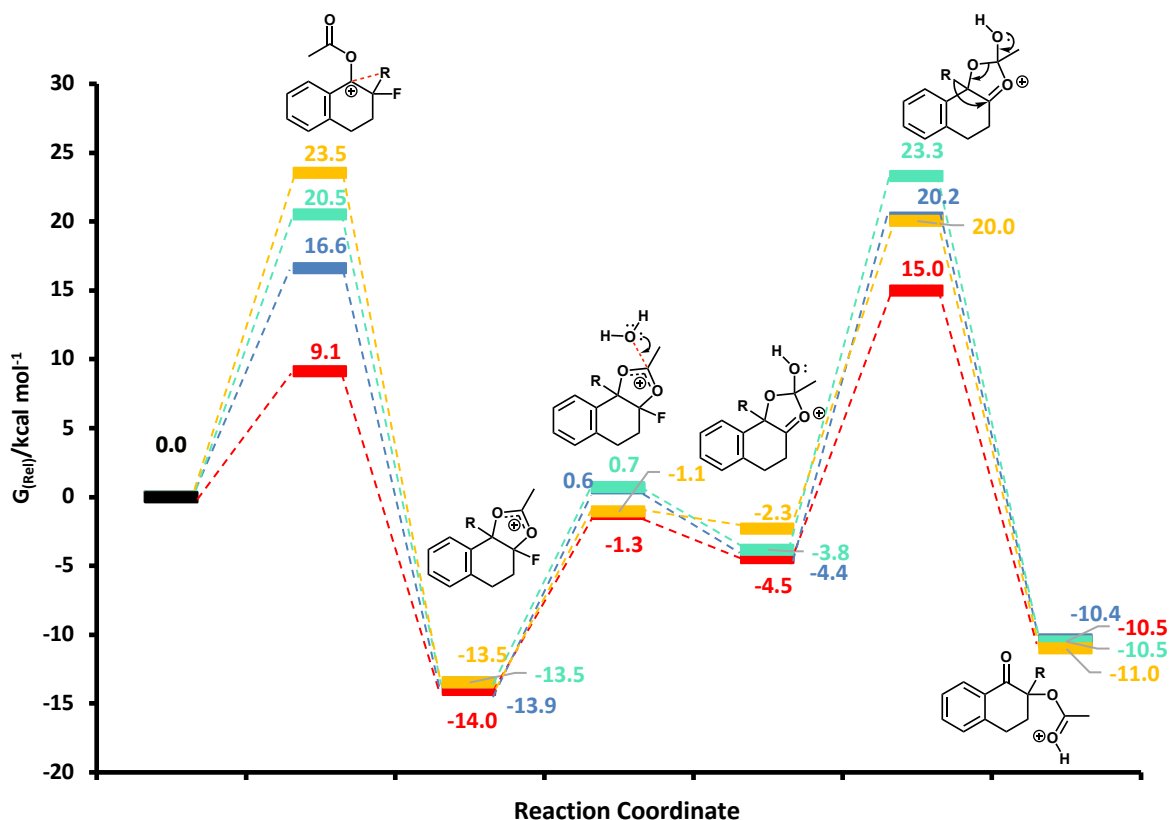
Figure 70: Comparison of Alpha-Substituents in Side Product Formation

Finally, a 1,2-hydride shift was computed for compound **100** as it is known that the side product does not form for this compound. The energy barrier for this transition state was 6.9 kcal mol^{-1} higher than that for the alpha-phenyl compound **120** and this hydride shift transition state was 13.5 kcal mol^{-1} higher than the hydrolysis transition state through the carbenium (*Figure 70*). The energy barriers for the initial 1,2-substituent shift are in the same order as is observed experimentally. If the computational model is correctly replicating the experimental behaviour it appears that the most significant step is the initial 1,2-shift. There is not a large difference in the energy barriers that have been estimated for the hydrolysis of the 5-membered intermediate, with all four being within 1 kcal mol^{-1}. The barrier to the final 1,2-shift appears to be less influential on the outcome of the pathway; the 4-methoxy compound again has the lowest barrier to this shift but the hydride shift now has a similar barrier to that observed with the alpha-phenyl compound. This suggests that the competition between the 1,2-shift and hydrolysis to the fluoroketone is what determines the outcome rather than steps further down the pathway.

Table 13: Correlation Between Side Product Formation and Computed Energy Barrier to 1,2-R Shift

R	% Side Product	ΔG from Carbenium to R-Shift/kcal mol^{-1}
● *H*	0	23.5
● *4-CF$_3$-C$_6$H$_4$*	13	20.5
● *Ph*	16	16.6
● *4-OMe-C$_6$H$_4$*	40	9.1

3.4.5. Hydrolysis of Alpha-Phenyl Compound

As evidenced by the [18]oxygen labelling experiment, the alpha-phenyl compound undergoes hydrolysis *via* a different mechanism to the other enol esters. Computation of alternative hydrolysis pathways to hydrolysis *via* carbon 1 proved to be challenging. Conducting a PES scan forming a bond between a water molecule and carbonyl carbon 9 of the ester results in the breaking of the C-O bond and the formation of an acylium ion as soon as the distance between the water molecule and carbonyl carbon is decreased to 2.04 Å.
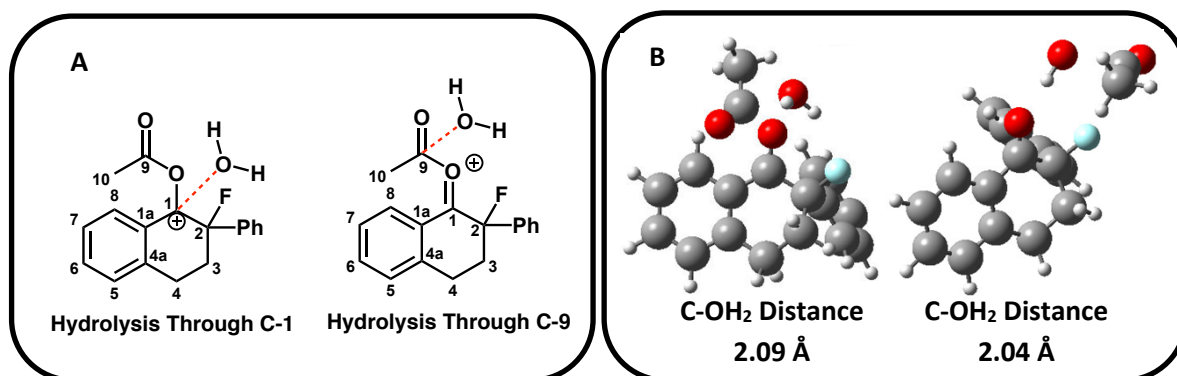
Figure 71: Possible Hydrolysis Pathways (A) Images from PES Scan (B)

A PES scan lengthening the bond between the 1-position oxygen and the carbon of the ester in the absence of a water molecule resulted in the formation of an acylium ion as an intermediate on the pathway (*Figure 72*). When a transition state optimisation was performed on this point in the scan a stationary point could not be found; however, a frequency calculation on the point in the scan that appeared close to a stationary point yielded a single imaginary frequency, corresponding to the breaking of the O-C bond. The energy barrier was 5.6 kcal mol^{-1} relative to the carbenium intermediate. The hydrolysis through carbon 1 was also computed and the energy barrier was found to be 7.6 kcal mol^{-1}. Whilst the identification of a transition state for the hydrolysis of this compound proved to be difficult. The formation of an acylium intermediate can now be postulated with the backing of the calculations described.
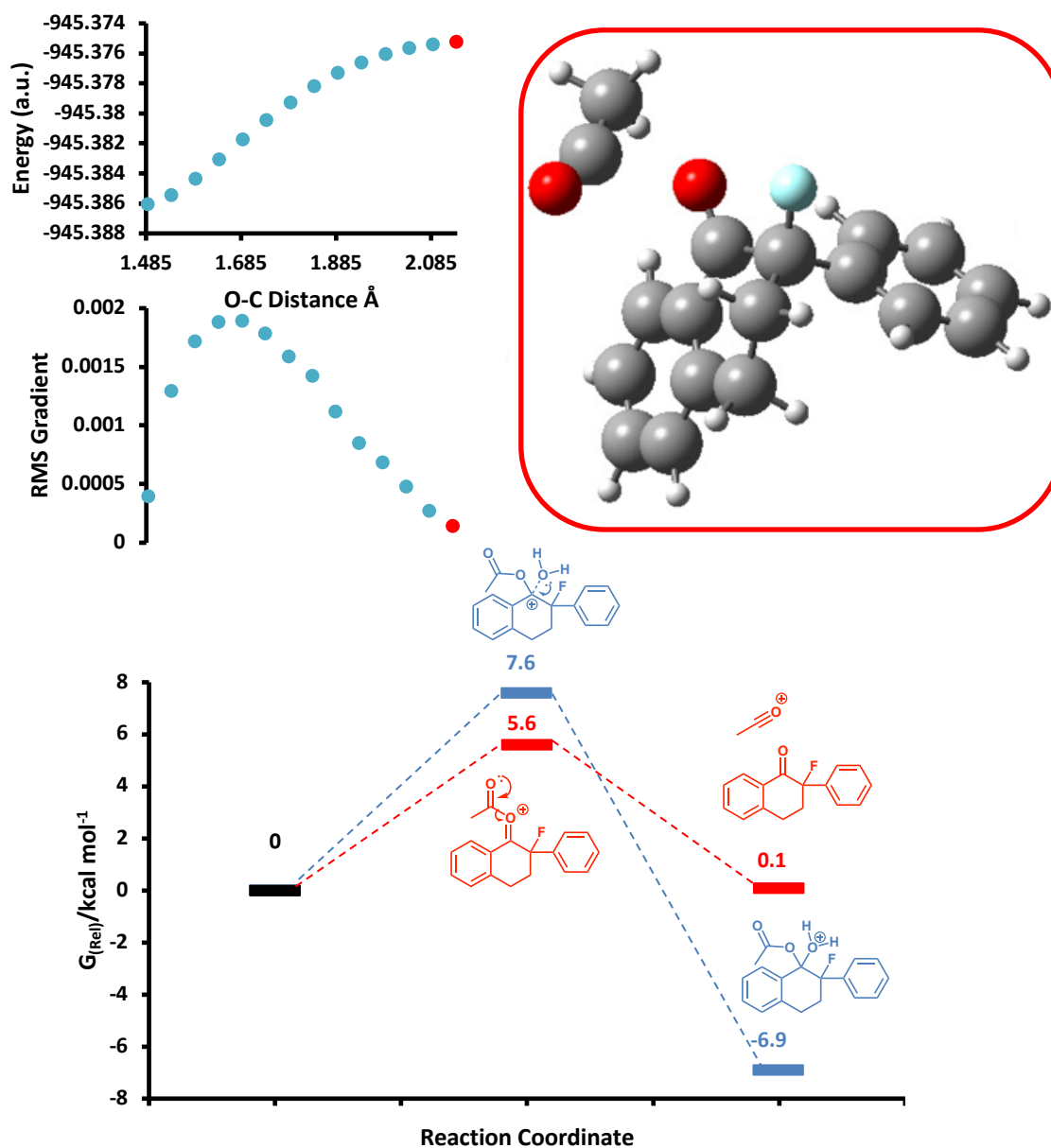
Figure 72: PES Lengthening O-C-9 Distance, Image of Scan Point Close to Stationary Point and Reaction Coordinate Comparing Relative Energy Barriers to Hydrolysis through C-1 and C-9

3.4.6. Computation of the Fluorination of the Steroid Models

The fluorination of the model compounds was examined computationally in order to gain further understanding into the reasons behind the rate enhancement observed relative to the tetralone-based compounds. The ωB97XD functional was used again for these compounds, as all of the preceding work shows that this is an appropriate level of

theory for this reaction (*Figure 73*). When the enone model (**148**) is fluorinated a mixture of diastereomeric products is produced, presumably as a result of two diastereomeric transition states, with the lower energy of the two being responsible for the formation of the major product.
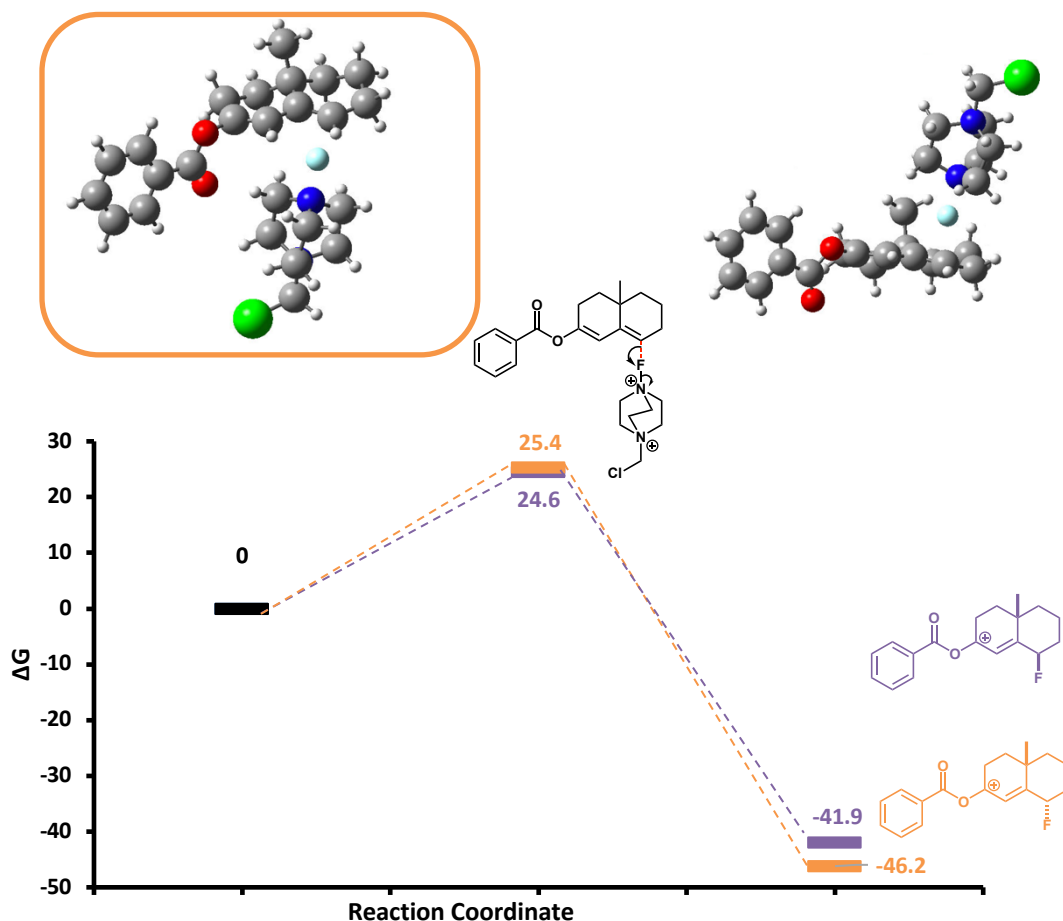
*Figure 73: Electronic Structure Calculations of the Fluorination of **148***

Further confidence in the accuracy of the computational model could be derived from the calculation of these transition states, with correct prediction of the more favourable transition state being indicative of a reasonable model. When the two transition states were computed, replication of the experimental preference for the axial diastereomer was observed. The free energy barrier to reaction for the formation of the axial product was calculated to be 0.8 kcal mol^{-1} lower than that for the equatorial diastereomer. The equatorial intermediate carbenium product is more

thermodynamically favourable by 4.3 kcal mol^{-1}. Electronic structure calculations of the ketone products also predict a thermodynamic advantage for the equatorial fluoride, indicating that were it possible to induce chemical equilibration between the two products that the equatorial product would be favoured.

3.4.7. Computation of the Fluorination of the Steroid 99b

Attention was turned to the computation of the energy barriers to each of the diastereomeric products of the fluorination of **99b** (*Figure 74*)**.** Once again utilising the ωB97XD functional and 6-31G* basis set with SMD solvation in acetonitrile the energy barrier for fluorine atom transfer on the α-face was found to be 1.4 kcal mol^{-1} lower in energy than transfer to the β-face, in contrast to the results obtained for model compound **148** but in good agreement with the experimentally observed behaviour.
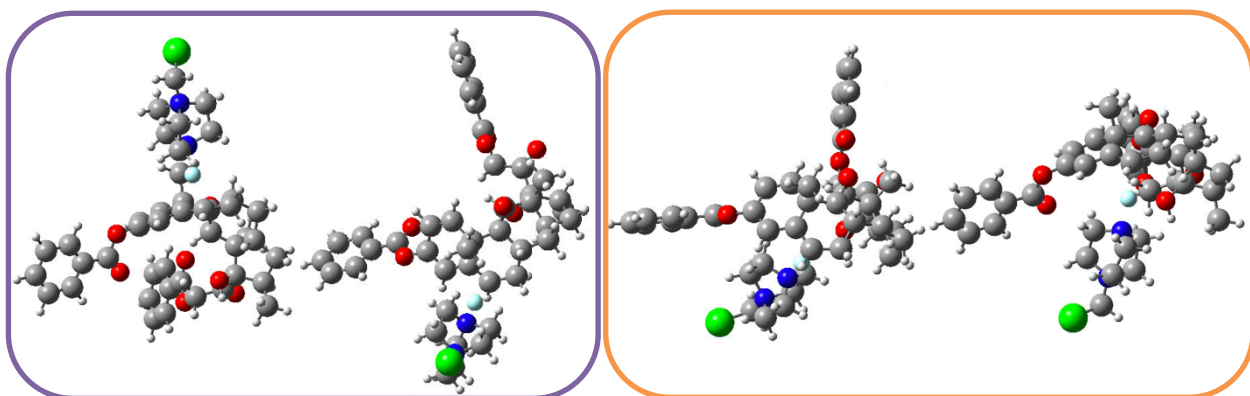
*Figure 74: Diastereomeric Transition States in the Fluorination of **99b** (left, axial TS, right, equatorial TS)*

The carbenium α-product was also predicted to be lower in energy than its β counterpart, indicating that upon equilibration of a mixture of α and β products the desired **6α-99** would be favoured. This is also in good agreement with results published in the patent literature in which equilibration from a mixture to pure α-fluorosteroid is well precedented.
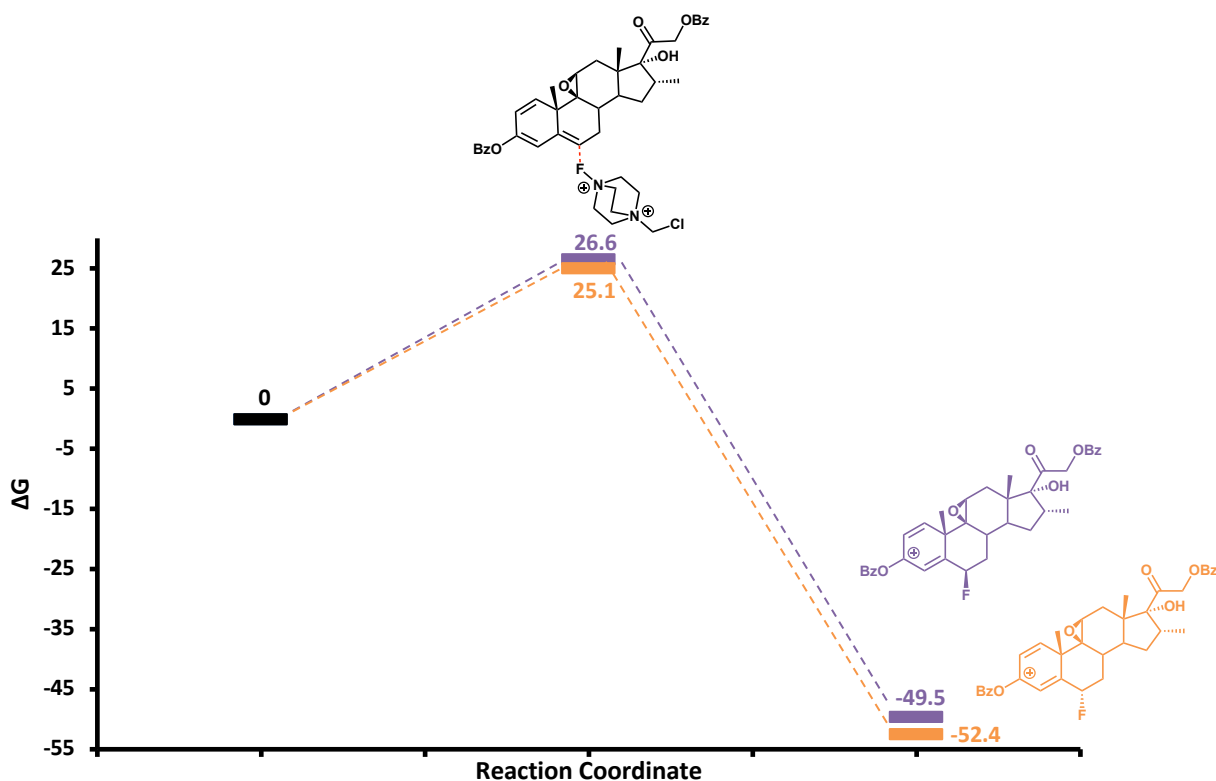
*Figure 75: Reaction Coordinate for the Fluorination of **99b***

3.4.8. Conclusions

The computational data corroborates the experimental evidence that suggests that the electrophilic fluorination of enol esters using SelectFluor proceeds *via* a polar mechanism. However, the margin between the predicted energy barrier to a polar fluorine atom transfer and a single electron transfer from enol ester **100** to SelectFluor is small, therefore a SET mechanism cannot be entirely ruled out for every possible substrate. Nevertheless, if a SET mechanism is in operation, the behaviour appears to be very similar to that which would be expected of a polar mechanism. This raises the question of how far removed the mechanisms are from each other; If these two mechanistic pathways are in fact much more closely related than they are traditionally described to be, it may prove extremely difficult to differentiate between them. In this case, it is therefore simpler to understand the fluorination of enol esters using SelectFluor as a polar mechanism, for which a computational model has been established

providing a reasonable approximation of the observed experimental behaviour. It is hoped that this model can further be utilised to further understand the fluorination of enol esters using SelectFluor and perhaps even in a predictive fashion to guide experimental work.

The possible mechanisms of formation of the side product in compounds **118-123, 127** and **138** have also been interrogated computationally resulting in a hypothesis which postulates that the side product is formed *via* a migration of the alpha-substituent rather than a ring contraction. The computational results are consistent with the experimental data observed in the formation of these side products therefore it is suggested that this is the current best understanding of how these side products are forming in the reaction mixture. Computational investigations into the hydrolysis of **120** have offered the formation of an acylium intermediate as a possible explanation for why no incorporation of [18]oxygen is observed in the labelling experiment (*Figure 76*).
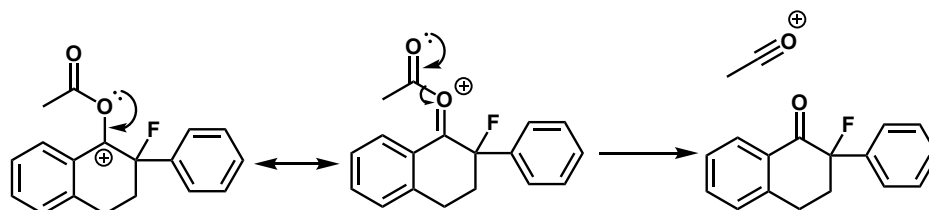
Figure 76: Acylium Forming Hydrolysis Mechanism

Further confidence in the computational model has been gained in its relative accuracy for the fluorination of enol esters by its ability to correctly replicate experiment in the fluorination of **99b**. The polar computational fluorine atom transfer model correctly predicts the lower energy diastereomeric transition state which leads to the major product as well as correctly identifying **6α-99** as the thermodynamically favoured product from the fluorination reaction. These data taken together allow the use of ωB97XD 6-31G* with SMD acetonitrile solvation to be presented as the best computationally inexpensive protocol for the computational study of the electrophilic fluorination of enol esters using SelectFluor.

3.5.   Investigation of the Use of Additives

A good understanding of the fluorination reaction in absence of additives has been established by the work discussed in the previous chapters of this thesis. However, the possibility remained that the behaviour in the industrial process is altered by the addition of pyridine and methanesulfonic acid to the reaction mixture, allowing an alternative mechanism to operate. Given that the understanding of the fluorination reaction using enol esters of tetralone is more complete the initial experiments explored the influence that the additives would have on this reaction.

3.5.1.   Effect of Additives on the Rate of Reaction Between SelectFluor and Compound 100

Considering how instrumental pyridine and methanesulfonic acid are to obtaining a high alpha/beta ratio in the isolated material from the fluorination of compound **99b** it was thought possible that they were involved in the rate determining step of the fluorination reaction. In order to determine whether this was the case the fluorination of compound **100** was performed in the presence of the additives (*Scheme 99*). To further understand their role, if any, in the reaction each additive was studied in isolation as well as in the combination utilised during the industrial fluorination process.
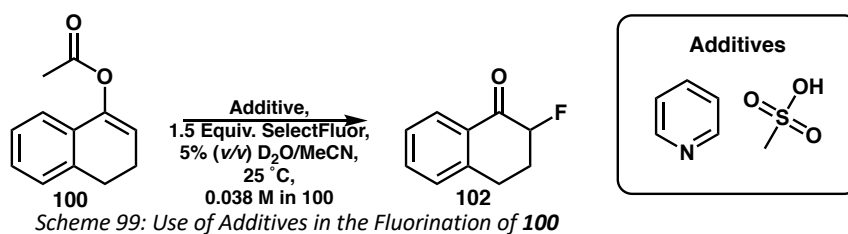
Scheme 99: Use of Additives in the Fluorination of **100**

The fluorination reaction was performed using 1 equivalent of methanesulfonic acid, which resulted in a negligible change to the rate of fluorination (*Figure 77*). This was also the case when 1 equivalent of pyridine was used. It was thought that perhaps the exact number of equivalents of each reagent was necessary to have an effect, therefore the reaction was performed using 1.2 equivalents methanesulfonic acid, which

also had little effect on the rate of reaction. The use of 2 equivalents of pyridine resulted in a slight increase in the rate of reaction. However, when 2 equivalents of pyridine and 1.2 equivalents of methanesulfonic acid were used in combination the rate of reaction was identical to the rate without any additives at all. The change in rate observed when 2 equivalents of pyridine were used was therefore thought to be due to some kind of change in dissociation of the SelectFluor reagent or the acidity of the medium rather than a change in the reaction mechanism. The inclusion of additives had no effect on the overall conversion of the substrate, indicating that the addition of methanesulfonic acid and/or pyridine had no distructive effect on the SelectFluor.
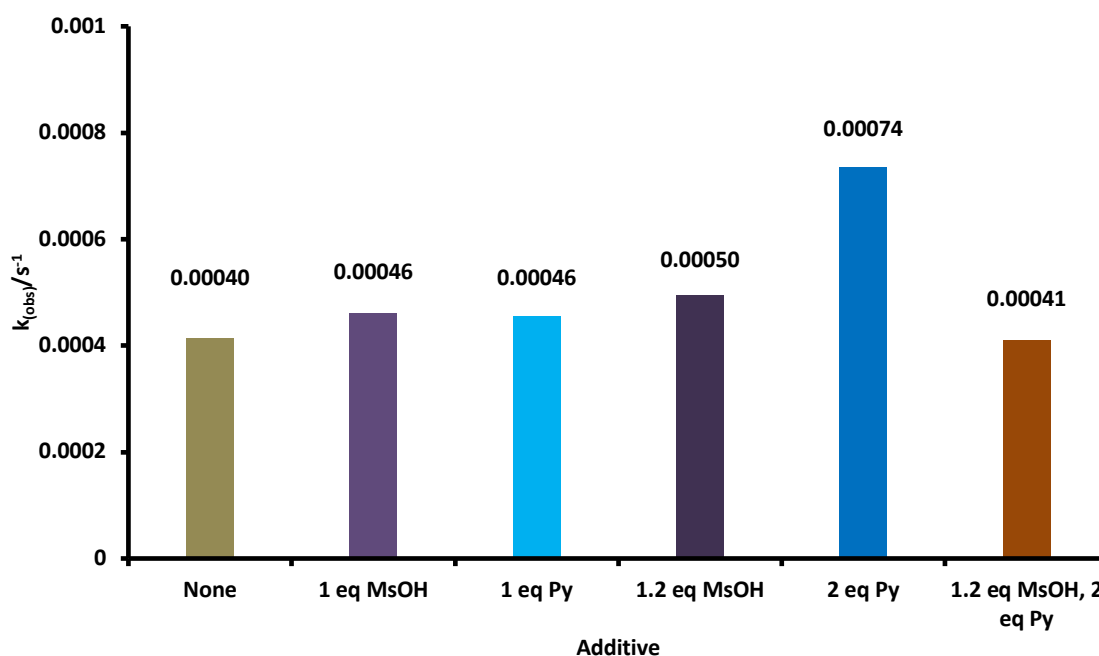
Figure 77: Comparison of Rates Using Additives in the Fluorination of **100**, 1.5 Equivalents of SelectFluor in 5% (v/v) $D_2O/MeCN$, 0.038 M initial **100** concentration, k is an average of two runs

3.5.2. Use of *N*-Fluoropyridinium Based Fluorinating Reagents

One possible role for pyridine in the industrial fluorination reaction is that the fluorine is transferred to pyridine, generating an *N*-fluoropyridinium reagent *in situ* and that it is this compound which is the active fluorine transfer reagent (*Scheme 100*). In order to probe the likelihood of this occurring the reactivity of the enol acetate of

tetralone **100** was investigated with two commercially available *N*-Fluoropyridinium reagents.
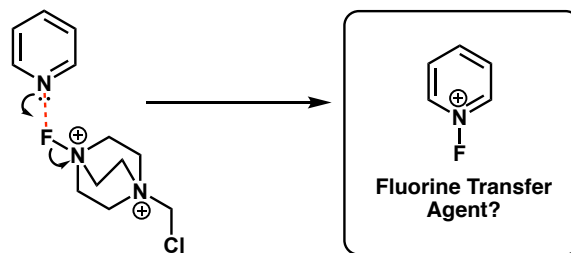
Scheme 100: Possible Fluorine Atom Transfer from SelectFluor to Pyridine

Initially, the reaction was trialled using 2,6-dichloro *N*-fluoropyridinium tetrafluoroborate as the fluorinating power of this reagent has been determined to be similar to that of SelectFluor.[150,153] The reaction components were combined in 5% *(v/v)* water in acetonitrile solution and the reaction was monitored by ^{1}H NMR (*Scheme 101*). Whilst there was some evidence of the formation of the fluorinated ketone product it soon became evident that the hydrolysis of the fluorinating reagent proceeded at a much higher rate than the fluorination reaction under these conditions.
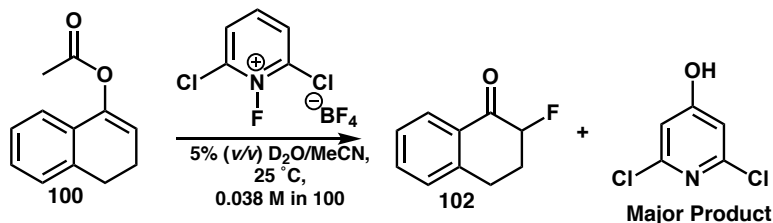
*Scheme 101: Attempted Fluorination of **100** Using 2,6-dichloro N-fluoropyridinium tetrafluoroborate*

The fluorination was then investigated with the use of *N*-fluoropyridinium tetrafluoroborate. It was thought to be important to uncover whether the enol ester compound **100** would react preferentially with SelectFluor or the pyridinium reagent when both were in solution. Were SelectFluor transferring the fluorine to form a transient *N*-fluoropyridinium it would be expected that this species would react with the enol ester faster than SelectFluor. A competition reaction was performed, using a 1:1 mixture of SelectFluor and *N*-fluoropyridinium tetrafluoroborate (overall 1 equivalent of fluorinating reagent) and 1.5 equivalents of enol ester (*Scheme 102*). The consumption of the fluorinating reagents was followed by ^{19}F NMR spectroscopy, following the

disappearance of the *N*-F signals in the NMR spectrum, in the presence of a capillary containing trifluoroethanol as an internal standard. The SelectFluor was consumed entirely over the course of the reaction with the integral of the signal corresponding to *N*-fluoropyridinium tetrafluoroborate remaining constant throughout. It was evident that SelectFluor was much more reactive than the *N*-fluoropyridinium reagent. This experiment was conducted prior to the Mayr *et al.* study quantifying the electrophilicity of *N*-F reagents and in good agreement with these results *N*-FPy was found to be significantly less electrophilic than SelectFluor.[150]
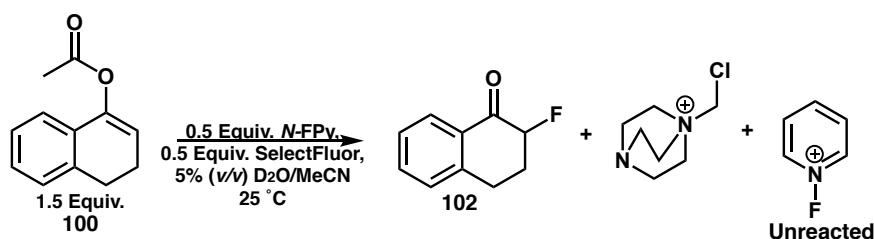
Scheme 102: Competition Reaction Between SelectFluor and N-*FPy*

During this experiment no reaction of *N*-fluoropyridinium tetrafluoroborate was observed over the course of 120 minutes. In order to establish whether the enol ester of tetralone was capable of reacting with *N*-fluoropyridinium tetrafluoroborate at all, a reaction between this substrate and *N*-fluoropyridinium tetrafluoroborate as the sole fluorinating reagent in the reaction mixture was conducted in 5% *(v/v)* water in acetonitrile. The progress of the reaction was periodically monitored by ^{1}H NMR (*Scheme 103*). No reaction was observed, and even after a reaction time of three days both the fluorinating reagent and the substrate were completely intact. These results indicate that SelectFluor is the fluorine transfer reagent in the reaction mixture during the industrial process, and rules out any involvement of *N*-fluoropyridinium intermediates.
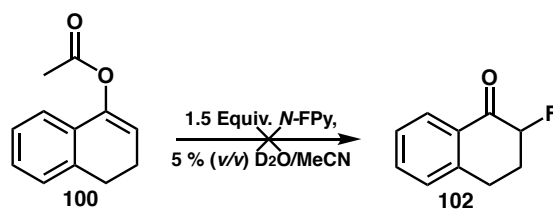
Scheme 103: Attempted Fluorination of **100** *with* N-*FPy*

3.5.3. Effect of Additives on the Reaction of Compound 152 with SelectFluor

Whilst the use of pyridine and methanesulfonic acid had little effect on the reaction of compound **100** with SelectFluor, reactions were performed to determine whether the additives would have an impact on the reaction of model compound **152** with SelectFluor as, like the steroid **99b**, there are two possible diastereomeric outcomes.
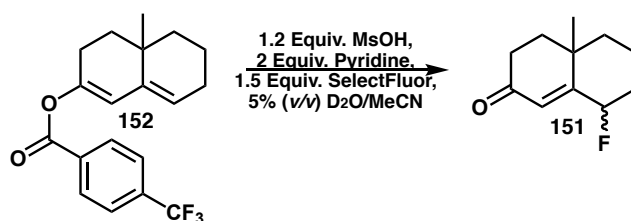
*Scheme 104: Fluorination of **152** Using Additives*

Compound **152** was selected for study due to the slightly decreased rate of reaction observed in relation to unsubstituted compound **148** *(Figure 78)*. The rate of reaction of compound **152** and SelectFluor with the use of 2 equivalents of pyridine and 1.2 equivalents of methanesulfonic acid was determined at 278 K. In a different outcome to that observed with tetralone-based **100** the rate of reaction was almost halved in comparison to the reaction in the absence of additives. The ratio of axial and equatorial products was unchanged from the reaction in the absence of the additives.
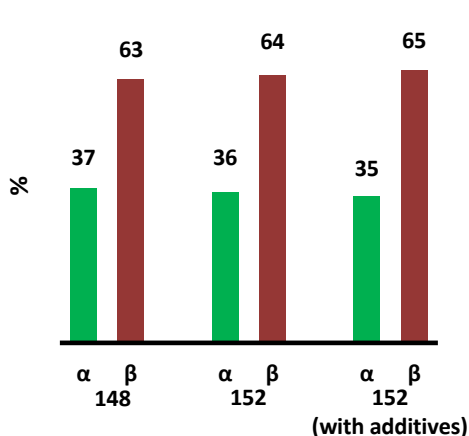
Compound	Additives	$k_{(obs)}$
100	None	4.1×10^{-4} s^{-1}
100	1.2 Equiv. MsOH, 2 Equiv. Pyridine	4.1×10^{-4} s^{-1}
152	None	1.84×10^{-3} s^{-1}
152	1.2 Equiv. MsOH, 2 Equiv. Pyridine	9.7×10^{-4} s^{-1}

*Figure 78: Comparison of α/β in the Fluorination of **148** and **152** in the Presence and Absence of Additives*

3.5.4. Attempted Equilibration of Diastereomers α- and β-151

The kinetic experiment indicated that the additives did not have an influence on the diastereomeric ratio of the products of the fluorination reaction. It was therefore possible that the additives were involved in transforming the axial product to the more thermodynamically stable equatorial fluorinated product in the industrial process. Electronic structure calculations suggest that the equatorial product of fluorination α-**151** is favoured over the axial product β-**151** by a similar margin to that predicted for the steroid (4.3 kcal mol^{-1} *vs.* 2.8 kcal mol^{-1}). If the additives were capable of inducing enolisation, formation of increased amounts of the thermodynamically favoured equatorial product would likely be observed (*Scheme 105*).
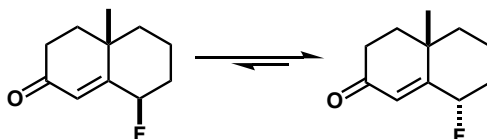
Scheme 105: Proposed Equilibration

In order to test this theory, isolated samples of both the equatorial (α-**151**) and axial products (β-**151**) were dissolved in 5% *(v/v)* water in acetonitrile and 1 equivalent of pyridinium methanesulfonate salt was added to each individual NMR tube (*Scheme 106*). The samples were analysed periodically in order to determine whether enolisation and subsequent equilibration was observed. No change in the samples was observed; each sample continued to contain only one diastereoisomer.
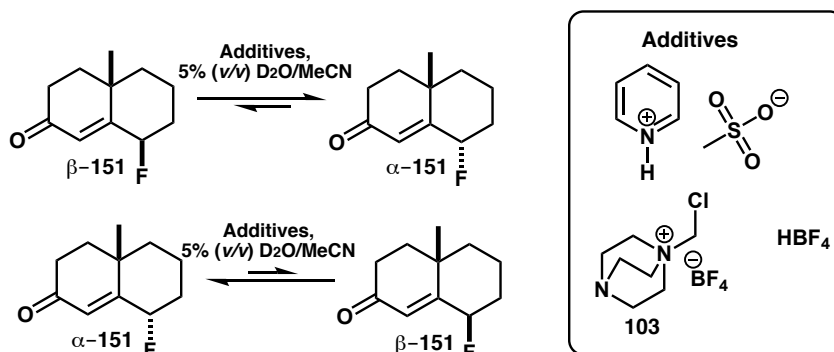
*Scheme 106: Attempted Equilibration of **151***

In an attempt to induce equilibration, 1 equivalent of **103** was added to each sample to mimic the conditions in the reaction mixture once fluorination has taken place. There were still no changes to the contents of the samples.

Aqueous tetrafluoroboric acid was then added to each sample in order to reduce the pH and induce equilibration. Still no change was observed. These results indicate that these compounds do not readily enolise and undergo subsequent equilibration under these conditions.

3.5.5. Conclusions

From the investigations that have been undertaken using the model compounds it is apparent that the inclusion of additives in the fluorination reaction effect no change on the reaction mechanism and any changes in reaction rate are likely to be the result of changing the physical properties of the reaction medium. Attempts at the equilibration of fluorinated model compounds α-**151** and β-**151** were unsuccessful and neither any change in the α/β ratio or any selective crystallisation of one stereoisomer over another was observed. From these results it is likely that the role of the additives in steroidal fluorinations is to either effect selective crystallisation of the desired 6α-product or to induce equilibration of the 6β-product to the thermodynamically favoured 6α-product or, a combination of the two.

4.   Conclusions

Through studying the fluorination of enol esters of tetralone compelling evidence has been established indicating that the reaction proceeds *via* a polar two electron mechanism, resulting in the formation of a carbenium intermediate. This is evidenced by the Hammett correlation observed in all three of the Hammett series studied based on the tetralone core. Further evidence for this mechanism is revealed by the kinetic isotope effect observed at the carbon in the 6-position in the tetralone ring, this is

consistent with the aryl ring participating in stabilisation of the carbenium generated in the 1-position. In addition to this, [18]oxygen-labelling studies result in the full incorporation of [18]oxygen from the solvent in the carbonyl of the product in all but one of the substrates analysed. No evidence for the participation of radicals in the reaction mechanism could be found, either by methods of directly observing radical intermediates or by indirect methods in which radical intermediates expect to be intercepted by competing reactivity.

The understanding developed on the tetralone system was then used as a tool to understand the fluorination of more steroid-like substrates and eventually the steroid itself. Common behaviour with tetralone substrates was observed in both the steroid and steroid model compounds when they were subjected to [18]oxygen labelling conditions. These experiments resulted in the complete incorporation of [18]oxygen into the ketone product of fluorination providing strong evidence for the presence of a carbenium intermediate on the pathway to fluorinated products for these substrates as well (*Figure 79*).
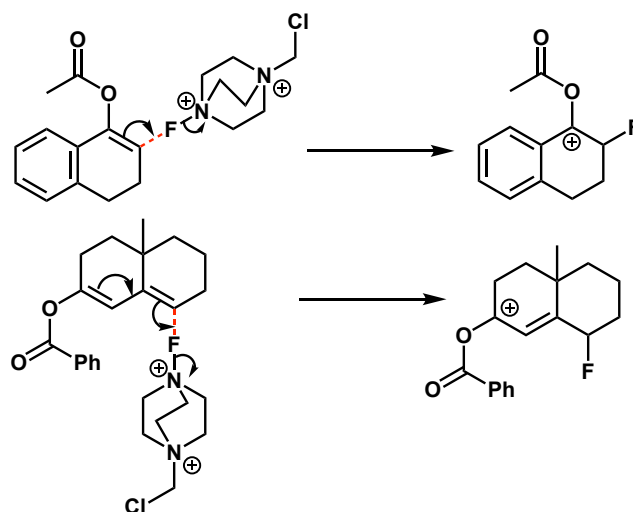
Figure 79: Polar Fluorination Generating Carbenium Intermediates

Attempts on detailed mechanistic studies of the behaviour of the steroid model compounds were thwarted by difficulties in synthesis and isolation of these compounds as well as their exceptionally fast reactivity with SelectFluor. Nevertheless, enough

insight had been gained from both these compounds and the extensive tetralone study to allow key kinetic experiments using the steroidal substrates to afford a high degree of insight.

The results from the Hammett study of the steroidal benzoates revealed a slightly different reactivity to their tetralone counterparts. Previously, the best correlation had been achieved using Hammett's σ_p^+ parameters, designed for use in reactions which result in the build-up of positive charge in the transition state however on this occasion, σ_p provided the best correlation to the rates of reaction measured for the fluorination of steroids, indicating that the build-up of positive charge in these substrates is less influenced by the substituent on the benzoate. A rationale for why this occurs is outlined in *Figure 80* below, considering the high degree of conjugation present in the A-ring of the steroid, it is possible that the positive charge that develops is delocalised around the ring, meaning that the *para*-substituents on the benzoate are less effective in changing the rate of reaction.
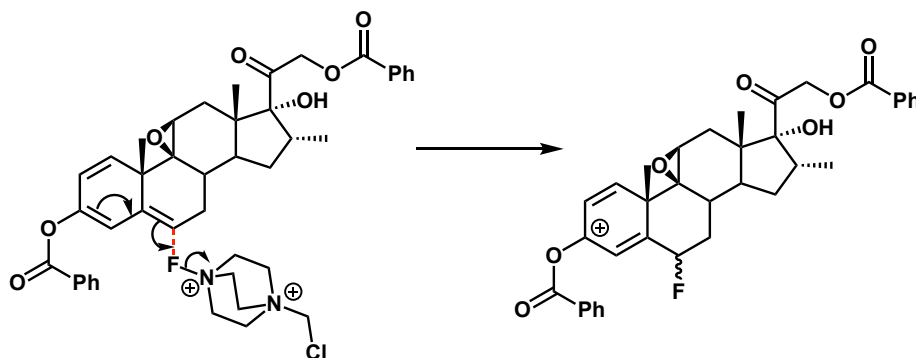
*Figure 80: Polar Fluorination of **99b***

The incorporation of [18]oxygen in the fluorinated product of this reaction provides very compelling evidence for the generation of a positive charge in the 3-position. Suggesting that a polar mechanism in this instance could also be likely. Eyring analysis of compound **99b** provided further insight into the mechanism of fluorination. The values of ΔH and ΔS were somewhat different from those that had been observed for the tetralone substrates, with ΔS being calculated as *ca.* 10 cal mol^{-1} K^{-1} larger in magnitude than in the tetralone compounds. This value is still consistent with a

bimolecular rate determining step, however indicates that the transition state is perhaps more tightly bound than in the tetralone compounds. The results using the steroid taken together with the understanding gained from the tetralone compounds makes the proposal of a polar rate determining step involving fluorine atom transfer to the substrate reasonable.

To further understand the experimental results DFT calculations were utilised. Once a level of theory that satisfactorily replicated the experimental data had been identified and calculations to determine the predicted energy barriers to single electron transfer and polar transition states had been determined this methodology was used to further understand not only the fluorination step in the pathway but also the hydrolysis to the products of the reaction and the formation of side product in compounds **118-123.** Guided by computational results, a mechanism for the formation of side products **118b-123b** is proposed (*Scheme 107*). Thus far the computational results replicate the experimental behaviour.
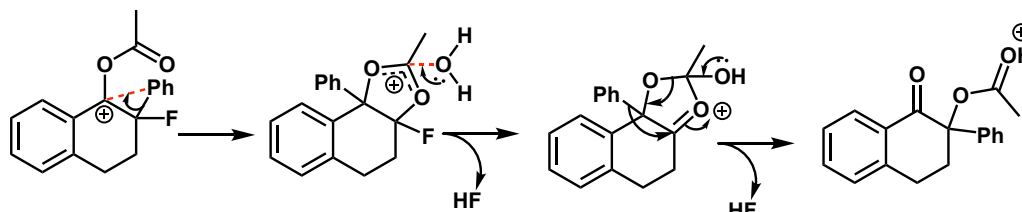
Scheme 107: Proposed Mechanism for the Formation of Side Products

The computational methodology was also applied to the steroid and steroid models. The chosen methodology replicates experimental behaviour well in predicting both the lower energy diastereomeric transition state and the thermodynamically favoured diastereoisomer. This provided further confidence in the computational method.

With an improved understanding of the mechanism of fluorination in hand, attention was focussed on the role of additives in this fluorination reaction. Kinetic experiments were conducted to determine that the additives provided no change in reaction rate of compound **100**. It was also established that the active fluorinating

species was not an *N*-Fluoropyridinium intermediate as utilising *N*-Fluoropyridinium reagents in fluorination reactions with **100** did not result in the formation of fluorinated products in appreciable amounts. The additives had no effect on the ratio of products produced from the fluorination of **152** making it likely that the high diastereoselectivity in the fluorination of **99b** was the result of either selective crystallisation or equilibration. The additives were unable to equilibrate the beta model compound to the alpha, likely due to the high solubility of the fluorinated products.
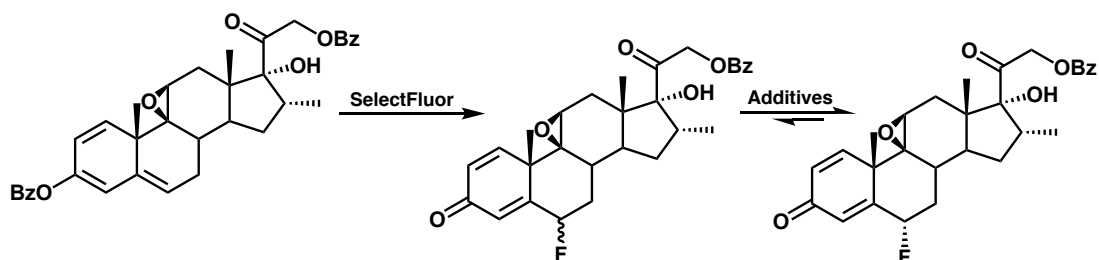
*Scheme 108: Fluorination of **99b***

5. Future Work

The mechanistic understanding of the behaviour of the steroidal and model compounds described has been sufficient to inform the proposal of conditions which afford a high α/β ratio however the understanding of the behaviour of more conjugated vinylic systems (such as **99b** and **148**) remains incomplete. There is scope for further study of the behaviour of these molecules which was hampered in this work by the difficulties in synthesis. Were a more tractable synthetic route designed to compounds such as **148** which allows the synthesis of more material to be developed it would be of use to carry out the Eyring and Hammett experiments that were not possible in this work, perhaps by React-IR. These data would provide valuable insight into the behaviour of these compounds, allowing further understanding of the steroidal substrates and shedding light on if and where the reaction mechanism deviates from the behaviour observed in the tetralone species.

In order to further understand these molecules, it may be of use to synthesise 4-substituted compounds of the type **163** (*Scheme 109*). If a Hammett series of this type were developed it would be of interest to determine whether a similar relationship to that observed for **118-123** between the rate of reaction and σ_p^+ exists for these compounds.[206] There is literature precedent for the synthesis of 4-brominated species as depicted in *Scheme 109*, affording the vinyl bromide which could then be utilised in a Suzuki-Miyaura coupling to yield the 4-aryl precursor to the enol ester.
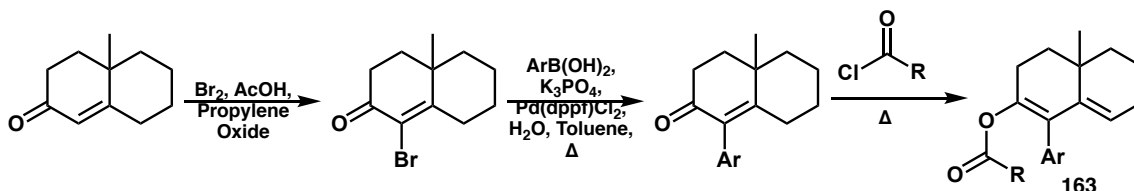
Scheme 109: Proposed Synthesis of 163

Further understanding is also desired into the formation of the side products **118b-123b**.   A reasonable mechanistic rationale has been developed using a computational model which thus far has proven reliable in its replication of the experimental behaviour. The [18]oxygen labelling experiment provides strong evidence for an intramolecular process however further experimentation is necessary to confirm that this is indeed the case. With the current proposed mechanism increasing the steric bulk on either the enol ester or on the alpha-substituent would be expected to have an effect. Introducing a nucleophilic functional group on the aryl ring may also allow the capture of the carbenium, allowing for the generation of observable intermediates (*Scheme 110*).

R^1 = ^{t}Bu, CF$_3$
R^2 = Me, OMe, ^{i}Pr, OH
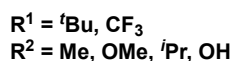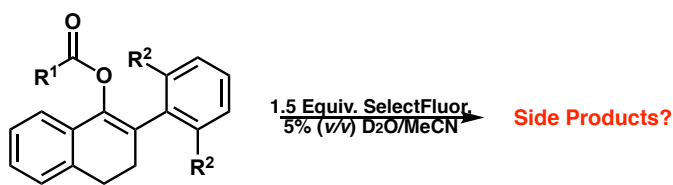
Scheme 110: Proposed Additional Alpha-Aryl Substrates

No evidence of radical involvement has been observed however no evidence to entirely rule out radical involvement has been observed either. In order to strengthen

the case for the proposed mechanism the synthesis of radical probe substrate **164** may be of interest (*Figure 82*). The cyclopropane would be expected to open much faster than that in compounds **137** and **138**. It is known that cyclopropane rings can open as a result of either an adjacent radical species or a carbenium therefore substrate **164** could be informative as a carbenium species would be expected to open the ring yielding **164b** product whereas a radical species would be expected to be stabilised better by the adjacent aryl ring and therefore open to yield the alternative product **164a**. Synthesis of the diphenyl-substituted variant **165** may also be of interest as the radical-induced ring opening of these compounds would be expected to proceed at a much enhanced rate relative to compound **138**.
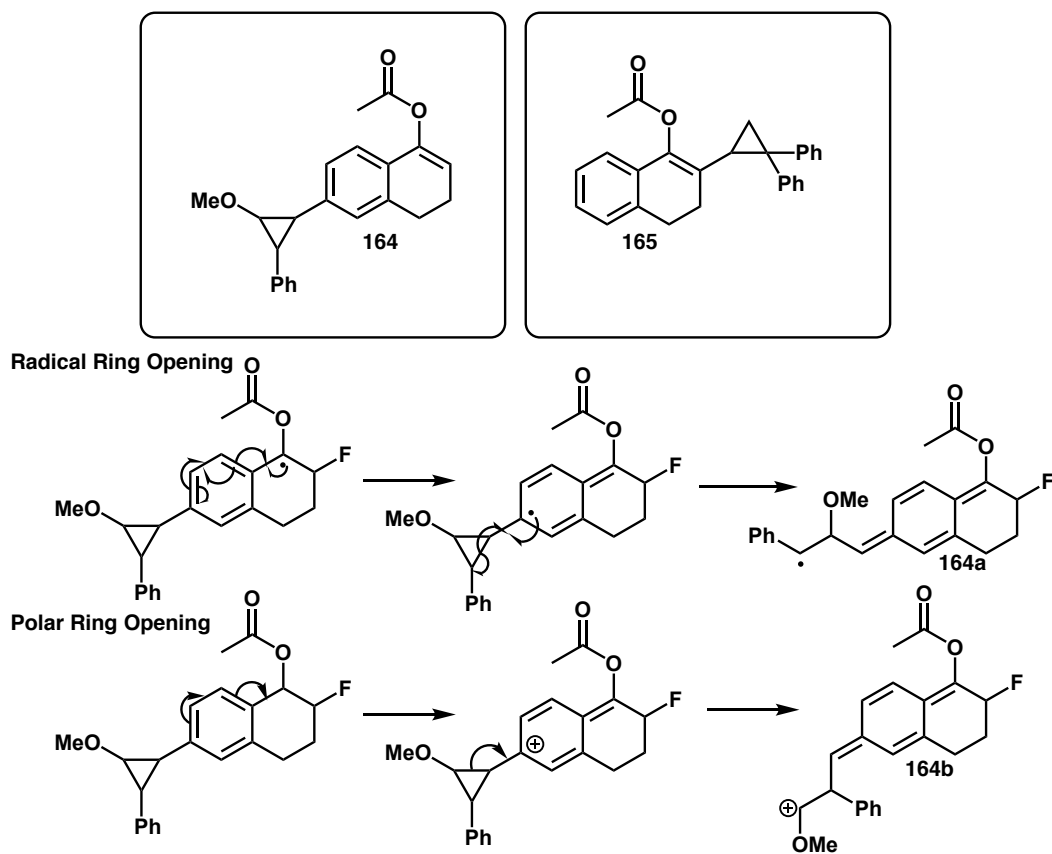
Figure 82: Proposed Radical Trap Substrates

6. Experimental

6.1. General Experimental

Unless stated otherwise, all compounds were obtained from commercial sources and used as supplied. Each batch of SelectFluor was analysed by iodometric titration and confirmed to be >95% pure. NMR characterisation was carried out using Bruker AV3-400 equipped with a liquid nitrogen Prodigy Cryoprobe, or a Bruker AV400 equipped with a BBFO-z-ATMA probe; kinetic data were obtained using a Bruker AVII-600 NMR spectrometer equipped with a BBO-z-ATMA probe. All NMR chemical shifts are quoted in units of parts per million (ppm). ^{1}H NMR spectra were referenced to residual solvent signals, ^{13}C{1H} spectra were referenced to the solvent signal, and ^{19}F spectra were externally referenced to CFCl$_3$. Assignments of the spectra were achieved by the use of [^{1}H, ^{1}H] COSY, [^{1}H, ^{13}C] HSQC, and [^{1}H, ^{13}C] HMBC experiments, as required. Mass spectrometry data was obtained using an Agilent 7890A GC system coupled to an Agilent 5975C mass spectrometer in electron impact mode, or an Agilent 6130 LC/MS system. High resolution mass spectrometry was carried out on a ThermoFinnigan Exactive mass spectrometer. Mass spectrometry/isolation was carried out on a Waters mass-directed auto-purification (MDAP) system. HPLC data were obtained on an Agilent 1200 HPLC system. Infrared spectra were obtained using a Shimadzu IRAffinity-1 IR spectrometer with an ATR accessory. UV/vis spectra were recorded on a Varian Cary 50 UV-Vis spectrophotometer using quartz cuvettes, in MeCN solvent. Thin layer chromatography was performed on pre-coated aluminium-backed silica gel plates (silica gel 60 F254, 0.2 mm thick). Column chromatography was performed on silica gel (40 – 63 μm).

6.2. Fluorination of Tetralone Derivatives with SelectFluor

6.2.1. General Procedures

6.2.1.1. A – Iodometric Titration of SelectFluor

A 0.01 M aqueous solution of SelectFluor (10 mL) was added to a 0.02 M aqueous solution of potassium iodide (20 mL), along with 1.9 M aqeous H_2SO_4 (5 mL). The liberated iodine was titrated against a 0.05 M aqueous solution of sodium thiosulfate.

6.2.1.2. General Procedure B – Synthesis of Enol Esters from Ketones using Isopropenyl Acetate

Ketone (1 equivalent) and *p*-toluenesulfonic acid monohydrate (0.1 equivalents) were suspended in isopropenyl acetate and heated to 120 °C for 2-4 hours. The reaction mixture was then cooled to room temperature, diluted with 10% ethyl acetate in hexane and extracted with saturated aqueous sodium bicarbonate solution. The organic phase was collected, dried over anhydrous $MgSO_4$ and filtered through silica.

6.2.1.3. General Procedure C – Fluorination of Enol Esters with SelectFluor (Synthetic Experiments)

Substrate (1 equiv.) was suspended in 95:5 MeCN:H_2O (0.38 M concentration) and the mixture left to stir at room temperature for 4-19 hours.

6.2.1.4. General Procedure D – Fluorination of Enol Esters with SelectFluor (^{1}H NMR Kinetic Experiments)

The substrate was weighed into an NMR tube, dissolved in 0.7 mL of the premade solvent mixture and a sealed capillary containing 5 µL cyclohexane and CDCl$_3$ was added to the tube. This sample was used to tune, match, lock and shim the spectrometer, and to set the receiver gain. SelectFluor was then added and ^{1}H NMR spectra (2 scans per spectrum) were acquired at 120 s intervals until more than 4 half-lives had elapsed.

6.2.1.5. General Procedure E – Synthesis of Enol Esters from 3,4-dihydronaphthalen-1-yl acetate (100)

Compound **100** (1 equiv.) was suspended in toluene (5 mL) and *p*-toluenesulfonic acid monohydrate (0.1 equiv.) and acid chloride (1.5 equiv.) were added. The mixture was then heated to 160°C with a Dean-Stark trap fitted for 7 hours. Upon cooling to room temperature the residue solidified. This brown solid was suspended in toluene and filtered. The filtrate was concentrated and the residue dissolved in dichloromethane. This solution was extracted with saturated aqueous sodium bicarbonate solution (to pH 8). The organic phase was collected, dried over anhydrous MgSO$_4$ and concentrated *in vacuo* on to silica. The silica was then washed (10% ethyl acetate in hexane) to yield a filtrate from which the compound precipitated on cooling.

6.2.1.6. General Procedure F – Synthesis of Enol Esters *via in situ* Generation of 3,4-dihydronaphthalen-1-yl acetate (100)

Tetralone (1 equiv.), isopropenyl acetate (2 equiv.) and acid chloride (1.25 equiv.) were combined and heated to 100°C for 1-2 hours in a flask equipped with still head, condenser and a collection flask. The temperature was then increased to 170 °C for 4 – 16 hours. The resulting brown residue was cooled to room temperature, suspended in

dichloromethane and concentrated onto silica. The silica was then washed (10% ethyl acetate in hexane) and the filtrate concentrated to 5 – 10 mL and chilled, resulting in precipitation of the desired product.

6.2.1.7. General Procedure G – Synthesis of Alpha-Substituted Enol Esters

Vinyl bromide (1 equiv.), boronic acid (1.1 equiv.), 1,1-Bis(diphenylphosphino)ferrocene]dichloropalladium(II) (5 mol%), potassium phosphate tribasic (3 equiv.) and water (10 equiv.) were suspended in toluene (0.25 M in bromide) under a nitrogen atmosphere and heated to 85˚C for 2.5 - 19 hours. The mixture was then allowed to cool to room temperature, filtered through silica and the silica washed with 10% ethyl acetate in hexane. The filtrate was concentrated *in vacuo* and the residue resuspended in hexane resulting in the precipitation of the desired compound.

6.2.1.8. General Procedure H – Synthesis of Alpha-ester Ketones

Enol ester (1 equiv.) and m-CPBA were combined in CH_2Cl_2 and heated to reflux for 24 hours. The mixture was then extracted with 1 M NaOH solution. The organic phase was collected, concentrated and passed through silica in 10% ethyl acetate in hexane. The filtrate was concentrated to yield the desired compound.

6.2.2. Synthesis of Compounds

6.2.2.1. Synthesis of 3,4-dihydronaphthalen-1-yl acetate (100):
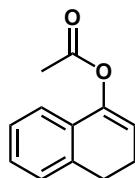
Method 1: According to the procedure of Basdevant and Legault,[207] tetralone (1 mL, 7.5 mmol) was suspended in anhydrous THF (32.8 mL) under a nitrogen atmosphere and the

mixture cooled to -78˚C, a solution of LDA in THF (1.75 M, 1.2 equiv., 9.1 mmol, 5.2 mL) was added and the mixture stirred at -78˚C for 45 minutes. Acetic anhydride (2 equiv., 15 mmol, 1.4 mL) was added and the mixture stirred at -78˚C for 45 minutes. The mixture was then allowed to warm to room temperature and stirred for 30 minutes. The suspension was poured into saturated aqueous NaHCO$_3$ solution (100 mL) and the aqueous and organic phases separated. The aqueous phase was extracted with ethyl acetate (50 mL) five times. The combined organic phases were dried over MgSO4 and concentrated *in vacuo*. The residue was distilled (185˚C, 2.2 mbar) to yield acetate **105** (0.91 g, 65%) as a pale yellow oil that crystallised on standing.

Method 2: Prepared according to general procedure B. The filtrate was concentrated *in vacuo* resulting in the precipitation of the title compound as a white solid (5.70 g, 81%).

^{1}H NMR (CDCl$_3$): δ$_H$ 7.23-7.11 (m, 4H, Ar CH), 5.74 (t, $^3J_{HH}$ = 4.7 Hz, 1H, C=CH), 2.90 (t, $^3J_{HH}$ = 8.1 Hz, 2H, CH$_2$), 2.48 (td, $^3J_{HH}$ = 8.5, 4.7 Hz, 2H, CH$_2$), 2.33 ppm (s, 3H).

^{13}C{^{1}H} NMR (CDCl$_3$): δ$_C$ 168.7, 145.2, 135.9, 130.0, 127.4, 127.1, 125.9, 120.2, 115.0, 27.0, 21.6, 20.4 ppm.

IR: 1753, 1662, 1203, 1076 cm^{-1}

m/z: (GC/MS EI) t$_R$ 11.785 min, [M] calculated 188.1, observed 188.1 ([M]$^+$).

M.P.: (Pentane) 58 – 60 °C.

Analytical data consistent with published values.[207]

6.2.2.2. Synthesis of 1*H*-inden-3-yl acetate (101):
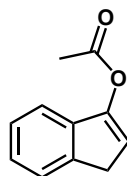
Method 1: Indanone (7.6 mmol, 1 g) as a solution in 5 mL THF was added to a suspension of sodium hydride (60% dispersion in mineral oil, 1.5 equiv., 11 mmol, 0.44 g) in anhydrous THF (10 mL) under nitrogen. The mixture was stirred at room temperature for 30 minutes during which time the reaction mixture changed colour from grey to green.

Acetyl chloride (1.5 equiv., 11 mmol, 0.8 mL) was added resulting in a colour change from green to red to orange. After 30 minutes, water (20 mL) then ethyl acetate (15 mL) were added and the aqueous and organic phases were separated. The aqueous phase was extracted with ethyl acetate (3 x 20 mL). The combined organic phases were dried over MgSO4 and concentrated. The residue was purified by flash silica column chromatography (0-20% ethyl acetate in hexane) to give enol acetate **101** (0.16 g, 12%) as a white solid.

Method 2:   Prepared according to general procedure B. The filtrate was concentrated *in vacuo* to *ca.* 5 mL and the title compound precipitated as a white solid on cooling (1.04 g, 78%).

^{1}H NMR (CDCl$_3$): δ_H 7.50 (d, $^3J_{HH}$ = 7.3 Hz, 1H, Ar CH), 7.42-7.30 (m, 3H, Ar CH), 6.41 (t, $^3J_{HH}$ = 2.4 Hz, 1H, C=CH), 3.47 (d, $^3J_{HH}$ = 2.4 Hz, 2H, CH$_2$), 2.38 (s, 3H, CH$_3$).

^{13}C{^{1}H} NMR (CDCl$_3$): δ_C 167.8, 148.8, 141.4, 138.7, 125.8, 125.3, 123.8, 117.7, 115.1, 34.5, 20.6.

IR: 1759, 1619, 1372, 1193, 1050, 1009, 766 cm^{-1}.

m/z (GC/MS EI): t$_R$ 11.134 min, [M] calculated 174.1, observed 174.1 ([M]$^+$).

M.P. (Hexane) 43-45°C

Analytical data consistent with published values.[208]

6.2.2.3.   Synthesis of 2-fluoro-2,3-dihydro-1*H*-inden-1-one (101a):
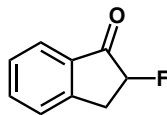
Prepared according to general procedure C. White solid (0.04 g, 80%).

^{1}H NMR (CDCl$_3$): δ_H 7.83 (d, $^3J_{HH}$ = 8.2 Hz, 1H, Ar CH), 7.69 (td, $^3J_{HH}$ = 7.5, 1.8 Hz, 1H, Ar CH), 7.50-7.44 (m, 2H, Ar CH), 5.30 (ddd, $^2J_{HF}$ = 51.0 Hz, $^3J_{HH}$ = 7.8, 4.4 Hz, 1H, CHF), 3.65 (dt, $^2J_{HH}$ = 17.1 Hz, $^3J_{HH}$,$^3J_{HF}$ = 7.8 Hz, 1H, CH$_2$), 2.26 (dt, $^3J_{HF}$ = 23.3 Hz, $^2J_{HH}$ = 17.1 Hz, $^3J_{HH}$ = 4.4 Hz, 1H, CH$_2$).

^{13}**C{^{1}H} NMR** (CDCl$_3$): δ_C 199.5 (d, $^2J_{CF}$ = 14.9 Hz), 149.2 (d, $^3J_{CF}$ = 5.66 Hz), 135.9, 133.4, 127.9, 126.3, 124.3, 90.2 (d, $^1J_{CF}$ = 190.3 Hz), 33.0 (d, $^2J_{CF}$ = 21.4 Hz).

^{19}**F NMR** (CDCl$_3$): δ_F -194.0 (ddd, $^2J_{HF}$ = 51.0, $^3J_{HF}$ = 23.3, 7.8 Hz).

IR: 1712, 1608, 1463, 1297, 1206, 1085, 811, 760 cm^{-1}.

m/z (GC/MS EI): t$_R$ 10.266 min, [M] calculated 150.0, observed 150.0 ([M]$^+$).

M.P. (Hexane) 59-61°C

Analytical data consistent with published values.[209]

6.2.2.4.   Synthesis of 2-fluoro-3,4-dihydronaphthalen-1(2*H*)-one (102):
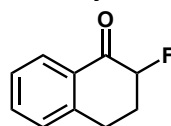
Prepared according to general procedure C. White solid (153.3 mg, 93%).

^{1}**H NMR** (CDCl$_3$): δ_H 8.07 (dd, $^3J_{HH}$ = 7.8 Hz, $^4J_{HH}$ = 1.3 Hz, 1H, Ar CH), 7.53 (td, $^3J_{HH}$ = 7.5 Hz, $^4J_{HH}$ = 1.4 Hz, 1H, Ar CH), 7.36 (t, $^3J_{HH}$ = 7.4 Hz, 1H, Ar CH), 7.29 (d, $^3J_{HH}$ = 7.8 Hz, 1H, Ar CH), 5.16 (ddd, $^2J_{HF}$ = 47.9, $^3J_{HH}$ = 12.7 Hz, $^3J_{HH}$ = 5.1 Hz, 1H, CHF), 3.15 (dd, $^3J_{HH}$ = 9.5, 4.0 Hz, 2H, CH$_2$), 2.64-2.55 (m, 1H, CH$_2$), 2.43-2.30 (m, 1H, CH$_2$).

^{13}**C{^{1}H} NMR** (CDCl$_3$): δ_C 192.8 (d, $^2J_{CF}$ = 14.6 Hz), 142.5, 133.7, 130.8, 128.2, 127.3, 126.7, 90.8 (d, $^1J_{CF}$ = 187.8 Hz), 29.6 (d, $^2J_{CF}$ = 19.1 Hz), 26.5 (d, $^3J_{CF}$ = 11.5 Hz).

^{19}**F NMR** (CDCl$_3$): δ_F -190.3 (dt, $^2J_{HF}$ = 47.9, $^3J_{HF}$ = 8.9 Hz).

IR: 1703, 1602, 1457, 1271, 1227, 1078, 927, 751 cm^{-1}.

m/z (GC/MS EI): t$_R$ 11.082 min, [M] calculated 164.1, observed 164.1 ([M]$^+$).

M. P.: (Chloroform/pentane) 41 – 43 °C.

Analytical data consistent with published values.[210]

6.2.2.5. 1-(Chloromethyl)-1,4-diazabicyclo[2.2.2]octan-1-ium tetrafluoroborate (103):
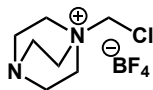
According to the procedure of Laali *et al.*,[211] DABCO (4 g) was suspended in anhydrous DCM (11.2 mL) under a nitrogen atmosphere and heated to reflux for 19 h. The mixture was cooled to room temperature and the white precipitate was collected. The solid was added to a solution of ammonium tetrafluoroborate (7 g) in acetonitrile (45 mL) and left to stir at room temperature for 22 h. The mixture was filtered, the filtrate was concentrated, and the white solid was recrystallised from hot ethanol to yield the title compound as a white solid (8.19 g, 93%). **^{1}H NMR** (MeCN-d_3): δH 4.96 (s, 2H, CH$_2$), 3.36 (t, $^3J_{HH}$= 7.5 Hz, 6H, CH$_2$), 3.18 (t, $^3J_{HH}$= 7.5 Hz, 6H, CH$_2$).

^{13}C{1H}NMR (MeCN-d_3): 118.3, 69.3, 52.4, 45.5.

IR: 1468, 1460, 1369, 1358, 1325, 1285, 1053 cm^{-1}

M.P.: (ethanol) 124°C.

Analytical data consistent with published values.[211]

6.2.2.6. Synthesis of cyclohex-1-en-1-yl acetate (104):
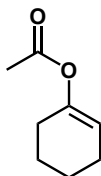
Prepared according to general procedure B. The filtrate was concentrated *in vacuo* and the residue distilled (0.1 mbar, 20-30 °C) to yield the title compound as a colourless oil (3.0 g, 56%).

^{1}H NMR (CDCl$_3$): δ_H 5.36 (tt, $^3J_{HH}$ = 5.7 Hz, $^4J_{HH}$ = 1.4 Hz, 1H, C=CH), 2.16-2.09 (m, 7H, 2 x CH$_2$, CH$_3$), 1.77-1.71 (m, 2H, CH$_2$), 1.63-1.57 (m, 2H, CH$_2$).

^{13}C{^{1}H} NMR (CDCl$_3$): δ_C 169.2, 148.3, 113.8, 26.7, 23.5, 22.5, 21.6, 20.8.

IR: 2932, 1751, 1364, 1224, 1119, 1043, 1011 cm^{-1}.

m/z (GC/MS EI): t_R 8.455 min, [M] calculated 140.1, observed 140.1 ([M]+).

Analytical data consistent with published values.[212]

6.2.2.7.   Synthesis of 4-(*tert*-butyl)cyclohex-1-en-1-yl acetate (105):
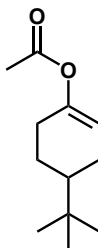
Prepared according to general procedure B. The filtrate was concentrated *in vacuo* and the residue was purified by flash silica column chromatography (40 g silica column, 0-10% ethyl acetate in hexane) to yield the title compound (0.50 g, 74%) as a colourless oil.

¹H NMR (CDCl₃): δ_H 5.36 (dt, $^3J_{HH}$ = 5.5, 2.4 Hz, $^4J_{HH}$ = 2.4 Hz, 1H, C=CH), 2.34-2.23 (m, 1H; H4), 2.17-2.06 (m, 5H, CH₂), 1.95-1.84 (m, 2H, CH₂), 1.39-1.33 (m, 2H, CH^{t}Bu, CH₂), 0.89 ppm (s, 9H, ^{t}Bu).

¹³C{¹H} NMR (CDCl₃): δ_C 169.0, 147.8, 113.4, 42.9, 31.7, 27.4, 26.8, 24.5, 23.5, 20.6.

IR: 2950, 2865, 1755, 1366, 1214, 1117, 907 cm⁻¹.

m/z (GC/MS EI): t_R 10.556 min, [M] calculated 196.2, observed 196.2 ([M]+).

Analytical data consistent with published values.[212]

6.2.2.8.   Synthesis of 2-fluorocyclohexan-1-one (106):
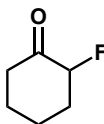
Prepared according to general procedure C. Colourless oil (1.2 g, 33%).

¹H NMR (CDCl₃): δ_H 4.86 (ddd, $^2J_{HF}$ = 49.0 Hz, $^3J_{HH}$ = 11.3, 6.3 Hz, 1H, CHF), 2.53-2.47 (m, 1H, CH₂), 2.41-2.26 (m, 2H, CH₂), 2.02-1.92 (m, 2H, CH₂), 1.84-1.57 (m, 3H, CH₂).

¹³C{¹H} NMR (CDCl₃): δ_C 205.2 (d, $^2J_{CF}$ = 14.4 Hz), 92.1 (d, $^1J_{CF}$ = 190.2 Hz), 39.7, 33.7 (d, $^2J_{CF}$ = 18.6 Hz), 26.4, 22.3 (d, $^3J_{CF}$ = 9.8 Hz).

19F NMR (CDCl$_3$): δ$_F$ -188.3 (m, incl. app. d, $^2J_{HF}$ = 49.0 Hz).

IR: 2943, 2867, 1729, 1069, 881, 745 cm^{-1}.

m/z (GC/MS EI): t$_R$ 7.034 min, [M] calculated 116.1, observed 116.2 ([M]$^+$).

Analytical data consistent with published values.[213]

6.2.2.9. **Synthesis of (2*R*,4*S*)-4-(*tert*-butyl)-2-fluorocyclohexan-1-one (107-ax)
and (2*S*,4*S*)-4-(*tert*-butyl)-2-fluorocyclohexan-1-one (107-eq):**
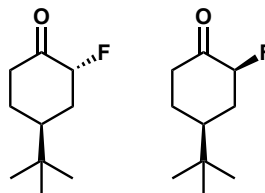
Prepared according to general procedure C. The residue was purified by flash silica
column chromatography (0-15%) to yield (2*S*,4*S*)-4-(*tert*-butyl)-2-fluorocyclohexan-1-
one **107-eq** (14.9 mg) and (2*R*,4*S*)-4-(*tert*-butyl)-2-fluorocyclohexan-1-one **107-ax** (29.8
mg) as a colourless oil and white solid respectively, 26% overall.

(2*R*,4*S*)-4-(*tert*-butyl)-2-fluorocyclohexan-1-one (107-ax):

1H NMR (CDCl$_3$): δ$_H$ 4.69 (dddd, $^2J_{HF}$ = 50.5 Hz, $^3J_{HH}$ = 3.3, 2.5 Hz, $^4J_{HH}$ = 1.3 Hz, 1H, CHF),
2.80 (tt, $^2J_{HH}$ = 13.7 Hz, $^4J_{HF}$ = 5.9 Hz, 1H, CH$_2$), 2.47-2.36 (m, 2H, CH$_2$), 2.18-2.10 (m, 1H,
CH$_2$), 1.88 (tt, $^3J_{HH}$ = 12.4, 3.6 Hz, 1H, CH^{t}Bu), 1.63 (dddd, $^3J_{HF}$ = 43.8 Hz, $^2J_{HH}$ = 14.8 Hz,
$^3J_{HH}$ = 12.5, 3.3 Hz, 1H, CH$_2$), 1.48 (qdd, $^2J_{HH}$,$^3J_{HH}$ = 13.1 Hz, $^3J_{HH}$ = 4.4 Hz, $^4J_{HH}$ = 1.5 Hz, 1H,
CH$_2$), 0.93 (s, 9H, ^{t}Bu).

13C{1H} NMR (CDCl$_3$): δ$_C$ 207.4 (d, $^2J_{CF}$ = 20.7 Hz), 92.1 (d, $^1J_{Cf}$ = 177.0 Hz), 40.0, 37.2, 33.9
(d, $^2J_{CF}$ = 22.1 Hz), 31.6, 27.4, 26.9.

19F NMR (CDCl$_3$): δ$_F$ -185.5 (dddd, $^2J_{HF}$ = 50.5 Hz, $^3J_{HF}$ = 43.8, 13.0 Hz, $^4J_{HF}$ = 5.9 Hz).

IR: 2952, 2868, 1709, 1455, 1190, 1110, 1013 cm^{-1}.

m/z (GC/MS EI): t$_R$ 10.288 min, [M] calculated 172.1, observed 172.1 ([M]$^+$).

M.P. (vapour diffusion DCM/hexane) 75-76°C

Analytical data consistent with published values.[214]

(2*S*,4*S*)-4-(*tert*-butyl)-2-fluorocyclohexan-1-one (107-eq):

¹H NMR (CDCl₃): δ_H 4.95 (dddd, $^2J_{HF}$ = 48.6 Hz, $^3J_{HH}$ = 12.0, 6.7 Hz, $^4J_{HH}$ = 1.1 Hz, 1H, CHF), 2.55-2.48 (m, 2H, CH₂), 2.32 (tdd, $^2J_{HH}$,$^3J_{HH}$ = 14.0 Hz, $^3J_{HH}$ = 6.1 Hz, $^4J_{HF}$ = 1.2 Hz, 1H, CH₂), 2.16-2.06 (m, 1H, CH₂), 1.70-1.56 (m, 2H, CH^{t}Bu, CH₂), 1.50-1.39 (m, 1H, CH₂), 0.95 (s, 9H, ^{t}Bu).

¹³C{¹H} NMR (CDCl₃): δ_C 205.2 (d, $^2J_{CF}$ = 13.7 Hz), 91.9 (d, $^1J_{CF}$ = 191.9 Hz), 44.8 (d, $^3J_{CF}$ = 8.2 Hz), 38.6, 34.9 (d, $^2J_{CF}$ = 14.3 Hz), 31.9, 27.3, 27.1.

¹⁹F NMR (CDCl₃): δ_F -188.0 (m, incl. app. d, $^2J_{HF}$ = 48.6 Hz).

IR: 2960, 2870, 1736, 1370, 1071, 870 cm⁻¹.

m/z (GC/MS EI): t_R 8.992 min, [M] calculated 172.1, observed 172.1 ([M]⁺).

Analytical data consistent with published values.[214]

6.2.2.10. Synthesis of 3,4-dihydronaphthalen-1-yl benzoate (108):
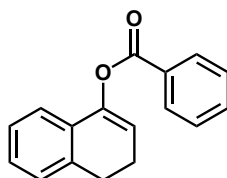
Prepared according to general procedure E. White solid, 103 mg (11%).

¹H NMR (CDCl₃): δ_H 8.24 (app. d, $^3J_{HH}$ = 8.2 Hz, 2H, Ar CH), 7.67 (tt, $^3J_{HH}$ = 7.5 Hz, $^4J_{HH}$ = 2.0 Hz, 1H, Ar CH), 7.55 (tt, $^3J_{HH}$ = 7.6 Hz, $^4J_{HH}$ = 2.0 Hz, 2H, Ar CH), 7.21-7.16 (m, 4H, Ar CH), 5.87 (t, $^3J_{HH}$ = 4.7 Hz, 1H, C=CH), 2.96 (t, $^3J_{HH}$ = 8.1Hz, 2H, CH₂), 2.54. (td, $^3J_{HH}$ = 8.1, 4.7 Hz, 2H, CH₂).

¹³C{¹H} NMR (CDCl₃): δ_C 164.5, 145.4, 136.0, 133.1, 130.0, 129.7, 129.1, 128.1, 127.5, 127.2, 126.0, 120.4, 115.3, 27.0, 21.7.

IR: 1730, 1618, 1545, 1487, 1360, 1334.74, 1171, 1124, 1086 cm⁻¹.

m/z HRMS calculated for C₁₇H₁₅O₂ = 251.1067 found 251.1066.

M. P.: (ethyl acetate/hexane) 51-52°C.

6.2.2.11. Synthesis of 3,4-dihydronaphthalen-1-yl 4-(dimethylamino)benzoate (109):
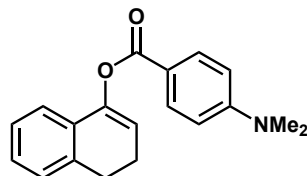
Prepared according to general procedure E. Yellow solid (253 mg, 23%).

¹H NMR (CDCl₃): δ_H 8.10 (dt, $^3J_{HH}$ = 9.8 Hz, $^4J_{HH}$ = 2.6 Hz, 2H, Ar CH), 7.23-7.12 (m, 4H, Ar CH), 6.74 (dt, $^3J_{HH}$ = 9.7 Hz, $^4J_{HH}$ = 2.6 Hz, 2H, Ar CH), 5.83 (t, $^3J_{HH}$ = 4.7 Hz, 1H, C=C*H*), 3.10 (s, 6H, CH₃), 2.92 (t, $^3J_{HH}$ = 8.1Hz, 2H, CH₂), 2.51 (td, $^3J_{HH}$ = 8.1, 4.7 Hz, 2H, CH₂).

¹³C{¹H} NMR (CDCl₃): δ_C 164.8, 153.2, 145.4, 136.0, 131.4, 130.6, 127.3, 127.0, 125.9, 120.5, 115.6, 114.9, 110.3, 39.6, 27.1, 21.7.

IR: 1713, 1605, 1572, 1375, 1269, 1175, 1124, 1080 cm⁻¹

m/z HRMS calculated for C₁₉H₂₀NO₂ [M+H] = 294.1489 found 294.1485

M. P.: (ethyl acetate/hexane) 120-122°C.

6.2.2.12. Synthesis of 3,4-dihydronaphthalen-1-yl 4-methoxybenzoate (110):
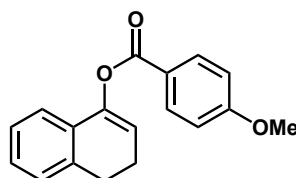
Prepared according to general procedure E. White solid (200 mg, 19%).

¹H NMR (CDCl₃): δ_H 8.19 (dt, $^3J_{HH}$ = 9.4, 2.4 Hz, 2H, Ar CH), 7.20-7.15 (m, 4H, Ar CH), 7.02 (dt, $^3J_{HH}$ = 9.3, 2.6 Hz, 2H, Ar CH), 5.85 (t, $^3J_{HH}$ = 4.7 Hz, 1H, C=CH), 3.93 (s, 3H, CH3), 2.95 (t, $^3J_{HH}$ = 8.1 Hz, 2H, CH*2*), 2.52 ppm (td, $^3J_{HH}$ = 8.1, 4.7 Hz, 2H, CH2).

¹³C{¹H} NMR (CDCl₃): δ_C 164.2, 163.4, 145.3, 136.0, 131.8, 130.2, 127.4, 127.1, 125.9, 121.4, 120.4, 115.1, 113.4, 55.0, 27.1, 21.7.

IR: 1722, 1605, 1259, 1221, 1180, 1167, 1126, 1084 cm⁻¹

m/z HRMS calculated for C₁₈H₁₇O₃ [M+H] = 281.1172 found 281.1170.

M. P.: (ethyl acetate/hexane) 118-120°C.

6.2.2.13. Synthesis of 3,4-dihydronaphthalen-1-yl 4-fluorobenzoate (111):
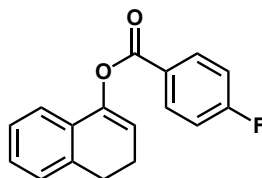
Prepared according to general procedure F. White solid, 20 mg (2%).

^{1}H NMR (CDCl$_3$): δ$_H$ 8.25 (ddt, $^3J_{HH}$ = 8.9 Hz, $^4J_{HF}$ = 5.4 Hz, $^4J_{HH}$ = 2.5 Hz, 2H, Ar CH), 7.24-7.12 (m, 6H, Ar CH), 5.86 (t, $^3J_{HH}$ = 4.7 Hz, 1H, C=CH), 2.95 (t, $^3J_{HH}$ = 8.1Hz, 2H, CH$_2$), 2.53 (td, $^3J_{HH}$ = 8.1, 4.7 Hz, 2H, CH$_2$).

^{13}C{^{1}H} NMR (CDCl$_3$): δ$_C$ 165.6 (d, $^1J_{CF}$ = 254.9 Hz), 163.5, 145.2, 136.0, 132.2 (d, $^3J_{CF}$ = 10.0 Hz), 129.9, 127.3 (d, $^2J_{CF}$ = 37.4 Hz), 125.9, 125.3 (d, $^4J_{CF}$ = 3.1 Hz), 120.2, 115.4, 115.3, 115.2, 27.0, 21.6.

^{19}F NMR (CDCl$_3$): δ$_F$ -104.6 (tt, $^3J_{HF}$ = 8.5 Hz, $^5J_{HF}$ = 5.4 Hz).

IR: 1728, 1692, 1487, 1410, 1364, 1258, 1240.23, 1084 cm^{-1}.

m/z HRMS calculated for C$_{17}$H$_{14}$FO$_2$ [M+H] = 269.0972 found 269.0962.

M. P.: (Ethyl acetate/hexane) 53-54°C.

6.2.2.14. Synthesis of 3,4-dihydronaphthalen-1-yl 4-chlorobenzoate (112):
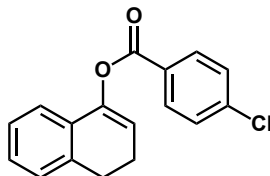
Prepared according to general procedure C. Off-white solid, 166 mg (15%).

^{1}H NMR (CDCl$_3$): δ$_H$ 8.16 (dt, $^3J_{HH}$ = 9.0 Hz, $^4J_{HH}$ = 2.2 Hz, 2H, Ar CH), 7.52 (dt, $^3J_{HH}$ = 9.1 Hz, $^4J_{HH}$ = 2.2 Hz, 2H, Ar CH), 7.22-7.11 (m, 4H, Ar CH), 5.86 (t, $^3J_{HH}$ = 4.7 Hz, 1H, C=CH), 2.95 (t, $^3J_{HH}$ = 8.1Hz, 2H, CH$_2$), 2.53 (td, $^3J_{HH}$ = 8.1, 4.7 Hz, 2H, CH$_2$).

^{13}C{^{1}H} NMR (CDCl$_3$): δ$_C$ 163.6, 145.2, 139.6, 136.0, 139.2, 131.0, 129.8, 128.8, 127.5, 127.2, 125.9, 120.2, 115.3, 27.0, 21.6.

IR: 1730, 1680, 1504, 1240, 1221, 1173, 1153, 1124, 1084 cm^{-1}.

m/z HRMS calculated for C$_{17}$H$_{14}$O$_2$Cl [M+H] 285.0677 found 285.0675

M. P. (Ethyl acetate/hexane) 68-70°C.

6.2.2.15. Synthesis of 3,4-dihydronaphthalen-1-yl methyl terephthalate (113):
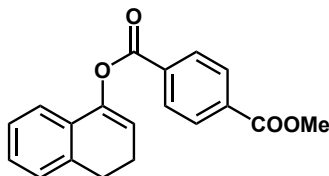
Prepared according to general procedure F. Off-white solid, 58 mg (5%).

^{1}H NMR (CDCl$_3$): δ_H 8.30 (dt, $^3J_{HH}$ = 8.5 Hz, $^4J_{HH}$ = 1.7 Hz, 2H, Ar CH), 8.20 (dt, $^3J_{HH}$ = 8.2 Hz, $^4J_{HH}$ = 1.7 Hz, 2H, Ar CH), 7.22-7.12 (m, 4H, Ar CH), 5.88 (t, $^3J_{HH}$ = 4.7 Hz, 1H, C=CH), 4.00 (s, 3H, CH$_3$), 2.96 (t, $^3J_{HH}$ = 8.1 Hz, 2H, CH$_2$), 2.54 (td, $^3J_{HH}$ = 8.1, 4.7 Hz, 2H, CH$_2$). [1]

^{3}C{^{1}H} NMR (CDCl$_3$): δ_C 165.7, 163.6, 145.2, 136.0, 133.9, 132.8, 129.6, 129.3, 127.6, 127.2, 126.0, 120.2, 115.3, 52.0, 27.0, 21.7.

IR: 1715, 1676, 1406, 1286, 1269, 1246, 1171, 1109, 1078 cm^{-1}.

m/z HRMS calculated for C$_{19}$H$_{17}$O$_4$ [M+H] 309.1121 found 309.1122

M. P.: (Ethyl acetate/hexane) 126-128°C.

6.2.2.16. Synthesis of 3,4-dihydronaphthalen-1-yl 4-(trifluoromethyl)benzoate (114):
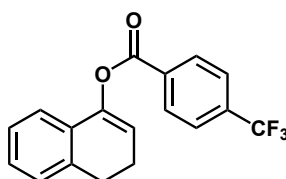
Prepared according to general procedure C. Off-white solid, 19 mg (6%).

^{1}H NMR (CDCl$_3$): δ_H 8.35 (d, $^3J_{HH}$ = 8.3 Hz, 2H, Ar CH), 7.82 (d, $^3J_{HH}$ = 8.7 Hz, 2H), 7.23-7.11 (m, 4H, Ar CH), 5.89 (t, $^3J_{HH}$ = 4.7 Hz, 1H, C=CH), 2.96 (t, $^3J_{HH}$ = 8.1Hz, 2H, CH$_2$), 2.54 (td, $^3J_{HH}$ = 8.1, 4.7 Hz, 2H, CH$_2$).

^{13}C{^{1}H} NMR (CDCl$_3$): δ_C 163.2, 145.2, 136.0, 134.5 (q, $^2J_{CF}$ = 32.6 Hz), 132.3, 130.0, 129.7, 127.6, 127.2, 123.1 (q, $^1J_{CF}$ = 273.6 Hz), 126.0, 125.2 (q, $^3J_{CF}$ = 3.7 Hz), 120.1, 115.4, 27.0, 21.6.

19F NMR (CDCl₃): δ_F -163.1 (s).

IR: 1730, 1408, 1323, 1267, 1124, 1113, 1092 cm⁻¹.

m/z HRMS calculated for $C_{18}H_{14}O_2F_3$ [M+H] 319.0940 found 319.

M. P. (Ethyl acetate/hexane) 96-98°C.

6.2.2.17. Synthesis of 3,4-dihydronaphthalen-1-yl 4-nitrobenzoate (115):
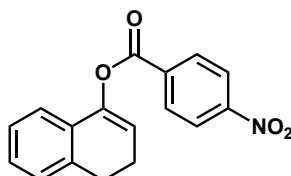
Prepared according to general procedure E. White solid, 355 mg (32%).

¹H NMR (CDCl₃): δ_H 8.44-8.36 (m, 4H, Ar CH), 7.23-7.16 (m, 3H, Ar CH), 7.12-7.10 (m, 1H, Ar CH), 5.91 (t, $^3J_{HH}$ = 4.6 Hz, 1H, C=CH), 2.96 (t, $^3J_{HH}$ = 8.1 Hz, 2H, CH₂), 2.56 (td, $^3J_{HH}$ = 8.1, 4.7 Hz, 2H, CH₂).

13C{¹H} NMR (CDCl₃): δ_C 168.7, 145.2, 135.9, 130.0, 127.4, 127.1, 125.9, 120.2, 115.0, 27.0, 21.6, 20.4.

IR: 1728, 1259, 1238, 1219, 1171, 1124, 1082 cm⁻¹.

m/z HRMS calculated for $C_{17}H_{14}NO_4$ [M+H] = 296.0917 found 296.0909

M. P.: (Ethyl acetate/hexane) 119-121°C.

6.2.2.18. Synthesis of 2-bromo-3,4-dihydronaphthalen-1-yl acetate (116):
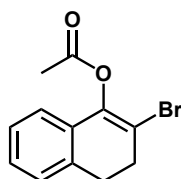
According to the procedure of Dwyer *et. al,*[215] tetralone (2 mL, 15 mmol), *p*-toluenesulfonic acid monohydrate (285 mg, 1.5 mmol) and *N*-bromosuccinimide (3.2 g, 18 mmol) were suspended in CH₂Cl₂ (10 mL) and heated to 40°C for 1 hour. The reaction mixture was then cooled to room temperature, filtered and concentrated. The resulting orange oil (crude **6**) was then suspended in THF (10 mL), cooled to -78°C under a nitrogen

atmosphere and NaHMDS (1 M solution in THF, 22.5 mL) added slowly. After 30 minutes acetic anhydride (13 mL, 35 mmol) was added resulting in the formation of a slurry. The reaction mixture was allowed to warm to room temperature and stirred for a further 30 minutes. The suspension was poured into 1 M aqueous HCl and diluted with Et_2O. The organic phase was washed with saturated aqueous $NaHCO_3$ solution and brine the dried over anhydrous $MgSO_4$. The concentrated organic phase was passed through silica in 10% EtOAc/hexane, concentrated and the residue resuspended in hexane resulting in the precipitation of the title compound as an off-white solid (2.81 g, 70%).

^{1}H NMR (CDCl$_3$): δ_H 7.19-7.06 (m, 4H, Ar CH), 3.00 (t, $^3J_{HH}$ = 8.0 Hz, 2H, CH$_2$), 2.90 (t, $^3J_{HH}$ = 8.0 Hz, 2H, CH$_2$), 2.35 (s, 3H, CH$_3$).

^{13}C{^{1}H} NMR (CDCl$_3$): δ_C. 167.1, 134.1, 129.5, 127.8, 127.1, 126.2, 120.5, 112.6, 32.3, 28.3, 20.1.

IR: 1765, 1641, 1487, 1439, 1425, 1371, 1275, 1180, 1124, 1103, 1053, 1038 cm^{-1}.

m/z (GC/MS EI): t$_R$ 13.714 min, [M] calculated 266.0, observed 266.1 ([M]$^+$).

M. P.: (Hexane) 94-95°C.

Analytical data consistent with published values.[216]

6.2.2.19.   Synthesis of 2-bromo-2-fluoro-3,4-dihydronaphthalen-1(2*H*)-one (117):
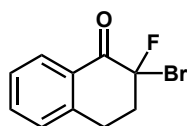
Prepared according to general procedure A. The reaction mixture was concentrated on to silica and washed with 10% ethyl acetate in hexane. The filtrate was concentrated to yield the title compound as a white solid (414 mg, 65%).

^{1}H NMR (CDCl$_3$): δ_H 8.15 (dd, $^3J_{HH}$ = 7.6 Hz, $^4J_{HH}$ = 1.2 Hz, 1H, Ar CH), 7.56 (td, $^3J_{HH}$ = 7.6 Hz, $^4J_{HH}$ = 1.4 Hz, 1H, Ar CH), 7.41 (t, $^3J_{HH}$ = 7.6 Hz, 1H, Ar CH), 7.30 (dd, $^3J_{HH}$ = 7.6 Hz, $^4J_{HH}$ = 1.2 Hz, 1H, Ar CH), 3.36 (dddd, $^2J_{HH}$ = 17.5 Hz, $^3J_{HH}$ = 11.7, 4.6 Hz, $^4J_{HF}$ = 1.3 Hz, 1H, CH$_2$), 3.12 (ddt, $^2J_{HH}$ = 17.5 Hz, $^3J_{HH}$ = 4.6, 2.4 Hz, 1H, CH$_2$), 2.86 (dddd, $^2J_{HH}$ = 14.2 Hz, $^3J_{HH}$ = 4.6,

2.4 Hz, $^3J_{HF}$ = 3.7 Hz, 1H, CH$_2$), 2.63 (dddd, $^2J_{HH}$ = 14.2 Hz, $^3J_{HH}$ = 11.7, 4.6 Hz, $^3J_{HF}$ = 7.0 Hz, 1H, CH$_2$).

^{13}C{^{1}H} NMR (CDCl$_3$): δ_C 184.9 (d, $^2J_{CF}$ = 19.1 Hz), 141.1, 134.2, 128.7, 128.3, 128.1, 127.1, 100.9 (d, $^1J_{CF}$ = 267.6 Hz), 38.0 (d, $^2J_{CF}$ = 19.1 Hz), 27.5 (d, $^3J_{CF}$ = 7.7 Hz).

^{19}F NMR (CDCl$_3$): δ_F-114.4 (ddt, $^3J_{HF}$ = 7.0, 3.7 Hz, $^4J_{HH}$ = 1.3 Hz).

IR: 1695, 1601, 1458, 1439, 1304, 1136, 1033 cm^{-1}.

m/z (GC/MS EI): t_R 12.884 minutes, [M] calculated 242.0, observed 242.1 [M].

M.P. (Hexane) 72-74°C.

Analytical data consistent with published values.[217]

6.2.2.20.   Synthesis of 2-(4-methoxyphenyl)-3,4-dihydronaphthalen-1-yl acetate (118):
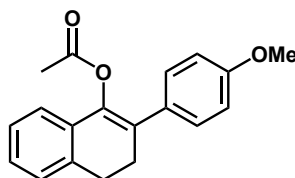
Prepared according to general procedure G. White solid (194 mg, 66%).

^{1}H NMR (CDCl$_3$): δ_H 7.34 (dt, $^3J_{HH}$ = 9.2 Hz, $^4J_{HH}$ = 2.5 Hz, 2H, Ar CH), 7.22-7.09 (m, 4H, Ar CH), 6.90 (dt, $^3J_{HH}$ = 9.2 Hz, $^4J_{HH}$ = 2.5 Hz, 2H, Ar CH), 3.83 (s, 3H, OCH$_3$), 2.99 (t, $^3J_{HH}$ = 7.9 Hz, 2H, CH$_2$), 2.78 (t, $^3J_{HH}$ = 7.9 Hz, 2H, CH$_2$), 2.16 (s, 3H, CH$_3$).

^{13}C{^{1}H} NMR (CDCl$_3$): δ_C. 168.5, 158.2, 140.0, 135.3, 130.7, 130.4, 128.2, 127.1, 126.8, 126.0, 125.9, 120.5, 113.2, 54.7, 28.3, 27.4, 20.3.

IR: 1749, 1603, 1508, 1485, 1450, 1369, 1277, 1244, 1225, 1177, 1155, 1128 cm^{-1}.

m/z HRMS calculated for C$_{19}$H$_{19}$O$_3$ [M+H] = 295.1329 found 295.1322

M. P.: (Hexane) 130-131°C.

Synthesis of 2-(*p*-tolyl)-3,4-dihydronaphthalen-1-yl acetate (119):
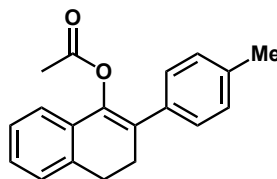
Prepared according to general procedure G. White solid (175 mg, 63%).

¹H NMR (CDCl₃): δ_H 7.29 (dt, $^3J_{HH}$ = 8.4 Hz, $^4J_{HH}$ = 1.9 Hz, 2H, Ar CH), 7.21-7.10 (m, 6H, Ar CH), 2.99 (t, $^3J_{HH}$ = 7.9 Hz, 2H, CH₂), 2.79 (t, $^3J_{HH}$ = 7.9 Hz, 2H, CH₂), 2.36 (s, 3H, CH₃), 2.15 (s, 3H, CH₃).

¹³C{¹H} NMR (CDCl₃): δ_C. 168.5, 140.2, 136.5, 135.4, 135.2, 130.6, 128.4, 127.2, 126.9, 126.3, 126.0, 120.6, 120.5, 28.3, 27.3, 20.7, 20.3.

IR: 1751, 1250, 1086, 1036 cm⁻¹.

m/z HRMS calculated for $C_{19}H_{19}O_2$ [M+H] = 279.1380 found 279.1370.

M. P.: (Hexane) 97-99°C.

6.2.2.21.   Synthesis of 2-phenyl-3,4-dihydronaphthalen-1-yl acetate (120):
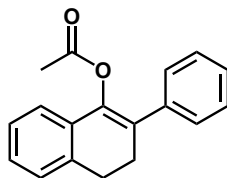
Prepared according to general procedure G. White solid (922 mg, 87%).

¹H NMR (CDCl₃): δ_H 7.40-7.34 (m, 4H, Ar CH), 7.29-7.25 (m, 1H, Ar CH), 7.21-7.18 (m, 3H, Ar CH), 7.13-7.11 (m, 1H, Ar CH), 3.00 (t, $^3J_{HH}$ = 8.1 Hz, 2H, CH₂), 2.81 (t, $^3J_{HH}$ = 8.1 Hz, 2H, CH₂), 2.14 (s, 3H, CH₃).

¹³C{¹H} NMR (CDCl₃): δ_C 168.5, 140.5, 138.2, 135.5, 130.5, 127.7, 127.3, 126.9, 126.8, 126.4, 126.0, 120.7, 28.3, 27.3, 20.2.

IR: 1763, 1640, 1485, 1364, 1190, 1124, 1051, 1038 cm⁻¹.

m/z (GC/MS EI): t_R 15.507 min, [M] calculated 264.1, observed ([M]⁺).

M. P.: (Hexane) 88-90°C.

Analytical data consistent with published values.[218]

6.2.2.22. Synthesis of methyl 4-(1-acetoxy-3,4-dihydronaphthalen-2-yl)benzoate (121):
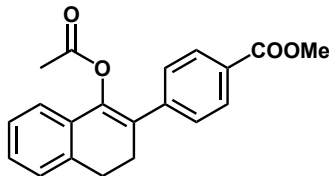
Prepared according to general procedure G. Off-white solid (107 mg, 93%).

^{1}H NMR (CDCl$_3$): δ_H 7.95 (dt, $^3J_{HH}$ = 8.5 Hz, $^4J_{HH}$ = 1.8 Hz, 2H, Ar CH), 7.48 (dt, $^3J_{HH}$ = 8.5 Hz, $^4J_{HH}$ = 1.8 Hz, 2H, Ar CH), 7.23-7.12 (m, 4H, Ar CH), 3.01 (t, $^3J_{HH}$ = 8.0 Hz, 2H, CH$_2$), 2.82 (t, $^3J_{HH}$ = 8.0 Hz, 2H, CH$_2$), 2.61 (s, 3H, CH$_3$), 2.14 (s, 3H, CH$_3$).

^{13}C{^{1}H} NMR (CDCl$_3$): δ_C 197.1, 168.2, 143.2, 141.6, 135.6, 135.3, 130.1, 127.9, 127.8, 127.8, 127.1, 127.1, 126.9, 126.2, 125.3, 121.0, 28.3, 27.3, 20.2.

IR: 1749, 1674, 1595, 1402, 1369, 1265, 1200, 1178, 1124, 1086, 1034 cm^{-1}.

m/z HRMS calculated for C$_{20}$H$_{19}$O$_3$ [M+H] 307.1329 found 307.1318.

M. P.: (Hexane) 157-159°C.

6.2.2.23. Synthesis of 2-(4-acetylphenyl)-3,4-dihydronaphthalen-1-yl acetate (122):
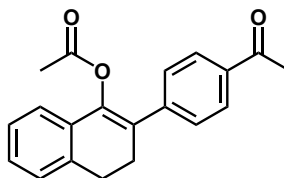
Prepared according to general procedure G. White solid, (671 mg, 69%).

^{1}H NMR (CDCl$_3$): δ_H 8.03 (dt, $^3J_{HH}$ = 8.5 Hz, $^4J_{HH}$ = 1.8 Hz, 2H, Ar CH), 7.46 (dt, $^3J_{HH}$ = 8.5 Hz, $^4J_{HH}$ = 1.8 Hz, 2H, Ar CH), 7.24-7.12 (m, 4H, Ar CH), 3.93 (s, 3H, CH$_3$), 3.01 (t, $^3J_{HH}$ = 8.1 Hz, 2H, CH$_2$), 2.82 (t, $^3J_{HH}$ = 8.1 Hz, 2H, CH$_2$), 2.61 (s, 3H, CH$_3$), 2.15 (s, 3H, CH$_3$).

^{13}C{^{1}H} NMR (CDCl$_3$): δ_C 168.2, 166.3, 143.0, 141.5, 135.6, 130.1, 129.0, 128.3, 127.8, 127.0, 126.9, 126.1, 125.4, 120.9, 51.6, 28.0, 27.2, 20.2.

IR: 1753, 1719, 1603, 1431, 1281, 1200, 1194, 1103, 1086, 1038 cm^{-1}.

m/z HRMS calculated for $C_{20}H_{19}O_4$ [M+H] = 281.1172 found 281.1169.

M. P.: (Hexane) 168-170°C.

6.2.2.24. Synthesis of 2-(4-(trifluoromethyl)phenyl)-3,4-dihydronaphthalen-1-yl acetate (123):
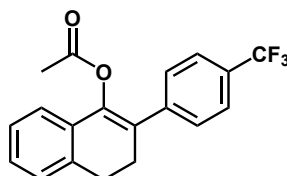
Prepared according to general procedure G. White solid (269 mg, 81%).

^{1}H NMR (CDCl$_3$): δ_H 7.61 (d, $^3J_{HH}$ = 8.0 Hz, 2H, Ar CH), 7.50 (d, $^3J_{HH}$ = 8.0 Hz, 2H), 7.24-7.12 (m, 4H, Ar CH), 3.02 (t, $^3J_{HH}$ = 8.2 Hz, 2H, CH$_2$), 2.81 (t, $^3J_{HH}$ = 8.2 Hz, 2H, CH$_2$), 2.15 (s, 3H, CH$_3$).

^{13}C{^{1}H} NMR (CDCl$_3$): δ_C 168.3, 142.0, 141.6, 135.6, 130.0, 128.7 (q, $^2J_{CF}$ = 32.9 Hz), 127.9, 127.0, 126.2, 125.0, 124.7 (q, $^3J_{CF}$ = 3.9 Hz), 123.6 (q, $^1J_{CF}$ = 271.9 Hz), 120.9, 28.1, 27.2, 20.2.

^{19}F NMR (CDCl$_3$): δ_F -62.5 (s).

IR: 1753, 1604, 1323, 1204, 1192, 1159, 1124, 1086, 1067 cm^{-1}.

m/z HRMS calculated for $C_{19}H_{16}O_2F_3$ [M+H] 333.1097 found 333.

M. P. (Ethyl acetate/hexane) 121-122°C.

6.2.2.25. 2-Fluoro-2-(4-methoxyphenyl)-3,4-dihydronaphthalen-1(2*H*)-one (118a):
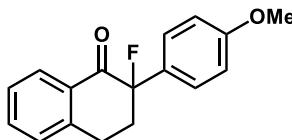
Prepared according to general procedure D.

^{1}H NMR (MeCN-d$_3$/D$_2$O, kinetic experiment) δ_H 8.06 (d, 1H, $^3J_{HH}$ = 8.0 Hz, 1H, Ar CH), 7.59 (t, $^3J_{HH}$ = 7.5 Hz, 1H, Ar CH), 7.42 (t, $^3J_{HH}$ = 8.0 Hz, 1H, Ar CH), 7.33 (d, $^3J_{HH}$ = 8.4 Hz, 2H, Ar

CH), 7.30-7.27 (m, 1H, Ar CH), 6.94 (d, $^3J_{HH}$ = 8.7 Hz, 2H, Ar CH), 3.78 (s, 3H, CH$_3$), 3.12 (apparent d, $^2J_{HH}$ = 16.9 Hz, 1H, CH$_2$), 2.88 (tt, $^3J_{HF}$,$^2J_{HH}$ = 11.5 Hz, $^3J_{HH}$ = 4.3 Hz, 1H, CH$_2$), 2.68-2.60 (m, 2H, CH$_2$).

Analytical data consistent with published values.[219]

6.2.2.26.   2-Fluoro-2-(p-tolyl)-3,4-dihydronaphthalen-1(2*H*)-one (119a):
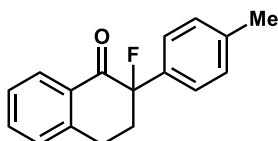
Prepared according to general procedure D.

¹H NMR (MeCN-d$_3$/D$_2$O, kinetic experiment) δ$_H$ 8.06 (d, $^3J_{HH}$ = 7.9 Hz, 1H, Ar CH), 7.59 (t, $^3J_{HH}$ = 7.5 Hz, 1H, Ar CH), 7.42 (t, $^3J_{HH}$ = 7.5 Hz, 1H, Ar CH), 7.31 (d, $^3J_{HH}$ = 7.9 Hz, 1H, Ar CH), 7.27 (d, $^3J_{HH}$ = 7.9, 2H, Ar CH), 7.22 (d, $^3J_{HH}$ = 7.9 Hz, 2H, Ar CH), 3.13 (apparent d, $^2J_{HH}$ = 16.9 Hz, 1H, CH$_2$), 2.84 (tt, $^3J_{HF}$,$^2J_{HH}$ = 12.2 Hz, $^3J_{HH}$ = 4.2 Hz, 1H, CH$_2$), 2.81-2.75 (m, 1H, CH$_2$), 2.67-2.61 (m, 1H, CH$_2$), 2.32 (s, 3H, CH$_3$).

Analytical data consistent with published values.[219]

6.2.2.27.   Synthesis   of   2-fluoro-2-phenyl-3,4-dihydronaphthalen-1(2*H*)-one (120a):
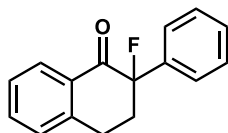
Prepared according to general procedure C. The crude reaction mixture was concentrated on to silica and purified by flash silica column chromatography (10% EtOAc/hexane) to yield the title compound as a colourless oil (29 mg, 64%).

¹H NMR (CDCl$_3$): δ$_H$ 8.18 (dd, $^3J_{HH}$ = 7.7 Hz, $^4J_{HH}$ = 1.2 Hz, 1H, Ar CH), 7.54 (td, $^3J_{HH}$ = 7.6 Hz, $^4J_{HH}$ = 1.4 Hz, 2H), 7.40 (t, $^3J_{HH}$ = 7.7 Hz, 1H, Ar CH), 7.35 (s, 5H, Ph), 7.24 (d, $^3J_{HH}$ = 7.6 Hz, 1H, Ar CH), 3.11 (dtt, $^2J_{HH}$ = 16.9 Hz, $^3J_{HH}$ = 4.8 Hz, $^4J_{HF}$ = 2 Hz, 1H, CH$_2$),2.84 (tt, $^3J_{HF}$,$^2J_{HH}$ = 11.1 Hz, $^3J_{HH}$ = 4.8 Hz, 1H, CH$_2$), 2.81-2.62 (m, 2H, CH$_2$).

¹H NMR (MeCN-d₃/D₂O, kinetic experiment) δ_H 8.07 (d, $^3J_{HH}$ = 7.7 Hz, 1H, Ar CH), 7.61 (t, $^3J_{HH}$ = 7.6 Hz, 1H, Ar CH), 7.44 (t, $^3J_{HH}$ = 7.6 Hz, 1H, Ar CH), 7.43-7.37 (m, 5H), 7.33 (d, $^3J_{HH}$ = 7.7 Hz, 1H, Ar CH), 3.33 (apparent d, $^2J_{HH}$ = 16.9 Hz, 1H, CH₂), 2.88-2.77 (m, 2H, CH₂), 2.70-2.63 (m, 1H, CH₂).

¹³C{¹H} NMR (CDCl₃): δ_C 193.3 (d, $^2J_{CF}$ = 18.1 Hz), 142.6, 136.3 (d, $^2J_{CF}$ = 22.5 Hz), 133.7, 131.7, 128.6, 128.3, 128.1, 127.7, 126.7, 125.6 (d, $^3J_{CF}$ = 6.4 Hz), 95.5 (d, $^1J_{CF}$ = 184.5 Hz), 35.0 (d, $^2J_{CF}$ = 25.1), 25.9 (d, $^3J_{CF}$ = 10.0 Hz).

¹⁹F NMR (CDCl₃): δ_F -145.4 (t, $^3J_{HF}$ = 11.1 Hz).

IR: 1730, 1408, 1323, 1267, 1124, 1113, 1092 cm⁻¹.

m/z (GC/MS EI) t_R 15.141 minutes, [M] calculated 240.1, observed 240.1.

Analytical data consistent with published values.[219]

6.2.2.28.   Synthesis of methyl 4-(2-fluoro-1-oxo-1,2,3,4-tetrahydronaphthalen-2-yl)benzoate (121a):
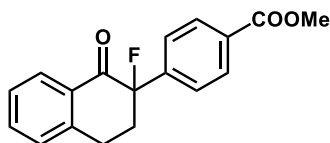
Prepared according to general procedure C. The crude reaction mixture was concentrated on to silica and purified by flash silica column chromatography (10% EtOAc/hexane) to yield the title compound as a white solid (109 mg, 73%).

¹H NMR (CDCl₃): δ_H 8.18 (dd, $^3J_{HH}$ = 7.7 Hz, $^4J_{HH}$ = 1.2 Hz, 1H, Ar CH), 7.54 (td, $^3J_{HH}$ = 7.6 Hz, $^4J_{HH}$ = 1.4 Hz, 2H), 7.40 (t, $^3J_{HH}$ = 7.7 Hz, 1H, Ar CH), 7.35 (s, 5H, Ph), 7.24 (d, $^3J_{HH}$ = 7.6 Hz, 1H, Ar CH), 3.11 (dtt, $^2J_{HH}$ = 16.9 Hz, $^3J_{HH}$ = 4.8 Hz, $^4J_{HF}$ = 2 Hz, 1H, CH₂), 2.84 (tt, $^3J_{HF}$, $^2J_{HH}$ = 11.1 Hz, $^3J_{HH}$ = 4.8 Hz, 1H, CH₂), 2.81-2.62 (m, 2H, CH₂).

¹H NMR (MeCN-d₃, kinetic experiment) δ_H 8.07 (d, $^3J_{HH}$ = 7.7 Hz, 1H, Ar CH), 7.61 (t, $^3J_{HH}$ = 7.6 Hz, 1H, Ar CH), 7.44 (t, $^3J_{HH}$ = 7.6 Hz, 1H, Ar CH), 7.43-7.37 (m, 5H), 7.33 (d, $^3J_{HH}$ = 7.7 Hz, 1H, Ar CH), 3.33 (apparent d, $^2J_{HH}$ = 16.9 Hz, 1H, CH₂), 2.88-2.77 (m, 2H, CH₂), 2.70-2.63 (m, 1H, CH₂).

^{13}C{^{1}H} NMR (CDCl$_3$): δ_C 193.3 (d, $^2J_{CF}$ = 18.1 Hz), 142.6, 136.3 (d, $^2J_{CF}$ = 22.5 Hz), 133.7, 131.7, 128.6, 128.3, 128.1, 127.7, 126.7, 125.6 (d, $^3J_{CF}$ = 6.4 Hz), 95.5 (d, $^1J_{CF}$ = 184.5 Hz), 35.0 (d, $^2J_{CF}$ = 25.1), 25.9 (d, $^3J_{CF}$ = 10.0 Hz).

^{19}F NMR (CDCl$_3$): δ_F -145.4 (t, $^3J_{HF}$ = 11.1 Hz).

IR: 1713, 1690, 1435, 1280, 1236, 1194, 1117, 1063, 1018 cm^{-1}.

m/z HRMS calculated for C$_{18}$H$_{16}$FO$_3$ [M+H] = 299.1078 found 299.1068

M.P. (Hexane) 103-105°C.

6.2.2.29. 2-(4-Acetylphenyl)-2-fluoro-3,4-dihydronaphthalen-1(2*H*)-one (122a):
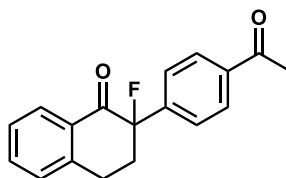
Prepared according to general procedure D.

^{1}H NMR (MeCN-d$_3$/D$_2$O, kinetic experiment) δ_H 8.08 (d, $^3J_{HH}$ = 7.7 Hz, 1H, Ar CH), 7.98 (d, $^3J_{HH}$ = 8.0 Hz, 2H, Ar CH), 7.64 (t, $^3J_{HH}$ = 7.7 Hz, 1H, Ar CH), 7.50 (d, $^3J_{HH}$ = 8.0 Hz, 2H, Ar CH), 7.46 (t, $^3J_{HH}$ = 7.7 Hz, 1H, Ar CH), 7.37 (d, $^3J_{HH}$ = 7.7 Hz, 1H, Ar CH), 3.20 (apparent d, $^2J_{HH}$ = 17.8 Hz, 1H, CH$_2$), 2.87-2.80 (m, 2H, CH$_2$), 2.72-2.65 (m, 1H, CH$_2$), 2.58 (s, 3H, CH$_3$). Analytical data consistent with published values.[219]

6.2.2.30. 2-Fluoro-2-(4-(trifluoromethyl)phenyl)-3,4-dihydronaphthalen-1(2*H*)-one (123a):
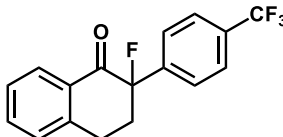
Prepared according to general procedure D.

^{1}H NMR (MeCN-d$_3$/D$_2$O, kinetic experiment) δ_H 8.08 (d, $^3J_{HH}$ = 7.9 Hz, 1H, Ar CH), 7.73 (d, $^3J_{HH}$ = 8.6 Hz, 2H, Ar CH), 7.65 (t, $^3J_{HH}$ = 7.7 Hz, 1H, Ar CH), 7.56 (d, $^3J_{HH}$ = 8.6 Hz, 2H, Ar

CH), 7.46 (t, $^3J_{HH}$ = 7.8 Hz, 1H, Ar CH), 7.38 (d, $^3J_{HH}$ = 7.7 Hz, 1H, Ar CH), 3.22 (apparent d, $^2J_{HH}$ = 14.9 Hz, 1H, CH_2), 2.88-2.79 (m, 2H, CH_2), 2.73-2.66 (m, 1H, CH_2).

Analytical data consistent with published values.[219]

6.2.2.31.   Synthesis of   1a-phenyl-2,3-dihydronaphtho[1,2-b]oxiren-7b(1aH)-yl acetate (125):
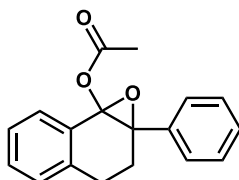
2-phenyl-3,4-dihydronaphthalen-1-yl acetate **8c** (200 mg) and *m*-CPBA (200 mg) were suspended in CH_2Cl_2 (4 mL) and the mixture stirred for 3 hours. The suspension was concentrated *in vacuo* and the residue purified by flash silica column chromatography (10% ethyl acetate in hexane) to yield the title compound as a while solid 172 mg (81%).

^{1}H NMR (CDCl$_3$): δ_H 7.50-7.47 (m, 2H, Ar CH), 7.38-7.29 (m, 5H, Ar CH), 7.24-7.19 (m, 2H, Ar CH), 2.97 (td, $^2J_{HH}$,$^3J_{HH}$ = 14.0 Hz, $^3J_{HH}$ = 6.3 Hz, 1H, CH_2), 2.75 (ddd, $^2J_{HH}$ = 14.0 Hz, $^3J_{HH}$ = 5.3, 1.3 Hz, 1H, CH_2), 2.67 (ddd, $^2J_{HH}$ = 14.1 Hz,$^3J_{HH}$ = 14.0 Hz, 5.3 Hz, 1H, CH_2), 2.46 (ddd, $^2J_{HH}$ = 14.1 Hz, $^3J_{HH}$ = 6.3, 1.3 Hz, 1H, CH_2), 1.79 (s, 3H, CH_3).

^{13}C{^{1}H} NMR (CDCl$_3$): δ_C 167.8, 136.0, 135.3, 130.6, 128.4, 128.1, 127.4, 127.3, 126.4, 125.8, 125.1, 85.0, 69.2, 26.1, 25.7, 19.7.

IR: 1753, 1484, 1444, 1380, 1069, 1034 cm^{-1}.

m/z HRMS calculated for $C_{18}H_{17}O_3$ [M+H] = 281.1172 found 281.1161.

M.P. (Hexane) 107-109°C.

6.2.2.32. Synthesis of 1-oxo-2-phenyl-1,2,3,4-tetrahydronaphthalen-2-yl acetate (120b):
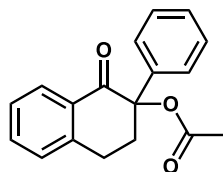
Method 1: Prepared according to general procedure C. The residue was purified by flash silica column chromatography to yield the title compound as a white solid.

Method 2: 1a-phenyl-2,3-dihydronaphtho[1,2-*b*]oxiren-7b(1a*H*)-yl acetate **125** (170 mg) was heated to 80°C for 2 hours resulting in the formation of the title compound as a white solid (170 mg, 100%).

Method 3: Prepared according to general procedure D.

¹H NMR (CDCl₃): δ_H 8.22 (dd, $^3J_{HH}$ = 7.9 Hz, $^4J_{HH}$ = 1.2 Hz, 1H, Ar CH), 7.49 (td, $^3J_{HH}$ = 7.4 Hz, $^4J_{HH}$ = 1.4 Hz, 1H, Ar CH), 7.39 (t, $^3J_{HH}$ = 7.7 Hz, 1H, Ar CH), 7.35-7.31 (m, 5H, Ph), 7.19 (d, $^3J_{HH}$ = 7.7 Hz, 1H, Ar CH), 3.36 (td, $^2J_{HH}$,$^3J_{HH}$ = 13.0 Hz, 1H, CH₂), 2.91 (ddd, $^2J_{HH}$ = 16.9 Hz, $^3J_{HH}$ = 4.4, 3.3 Hz, 1H, CH₂), 2.72 (ddd, $^2J_{HH}$ = 16.9 Hz, $^3J_{HH}$ = 13.0, 4.3 Hz, 1H, CH₂), 2.48 (ddd, $^2J_{HH}$ = 13.0 Hz, $^3J_{HH}$ = 4.4, 3.3 Hz, 1H, CH₂), 2.15 (s, 3H, CH₃).

¹H NMR (MeCN-d₃, kinetic experiment) δ_H 8.10 (d, $^3J_{HH}$ = 8.4 Hz, 1H, Ar CH), 7.61 (t, $^3J_{HH}$ = 7.4, 1H, Ar CH), 7.45-7.29 (m, 7H, Ar CH), 3.23 (td, $^2J_{HH}$,$^3J_{HH}$ = 13.0 Hz, $^3J_{HH}$ = 4.7 Hz, 1H, CH₂), 3.01-2.96 (m, 1H, CH₂), 2.70-2.61 (m, 1H, CH₂), 2.53 (ddd, $^2J_{HH}$ = 13.0 Hz, $^3J_{HH}$ = 4.6, 3.6 Hz, 1H, CH₂), 2.09 (s, 3H, CH₃).

¹³C{¹H} NMR (CDCl₃): δ_C 193.5, 169.3, 142.3, 137.0, 133.4, 132.3, 128.2, 128.2, 128.0, 127.7, 126.6, 126.3, 84.4, 33.4, 26.4, 221.1

IR: 1738, 1693, 1240, 1211, 1050 cm⁻¹.

m/z HRMS calculated for C₁₈H₁₇O₃ = 281.1172 found 281.1163.

M.P. (Hexane) 134-135°C.

6.2.2.33.   Synthesis of 2-(4-methoxyphenyl)-1-oxo-1,2,3,4-tetrahydronaphthalen-2-yl acetate (118b):
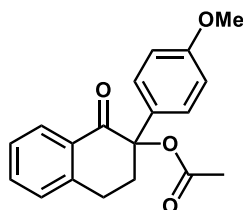
Prepared according to general procedure H. Yellow gum, (9 mg, 83%).

¹H NMR (CDCl₃): δ_H 8.24 (dd, $^3J_{HH}$ = 7.8 Hz, $^4J_{HH}$ = 1.2 Hz, 1H, Ar CH), 7.50 (td, $^3J_{HH}$ = 7.4 Hz, $^4J_{HH}$ = 1.4 Hz, 2H), 7.39 (td, $^3J_{HH}$ = 9.0 Hz, $^4J_{HH}$ = 2.7 Hz, 2H, Ar CH), 7.20 (d, $^3J_{HH}$ = 7.5 Hz, 1H, Ar CH), 6.87 (dt, $^3J_{HH}$ = 9.0 Hz, $^4J_{HH}$ = 2.7 Hz, 2H, Ar CH), 3.80 (s, 3H, CH₃), 3.39 (td, $^2J_{HH}, ^3J_{HH}$ = 13 Hz, $^3J_{HH}$ = 4.8 Hz, 1H, CH₂), 2.16 (s, 3H, CH₃).

¹H NMR (MeCN-d₃, kinetic experiment) δ_H 8.10 (d, $^3J_{HH}$ = 7.9 Hz, 1H, Ar CH), 7.58 (t, $^3J_{HH}$ = 7.5 Hz, 1H, Ar CH), 7.42 (t, $^3J_{HH}$ = 7.4 Hz, 1H, Ar CH), 7.30-7.27 (m, 3H, Ar CH), 6.91 (d, $^3J_{HH}$ = 7.7 Hz, 1H, Ar CH), 3.77 (s, 3H, CH₃), 3.23 (td, $^2J_{HH}, ^3J_{HH}$ = 13.0 Hz, $^3J_{HH}$ = 4.2 Hz, 1H, CH₂), 2.99-2.94 (m, 1H, CH₂), 2.78 (ddd, $^2J_{HH}$ = 17.0 Hz, $^3J_{HH}$ = 13.0, 4.2 Hz, 1H, CH₂), 2.55 (apparent d, $^2J_{HH}$ = 13.0 Hz, 1H, CH₂), 2.01 (s, 3H, CH₃).

¹³C{¹H} NMR (CDCl₃): δ_C 193.4, 169.4, 159.3, 142.2, 133.4, 123.1, 128.4, 128.2, 127.9, 127.8, 127.7, 126.5, 113.4, 84.3, 54.8, 32.9, 26.5, 21.1.

IR: 1678, 1599, 1460, 1389, 1244, 1205, 1059 cm⁻¹.

m/z HRMS calculated for $C_{19}H_{18}O_4Na$ [M+Na] = 333.1097 found 333.1096.

6.2.2.34. Synthesis of 1-oxo-2-(*p*-tolyl)-1,2,3,4-tetrahydronaphthalen-2-yl acetate (119b):
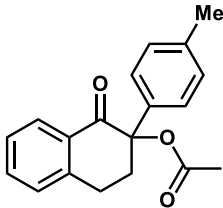
Method 1: Prepared according to general procedure H. Orange gum, 24 mg (51%).

Method 2: Prepared according to general procedure D.

¹H NMR (CDCl₃): δ$_H$ 8.24 (dd, $^3J_{HH}$ = 7.8 Hz, $^4J_{HH}$ = 1.3 Hz, 1H, Ar CH), 7.50 (td, $^3J_{HH}$ = 7.4 Hz, $^4J_{HH}$ = 1.4 Hz, 1H, Ar CH), 7.40 (t, $^3J_{HH}$ = 7.6 Hz, 1H, Ar CH), 7.26 (d, $^3J_{HH}$ = 8.0 Hz, $^4J_{HH}$ = 1.9 Hz, 2H, Ar CH), 7.20 (d, $^3J_{HH}$ = 8.0 Hz, 1H, Ar CH), 7.15 (d, $^3J_{HH}$ = 8.0 Hz, 2H, CH₂), 3.37 (td, $^2J_{HH}$,$^3J_{HH}$ = 13.0 Hz, $^3J_{HH}$ = 4.8 Hz, 1H, CH₂), 2.92 (ddd, $^2J_{HH}$ = 16.9 Hz, $^3J_{HH}$ = 4.5, 3.1 Hz, 1H, CH₂), 2.75 (ddd, $^2J_{HH}$ = 16.9 Hz, $^3J_{HH}$ = 13.0, 4.4 Hz, 1H, CH₂), 2.51 (ddd, $^2J_{HH}$ = 13.0 Hz, $^3J_{HH}$ = 4.4, 3.1 Hz, 1H, CH₂), 2.16 (s, 3H, CH₃).

¹H NMR (MeCN-d₃, kinetic experiment) δ$_H$ 8.09 (d, $^2J_{HH}$ = 7.7, 1H, Ar CH), 7.59 (t, $^2J_{HH}$ = 7.5 Hz, 1H, Ar CH), 7.43 (t, $^3J_{HH}$ = 7.6 Hz, 1H, Ar CH), 7.31-7.18 (m, 8H, Ar CH), 3.21 (td, $^2J_{HH}$,$^3J_{HH}$ = 13.0 Hz, $^3J_{HH}$ = 4.6 Hz, 1H, CH₂), 2.07 (s, 3H, CH₃).

¹³C{¹H} NMR (CDCl₃): δ$_C$ 193.5, 169.4, 142.3, 138.1, 133.7, 133.3, 132.2, 128.7, 128.2, 127.7, 126.5, 126.3, 84.4, 33.0, 26.5, 21.1, 20.6.

IR: 1740, 1688, 1599, 1240, 1231, 1211, 1053 cm⁻¹.

m/z HRMS calculated for C₁₉H₁₉O₃ [M+H] = 295.1329 found 295.1329.

6.2.2.35. Synthesis of methyl 4-(2-acetoxy-1-oxo-1,2,3,4-tetrahydronaphthalen-2-yl)benzoate (121b):
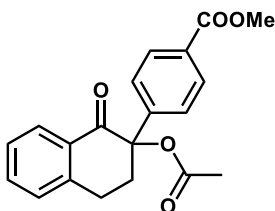
Method 1: Prepared according to general procedure H. Yellow gum, 12 mg (56%).

Method 2: Prepared according to general procedure D.

^{1}H NMR (CDCl$_3$): δ$_H$ 8.24 (dd, $^3J_{HH}$ = 7.9 Hz, $^4J_{HH}$ = 1.2 Hz, 1H, Ar CH), 8.01 (dt, $^3J_{HH}$ = 8.7 Hz, $^4J_{HH}$ = 1.9 Hz, 2H, Ar CH), 7.554 (td, $^3J_{HH}$ = 7.5 Hz, $^4J_{HH}$ = 1.4 Hz, 1H, Ar CH), 7.45-7.41 (m, 3H, Ar CH), 7.23 (d, $^3J_{HH}$ = 7.6 Hz, 1H, Ar CH), 3.92 (s, 3H, CH$_3$), 3.38 (td, $^2J_{HH}$,$^3J_{HH}$ = 12.8 Hz, $^3J_{HH}$ = 4.7 Hz, 1H, CH$_2$), 2.96 (ddd, $^2J_{HH}$ = 16.7 Hz, $^3J_{HH}$ = 4.6, 3.2 Hz, 1H, CH$_2$), 2.71 (ddd, $^2J_{HH}$ = 16.9 Hz, $^3J_{HH}$ = 4.4, 2.8 Hz, 1H, CH$_2$), 2.48 (ddd, $^2J_{HH}$ = 12.8 Hz, $^3J_{HH}$ = 4.4, 3.2 Hz, 1H, CH$_2$), 2.19 (s, 3H, CH$_3$).

^{1}H NMR (MeCN-d$_3$, kinetic experiment) δ$_H$ 8.10 (d, $^3J_{HH}$ = 8.6, 1H, Ar CH), 7.97 (d, $^3J_{HH}$ = 8.4 Hz, 2H, Ar CH), 7.47-7.44 (m, 3H, Ar CH), 7.33 (d, $^3J_{HH}$ = 7.5 Hz, 1H, Ar CH), 3.87 (s, 3H, CH$_3$), 3.24-3.17 (m, 1H, CH$_2$), 2.01 (ddd, $^2J_{HH}$ = 17.4 Hz, $^3J_{HH}$ = 4.1 Hz, 1H, CH$_2$), 2.72-2.62 (m, 1H, CH$_2$), 2.51 (ddd, $^2J_{HH}$ = 13.4 Hz, $^3J_{HH}$ = 4.1 Hz, 1H, CH$_2$).

^{13}C{^{1}H} NMR (CDCl$_3$): δ$_C$ 193.0, 169.1, 166.0, 142.2, 142.1, 133.6, 132.2, 129.8, 129.2, 128.3, 127.8, 126.8, 126.3, 83.9, 51.7, 33.4, 26.1, 21.0.

IR 1722, 1693, 1603, 1281, 1238, 1113, 1018 cm^{-1}.

m/z HRMS calculated for C$_{20}$H$_{19}$O$_5$ [M+H] = 339.1227 found 339.1215.

6.2.2.36.   2-(4-Acetylphenyl)-1-oxo-1,2,3,4-tetrahydronaphthalen-2-yl   acetate (122b):
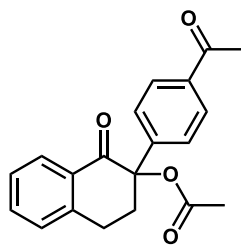
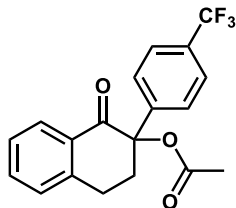Prepared according to general procedure D.

^{1}H NMR (MeCN-d$_3$/D$_2$O, kinetic experiment) δ$_H$ 8.10 (d, $^3J_{HH}$ = 7.9 Hz, 1H, Ar CH), 7.95 (d, $^3J_{HH}$ = 9.0 Hz, 2H, Ar CH), 7.62 (t, $^3J_{HH}$ = 7.8 Hz, 1H, Ar CH), 7.54 (d, $^3J_{HH}$ = 8.4 Hz, 1H, Ar CH), 7.47-7.44 (m, 2H, Ar CH), 7.33 (d, $^3J_{HH}$ = 7.7 Hz, 1H, Ar CH), 3.24-3.18 (m, 1H, CH$_2$), 3.02 (ddd, $^2J_{HH}$ = 17.0 Hz, $^3J_{HH}$ = 4.0 Hz, 1H, CH$_2$), 2.72-2.67 (m, 1H, CH$_2$), 2.56 (s, 3H, CH$_3$), 2.54 (ddd, $^2J_{HH}$ = 13.0 Hz, $^3J_{HH}$ = 4.0 Hz, 1H, CH$_2$), 2.10 (s, 3H, CH$_3$).

m/z HRMS calculated for $C_{20}H_{19}O_4$ [M+H] = 323.1278 found 323.1269.

6.2.2.37. **Synthesis** **of** **1-oxo-2-(4-(trifluoromethyl)phenyl)-1,2,3,4-tetrahydronaphthalen-2-yl acetate (123b):**

Method 1: Prepared according to general procedure H. Yellow gum, 8 mg (35%).

Method 2: Prepared according to general procedure D.

¹H NMR (CDCl₃): δ_H 8.24 (dd, $^3J_{HH}$ = 7.8 Hz, $^4J_{HH}$ = 1.3 Hz, 1H, Ar CH), 7.50 (td, $^3J_{HH}$ = 7.4 Hz, $^4J_{HH}$ = 1.4 Hz, 1H, Ar CH), 7.40 (t, $^3J_{HH}$ = 7.6 Hz, 1H, Ar CH), 7.26 (d, $^3J_{HH}$ = 8.0 Hz, $^4J_{HH}$ = 1.9 Hz, 2H, Ar CH), 7.20 (d, $^3J_{HH}$ = 8.0 Hz, 1H, Ar CH), 7.15 (d, $^3J_{HH}$ = 8.0 Hz, 2H, CH₂), 3.37 (td, $^2J_{HH}$,$^3J_{HH}$ = 13.0 Hz, $^3J_{HH}$ = 4.8 Hz, 1H, CH₂), 2.92 (ddd, $^2J_{HH}$ = 16.9 Hz, $^3J_{HH}$ = 4.5, 3.1 Hz, 1H, CH₂), 2.75 (ddd, $^2J_{HH}$ = 16.9 Hz, $^3J_{HH}$ = 13.0, 4.4 Hz, 1H, CH₂), 2.51 (ddd, $^2J_{HH}$ = 13.0 Hz, $^3J_{HH}$ = 4.4, 3.1 Hz, 1H, CH₂), 2.16 (s, 3H, CH₃).

¹H NMR (MeCN-d₃, kinetic experiment) δ_H 8.10-8.08 (m, 1H, Ar CH), 7.74-7.73 (m, 1H, Ar CH), 7.69 (d, $^3J_{HH}$ = 8.4 Hz, 2H, Ar CH), 7.66-7.61 (m, 1H, Ar CH), 7.53 (d, $^3J_{HH}$ = 8.4 Hz, 2H, Ar CH), 7.33 (d, $^3J_{HH}$ = 7.7 Hz, 1H, Ar CH), 3.24-3.19(m, 1H, CH₂), 3.03 (apparent d, $^2J_{HH}$ = 17.8 Hz, 1H, CH₂), 2.73-2.63 (m, 1H, CH₂), 2.53 (apparent d, $^2J_{HH}$ = 13.0 Hz, 1H, CH₂), 2.10 (s, 3H, CH₃).
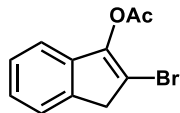
¹³C{¹H} NMR (CDCl₃): δ_C 192.3, 168.5, 141.5, 140.8, 133.2, 131.6, 129.8 (q, $^2J_{CF}$ = 31.2 Hz), 127.8, 127.3, 126.3, 126.2, 124.4 (q, $^3J_{CF}$ = 3.7 Hz), 122.7 (q, $^1J_{CF}$ = 271.9 Hz), 83.2, 32.8, 25.6, 20.5.

¹⁹F NMR (CDCl₃): δ_F -62.9 (s).

IR: 1730, 1692, 1327, 1238, 1130, 1070 cm⁻¹.

m/z HRMS calculated for $C_{19}H_{16}F_3O_3$ [M+H] = 349.1046 found 349.1044.

6.2.2.38.   Synthesis of 2-bromo-1*H*-inden-3-yl acetate (126):

Indanone (990 mg), *N*-bromosuccinimide (1.6 g) and p-toluenesulfonic acid monohydrate (142 mg) were suspended in CH_2Cl_2 (5 mL) and the mixture heated to reflux 1 hour. The reaction mixture was then cooled to room temperature, filtered and concentrated. The resulting orange oil (crude **6**) was then suspended in THF (20 mL), cooled to -78°C under a nitrogen atmosphere and NaHMDS (1 M solution in THF, 11 mL) added slowly. After 30 minutes acetic anhydride (2 mL) was added resulting in the formation of a slurry. The reaction mixture was allowed to warm to room temperature and stirred for a further 30 minutes. The suspension was poured into 1 M aqueous HCl and diluted with Et_2O. The organic phase was washed with saturated aqueous $NaHCO_3$ solution and brine the dried over anhydrous $MgSO_4$. The concentrated organic phase was passed through silica in 10% EtOAc/hexane, concentrated and the residue resuspended in hexane resulting in the precipitation of the title compound as an off-white solid (545 mg, 30%).

¹H NMR (CDCl₃): δ_H 7.37 (d, $^3J_{HH}$ = 7.0 Hz, 1H, Ar CH), 7.29 (dd, $^3J_{HH}$ = 7.5 Hz, $^4J_{HH}$ = 1.3 Hz, 1H Ar CH), 7.22 (td, $^3J_{HH}$ = 7.5 Hz, $^4J_{HH}$ = 1.3 Hz, 1H, Ar CH), 7.16 (d, $^3J_{HH}$ = 7.5 Hz, 1H, Ar CH), 3.63 (s, 2H, CH₂), 2.40 (s, 3H, CH₃).

¹³C{¹H} NMR (CDCl₃): δ_C 166.5, 147.4, 139.7, 137.6, 126.2, 125.3, 123.3, 117.2, 109.5, 40.6, 20.0.
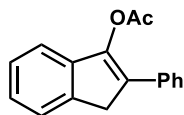
IR: 1774, 1624, 1464, 1369, 1209, 1190, 1113, 1067 cm⁻¹.

m/z (GC/MS EI): t_R 12.834 minutes [M] calculated 252.0, observed 251.8 [M].

M.P. (Hexane) 96°C.

Analytical data consistent with published values.[216]

6.2.2.39. Synthesis of 2-phenyl-1*H*-inden-3-yl acetate (127):

Prepared according to general procedure E. White solid (258 mg, 52%)

¹H NMR (CDCl₃): δ_H 7.63 (dd, $^3J_{HH}$ = 8.5 Hz, $^4J_{HH}$ = 1.0 Hz, 2H, Ar CH), 7.46 (d, $^3J_{HH}$ = 7.3 Hz, 1H, Ar CH), 7.32-7.27 (m, 2H, Ar CH), 7.25-7.24 (m, 1H, Ar CH), 7.16 (dt, $^3J_{HH}$ = 7.5 Hz, $^4J_{HH}$ = 1.0 Hz, 1H, Ar CH), 3.82 (s, 2H, CH₂), 2.43 (s, 3H, CH₃)

¹³C{¹H} NMR (CDCl₃): δ_C 167.6, 144.7, 139.5, 133.6, 128.5, 128.2, 127.0, 126.5, 126.1, 125.3, 123.5, 117.9, 36.4, 20.4.
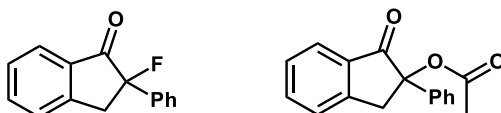
IR: 1767, 1493, 1198, 1178, 1117, 1070 cm^{-1}.

m/z (GC/MS EI): t_R 15.410 minutes, [M] calculated 250.1, observed 250.0 [M].

M.P. (Hexane) 109-110°C.

Analytical data consistent with published values.[220]

6.2.2.40. Synthesis of 2-fluoro-2-phenyl-2,3-dihydro-1*H*-inden-1-one (127a) and 1-oxo-2-phenyl-2,3-dihydro-1*H*-inden-2-yl acetate (127b):

Prepared according to general procedure C. The reaction mixture was concentrated on to silica and purified by flash silica column chromatography (10% ethyl acetate in hexane) to yield 2-fluoro-2-phenyl-2,3-dihydro-1*H*-inden-1-one as a colourless oil (68 mg, 75%) and 1-oxo-2-phenyl-2,3-dihydro-1*H*-inden-2-yl acetate as a white solid (10 mg, 9%).

2-Fluoro-2-phenyl-2,3-dihydro-1*H*-inden-1-one (127a):

¹H NMR (CDCl₃): δ_H 7.85 (d, $^3J_{HH}$ = 7.6 Hz, 1H, Ar CH), 7.74 (td, $^3J_{HH}$ = 7.5 Hz, $^4J_{HH}$ = 1.2 Hz, 1H, Ar CH), 7.57 (dt, $^3J_{HH}$ = 7.6 Hz, 1H, Ar CH), 7.49 (t, $^3J_{HH}$ = 7.5 Hz, 1H, Ar CH), 7.40-7.35 (m, 5H, Ph), 3.84-3.69 (m, 2H, CH₂).

13C{1H} NMR (CDCl$_3$): δ_C 198.8 (d, $^2J_{CF}$ = 20.2 Hz), 149.8 (d, $^3J_{CF}$ = 5.5 Hz), 137.2 (d, $^2J_{CF}$ = 24.2 Hz), 135.9, 133.3, 128.2, 128.1, 128.0, 125.9, 125.2, 124.0, 123.9, 97.4 (d, $^1J_{CF}$ = 190.3 Hz), 41.3 (d, $^2J_{CF}$ = 23.1 Hz).

19F NMR (CDCl$_3$): δ_F-157.3 (dd, $^3J_{HF}$ = 20.9, 11.7 Hz).

IR: 1724, 1609, 1445, 1301, 1063 cm^{-1}.

m/z (GC/MS EI): t$_R$ 14.253 minutes, [M] calculated 226.1, observed 226.0 [M].

Analytical data consistent with published values.[221]

1-Oxo-2-phenyl-2,3-dihydro-1*H*-inden-2-yl acetate (127b):

1H NMR (CDCl$_3$): δ_H 7.81 (d, $^3J_{HH}$ = 7.7 Hz, 1H, Ar CH), 7.69 (td, $^3J_{HH}$ = 7.5 Hz, $^4J_{HH}$ = 1.1 Hz, 1H, Ar CH), 7.54 (d, $^3J_{HH}$ = 7.7 Hz, 1H, Ar CH), 7.45 (t, $^3J_{HH}$ = 7.5 Hz, 1H, Ar CH), 7.40-7.37 (m, 2H, Ar CH), 7.35-7.27 (m, 3H, Ar CH), 3.84 (d, $^2J_{HH}$ = 17.0 Hz, 1H, CH$_2$), 3.78 (d, $^2J_{HH}$ = 17.0 Hz, $^2J_{HH}$ = 17.0 Hz, 1H, CH$_2$), 2.26 (s, 3H, CH$_3$).

13C{1H} NMR (CDCl$_3$): δ_C 198.9, 169.4, 149.2, 137.1, 135.1, 133.9, 128.2, 127.7, 127.7, 125.5, 124.9, 124.4, 85.0, 40.5, 20.6.

IR: 1738, 1606, 1460, 1383, 1240, 1066, 1011 cm^{-1}.

m/z z HRMS calculated for C$_{17}$H$_{15}$O$_3$ [M+H] 267.1016 found 267.1014.

M.P. (Hexane) 157°C.

6.2.2.41.   Synthesis of 6-methoxy-3,4-dihydronaphthalen-1-yl acetate (131):
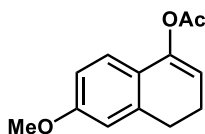
Prepared according to general procedure B. The filtrate was concentrated and the oily residue dissolved in methanol which crystallised on cooling. Pale yellow solid (2.48 g, 40%).

1H NMR (CDCl$_3$): δ_H 7.01 (d, $^3J_{HH}$ = 8.3 Hz, 1H, Ar CH), 6.71-6.67 (m, 2H, Ar CH), 5.56 (t, $^3J_{HH}$ = 4.7 Hz, 1H, C=CH), 3.79 (s, 3H, CH$_3$), 2.83 (t, $^2J_{HH}$ = 8.2 Hz, 2H, CH$_2$), 2.41 (td, $^2J_{HH}$ = 8.2 Hz, $^3J_{HH}$ = 4.7 Hz, 2H, CH$_2$), 2.28 (s, 3H, CH$_3$).

$^{13}C\{^1H\}$ **NMR** (CDCl$_3$): δ_C 168.8, 158.9, 145.0, 137.9, 123.0, 121.5, 113.4, 112.2, 110.5, 54.7, 27.5, 21.5, 20.4.
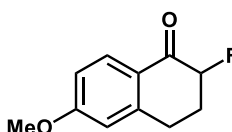
IR: 1764, 1602, 1499, 1380, 1203, 1160, 1013 cm^{-1}.

m/z (GC/MS EI): t_R 13.795 minutes, [M] calculated 218.1, observed 218.0.

M.P. (Methanol) 30-32°C.

Analytical data consistent with published values.[222]

6.2.2.42. Synthesis of 2-fluoro-6-methoxy-3,4-dihydronaphthalen-1(2*H*)-one (131a):

Prepared according to general procedure C. The reaction mixture was concentrated on to silica and washed with 10% ethyl acetate in hexane. The filtrate was concentrated to yield the title compound as a white solid (20 mg, 45%).

^{1}**H NMR** (CDCl$_3$): δ_H 8.02 (d, $^3J_{HH}$ = 8.8 Hz, 1H, Ar CH), 6.85 (dd, $^3J_{HH}$ = 8.8 Hz, $^4J_{HH}$ = 2.5 Hz, 1H, Ar CH), 6.69 (d, $^4J_{HH}$ = 2.5 Hz, 1H, Ar CH), 5.07 (ddd, $^2J_{HF}$ = 48.0 Hz, $^3J_{HH}$ = 12.4, 5.1 Hz, 1H, CHF), 3.85 (s, 3H, CH$_3$), 3.06 (dd, $^2J_{HH}$ = 9.2 Hz, $^3J_{HH}$ = 4.1 Hz, 2H, CH$_2$), 2.57-2.48 (m, 1H, CH$_2$), 2.37-2.25 (m, 1H, CH$_2$).

$^{13}C\{^1H\}$ **NMR** (CDCl$_3$): δ_C 191.4 (d, $^2J_{CF}$ = 14.1 Hz), 163.7, 145.1, 129.8, 124.2, 113.3, 112.0, 90.4 (d, $^1J_{CF}$ = 186.7 Hz), 55.0, 29.6 (d, $^2J_{CF}$ = 19.3 Hz), 26.7 (d, $^3J_{CF}$ = 11.4 Hz).

^{19}**F NMR** (CDCl$_3$): δ_F-190.4 (apparent d, 48.0 Hz).

IR: 1760, 1681, 1599, 1501, 1453, 1370, 1246, 1203, 1068 cm^{-1}.
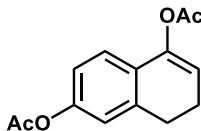
m/z (GC/MS EI): t_R 13.367 minutes, [M] calculated 194.1, observed 193.9 [M].

M.P. 104-106°C.

Analytical data consistent with published values.[223]

6.2.2.43.   Synthesis of 3,4-dihydronaphthalene-1,6-diyl diacetate (132):

Methoxytetralone (1 g) was suspended in 48% aqueous HBr (3.4 mL) and the mixture heated to reflux. After 3 hours the mixture was cooled to room temperature and the crude 6-hydroxytetralone collected by filtration. The solid was suspended in isopropenyl acetate (10 mL) along with p-toluenesulfonic acid (108 mg) and heated to relux for 4 hours. The mixture was cooled to room temperature, diluted with ethyl acetate and extracted with saturated aqueous sodium bicarbonate. The organic phase was dried over anhydrous $MgSO_4$ and concentrated *in vacuo.* The residue was passed through silica in 10% ethyl acetate in hexane and filtrate collected. The desired compound precipitated on cooling as an off-white solid (503 mg, 36%).

^{1}H NMR (CDCl$_3$): δ_H 7.96 (d, $^3J_{HH}$ = 8.0, 1H, Ar CH), 6.89-6.87 (m, 2H, Ar CH), 5.69 (t, $^3J_{HH}$ = 4.7 Hz, 1H, C=CH), 2.86 (t, $^3J_{HH}$ = 8.1 Hz, 2H, CH$_2$), 2.44 (td, $^3J_{HH}$ = 8.1, 4.7 Hz, 2H, CH$_2$), 2.28 (s, 6H, CH$_3$).

^{13}C{^{1}H} NMR (CDCl$_3$): δ_C 169.0, 168.6, 149.6, 144.6, 137.6, 127.8, 121.3, 120.4, 118.7, 114.8, 27.0, 21.3, 20.6, 20.4.

IR: 1764, 1748, 1383, 1196, 1191, 1163, 1038 cm^{-1}.

m/z HRMS calculated for C$_{14}$H$_{15}$O$_4$ [M+H] = 247.0965 found 247.0954.

M.P. (Ethyl acetate/hexane) 90°C.

6.2.2.44. Synthesis of 6-fluoro-5-oxo-5,6,7,8-tetrahydronaphthalen-2-yl acetate (132a):
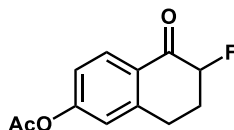
Prepared according to general procedure A. The reaction mixture was concentrated on to silica and washed with 10% ethyl acetate in hexane. The filtrate was concentrated to yield the title compound as an off-white solid (29 mg, 65%).

^{1}H NMR (CDCl$_3$): δ_H 8.11 (d, $^3J_{HH}$ = 8.6 Hz, 1H, Ar CH), 7.08 (dd, $^3J_{HH}$ = 8.6 Hz, $^4J_{HH}$ = 2.2 Hz, 1H, Ar CH), 7.03 (d, $^4J_{HH}$ = 2.2 Hz, 1H, Ar CH), 5.13 (ddd, $^2J_{HF}$ = 47.9 Hz, $^3J_{HH}$ = 12.6, 5.2 Hz, 1H, CHF), 3.12 (dd, $^2J_{HH}$ = 9.2 Hz, $^3J_{HH}$ = 4.1 Hz, 2H, CH$_2$), 2.62-2.52 (m, 1H, CH$_2$), 2.43-2.34 (m, 1H, CH$_2$).

^{13}C{^{1}H} NMR (CDCl$_3$): δ_C 191.6 (d, $^2J_{CF}$ = 14.9 Hz), 168.2, 154.5, 144.3, 129.4, 128.5, 120.9, 120.4, 90.4 (d, $^1J_{CF}$ = 188.1 Hz), 29.4 (d, $^2J_{CF}$ = 19.4 Hz), 26.5 (d, $^3J_{CF}$ = 11.5 Hz).
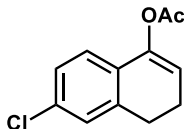
^{19}F NMR (CDCl$_3$): δ_F-190.7 (apparent d, 47.8 Hz).

IR: 1753, 1691, 1607, 1373, 1196, 1072 cm^{-1}.

m/z HRMS calculated for C$_{12}$H$_{12}$FO$_3$ [M+H] = 223.0765 found 223.0763.

M.P. (Hexane) 122-123°C.

6.2.2.45. Synthesis of 6-chloro-3,4-dihydronaphthalen-1-yl acetate (133):

6-Aminotetralone (500 mg) was suspended in 37% aqeous HCl (6 mL) at 0°C and NaNO$_2$ (235 mg) added as a suspension in H$_2$O (2 mL). The mixture was stirred at 0°C for 20 minutes before the addition of Cu(I)Cl (675 mg) was added resulting in the evolution of gas. The mixture was stirred for a further 10 minutes at 0°C before being allowed to warm to room temperature and stirred for a further 1.5 hours. The mixture was then diluted with water and extracted with Et$_2$O. The organic phase was dried over anhydrous MgSO$_4$, concentrated *in vacuo* and the residue filtered through silica in 10% ethyl acetate

in hexane. The filtrate was concentrated to yield crude 6-chlorotetralone as a red oil. The oil was suspended in isopropenyl acetate (2 mL) and p-toluenesulfonic acid monohydrate (59 mg) added and the mixture heated to reflux for 5 hours. The mixture was then diluted with ethyl acetate, extracted with saturated aqueous sodium bicarbonate solution and the organic phase dried over anhydrous MgSO$_4$. The organic phase was concentrated *in vacuo* and the residue purified by flash silica column chromatography (10% ethyl acetate in hexane) to yield the title compound as a yellow oil (117 mg, 17%).
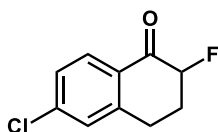
^{1}H NMR (CDCl$_3$): δ$_H$ 7.15-7.12 (m, 2H, Ar CH), 7.01-6.99 (m, 1H, Ar CH), 5.71 (t, $^{3}J_{HH}$ = 4.7 Hz, 1H, C=CH), 2.84 (t, $^{3}J_{HH}$ = 8.1 Hz, 2H, CH$_2$), 2.43 (dt, $^{3}J_{HH}$ = 8.1, 4.7 Hz, 2H, CH$_2$), 2.29 (s, 3H, CH$_3$).

^{13}C{^{1}H} NMR (CDCl$_3$): δ$_C$ 168.6, 144.4, 137.7, 132.8, 128.5, 127.2, 125.9, 121.5, 115.3, 26.8, 21.4, 20.4.

IR: 1763, 1442, 1200, 1191, 1043, 1020 cm^{-1}.

 m/z HRMS calculated for C$_{12}$H$_{12}$ClO$_2$ [M+H] = 223.0520 found 223.0518.

6.2.2.46.　　**Synthesis of 6-chloro-2-fluoro-3,4-dihydronaphthalen-1(2*H*)-one (133a):**

Prepared according to general procedure A. The reaction mixture was concentrated on to silica and washed with 10% ethyl acetate in hexane. The filtrate was concentrated to yield the title compound as a white solid (33 mg, 79%).

^{1}H NMR (CDCl$_3$): δ$_H$ 8.03 (d, $^{3}J_{HH}$ = 8.4 Hz, 1H, Ar CH), 7.36 (dd, $^{3}J_{HH}$ = 8.4 Hz, $^{4}J_{HH}$ = 2.0 Hz, 1H, Ar CH), 7.30 (d, $^{4}J_{HH}$ = 2.0 Hz, 1H, Ar CH), 5.15 (ddd, $^{2}J_{HF}$ = 47.6 Hz, $^{3}J_{HH}$ = 12.6, 52 Hz, 1H, CHF), 3.13 (dd, $^{2}J_{HH}$ = 9.2 Hz, $^{3}J_{HH}$ = 4.2 Hz, 2H, CH$_2$), 2.64-2.55 (m, 1H, CH$_2$), 2.45-2.32 (m, 1H, CH$_2$).

13C{1H} NMR (CDCl$_3$): δ$_C$ 191.6 (d, $^2J_{CF}$ = 15.1 Hz), 144.0, 140.2 129.2, 129.0, 128.1, 127.3, 90.3 (d, $^1J_{CF}$ = 188.3 Hz), 29.3 (d, $^2J_{CF}$ = 19.6 Hz), 26.2 (d, $^3J_{CF}$ = 11.3 Hz).

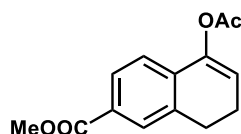**19F NMR** (CDCl$_3$): δ$_F$ -190.7 (ddd, $^2J_{HF}$ 47.8 Hz, $^3J_{HF}$ = 12.6, 8.0 Hz).

IR: 1701, 1591, 1458, 1358, 1190, 1066 cm^{-1}.

m/z HRMS calculated for C$_{10}$H$_9$ClF [M+H] = 199.0320 found 199.0320.

M.P. 95-96°C.

6.2.2.47.   Synthesis of methyl 5-acetoxy-7,8-dihydronaphthalene-2-carboxylate (134):

TMSCl (3 mL) and methanol (6 mL) were stirred for 5 minutes before 5-oxo-5,6,7,8-tetrahydronaphthalene-2-carboxylic acid (100 mg) was added and the mixture heated to reflux for 1.5 hours. The methanol was then removed *via* distillation and isopropenyl acetate (20 mL) was added. The mixture was heated to reflux for 4 hours. After cooling to room temperature the mixture was diluted with ethyl acetate and extracted with aqueous saturated sodium bicarbonate solution. The organic phase was dried over anhydrous MgSO$_4$ and concentrated *in vacuo*. The residue was filtered through silica in 10% ethyl acetate in hexane and the filtrate concentrated. The oily residue was dissolved in methanol and cooled resulting in the precipitation of the desired compound as a white solid (30 mg, 23%).

1H NMR (CDCl$_3$): δ$_H$ 7.85-7.81 (m, 2H, Ar CH), 7.13 (d, $^3J_{HH}$ = 8.0 Hz, Ar CH), 5.84 (t, $^3J_{HH}$ = 4.7 Hz, 1H, C=CH), 3.90 (s, 3H, CH$_3$), 2.91 (t, $^3J_{HH}$ = 8.3 Hz, 2H, CH$_2$), 2.47 (td, $^3J_{HH}$ = 8.3, 4.7 Hz, 2H, CH$_2$), 2.31 (s, 3H, CH$_3$).

13C{1H} NMR (CDCl$_3$): δ$_C$ 168.6, 166.3, 144.6, 135.9, 134.2, 128.1, 127.5, 120.2, 117.9, 51.6, 26.7, 21.5, 20.4.

IR: 1749, 1713, 1433, 1288, 1263, 1196, 1036 cm^{-1}.

m/z HRMS calculated for C$_{14}$H$_{15}$O$_4$ [M+H] = 247.0965 found 247.0955.

M.P. (Methanol) 101-103°C.

6.2.2.48. **Synthesis of methyl 6-fluoro-5-oxo-5,6,7,8-tetrahydronaphthalene-2-carboxylate (134a):**
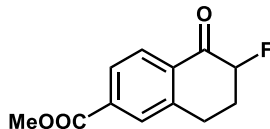
Prepared according to general procedure A. The reaction mixture was concentrated on to silica and washed with 10% ethyl acetate in hexane. The filtrate was concentrated to yield the title compound as a white solid (9 mg, 74%).

^{1}H NMR (CDCl$_3$): δ_H 8.15 (d, $^3J_{HH}$ = 8.6 Hz, 1H, Ar CH), 8.01 (dd, $^3J_{HH}$ = 8.6 Hz, $^4J_{HH}$ = 1.7 Hz, 1H, Ar CH), 7.98 (d, $^4J_{HH}$ = 1.7 Hz, 1H, Ar CH), 5.20 (ddd, $^2J_{HF}$ = 47.7 Hz, $^3J_{HH}$ = 12.6, 5.1 Hz, 1H, CHF), 3.98 (s, 3H, CH$_3$), 3.23-3.19 (m, 2H, CH$_2$), 2.68-2.59 (m, 1H, CH$_2$), 2.47-2.35 (m, 1H, CH$_2$).

^{13}C{^{1}H} NMR (CDCl$_3$): δ_C 192.3 (d, $^2J_{CF}$ = 15.3 Hz), 165.5, 142.4, 134.3, 133.7, 129.5, 127.6, 127.4, 90.4 (d, $^1J_{CF}$ = 188.9 Hz), 52.1, 29.4 (d, $^2J_{CF}$ = 19.4 Hz), 26.4 (d, $^3J_{CF}$ = 11.3 Hz).

^{19}F NMR (CDCl$_3$): δ_F -190.4 (dddd, $^2J_{HF}$ = 47.7 Hz, $^3J_{HF}$ = 10.9, 6.6 Hz, $^4J_{HF}$ = 3.5 Hz).

IR: 1774, 1624, 1466, 1369, 1209, 1193, 1113, 1067 cm^{-1}.

m/z HRMS calculated for C$_{12}$H$_{12}$FO$_3$ [M+H] = 223.0765 found 223.0762.

M.P. (Hexane) 144-145°C.

6.2.2.49. **Synthesis of 3,4-dihydronaphthalen-1-yl cyclopropanecarboxylate (137):**
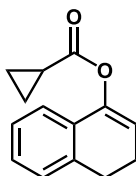
Prepared according to general procedure F. Glassy crystalline colourless solid (203 mg, 25%).

¹H NMR (CDCl₃): δ_H 7.21-7.13 (m, 4H, Ar CH), 5.73 (t, $^3J_{HH}$ = 4.7 Hz, 1H, C=CH), 2.88 (t, $^3J_{HH}$ = 8.1 Hz, 2H, CH₂), 2.46 (td, $^3J_{HH}$ = 8.1, 4.8 Hz, 2H, CH₂), 1.87 (tt, $^3J_{HH}$ = 7.9, 4.7 Hz, 1H, CH), 1.18 (dt, $^3J_{HH}$ = 7.2, 4.3 Hz, 2H, CH₂), 1.04 (dt, $^3J_{HH}$ = 7.2, 3.9 Hz, 2H, CH₂).

¹³C{¹H} NMR (CDCl₃): δ_C 172.8, 145.1, 135.9, 130.1, 127.4, 127.0, 125.9, 120.2, 114.9, 27.0, 21.6, 12.3, 8.5.

IR: 1736, 1385, 1356, 1335, 1178, 1163, 1099 cm⁻¹.

m/z HRMS calculated for C₁₄H₁₅O₂ [M+H] = 215.1067 found 215.1061
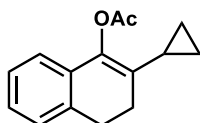
M.P.: (ethyl acetate/hexane) 57 – 59 °C.

6.2.2.50. Synthesis of 2-cyclopropyl-3,4-dihydronaphthalen-1-yl acetate (138):

Prepared according to general procedure E. Yellow solid (738 mg, 74%).

¹H NMR (CDCl₃): δ_H 7.18-7.12 (m, 1H, Ar CH), 7.11-7.09 (m, 2H, Ar CH), 7.01 (d, $^3J_{HH}$ = 7.3 Hz, 1H, Ar CH), 2.79 (t, $^3J_{HH}$ = 8.4 Hz, CH₂), 2.34 (s, 3H, CH₃), 1.99 (t, $^3J_{HH}$ = 8.4 Hz, 2H, CH₂), 1.73 (tt, $^3J_{HH}$ = 8.2, 5.2 Hz, 1H, CH), 0.78-0.73 (m, 2H, CH₂), 0.66-0.61 (m, 2H, CH₂).

¹³C{¹H} NMR (CDCl₃): δ_C 168.5, 140.5, 134.5, 130.8, 127.7, 126.6, 126.2, 125.9, 119.4, 27.0, 21.3, 20.1, 10.2, 4.1.

IR: 1747, 1485, 1366, 1207, 1123, 1065, 1043 cm⁻¹.

m/z HRMS calculated for C₁₅H₁₇O₂ [M+H] = 229.1223 found 229.1219.

M.P. (Hexane) 92-94°C.

6.2.2.51. Synthesis of 2-cyclopropyl-2-fluoro-3,4-dihydronaphthalen-1(2*H*)-one (138a) and 2-cyclopropyl-1-oxo-1,2,3,4-tetrahydronaphthalen-2-yl acetate (138b):
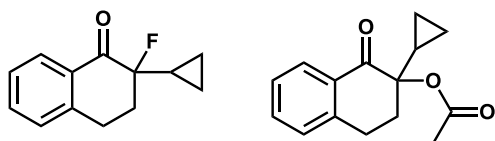
Prepared according to general procedure A. The crude reaction mixture was concentrated *in vacuo* and the residue purified by flash silica column chromatography

(10% ethyl acetate in hexane) to yield 2-cyclopropyl-2-fluoro-3,4-dihydronaphthalen-1(2*H*)-one as a colourless oil (98 mg, 48%) and 2-cyclopropyl-1-oxo-1,2,3,4-tetrahydronaphthalen-2-yl acetate as a colourless oil (19 mg, 8%).

2-Cyclopropyl-2-fluoro-3,4-dihydronaphthalen-1(2*H*)-one (138a):

^{1}H NMR (CDCl$_3$): δ_H 8.02 (dd, $^3J_{HH}$ = 7.7 Hz, $^4J_{HH}$ = 1.2, 1H, Ar CH), 7.50 (td, $^3J_{HH}$ = 7.5 Hz, $^4J_{HH}$ = 1.2 Hz, 1H, Ar CH), 7.34 (t, $^3J_{HH}$ = 7.7 Hz, 1H, Ar CH), 3.27 (ddd, $^2J_{HH}$ = 17.1 Hz, $^3J_{HH}$ = 11.7, 5.2 Hz, 1H, CH$_2$), 3.10 (apparent d, $^2J_{HH}$ = 17.1 Hz, 1H, CH$_2$), 2.51-2.34 (m, 2H, CH$_2$), 1.35-1.24 (m, 1H, CH), 0.68-0.48 (m, 4H, CH$_2$).

^{13}C{^{1}H} NMR (CDCl$_3$): δ_C 193.7 (d, $^2J_{CF}$ = 18.3 Hz), 142.2, 133.4, 130.9, 128.2, 127.5, 126.5, 93.9 (d, $^1J_{CF}$ = 185.9 Hz), 33.8 (d, $^2J_{CF}$ = 23.5 Hz), 26.0 (d, $^3J_{CF}$ = 10.5 Hz), 13.7 (d, $^2J_{CF}$ = 25.2 Hz), 0.98 (d, $^3J_{CF}$ = 6.4 Hz), -0.33 (d, $^3J_{CF}$ = 4.0 Hz).

^{19}F NMR (CDCl$_3$): δ_F-165.0 (dt, $^3J_{HF}$ = 17.6, 8.8 Hz).

IR: 1699, 1600, 1448, 1300, 1226 cm^{-1}.

m/z HRMS calculated for C$_{13}$H$_{14}$FO [M+H] = 205.1025 found 205.1018.

2-Cyclopropyl-1-oxo-1,2,3,4-tetrahydronaphthalen-2-yl acetate (138b):

^{1}H NMR (CDCl$_3$): δ_H 8.07 (dd, $^3J_{HH}$ = 7.9 Hz, $^4J_{HH}$ = 1.3 Hz, 1H, Ar CH), 7.47 (td, $^3J_{HH}$ = 7.5 Hz, $^4J_{HH}$ = 1.4 Hz, 1H, Ar CH), 7.32 (t, $^3J_{HH}$ = 7.7 Hz, 1H, Ar CH), 7.23 (d, $^3J_{HH}$ = 7.7 Hz, 1H, Ar CH), 3.33 (ddd, $^2J_{HH}$ = 16.5 Hz, $^3J_{HH}$ = 12.6, 4.7 Hz, 1H, CH$_2$), 3.09 (td, $^2J_{HH}$,$^3J_{HH}$ = 12.6 Hz, $^3J_{HH}$ = 5.1 Hz, 1H, CH$_2$), 3.01 (ddd, $^2J_{HH}$ = 16.5 Hz, $^3J_{HH}$ = 5.1, 2.5 Hz, 1H, CH$_2$), 2.20 (ddd, $^2J_{HH}$ = 12.6 Hz, $^3J_{HH}$ = 4.7, 2.5 Hz, 1H, CH$_2$), 2.06 (s, 3H, CH$_3$), 1.33 (tt, $^3J_{HH}$ = 8.5, 5.3 Hz, 1H, CH), 0.69-0.65 (m, 1H, CH$_2$), 0.57-0.45 (m, 3H, CH$_2$).

^{13}C{^{1}H} NMR (CDCl$_3$): δ_C 192.6, 169.1, 141.9, 133.1, 131.2, 128.1, 127.6, 126.4, 81.0, 32.5, 26.4, 20.8, 14.6, 1.2, -0.4.

IR: 1736, 1692, 1603, 1367, 1302, 1243, 1215 cm^{-1}.

m/z HRMS calculated for C$_{15}$H$_{17}$O$_3$ [M+H] = 245.1172 found 245.1163.

6.2.2.52. Synthesis of 2,2,6,6-tetramethyl-1-oxopiperidin-1-ium tetrafluoroborate (139):
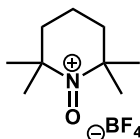
According to the procedure of Hayashi *et al.*,[224] TEMPO (1 g), 48% aqueous HBF$_4$ (1 mL) and water 3 mL were combined and stirred at room temperature for 20 minutes until the orange colour of TEMPO was no longer visible. The mixture was then cooled to 0°C and aqueous NaOCl solution (4.3 mL) was added dropwise. The mixture was stirred at 0°C for 45 minutes and the precipitate collected, washed with H$_2$O and CH$_2$Cl$_2$ and dried at 40°C *in vacuo* to yield the title compound as a bright yellow solid (880 mg, 57%).

IR 1626, 1472, 1462, 1398, 1381, 1288, 1097, 1032 cm^{-1}.

M.P. (water): 159-162°C.

Analytical data consistent with published values.[224]

6.2.2.53. Synthesis of 2-phenylnaphthalen-1-yl acetate (140):
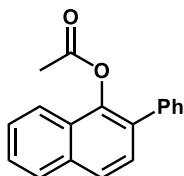
2-phenyl-3,4-dihydronaphthalen-1-yl acetate **120** (146 mg) and 2,2,6,6-tetramethyl-1-oxopiperidin-1-ium tetrafluoroborate (202 mg) were suspended in 95:5 acetonitrile/water and the mixture stirred at room temperature for 24 hours. The mixture was diluted with CH$_2$Cl$_2$ and extracted with saturated aqueous sodium thiosulfate solution. The organic phase was concentrated to yield the title compound as a white solid (113 mg, 78%).

^{1}H NMR (CDCl$_3$): δ_H 7.93-7.83 (m, 3H, Ar CH), 7.60-7.52 (m, 5H, Ar CH), 7.48 (tt, $^3J_{HH}$ = 7.5 Hz, $^4J_{HH}$ = 1.7 Hz, 2H, Ar CH), 7.40 (t, $^3J_{HH}$ = 7.5 Hz, 1H, Ar CH)

^{13}C{^{1}H} NMR (CDCl$_3$): δ_C 168.7, 142.9, 137.6, 133.5, 130.6, 128.6, 127.5, 127.4, 127.0, 126.8, 126.4, 126.0, 125.8, 121.1, 20.2.

IR: 1755, 1493, 1364, 1206, 1189, 1051 cm^{-1}.

m/z (GC/MS EI): t$_R$ 15.556 minutes [M] calculated 262.1, observed 219.9 [M-CH$_3$C=O]

M.P. (DCM) 126°C.

Analytical data consistent with published values.[217]

6.2.2.54.   Synthesis of 2-cyclopropylnaphthalen-1-yl acetate (141):
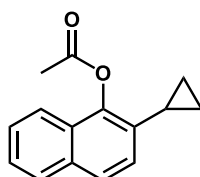
2-cyclopropyl-3,4-dihydronaphthalen-1-yl acetate **138** (20 mg) and DDQ (28 mg) were suspended in 1,4-dioxane (0.5 mL) and the mixture stirred for 3 hours. The mixture was then diluted with 10% ethyl acetate in hexane and passed through silica. The filtrate was concentrated *in vacuo* to yield the title compound as a colourless oil (17 mg, 83%).

^{1}H NMR (CDCl$_3$): δ$_H$ 7.81 (d, $^3J_{HH}$ = 8.2 Hz, 1H, Ar CH), 7.76 (d, $^3J_{HH}$ = 8.2 Hz, 1H, Ar CH), 7.67 (d, $^3J_{HH}$ = 8.6 Hz, 1H, Ar CH), 7.50 (t, $^3J_{HH}$ = 8.2 Hz, 1H, Ar CH), 7.43 (t, $^3J_{HH}$ = 8.2 Hz, 1H, Ar CH), 7.08 (d, $^3J_{HH}$ = 8.6 Hz, 1H, Ar CH), 2.51 (s, 3H, CH$_3$), 2.02 (tt, $^3J_{HH}$ = 8.7, 5.2 Hz, 1H, CH), 1.00 (ddd, $^3J_{HH}$ = 8.7, 6.2, 4.4 Hz, 2H, CH$_2$), 0.79 (dt, $^3J_{HH}$ = 6.2, 5.2 Hz, CH$_2$).

^{13}C{^{1}H} NMR (CDCl$_3$): δ$_C$ 168.7, 144.7, 132.3, 130.9, 127.3, 126.4, 126.1, 125.6, 125.6, 125.1, 123.1, 120.2, 20.2, 10.0, 6.9.

IR: 1763, 1366, 1207, 1069 cm^{-1}.

m/z HRMS calculated for C$_{15}$H$_{15}$O$_2$ [M+H] = 227.1067 found 227.1065.

6.3. Steroid Models

6.3.1. Synthesis of Compounds

6.3.1.1. Synthesis of 4a-methyl-4,4a,5,6,7,8-hexahydronaphthalen-2(3*H*)-one (142):
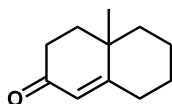
Method 1: According to the procedure of Pfau and Revial, 2-methylcyclohexanone (0.12 mol, 15 mL) and α-methylbenzylamine (1 equiv., 0.12 mol, 16 mL) were combined in toluene (15 mL). A Dean-Stark trap was fitted and the mixture was heated to 85 °C for 16 hours after which time no water had collected in the trap. The temperature was increased to 150°C and stirred for a further 136 hours. The deep red reaction mixture was then cooled to 0°C and freshly-distilled methyl vinyl ketone (1.2 equiv., 0.15 mol, 12 mL) added. The mixture was allowed to warm to room temperature before heating to 40°C with stirring for 18 hours. After this time the mixture was cooled to 0°C and glacial acetic acid (1.2 equiv., 0.15 mol, 9 mL) then water (8 mL) added with stirring at 0°C, warming to room temperature over 2.5 hours. Further water (8 mL) and brine (9 mL) were added and the organic and aqueous phases were separated. The aqueous phase was then extracted with pet. ether/diethyl ether (5 x 30 mL of a 1:1 v/v mixture) and the combined organic phases dried over MgSO₄ and concentrated *in vacuo*. The residue was then suspended in anhydrous methanol (90 mL); sodium methoxide (0.59 g) in methanol (3 mL) was added and the mixture stirred at 60°C for 16 hours. Glacial acetic acid (20 mL) was added to pH 6 and the mixture was concentrated *in vacuo.* Water (40 mL) added to the residue and the aqueous solution was extracted with 50:50 pet. ether:diethyl ether (3 x 25 mL) three times. The combined organic extracts were dried over MgSO4 and concentrated *in vacuo* to leave a dark brown oily residue. Purification was attempted *via* reduced pressure distillation (128°C, 6.8 mbar), producing a dark yellow oil

comprising impure desired product. The oil was then repurified by flash silica column chromatography (240 g silica column, 0-15% ethyl acetate in hexane) yielding the enone (2.68 g, 13%) as a yellow oil.

Method 2: 2-Methylcyclohexanone (0.12 mol, 16 mL), α-methylbenzylamine (1 equiv., 0.12 mol, 15 mL) and *p*-toluenesulfonic acid (0.01 equiv., 1 mmol, 0.19 g) were combined in toluene (45 mL), Dean-Stark trap was fitted, and the mixture heated to 145°C for 136 hours. The deep red reaction mixture was concentrated *in vacuo* then cooled to 0°C and freshly distilled methyl vinyl ketone (1.2 equiv., 0.148 mol, 12 mL) was added. The mixture was allowed to warm to room temperature before heating to 40°C with stirring for 18 hours. After this time the mixture was cooled to 0°C and glacial acetic acid (1.2 equiv., 0.150 mol, 9 mL) and water (8 mL) added with stirring at 0°C, warming to room temperature over 2.5 hours. Further water (8 mL) and brine (9 mL) were added and the organic and aqueous phases separated. The aqueous phase was then extracted five times with 50:50 pet. ether:diethyl ether (30 mL portions) and the combined organic phases dried over MgSO$_4$ and concentrated *in vacuo*. The residue was then suspended in anhydrous methanol (90 mL), sodium methoxide (25% by weight in methanol, 3 mL) was added and the mixture stirred at 60°C for 16 hours. Glacial acetic acid was added to pH 6 and the mixture was concentrated *in vacuo* and water (40 mL) added to the residue and the aqueous solution extracted with 50:50 pet. ether:diethyl ether (25 mL) three times. The combined organic extractions were dried over MgSO$_4$ and concentrated *in vacuo* to leave a dark brown oily residue. Purification was attempted *via* reduced pressure distillation (128°C, 6.8 mbar), producing a dark yellow oil consisting of impure desired product. The oil was then re-purified by flash silica column chromatography (240 g silica column, 0-15% ethyl acetate in hexane) yielding the enone (4.44 g, 22%) a yellow oil.

Method 3: 2-Methylcyclohexanone (0.06 mol, 7 mL), α-methylbenzylamine (1 equiv., 0.06 mol, 8 mL) and *p*-toluenesulfonic acid (0.05 equiv., 3 mmol, 0.57 g) were combined in toluene (4 mL) and MgSO$_4$ (9 g) added. The mixture was heated to 40°C for 19 hours

then allowed to cool to room temperature. The mixture was filtered and the MgSO$_4$ cake washed with toluene. The yellow filtrate was concentrated *in vacuo* then cooled to 0°C and freshly-distilled methyl vinyl ketone (1.2 equiv., 0.148 mol, 12 mL) added. The mixture was allowed to warm to room temperature before heating to 40°C with stirring for 21 hours. The mixture was cooled to 0°C and glacial acetic acid (1.1 equiv., 0.06 mol, 4 mL) and water (3.5 mL) added with stirring at 0°C, warming to room temperature over 2 hours. Further water (15 mL) and brine (20 mL) were added and the organic and aqueous phases separated. The aqueous phase was then extracted with 50:50 pet. ether:diethyl ether (3 x 50 mL) and the combined organic phases dried over MgSO$_4$ and concentrated in vacuo. The residue was then suspended in anhydrous methanol (25 mL), sodium methoxide (1.1 g) in methanol (5.5 mL) was added and the mixture stirred at 60°C for 16 hours. Glacial acetic acid was added to pH 6 and the mixture was concentrated in vacuo and water (20 mL) added to the residue and the aqueous solution extracted with 50:50 pet. ether:diethyl ether (25 mL) three times. The combined organic extractions were dried over MgSO$_4$ and concentrated *in vacuo* to leave a dark brown oily residue. Purification was attempted via reduced pressure distillation (128°C, 6.8 mbar), producing a dark yellow oil comprising impure desired product. The oil was then repurified by flash silica column chromatography (90 g silica column, 0-15% ethyl acetate in hexane) yielding the enone (1.47 g, 15%) as a yellow oil.

Method 4: 2-Methylcyclohexanone (0.08 mol, 10 mL), α-methylbenzylamine (1 equiv., 0.08 mol, 10 mL) and *p*-toluenesulfonic acid (0.05 equiv., 4 mmol, 0.76 g) were combined in toluene (5 mL) and 3 Å mol. Sieves added and the mixture heated to 110 ˚C for 2 hours. The mixture was cooled to 40 ˚C and methyl vinyl ketone (1.2 equiv., 0.1 mol, 8 mL) added and the mixture stirred at 40 ˚C for 3 hours. The mixture was cooled to room temperature and the mol. Sieves were removed by filtration. Glacial acetic acid (6 mL) and water (5 mL) were added to the filtrate and this mixture was stirred at room temperature for 45 minutes. The mixture was extracted with 1:1 pet. Ether:diethyl ether. The organic phase was extracted with brine, dried over anhydrous MgSO$_4$ and

concentrated *in vacuo*. The residue was suspended in methanol (40 mL) and sodium methoxide (1.5 g) in methanol (7.3 mL) was added slowly and the resulting mixture stirred at 60 ˚C for 19 hours. The mixture was cooled to room temperature and glacial acetic acid added to pH 6, concentrated *in vacuo* and water (25 mL) added to the residue. The suspension was extracted with 50:50 pet. Ether:diethyl ether (30 mL) three times. The combined organic extractions were dried over anhydrous MgSO$_4$ and concentrated *in vacuo.* The residue was distilled (128°C, 6.8 mbar) resulting in the collection of the desired product as a pale yellow oil (3.0 g, 23%).

^{1}H NMR (CDCl$_3$): δ$_H$ 5.68 (s, 1H, C=CH), 2.47 (ddd, $^2J_{HH}$ = 17.0 Hz, $^3J_{HH}$ = 14.0, 5.7 Hz, 1H, CH$_2$), 2.37-2.27 (m, 2H, CH$_2$), 2.24-2.19 (m, 1H, CH$_2$), 1.90-1.61 (m, 6H, CH$_2$), 1.42-1.28 (m, 2H, CH$_2$), 1.21 (s, 3H, CH$_3$).

^{13}C{^{1}H} NMR (CDCl$_3$): δ$_C$ 199.2, 170.1, 123.6, 41.1, 37.5, 35.5, 33.5, 32.3, 26.7, 21.6, 21.3.

IR: 2922, 2854, 1654, 1617, 1236, 1172 cm^{-1}.

m/z (GC/MS EI): t$_R$ 11.902 minutes [M+H] calculated 165.1, observed 165.0 [M+H] Analytical data consistent with published values.[225]

6.3.1.2.   Synthesis   of   4a-methyl-3,4,4a,5,6,7-hexahydronaphthalen-2-yl benzoate (148):
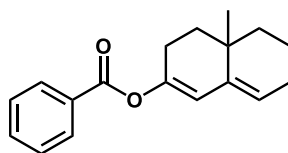
Method 1 – Attempted Synthesis: 4a-Methyl-4,4a,5,6,7,8-hexahydronaphthalen-2(3*H*)-one (**142**) (1 equiv.) was suspended in pyridine (1.25 M in ketone) or toluene (1.25 M in ketone) and pyridine (0.1, 1, 1.5, 2 or 3 equiv.) added (if in toluene) along with benzoyl chloride (3 equiv.). The resulting mixture was heated to 80°C under an atmosphere of air, nitrogen or argon for 4, 3.5, 14 or 16 hours. The crude reaction mixture was analysed by ^{1}H NMR to determine the ratio of starting material (**142**) to product (**148**) to side product (**149**). *Table 14* shows variables changed.

*Table 14: Attempted Synthesis of **148***

a = degassed under N_2, b = conducted in carousel tubes, c = possible presence of air (deflated balloon), d = separate gas supply

Entry	Equiv. Py	Atmosphere	142/%	148/%	149/%	Time/h	Scale/mmol
1	Solvent	Nitrogen	50	16	34	4	2.5
2[a]	Solvent	Nitrogen	49	18	33	3.5	1
3[a]	Solvent	Nitrogen	47	32	21	14	0.3
4[a]	Solvent	Argon	37	44	19	14	0.3
5[a]	1	Nitrogen	8	39	52	14	0.3
6[a,b,c]	1	Argon	90	10	0	16	0.1
7[a,b]	1	Air	100	0	0	16	0.1
8[a,b,c]	1	Argon	86	14	0	16	0.1
9[a,b,c]	0.1	Argon	100	0	0	16	0.1
10[a,b]	0	Argon	81	0	19	16	0.1
11[a,b]	1	Argon	100	0	0	16	0.1
12[a,b]	0	Argon	100	0	0	16	0.1
13[a,b]	1.5	Argon	100	0	0	16	0.1
14[a.b]	3	Argon	89	0	11	16	0.1
15[a,b]	1	Air	100	0	0	16	0.1
16[a,b,d]	1	Argon	100	0	0	16	0.1
17[a]	1	Argon	0	100	0	16	0.1
18[a]	0	Argon	0	100	0	16	0.1
19[a]	1	Argon	18	82	0	16	1
20[a]	0	Argon	63	18	19	16	0.3
21[a]	1	Argon	60	5	35	16	1
22[a]	0	Argon	26	74	0	16	0.3
23[a]	2	Argon	21	79	0	16	0.3
24[a]	1	Argon	63	18	19	16	0.3
25[a]	0	Argon	59	41	0	16	0.3
26[a]	2	Argon	36	13	51	16	0.9
27[a]	1	Argon	65	6	29	16	3
28[a]	1	Argon	100	0	0	16	0.3

Method 2: According to the procedure of Vandenheuvel *et al.*,[204] 4a-Methyl-4,4a,5,6,7,8-hexahydronaphthalen-2(3*H*)-one (**142**) (1 equiv., 164 mg, 1 mmol) was suspended in hexane (1 mL) and benzoyl chloride (1.1 equiv., 1.1 mmol, 0.15 mL) added. The resulting mixture was then stirred at 80 ˚C for 4 hours under a nitrogen atmosphere. The mixture was allowed to cool to room temperature, diluted with 10% ethyl acetate in hexane and the solution passed through a pad of silica. The filtrate was collected, concentrated *in vacuo* and the residue suspended in methanol. The title compound precipitated as a white solid upon cooling to yield 45 mg (17%).

Method 3: Benzoyl chloride (3.3 mmol, 0.4 mL, 1.1 equiv.) was added to 4a-Methyl-4,4a,5,6,7,8-hexahydronaphthalen-2(3*H*)-one (**142**) (1 equiv., 3 mmol, 492 mg) and the mixture heated to 170 ˚C under a nitrogen atmosphere for 2 hours. The mixture was then allowed to cool to room temperature and the residue diluted with 10% ethyl acetate in hexane and the solution passed through silica. The filtrate was concentrated *in vacuo* and diluted with methanol. The title compound crystallised on cooling to yield 229 mg (28%) as a white solid.

^{1}H NMR (CDCl$_3$): δ_H 8.11 (dt, $^3J_{HH}$ = 6.6 Hz, $^4J_{HH}$ = 1.7 Hz, 2H, Ar CH), 7.61 (tt, $^3J_{HH}$ = 7.5 Hz, $^4J_{HH}$ = 1.4 Hz, 1H, Ar CH), 7.49 (tt, $^3J_{HH}$ = 7.6 Hz, $^4J_{HH}$ = 1.4 Hz, 2H, Ar CH), 5.88 (d, $^4J_{HH}$ = 2.1 Hz, 1H, C=CH), 5.47 (t, $^3J_{HH}$ = 4.0 Hz, 1H, C=CH), 2.68 (dt, $^2J_{HH}$ = 17.7 Hz, $^3J_{HH}$ = 8.9 Hz, CH$_2$), 2.31-2.25 (m, 1H, CH$_2$), 2.23-2.07 (m, 2H, CH$_2$), 1.84-1.78 (m, 1H, CH$_2$), 1.76-1.70 (m, 1H, CH$_2$), 1.63-1.60 (m, 3H, CH$_2$), 1.37 (td, $^2J_{HH}$,$^3J_{HH}$ = 13.2 Hz, $^3J_{HH}$ = 3.5 Hz, 1H, CH$_2$), 1.15 (s, 3H, CH$_3$).

^{13}C{^{1}H} NMR (CDCl$_3$): δ_C 164.6, 147.2, 138.1, 132.7, 129.4, 127.9, 123.9, 116.7, 36.4, 36.3, 31.4, 25.1, 24.5, 22.8, 17.9.
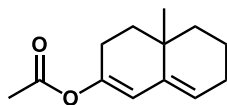
IR: 2928, 2911, 2836, 1722, 1660, 1263, 1246, 1119, 1101, 1074, 1057, 1022 cm^{-1}.

m/z (GC/MS EI): t$_R$ 15.573 minutes [M] calculated 268.1, observed 268.1 [M]

M.P. (Methanol) 49-50 ˚C.

Analytical data consistent with published values.[204]

6.3.1.3. Synthesis of 4a-methyl-3,4,4a,5,6,7-hexahydronaphthalen-2-yl acetate (150):

Prepared according to the procedure of Waalboer *et al*. 4a-methyl-4,4a,5,6,7,8-hexahydronaphthalen-2(3*H*)-one (**142**) (2 mmol, 0.33 g), chlorotrimethylsilane (4 equiv., 8 mmol, 1 mL) and sodium iodide (0.8 equiv., 1.6 mmol, 0.24 g) were combined in acetic anhydride (3.7 equiv., 7.4 mmol, 0.7 mL) at 0°C under a nitrogen atmosphere for 1 hour. Pyridine (0.7 equiv., 1.4 mmol, 0.1 mL) was then added and the mixture stirred, gradually warming to room temperature for 16 hours. The mixture was diluted with ethyl acetate (25 mL) and extracted with saturated aqueous NaHCO3 solution (20 mL). The organic phase was then extracted with CuSO4 solution (3 x 30 mL of a saturated aqueous solution). The organic phase was then dried over MgSO4, concentrated and the residue purified by flash silica column chromatography (0-15% ethyl acetate in hexane) to yield dienol acetate **150** (0.31 g, 74%) as a pale yellow oil.

^{1}H NMR (CDCl$_3$): δ_H 5.70 (d, $^4J_{HH}$ = 1.9 Hz, 1H, C=CH), 5.40 (t, $^3J_{HH}$ = 3.7 Hz, 1H, C=CH), 2.55-2.47 (m, 1H, CH$_2$), 2.14-2.04 (m, 6H, CH$_2$), 1.85-1.65 (m, 2H, CH$_2$), 1.56-1.43 (m, 3H, CH$_2$), 1.30 (td, $^2J_{HH}$,$^3J_{HH}$ = 13.0 Hz, $^3J_{HH}$ = 3.5 Hz, 1H, CH$_2$), 1.08 (s, 3H, CH$_3$).

^{13}C{^{1}H} NMR (CDCl$_3$): δ_C 168.9, 146.9, 138.0, 123.8, 116.4, 36.4, 36.2, 31.3, 25.0, 24.2, 22.7, 20.5, 17.9.

m/z (GC/MS EI): t_R 11.797 minutes [M] calculated 206.1, observed 206.1 [M].Analytical data consistent with published values.[226]

6.3.1.4. **Synthesis** **of** **(4a*S*,8*R*)-8-fluoro-4a-methyl-4,4a,5,6,7,8-hexahydronaphthalen-2(3*H*)-one** **(β-151)** **and** **(4a*S*,8*S*)-8-fluoro-4a-methyl-4,4a,5,6,7,8-hexahydronaphthalen-2(3*H*)-one (α-151):**
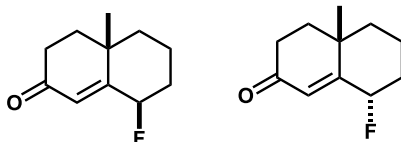
4a-Methyl-3,4,4a,5,6,7-hexahydronaphthalen-2-yl acetate (**142**) (1.46 mmol, 0.30 g) was reacted following general procedure C. The residue was purified by flash silica column chromatography (0-25% ethyl acetate in hexane) to yield β-**151** as a colourless oil and α-**151** as a white solid (0.02 g and 0.01 g respectively, 25%).

(4a*S*,8*R*)-8-fluoro-4a-methyl-4,4a,5,6,7,8-hexahydronaphthalen-2(3*H*)-one (β-151):

^{1}H NMR (CDCl$_3$): δ$_H$ 5.88 (d, $^3J_{HF}$ = 5.0 Hz, 1H, C=CH), 5.00 (dt, $^2J_{HF}$ = 48.7 Hz, $^3J_{HH}$ = 2.5 Hz, 1H, CHF), 2.64 (ddd, $^2J_{HH}$ = 17.2 Hz, $^3J_{HH}$ = 14.5 Hz, 5.4 Hz, 1H, CH$_2$), 2.41 (dt, $^2J_{HH}$ = 17.7 Hz, $^3J_{HH}$ = 3.4 Hz, 1H, CH$_2$), 2.30-2.20 (m, 1H, CH$_2$), 2.01 (qt, $^2J_{HH}$,$^3J_{HH}$ = 13.3 Hz, $^3J_{HH}$ = 3.4 Hz, 1H, CH$_2$), 1.88 (td, $^2J_{HH}$,$^3J_{HH}$ = 14.0 Hz, $^3J_{HH}$ = 4.4 Hz, 1H, CH$_2$), 1.80 (dq, $^2J_{HH}$ = 13.4 Hz, $^3J_{HH}$,$^4J_{HH}$ = 2.8 Hz, 1H, CH$_2$), 1.77-1.67 (m, 1H, CH$_2$), 1.64-1.51 (m, 2H, CH$_2$), 1.41-1.33 (m, 4H, CH$_2$, CH$_3$).

^{13}C{^{1}H} NMR (CDCl$_3$): δ$_C$ 199.6, 160.7 (d, $^2J_{CF}$ = 12.4 Hz), 128.1 (d, $^3J_{CF}$ = 8.9 Hz), 92.5 (d, $^1J_{CF}$ = 167.2 Hz), 40.2, 38.7, 34.7, 33.8, 31.6 (d, $^2J_{CF}$ = 24.2 Hz), 22.6, 15.7.

^{19}F NMR (CDCl$_3$): δ$_F$-168.0 (tdd, $^2J_{HF}$,$^3J_{HF}$ = 48.7 Hz, $^3J_{HF}$ = 12.8 Hz, $^4J_{HF}$ = 5.0 Hz).

IR: 2924, 2852, 1679, 1180, 1033, 877 cm^{-1}.

m/z (GC/MS): t$_R$ 11.207 minutes [M] calculated 182.1, observed 182.1 [M]

Analytical data consistent with published values.[227]

(4a*S*,8*S*)-8-fluoro-4a-methyl-4,4a,5,6,7,8-hexahydronaphthalen-2(3*H*)-one (α-151):

^{1}H NMR (CDCl$_3$): δ$_H$ 6.10 (s, 1H, C=CH), 5.12 (dddd, $^2J_{HF}$ = 47.8 Hz, $^3J_{HH}$ = 11.8, 5.8 Hz, $^4J_{HH}$ = 2.0 Hz, 1H, CHF, 2.53 (ddd, $^2J_{HH}$ = 16.9 Hz, $^3J_{HH}$ = 13.8, 5.6 Hz, 1H, CH$_2$), 2.42-2.32 (m, 2H, CH$_2$), 1.98-1.78 (m, 3H, CH$_2$), 1.75-1.59 (m, 3H, CH$_2$), 1.63 (td, $^2J_{HH}$,$^3J_{HH}$ = 13.3 Hz, $^3J_{HH}$ = 1.38 Hz, CH$_2$), 1.26 (s, 3H, CH$_3$).

^{13}C{^{1}H} NMR (CDCl$_3$): δ_C 198.5, 164.8 (d, $^2J_{CF}$ = 11.7 Hz), 119.6 (d, $^3J_{CF}$ = 14.0 Hz), 88.3 (d, $^1J_{CF}$ = 184.8 Hz), 40.2, 27.7, 36.5, 33.5, 33.3, 22.2, 18.7 (d, $^2J_{CF}$ = 12.4 Hz).

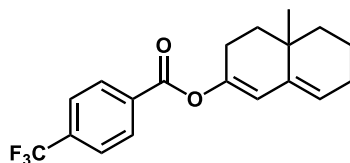**^{19}F NMR** (CDCl$_3$): δ_F -184.1 (apparent d, $^2J_{HF}$ = 47.8 Hz).

IR: 2943, 2843, 1667, 1627, 1318, 1059, 877 cm^{-1}.

m/z (GC/MS): t_R 11.852 minutes [M] calculated 182.1, observed 182.1 [M]

M.P. (DCM/pentane) 45-46 °C.

Analytical data consistent with published values.[227]

6.3.1.5. Synthesis of 4a-methyl-3,4,4a,5,6,7-hexahydronaphthalen-2-yl 4-(trifluoromethyl)benzoate (152)

4-Trifluoromethylbenzoyl chloride (1.1 mmol, 0.2 mL, 1.1 equiv.) was added to 4a-Methyl-4,4a,5,6,7,8-hexahydronaphthalen-2(3*H*)-one (**142**) (1 equiv., 1 mmol, 164 mg) and the mixture heated to 170 °C under a nitrogen atmosphere for 2 hours. The mixture was then allowed to cool to room temperature and the residue diluted with 10% ethyl acetate in hexane and the solution passed through silica. The filtrate was concentrated *in vacuo* and diluted with methanol. The title compound crystallised on cooling to yield 107 mg (32%) as a white solid.

^{1}H NMR (CDCl$_3$): δ_H 8.22 (d, $^3J_{HH}$ = 8.3 Hz, 2H, Ar CH), 7.75 (d, $^3J_{HH}$ = 8.3 Hz, 2H, Ar CH), 5.90 (d, $^4J_{HH}$ = 2.0 Hz, 1H, C=CH), 5.50 (t, $^3J_{HH}$ = 3.7 Hz, 1H, C=CH), 2.69 (dt, $^2J_{HH}$ = 17.5 Hz, $^3J_{HH}$ = 8.8 Hz, 1H, CH$_2$), 2.31-2.25 (m 1H, CH$_2$), 2.23-2.07 (m, 2H, CH$_2$), 1.91-1.81 (m, 1H, CH$_2$), 1.75-1.71 (m, 1H, CH$_2$), 1.66-1.57 (m, 3H, CH$_2$), 1.37 (td, $^2J_{HH}$, $^3J_{HH}$ = 13.5 Hz, $^3J_{HH}$ = 3.4 Hz, 1H, CH$_2$), 1.15 (s, 3H, CH$_3$).

^{13}C{^{1}H} NMR (CDCl$_3$): δ_C 163.8, 147.4, 138.4, 134.7 (q, $^2J_{CF}$ = 32.7 Hz), 133.2, 130.3, 125.5 (q, $^3J_{CF}$ = 3.8 Hz), 125.0, 123.6 (q, $^1J_{CF}$ = 273.0 Hz), 117.5, 36.8, 36.7, 31.9, 25.6, 24.9, 23.2, 18.3.

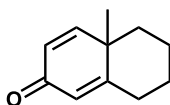**¹⁹F NMR** (CDCl₃): δ_F-63.1 (s, CF₃).

IR: 2932, 2911, 2841, 1732, 1325, 1265, 1179, 1099, 1067, 1015 cm⁻¹.

m/z (GC/MS EI): t_R 15.172 minutes [M] calculated 336.1, observed 336.1 [M].

M.P. (Methanol) 42-44 °C.

6.3.1.6.   Synthesis of 4a-methyl-5,6,7,8-tetrahydronaphthalen-2(4a*H*)-one (153)

Based on the procedures of Ainsworth,[228] Davis[229] and Bloom.[230] Anhydrous diethyl ether (660 mL) and sodium (0.33 mol, 7.6 g), freshly distilled cyclohexanone (1 equiv., 0.33 mol, 34 mL), ethyl formate (1.5 equiv., 0.49 mol, 40 mL) and ethanol (0.08 equiv., 0.026 mol, 1.5 mL) were added to an oven dried flask under a nitrogen atmosphere with stirring and the mixture was cooled to 0°C. The mixture changed from colourless to pale yellow to orange over 6 hours. After stirring for 7.5 hours, the now viscous and opaque orange suspension was left to stand without stirring at room temperature under nitrogen for 16 hours. Ethanol (8.5 mL) was added and the mixture stirred for 1 hour. Water (70 mL) was added and the aqueous and organic phases separated. The organic phase was then extracted with water (20 mL). The combined aqueous phases were extracted with diethyl ether (40 mL). The aqueous phase was then acidified to pH 1 with aqueous 1 M HCl solution and the aqueous phase extracted with diethyl ether (100 mL) a further two times. The combined organic phases were washed with brine (10 mL) and dried over MgSO₄ before concentration. The residue was then distilled (58°C, 1.3 mbar) to yield 26.84 g crude 2-oxocyclohexane-1-carbaldehyde. The crude material (taken as 0.21 mol, 26.84 g) was suspended in anhydrous acetone (426 mL), methyl iodide (2 equiv., 0.43 mol, 27 mL) and K₂CO₃ (2 equiv., 0.43 mol, 58.9 g) were added and the mixture stirred at room temperature for 16 hours. The K₂CO₃ was removed by vacuum filtration and washed with diethyl ether (200 mL). The filtrate was concentrated *in vacuo* to yield crude 1-methyl-2-oxocyclohexane-1-carbaldehyde. The crude material was suspended in

anhydrous acetone (288 mL), piperidine (1.05 equiv., 0.22 mol, 22 mL) and glacial acetic acid (1.05 equiv., 0.22 mol, 13 mL) were added. The yellow suspension was then heated to reflux for 89 hours resulting in the formation of an orange solution. The mixture was allowed to cool to room temperature and concentrated *in vacuo*. The residue was suspended in diethyl ether (100 mL) and water (100 mL) was added. The aqueous and organic phases were separated and the organic phase extracted with aqueous HCl solution (1 M, 100 mL), water (100 mL) and $NaHCO_3$ solution (1 M, 100 mL). The organic phase was dried over $MgSO_4$, concentrated *in vacuo* and the residue resuspended in methanol (250 mL). Aqueous KOH (18 M, 16 mL) was added resulting in a colour change from orange to deep red and the mixture heated to reflux for 4.5 hours. After cooling to room temperature the mixture was concentrated *in vacuo*. The residue was distilled (115°C, 1.8 mbar) to afford 9.62 g (18%) of the title compound as a yellow oil.

^{1}H NMR (CDCl$_3$): δ_H 6.78 (d, $^3J_{HH}$ = 10.0 Hz, 1H, HC=CH), 6.22 (dd, $^3J_{HH}$ = 9.9 Hz, $^4J_{HH}$ = 1.8 Hz, 1H, HC=CH), 6.11 (t, $^4J_{HH}$ = 1.7 Hz, 1H, C=CH), 2.45 (tdd, $^2J_{HH}$ = 13.2 Hz, $^3J_{HH}$ = 5.1 Hz, $^4J_{HH}$ = 1.6 Hz, 1H, CH$_2$), 2.38 (dt, $^2J_{HH}$ = 13.2 Hz, $^3J_{HH}$ = 2.9 Hz, 1H, CH$_2$), 2.04 (apparent d, $^2J_{HH}$ = 13.1 Hz, 1H, CH$_2$), 1.85 (apparent d, $^2J_{HH}$ = 13.9 Hz, 1H, CH$_2$), 1.80-1.69 (m, 2H, CH$_2$), 1.41-1.30 (m, 2H, CH$_2$), 1.29 (s, 3H, CH$_3$).
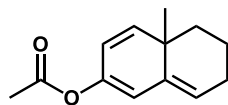
^{13}C{^{1}H} NMR (CDCl$_3$): δ_C 186.5, 167.2, 157.1, 126.1, 123.6, 40.4, 37.7, 32.3, 27.5, 22.4, 20.4.

IR: 2928, 2854, 1710, 1660, 1606, 847 cm^{-1}.

m/z (GC/MS): t$_R$ 11.591 minutes [M] calculated 162.1, observed 162.1 [M]

Analytical data consistent with published values.[231]

6.3.1.7. Attempted Synthesis of 4a-methyl-4a,5,6,7-tetrahydronaphthalen-2-yl acetate (157):

Attempted using general procedure B. Isolation *via* column chromatography (15% EtOAc/hexane) or crystallisation (hexane or methanol) failed to yield pure **157**.

^{1}H NMR (CDCl$_3$, crude reaction mixture): δ_H 5.72 (apparent d, $^3J_{HH}$ = 10.0 Hz, 2H, C=CH, HC=CH), 5.68 (dd, $^3J_{HH}$ = 10.0 Hz, $^4J_{HH}$ = 2.1 Hz, 1H, HC=CH), 5.54 (t, $^3J_{HH}$ = 4.0 Hz, 1H, C=CH), 2.22-2.18 (m, 1H, CH$_2$), 1.95-1.89 (m, 1H, CH$_2$), 1.79-1.69 (m, 3H, CH$_2$), 1.58-1.51 (m, 1H, CH$_2$), 1.23 (s, 3H, CH$_3$).

6.3.1.8. Attempted Synthesis of 4a-methyl-4a,5,6,7-tetrahydronaphthalen-2-yl benzoate (156):
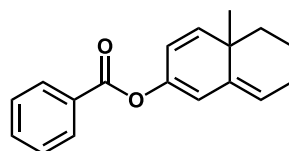
Compound **153** was suspended in pyridine and degassed under N$_2$, benzoyl chloride (3 equiv.) was then added and the mixture stirred under N$_2$ at 80 °C for 3 hours. The mixture was cooled to room temperature, diluted with ethyl acetate and extracted with saturated aqueous CuSO$_4$ solution. The organic phase was collected, dried over MgSO$_4$ and passed through silica in 20% ethyl acetate in hexane. Isolation *via* column chromatography (10% EtOAc/hexane) or crystallisation (hexane or methanol) failed to yield pure **156**.

^{1}H NMR (CDCl$_3$, crude reaction mixture): δ_H 8.13 (dt, $^3J_{HH}$ = 7.0 Hz, $^4J_{HH}$ = 1.7 Hz, 2H, Ar CH), 7.74-7.69 (m, 1H, Ar CH), 7.48 (tt, $^3J_{HH}$ = 7.0 Hz, $^4J_{HH}$ = 1.7 Hz, 2H, Ar CH), 5.87 (d, $^4J_{HH}$ = 1.8 Hz, 1H, C=CH), 5.82 (dd, $^3J_{HH}$ = 9.8 Hz, $^4H_{HH}$ = 1.8 Hz, 1H, HC=CH), 5.78 (d, $^3J_{HH}$ = 9.8 Hz, 1H, HC=CH), 2.26-2.19 (m, 2H, CH$_2$), 1.99-1.90 (m, 1H, CH$_2$), 1.82-1.71 (m, 2H, CH$_2$), 1.62-1.57 (m, 1H, CH$_2$), 1.30 (s, 3H, CH$_3$).

6.4. Steroids

6.4.1. General Procedures

6.4.1.1.   General Procedure I – Synthesis of Trienol Benzoates from Alpha-Methyl Epoxide:

Alpha methyl epoxide was suspended in pyridine (0.8 M in ketone), degassed under N_2, benzoyl chloride (3 equiv.) added and heated to 80 °C with stirring for 4.5 hours. The mixture was then cooled to room temperature and water (0.15 vol.*) added followed by MeCN (3 vol.) and water (1.5 vol.).

*vol. refers to volume of pyridine (ie. If 20 mL pyridine used 0.15 vol. water would be 3 mL).

6.4.1.2.   General Procedure J – Synthesis of Poorly Soluble Trienol Benzoates from Alpha-Methyl Epoxide:

Alpha methyl epoxide was suspended in pyridine (0.8 M in ketone), degassed under N_2, benzoyl chloride (3 equiv.) added and heated to 80 °C with stirring for 4.5 hours. The mixture was then cooled to room temperature and water (0.15 vol.*) added followed by MeCN (3 vol.), acetone (2 vol.) and water (1.5 vol.).

*vol. refers to volume of pyridine (ie. If 20 mL pyridine used 0.15 vol. water would be 3 mL).

6.4.2. General Procedure K – Fluorination of Trienol Benzoates with SelectFluor (React-IR kinetic experiments):

Enol ester substrate was dissolved in 30 mL solvent mixture (usually 2:1 5% *(v/v)* water in MeCN:2-MeTHF) to a concentration of 0.038 M or 0.019 M, stirred, cooled to the

desired temperature using Mettler Toledo EasyMax and Mettler Toledo ReactIR probe inserted into the reaction mixture. When the desired temperature had been reached IR spectra were acquired (at a frequency of one spectrum per 15 seconds) and 1.5 equivalents of SelectFluor added to the reaction mixture. Spectra were acquired until no apparent change in intensity of the starting material ester C-O signal (*ca.* 1250 cm^{-1}) was visible. Confirmation that the reaction had reached completion was obtained *via* HPLC.

6.4.3. Synthesis of Compounds

6.4.3.1. Synthesis of 2-((4a*S*,4b*S*,5a*S*,6a*S*,7*R*,8*R*)-2-(benzoyloxy)-7-hydroxy-4a,6a,8-trimethyl-4a,5a,6,6a,7,8,9,9a,9b,10-decahydrocyclopenta[1,2]phenanthro[4,4a-b]oxiren-7-yl)-2-oxoethyl benzoate (99b):
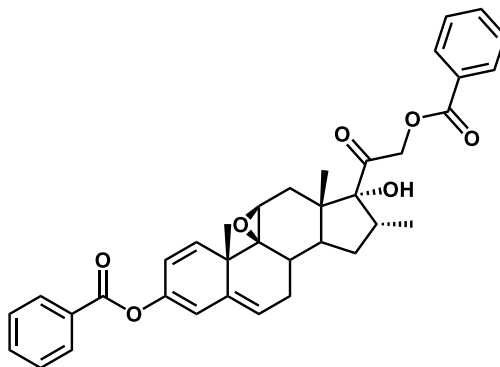
Prepared according to general procedure I. The desired compound precipitated from the reaction mixture and was collected by filtration, washed with 2:1 MeCN:water and dried *in vacuo* to yield 8.0 g of the title compound (86%) as an off-white solid.

^{1}H NMR (CDCl$_3$): δ_H 8.12 (dt, $^3J_{HH}$ = 7.3 Hz, $^4J_{HH}$ = 1.2 Hz, 2H, Ar CH), 8.11 (dt, $^3J_{HH}$ = 7.3 Hz, $^4J_{HH}$ = 1.25 Hz, 2H, Ar CH), 7.63 (tt, $^3J_{HH}$ = 7.3 Hz, $^4J_{HH}$ = 1.4 Hz, 1H, Ar CH), 7.60 (tt, $^3J_{HH}$ = 7.3 Hz, $^4J_{HH}$ = 1.4 Hz, 1H, Ar CH), 7.52-7.45 (m, 4H, Ar CH), 5.98 (d, $^4J_{HH}$ = 2.0 Hz, 1H, A-ring C=CH), 5.84 (apparent dd, $^3J_{HH}$ = 10.3 Hz, $^4J_{HH}$ = 2.0 Hz, 2H, A-ring HC=CH, B-ring C=CH), 5.54 (d, $^3J_{HH}$ = 10.3 Hz, 1H, A-ring HC=CH), 5.33 (d, $^2J_{HH}$ = 17.1 Hz, 1H, CH$_2$OBz), 4.94 (d, $^2J_{HH}$ = 17.1 Hz, 1H, CH$_2$OBz), 3.17 (t, $^3J_{HH}$ = 2.0 Hz, C-ring C-O-CH), 3.14- 3.05 (m,

1H, D-ring CHCH$_3$), 2.89 (ddd, $^2J_{HH}$ = 18.1 Hz, $^3J_{HH}$ = 9.1, 2.9 Hz, 1H, B-ring CH$_2$), 2.54 (s, 1H, OH), 2.46 (dd, $^2J_{HH}$ = 14.5 Hz, $^3J_{HH}$ = 2.0 Hz, 1H, C-ring CH$_2$), 2.29 (dd, $^3J_{HH}$ = 12.5, 9.1 Hz, 1H, B/C-ring junction CH), 2.19 (dd, $^2J_{HH}$ = 18.1 Hz, $^3J_{HH}$ = 7.8 Hz, 1H, B-ring CH$_2$), 1.99-1.90 (m, 2H, C-ring CH$_2$, C/D ring junction CH), 1.75-1.69 (m, 1H, D-ring CH$_2$), 1.39 (ddd, $^2J_{HH}$ = 13.0 Hz, $^3J_{HH}$ = 8.5, 5.0 Hz, 1H, D-ring CH$_2$), 1.32 (s, 3H, A/B ring junction CH$_3$), 1.01 (s, 3H, C/D ring junction CH$_3$), 0.96 (d, $^3J_{HH}$ = 7.0 Hz, 3H, D-ring CH$_3$).

^{13}C{^{1}H} NMR (CDCl$_3$): δ_C 204.0, 165.7, 164.3, 143.8, 139.4, 134.1, 133.0, 132.8, 129.5, 129.4, 129.0, 128.9, 128.0, 127.9, 125.3, 119.7, 113.3, 90.4, 67.5, 65.6, 63.5, 47.8, 47.1, 41.3, 35.0, 33.0, 30.9, 29.4, 26.4, 20.0, 16.4, 14.1.

IR: 1728, 1712, 1450, 1404, 1263, 1247, 1148, 1138, 1117 cm^{-1}.

HPLC: t$_R$ 4.055 min,

m/z (LC/MS ES+): t$_R$ 10.137 min, [M+H] calculated 581.3, observed 581.3 ([M+H]$^+$).

M.P. (MeCN/Water) 144-146 °C (decomposition).

6.4.3.2.   **Synthesis   of   2-((4aS,4bS,5aS,6aS,7R,8R,11S)-11-fluoro-7-hydroxy-4a,6a,8-trimethyl-2-oxo-2,4a,5a,6,6a,7,8,9,9a,9b,10,11-dodecahydrocyclopenta[1,2]phenanthro[4,4a-b]oxiren-7-yl)-2-oxoethyl benzoate (6α-99) and 2-((4aS,4bS,5aS,6aS,7R,8R,11R)-11-fluoro-7-hydroxy-4a,6a,8-trimethyl-2-oxo-2,4a,5a,6,6a,7,8,9,9a,9b,10,11-dodecahydrocyclopenta[1,2]phenanthro[4,4a-b]oxiren-7-yl)-2-oxoethyl benzoate (6β-99):**
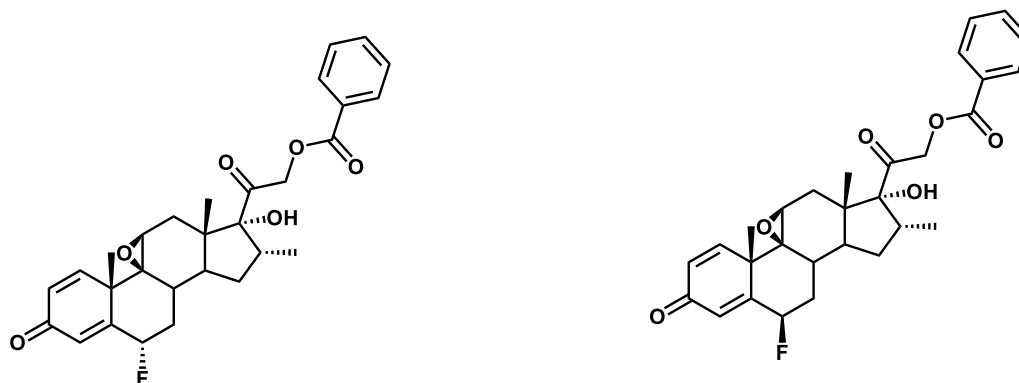
Prepared according to general procedure K. Combined reaction mixtures from kinetic runs of compound **99a** were concentrated to yield crude white solid. Compound **6α-99**

was isolated by suspending the crude solid in 2:1 1 M aqueous $NaHCO_3$ solution:MeCN and shaking for 3 hours at room temperature. Compound **6α-99** was collected by filtration and the white solid washed with water to yield a pure analytical sample. Compound **6β-99** was isolated by dissolving 100 mg crude solid in 1 mL DMSO and purified using MDAP to yield a pure analytical sample.

2-((4a*S*,4b*S*,5a*S*,6a*S*,7*R*,8*R*,11*S*)-11-fluoro-7-hydroxy-4a,6a,8-trimethyl-2-oxo-2,4a,5a,6,6a,7,8,9,9a,9b,10,11-dodecahydrocyclopenta[1,2]phenanthro[4,4a-b]oxiren-7-yl)-2-oxoethyl benzoate (6α-99):

^{1}H NMR (CDCl$_3$): δ$_H$ 8.09 (d, $^3J_{HH}$ = 7.2 Hz, 2H, Ar CH), 7.6 (t, $^3J_{HH}$ = 7.2 Hz, 1H, Ar CH), 7.46 (t, $^3J_{HH}$ = 7.2 Hz, 2H, Ar CH), 6.55 (d, $^3J_{HH}$ = 10.1 Hz, 1H, A-ring HC=CH), 6.47 (t, $^4J_{HH}$ = 1.8 Hz, 1H, A-ring C=CH), 6.27 (dd, $^3J_{HH}$ = 10.1 Hz, $^4J_{HH}$ = 1.8 Hz, 1H, A-ring HC=CH), 5.46 (dddd, $^2J_{HF}$ = 49.4 Hz, $^3J_{HH}$ = 10.6, 6.1 Hz, $^4J_{HH}$ = 1.8 Hz, 1H, CHF), 5.25 (d, $^2J_{HH}$ = 17.2, 1H, CH$_2$OBz), 4.93 (d, $^2J_{HH}$ = 17.2 Hz, 1H, CH$_2$OBz), 3.36 (t, $^3J_{HH}$ = 1.8 Hz, 1H, C-ring C-O-CH), 3.17-3.07 (m, 1H, D-ring CHCH$_3$), 2.69-2.62 (m, 1H, B-ring CH$_2$), 2.50 (s, 1H, OH), 2.46 (dd, $^2J_{HH}$ = 14.1 Hz, $^3J_{HH}$ = 1.8 Hz, C-ring CH$_2$), 2.35 (td, $^3J_{HH}$ = 10.6, 7.3 Hz, 1H, B/C ring junction CH), 2.01 (dd, $^2J_{HH}$ = 14.1 Hz, $^3J_{HH}$ = 1.8 Hz, C-ring CH$_2$), 1.89 (td, $^3J_{HH}$ = 10.6, 8.3 Hz, C/D ring junction CH), 1.70-1.60 (m, 2H, B-ring CH$_2$, D-ring CH$_2$), 1.44 (s, 3H, A/B ring junction CH$_3$), 1.39 (ddd, $^2J_{HH}$ = 12.9 Hz, $^3J_{HH}$ = 8.3, 4.7 Hz, D-ring CH$_2$), 1.00 (s, 3H, C/D ring junction CH$_3$), 0.94 (d, $^3J_{HH}$ = 7.3 Hz, D ring CH$_3$).

^{13}C{^{1}H} NMR (CDCl$_3$): δ$_C$ 204.3, 185.4, 166.3, 160.7 (d, $^2J_{CF}$ = 13.6 Hz), 151.5, 133.4, 129.9, 129.3, 128.4, 128.3, 121.6 (d, $^3J_{CF}$ = 11.5 Hz), 90.6, 86.3 (d, $^1J_{CF}$ = 182.9 Hz), 68.0, 65.9 (d, $^4J_{CF}$ = 1.0 Hz), 63.2, 49.4, 47.6, 43.8 (d, $^3J_{CF}$ = 3.9 Hz), 38.0 (d, $^2J_{CF}$ = 19.6 Hz), 35.4, 33.2, 33.1, 30.5, 23.5, 17.2, 14.5.

^{19}F NMR (CDCl$_3$): δ$_F$-184.4 (ddd, $^2J_{HF}$ = 49.4 Hz, $^3J_{HF}$ = 15.5, 10.4 Hz).

IR: 2941, 1724, 1666, 1627, 1267, 1132, 1109 cm^{-1}.

HPLC: t$_R$ 3.290 min,

m/z (LC/MS MDAP ES+): t$_R$ 14.29 min, [M-HF] calculated 474.2, observed 474.2 ([M]$^+$).

M.P. (MeCN/Water) 182-184 °C (decomposition).

2-((4aS,4bS,5aS,6aS,7R,8R,11R)-11-fluoro-7-hydroxy-4a,6a,8-trimethyl-2-oxo-2,4a,5a,6,6a,7,8,9,9a,9b,10,11-dodecahydrocyclopenta[1,2]phenanthro[4,4a-b]oxiren-7-yl)-2-oxoethyl benzoate (6β-99):

^{1}H NMR (CDCl$_3$): δ$_H$ 8.09 (dt, $^3J_{HH}$ = 8.3 Hz, $^4J_{HH}$ = 1.6 Hz, 2H, Ar CH), 7.89 (tt, $^3J_{HH}$ = 8.3 Hz, $^4J_{HH}$ = 1.6 Hz, 1H, Ar CH), 7.46 (tt, $^3J_{HH}$ = 8.3 Hz, $^4J_{HH}$ = 1.6 Hz, 2H, Ar CH), 6.63 (d, $^3J_{HH}$ = 10.1 Hz, 1H, A-ring HC=CH), 6.42 (ddd, $^4J_{HF}$ = 3.3 Hz, $^4J_{HH}$ = 1.8, 1.0 Hz, 1H, A-ring C=CH), 6.23 (dd, $^3J_{HH}$ = 10.1 Hz, $^4J_{HH}$ = 1.8 Hz, 1H, A-ring HC=CH), 5.32 (ddd, $^2J_{HF}$ = 49.6 Hz, $^3J_{HH}$ = 7.4, 4.9 Hz, 1H, CHF), 5.26 (d, $^2J_{HH}$ = 16.9 Hz, 1H, CH$_2$OBz), 4.90 (d, $^2J_{HH}$ = 16.9 Hz, 1H, CH$_2$OBz), 3.23 (t, $^3J_{HH}$ = 2.3 Hz, 1H, C-O-CH), 3.16-3.07 (m, 1H, D-ring CHCH$_3$), 2.66 (ddd, $^3J_{HF}$ = 27.9 Hz, $^2J_{HH}$ = 14.6 Hz, $^3J_{HH}$ = 7.4 Hz, 1H, B-ring CH$_2$), 2.48 (dt, $^3J_{HH}$ = 12.6, 7.4 Hz, 1H, B/C ring junction CH), 2.41 (dd, $^2J_{HH}$ = 14.9 Hz, $^3J_{HH}$ = 2.3 Hz, 1H, C-ring CH$_2$), 1.98 (dd, $^2J_{HH}$ = 14.9 Hz, $^3J_{HH}$ = 2.3 Hz, 1H, C-ring CH$_2$), 1.95-1.82 (m, 2H, B-ring CH$_2$, D-ring CH$_2$), 1.72-167 (2H, C/D ring junction CH, OH), 1.59 (d, $^5J_{HF}$ = 1.5 Hz, 3H, A/B ring junction CH$_3$), 1.41 (ddd, $^2J_{HH}$ = 17.5 Hz, $^3J_{HH}$ = 8.1, 4.9 Hz, 1H, D-ring CH$_2$), 1.01 (s, 3H, C/D ring junction CH$_3$), 0.95 (d, $^3J_{HH}$ = 7.3 Hz, 3H, D-ring CH$_3$).

^{13}C{^{1}H} NMR (CDCl$_3$): δ$_C$ 204.2, 185.6, 166.2, 157.7 (d, $^2J_{CF}$ = 13.0 Hz), 152.4, 133.4, 129.9, 129.2, 128.7 (d, $^3J_{CF}$ = 6.9 Hz), 128.4, 127.5, 90.5, 88.9 (d, $^1J_{CF}$ = 176.8 Hz), 67.7, 64.6 (d, $^4J_{CF}$ = 2.9 Hz), 62.3, 47.6 (d, $^3J_{CF}$ = 2.9 Hz), 43.3, 35.3, 34.1 (d, $^2J_{CF}$ = 21.1 Hz), 33.1, 31.7, 31.6, 30.2, 24.4 (d, $^4J_{CF}$ = 2.4 Hz) 17.1, 14.5.

^{19}F NMR (CDCl$_3$): δ$_F$-171.1 (dddd, $^2J_{HF}$ = 49.6 Hz, $^3J_{HF}$ = 27.9, 13.9 Hz, $^4J_{HF}$ = 3.3 Hz)

IR: 1717, 1663, 1626, 1277, 1117 cm^{-1}.

HPLC: t$_R$ 3.414 min,

m/z (LC/MS MDAP ES+): t$_R$ 15.42 min, [M-HF] calculated 474.2, observed 474.2 ([M-HF]$^+$).

M.P. (MeCN/Water) 158-160 °C (decomposition).

6.4.3.3. **Synthesis** **of** **2-((4a*S*,4b*S*,5a*S*,6a*S*,7*R*,8*R*)-7-hydroxy-2-((4-methoxybenzoyl)oxy)-4a,6a,8-trimethyl-4a,5a,6,6a,7,8,9,9a,9b,10-decahydrocyclopenta[1,2]phenanthro[4,4a-b]oxiren-7-yl)-2-oxoethyl** **4-methoxybenzoate (158a):**
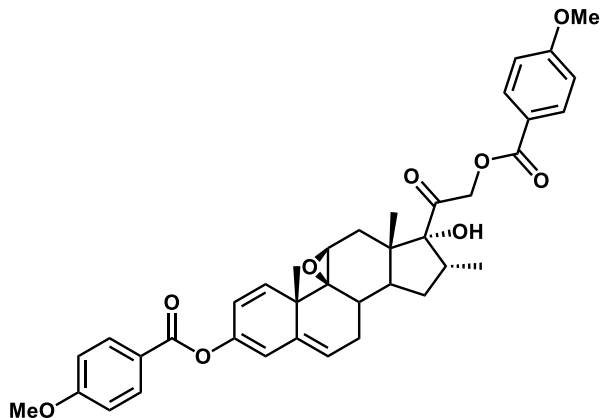
Prepared according to general procedure I. Reaction mixture was diluted with CH_2Cl_2 and extracted with saturated aqueous $CuSO_4$ solution. The organic phase was collected and concentrated. The oily residue was diluted with acetone and 2:1 MeCN:water added resulting in the precipitation of a pale yellow solid. The precipitate was collected *via* filtration and washed with 2:1 MeCN:water and the solid collected and dried *in vacuo* to yield 3.68 g of the title compound (37%).

^{1}H NMR (CDCl$_3$): δ_H 8.07 (dd, $^3J_{HH}$ = 9.0 Hz, $^4J_{HH}$ = 3.0 Hz, 4H, Ar CH), 6.96 (apparent t, $^3J_{HH}$ = 9.0 Hz, 4H, Ar CH), 5.96 (d, $^4J_{HH}$ = 1.3 Hz, 1H, A-ring C=CH), 5.83 (apparent dd, $^3J_{HH}$ = 10.2 Hz, $^4J_{HH}$ = 1.3 Hz, 2H, A-ring HC=CH, B-ring C=CH), 5.53 (d, $^3J_{HH}$ = 10.2 Hz, 1H, A-ring HC=CH), 5.28 (d, $^2J_{HH}$ = 17.0 Hz, 1H, CH$_2$OBz), 4.89 (d, $^2J_{HH}$ = 17.0 Hz, 1H, CH$_2$OBz), 3.90 (s, 3H, OCH$_3$), 3.89 (s, 3H, OCH$_3$), 3.16 (t, $^3J_{HH}$ = 2.2 Hz, 1H, C-ring C-O-CH), 3.13-3.05 (m, 1H, D-ring CHCH$_3$), 2.89 (ddd, $^2J_{HH}$ = 17.9 Hz, $^3J_{HH}$ = 9.0 Hz, 2.8 Hz, 1H, B-ring CH$_2$), 2.46 (s, 1H, OH), 2.45 (dd, $^2J_{HH}$ = 14.7 Hz, $^3J_{HH}$ = 2.2 Hz, 1H, C-ring CH$_2$), 2.28 (dd, $^3J_{HH}$ = 12.4, 9.0 Hz, 1H, B/C ring junction), 2.18 (dd, $^2J_{HH}$ = 17.9 Hz, $^3J_{HH}$ = 7.8 Hz, 1H, B-ring CH$_2$), 1.97-1.91 (m, 2H, C-ring CH$_2$, D-ring CH$_2$), 1.71 (dt, $^3J_{HH}$ = 12.4, 11.3 Hz, 1H, C/D ring junction), 1.43-1.36 (m, 1H, D-ring CH$_2$), 1.31 (s, 3H, A/B ring junction CH$_3$), 1.01 (s, 3H, C/D ring junction CH$_3$), 0.95 (d, $^3J_{HH}$ = 7.2 Hz, D-ring CHCH$_3$).

^{13}C{^{1}H} NMR (CDCl$_3$): δ_C 204.8, 165.9, 164.5, 163.8, 163.7, 144.4, 140.0, 134.5, 132.1, 132.0, 125.5, 121.8, 121.7, 120.4, 113.8, 113.7, 113.6, 90.9, 67.6, 66.1, 64.0, 55.5, 55.4, 48.3, 47.6, 41.7, 35.4, 33.5, 31.4, 29.9, 26.9, 20.5, 16.9, 14.6.

IR: 1719, 1607, 1512, 1269, 1151, 1115, 1059, 1030 cm^{-1}.

HPLC: t$_R$ 4.021 min,

m/z (LC/MS): t$_R$ 9.990 min, [M+H] calculated 641.3, observed 641.3 ([M+H]$^+$).

M.P. (MeCN/water) 157-159 °C (decomposition).

6.4.3.4. Synthesis of 2-((4a*S*,4b*S*,5a*S*,6a*S*,7*R*,8*R*,11*S*)-11-fluoro-7-hydroxy-4a,6a,8-trimethyl-2-oxo-2,4a,5a,6,6a,7,8,9,9a,9b,10,11-dodecahydrocyclopenta[1,2]phenanthro[4,4a-b]oxiren-7-yl)-2-oxoethyl 4-methoxybenzoate (6α-158):
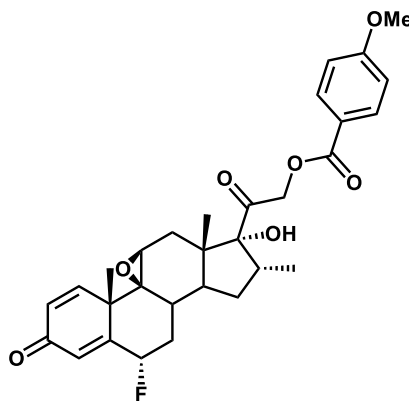
Prepared according to general procedure K. Combined reaction mixtures from kinetic runs of compound **158a** were concentrated to yield crude white solid. Compound **6α-158** was isolated by suspending the crude solid in 2:1 1 M aqueous NaHCO$_3$ solution:MeCN and shaking for 3 hours at room temperature. Compound **6α-158** was collected by filtration and the white solid washed with water to yield a pure analytical sample.

^{1}H NMR (CDCl$_3$): δ_H 8.04 (d, $^3J_{HH}$ = 9.0 Hz, 2H, Ar CH), 6.94 (d, $^3J_{HH}$ = 9.0 Hz, 2H, Ar CH), 6.55 (dd, $^3J_{HH}$ = 10.1 Hz, $^5J_{HF}$ = 1.7 Hz, 1H, A-ring HC=CH), 6.47 (t, $^4J_{HH}$ = 1.9 Hz, 1H, A-ring C=CH), 6.27 (dd, $^3J_{HH}$ = 10.1 Hz, $^4J_{HH}$ = 1.9 Hz, 1H, A-ring HC=CH), 5.46 (dddd, $^2J_{HF}$ = 49.3

Hz, $^3J_{HH}$ = 10.8, 6.0 Hz, $^4J_{HH}$ = 1.9 Hz, 1H, CHF), 5.21 (d, $^2J_{HH}$ = 16.9 Hz, 1H, CH$_2$OBz), 4.86 (d, $^2J_{HH}$ = 16.9 Hz, 1H, CH$_2$OBz), 3.9 (s, 3H, OCH$_3$), 3.36 (t, $^3J_{HH}$ = 1.8 Hz, 1H, C-ring C-O-OCH), 3.16-3.07 (m, 1H, D-ring CHCH$_3$), 2.71-2.62 (m, 1H, B-ring CH$_2$), 2.55 (s, 1H, OH), 2.45 (dd, $^2J_{HH}$ = 14.6 Hz, $^3J_{HH}$ = 1.8 Hz, 1H, C-ring CH$_2$), 2.33 (td, $^3J_{HH}$ = 10.7, 6.9 Hz, 1H, B/C ring junction CH), 1.99 (dd, $^2J_{HH}$ = 14.6 Hz, $^3J_{HH}$ = 1.8 Hz, 1H, C-ring CH$_2$), 1.89 (td, 10.7, 8.4 Hz, 1H, C/D ring junction CH), 1.71-1.59 (m, B-ring CH$_2$, D-ring CH$_2$), 1.43 (s, 3H, A/B ring junction CH$_3$), 1.39(ddd, $^2J_{HH}$ = 12.8 Hz, $^3J_{HH}$ = 8.4, 4.6 Hz), 1.00 (s, 3H, C/D ring junction CH$_3$), 0.94 (d, $^3J_{HH}$ = 7.2 Hz).

^{13}C{^{1}H} NMR (CDCl$_3$): δ_C 204.1, 184.8, 165.5, 163.2, 160.0 (d, $^2J_{CF}$ = 14.3 Hz), 150.8, 131.5, 127.9, 121.1, 121.1 (d, $^3J_{CF}$ = 7.6 Hz), 113.2, 90.0, 85.7 (d, $^1J_{CF}$ = 181.2 Hz), 67.1, 65.3, 62.7, 55.0, 47.1, 43.2 (d, $^3J_{CF}$ = 3.9 Hz), 37.5 (d, $^2J_{CF}$ = 19.6 Hz), 34.8, 32.7, 32.6 (d, $^4J_{CF}$ = 3.1 Hz), 30.0, 23.0, 16.7, 14.0.

^{19}F NMR (CDCl$_3$): δ_F-184.6 (ddd, $^2J_{HF}$ = 49.3 Hz, $^3J_{HF}$ = 15.5, 10.3 Hz)

IR: 2941, 1713, 1666, 1631, 1600, 1226, 1120, 1083, 1020 cm^{-1}.

HPLC: t_R 3.286 min,

m/z (LC/MS MDAP ES+): t_R 14.00 min, [M] calculated 524.2, observed 524.2 ([M]$^+$), 504.2 ([M-HF]).

M.P. (MeCN/Water) 204-206 °C (decomposition).

6.4.3.5. Synthesis of 2-((4aS,4bS,5aS,6aS,7R,8R)-7-hydroxy-4a,6a,8-trimethyl-2-((4-methylbenzoyl)oxy)-4a,5a,6,6a,7,8,9,9a,9b,10-decahydrocyclopenta[1,2]phenanthro[4,4a-b]oxiren-7-yl)-2-oxoethyl 4-methylbenzoate (159a):
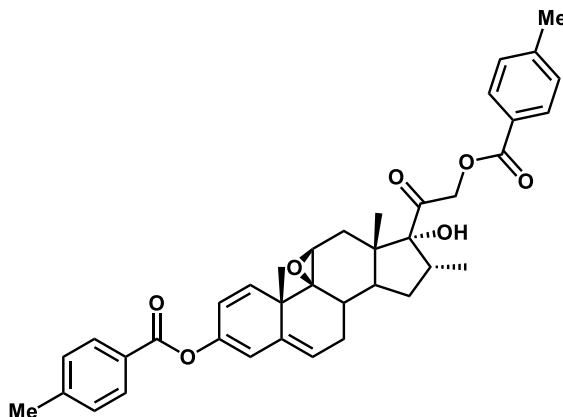
Prepared according to general procedure J. The desired compound precipitated from the reaction mixture and was collected by filtration, washed with 2:1 MeCN:water and dried *in vacuo* to yield 6.11 g of the title compound (63%) as an off-white solid.

^{1}H NMR (CDCl$_3$): δ_H 8.00-7.94 (m, 4H, Ar CH), 7.30-7.25 (m, 4H, Ar CH), 5.95 (d, $^4J_{HH}$ = 1.8 Hz, 1H, A-ring C=CH), 5.81 (apparent dd, $^3J_{HH}$ = 10.2 Hz, $^4J_{HH}$ = 1.8 Hz, 2H, A-ring CH=CH, B-ring C=CH), 5.52 (d, $^3J_{HH}$ = 10.2 Hz, 1H, A-ring HC=CH), 5.28 (d, $^2J_{HH}$ = 17.1 Hz, 1H, CH$_2$OBz), 4.90 (d, $^2J_{HH}$ = 17.1 Hz, 1H, CH$_2$OBz), 3.15 (t, $^3J_{HH}$ = 2.0 Hz, 1H, C-ring C-O-CH), 3.12-3.03 (m, 1H, D-ring CHCH$_3$), 2.87 (ddd, $^2J_{HH}$ = 18.1 Hz, $^3J_{HH}$ = 8.8, 3.5 Hz, 1H, B-ring CH$_2$), 2.48-2.45 (m, 1H, C-ring CH$_2$), 2.44 (s, 3H, Ar CH$_3$), 2.42 (s, 3H, Ar CH$_3$), 2.27 (dd, $^3J_{HH}$ = 12.4, 9.1 Hz, B/C ring junction CH$_2$), 2.17 (dd, $^2J_{HH}$ = 18.1 Hz, $^3J_{HH}$ = 7.7 Hz, 1H, B-ring CH$_2$), 1.96-1.88 (m, 2H, C-ring CH$_2$, C/D ring junction CH), 1.73-1.64 (m, 1H, D-ring CH$_2$), 1.38 (ddd, $^2J_{HH}$ = 13.1 Hz, $^3J_{HH}$ = 8.4, 4.9 Hz, 1H, D-ring CH$_2$), 1.30 (s, 3H, A/B ring junction CH$_3$), 1.02 (s, 3H, C/D ring junction CH$_3$), 0.94 (d, $^3J_{HH}$ = 7.2 Hz, 3H, D-ring CH$_3$).

^{13}C{^{1}H} NMR (CDCl$_3$): δ_C 204.6, 166.2, 164.8, 144.4, 144.3, 144.0, 139.9, 134.5, 130.1, 129.9, 129.2, 129.1, 126.7, 126.6, 125.6, 120.3, 113.7, 90.9, 67.8, 66.1, 64.0, 48.3, 47.6, 41.8, 35.4, 33.5, 31.4, 29.9, 26.9, 21.7, 21.7, 20.5, 16.9, 14.6.

IR: 1720, 1269, 1151, 1138, 1126, 1113, 1059, 1020 cm^{-1}.

HPLC: t_R 4.251 min,

m/z (LC/MS ES+): t_R 10.525 min, [M+H] calculated 609.3, observed 609.3 ([M]$^+$).

M.P. (MeCN/Water) 222-224 °C (decomposition).

6.4.3.6. Synthesis of 2-((4aS,4bS,5aS,6aS,7R,8R,11S)-11-fluoro-7-hydroxy-4a,6a,8-trimethyl-2-oxo-2,4a,5a,6,6a,7,8,9,9a,9b,10,11-dodecahydrocyclopenta[1,2]phenanthro[4,4a-b]oxiren-7-yl)-2-oxoethyl 4-methylbenzoate (6α-159):
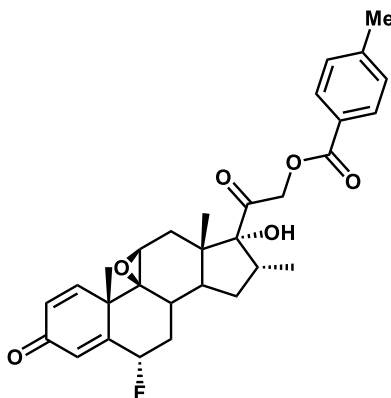
Prepared according to general procedure K. Combined reaction mixtures from kinetic runs of compound **159a** were concentrated to yield crude white solid. Compound **6α-159** was isolated by suspending the crude solid in 2:1 1 M aqueous NaHCO$_3$ solution:MeCN and shaking for 3 hours at room temperature. Compound **6α-159** was collected by filtration and the white solid washed with water to yield a pure analytical sample.

¹H NMR (CDCl$_3$): δ_H 7.97 (d, $^3J_{HH}$ = 8.1 Hz, 2H, Ar CH), 7.26 (d, $^3J_{HH}$ = 8.1 Hz, Ar CH), 6.55 (dd, $^3J_{HH}$ = 10.1 Hz, $^5J_{HF}$ = 1.5 Hz, 1H, A-ring HC=CH), 6.47 (t, $^4J_{HH}$ = 1.8 Hz, 1H, A-ring C=CH), 6.27 (dd, $^3J_{HH}$ = 10.1 Hz, $^4J_{HH}$ = 1.8 Hz, 1H, A-ring HC=CH), 5.46 (dddd, $^2J_{HF}$ = 49.3 Hz, $^3J_{HH}$ = 10.7, 5.9 Hz, $^4J_{HH}$ = 1.8 Hz, CHF), 5.23 (d, $^2J_{HH}$ = 17.2 Hz, 1H, CH$_2$OBz), 4.88 (d, $^2J_{HH}$ = 17.2 Hz, 1H, CH$_2$OBz), 3.36 (t, $^3J_{HH}$ = 2.5 Hz, 1H, C-ring C-O-CH), 3.16-3.07 (m, 1H, D-ring CHCH$_3$), 2.71-2.62 (m, 1H, B-ring CH$_2$), 2.53 (s, 1H, OH), 2.47-2.43 (m, 1H, C-ring CH$_2$), 2.42 (s, 3H, Ar CH$_3$), 2.33 (td, $^3J_{HH}$ = 11.0, 7.0 Hz, 1H, B/C ring junction CH), 2.00 (dd, $^2J_{HH}$ = 14.6 Hz, $^3J_{HH}$ = 2.5 Hz, 1H, C-ring CH$_2$), 1.88 (td, $^3J_{HH}$ = 11.0, 8.4 Hz, 1H, C/D ring junction

CH), 1.71-1.58 (m, 2H, B-ring CH$_2$, D-ring CH$_2$), 1.43 (s, 3H, A/B ring junction CH$_3$), 1.39 (ddd, $^2J_{HH}$ = 12.9 Hz, $^3J_{HH}$ = 8.4, 4.7 Hz, D-ring CH$_2$), 1.00 (s, 3H, C/D ring junction CH$_3$), 0.94 (d, $^3J_{HH}$ = 7.1 Hz, 3H, D-ring CH$_3$).

^{13}C{^{1}H} NMR (CDCl$_3$): δ_C 203.9, 184.8, 165.8, 160.1 (d, $^2J_{CF}$ = 14.4 Hz), 150.8, 143.6, 129.4, 128.7, 127.8, 126.0, 121.1 (d, $^3J_{CF}$ = 11.6 Hz), 90.0, 85.7 (d, $^1J_{CF}$ = 181.3 Hz), 67.3, 65.3, 62.7, 49.0, 47.1, 43.2 (d, $^3J_{CF}$ = 3.9 Hz), 37.6 (d, $^2J_{CF}$ = 19.6 Hz), 34.8, 32.7, 32.6, 30.0, 23.0, 21.2, 16.7, 14.0.

^{19}F NMR (CDCl$_3$): δ_F-184.5 (ddd, $^2J_{HF}$ = 49.3 Hz, $^3J_{HF}$ = 15.6, 10.4 Hz)

IR: 2941, 1717, 1666, 1624, 1404, 1235, 1177, 1130, 1105, 1078 cm^{-1}.

HPLC: t$_R$ 3.470 min,

m/z (LC/MS MDAP ES+): t$_R$ 16.80 min, [M-HF] calculated 488.2, observed 488.2 ([M-HF]$^+$).

M.P. (MeCN/Water) 229-230 °C (decomposition).

6.4.3.7. **Synthesis of 2-((4aS,4bS,5aS,6aS,7R,8R)-2-((4-chlorobenzoyl)oxy)-7-hydroxy-4a,6a,8-trimethyl-4a,5a,6,6a,7,8,9,9a,9b,10-decahydrocyclopenta[1,2]phenanthro[4,4a-b]oxiren-7-yl)-2-oxoethyl 4-chlorobenzoate (160a):**
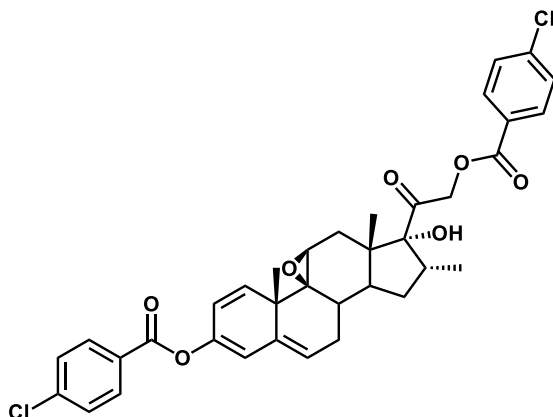
Prepared according to general procedure J. The desired compound precipitated from the reaction mixture and was collected by filtration, washed with 2:1 MeCN:water and dried *in vacuo* to yield 6.23 g of the title compound (60%) as a pale yellow solid.

¹H NMR (CDCl₃): δ$_H$ 8.08-8.01 (m, 4H, Ar CH), 7.46 (d, $^3J_{HH}$ = 8.9 Hz, 2H, Ar CH), 7.44 (d, $^3J_{HH}$ = 8.7 Hz, 2H, Ar CH), 5.96 (d, $^4J_{HH}$ = 1.6 Hz, 1H, A-ring C=CH), 5.83 (dd, $^3J_{HH}$ = 7.0, 2.7 Hz, 1H, B-ring C=CH), 5.80 (dd, $^3J_{HH}$ = 10.2 Hz, $^4J_{HH}$ = 1.6 Hz, 1H, A-ring HC=CH), 5.52 (d, $^3J_{HH}$ = 10.2 Hz, 1H, A-ring HC=CH), 5.28 (d, $^2J_{HH}$ = 17.2 Hz, 1H, CH₂OBz), 4.94 (d, $^2J_{HH}$ = 17.2 Hz, CH₂OBz), 3.14 (t, $^3J_{HH}$ = 2.1 Hz, 1H, C-ring C-O-CH), 3.11-3.04 (m, 1H, D-ring CHCH₃), 2.88 (ddd, $^2J_{HH}$ = 18.1 Hz, $^3J_{HH}$ = 9.1, 2.7 Hz, 1H, B-ring CH₂), 2.43 (dd, $^2J_{HH}$ = 14.7, $^3J_{HH}$ = 2.1 Hz, 1H, C-ring CH₂), 2.36 (s, 1H, OH), 2.28 (dd, $^3J_{HH}$ = 12.5, 9.0 Hz, 1H, B/C ring junction CH), 2.17 (dd, $^2J_{HH}$ = 18.1 Hz, $^3J_{HH}$ = 7.0 Hz, 1H, B-ring CH₂), 1.95 (dd, $^2J_{HH}$ = 14.7 Hz, $^3J_{HH}$ = 2.1 Hz, 1H, C-ring CH₂), 1.95-1.87 (m, 1H, C/D ring junction CH), 1.74-1.65 (m, 1H, B/C ring junction CH), 1.38 (ddd, $^2J_{HH}$ = 13.1 Hz, $^3J_{HH}$ = 8.4, 4.9 Hz, 1H, D-ring CH₂), 1.30 (s, 3H, A/B ring junction CH₃), 0.99 (s, 3H, C/D ring junction CH₃), 0.94 (d, $^3J_{HH}$ = 7.2 Hz, 3H, D-ring CH₃).

¹³C{¹H} NMR (CDCl₃): δ$_C$ 204.2, 165.3, 163.9, 144.2, 140.1, 139.8, 134.7, 131.9, 131.4, 131.3, 139.4, 128.9, 128.8, 127.9, 127.8, 126.0, 113.8, 90.9, 68.2, 66.0, 64.0, 48.3, 47.6, 41.8, 35.5, 33.4, 31.3, 29.9, 26.9, 20.5, 16.8, 14.5.

IR: 1728, 1713, 1402, 1263, 1147, 1138, 1117, 1096, 1061, 1022 cm⁻¹.

HPLC: t$_R$ 4.346 min,

m/z (LC/MS ES+): t$_R$ 10.799 min, [M+H] calculated 649.2, observed 649.2 ([M+H]⁺).

M.P. (MeCN/Water) 182-184 °C (decomposition).

6.4.3.8. **Synthesis** of 2-((4aS,4bS,5aS,6aS,7R,8R,11S)-11-fluoro-7-hydroxy-4a,6a,8-trimethyl-2-oxo-2,4a,5a,6,6a,7,8,9,9a,9b,10,11-dodecahydrocyclopenta[1,2]phenanthro[4,4a-b]oxiren-7-yl)-2-oxoethyl 4-chlorobenzoate (6α-160):
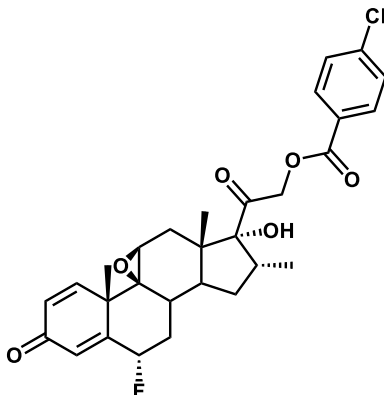
Prepared according to general procedure K. Combined reaction mixtures from kinetic runs of compound **160a** were concentrated to yield crude white solid. Compound **6α-160** was isolated by suspending the crude solid in 2:1 1 M aqueous NaHCO$_3$ solution:MeCN and shaking for 3 hours at room temperature. Compound **6α-160** was collected by filtration and the white solid washed with water to yield a pure analytical sample.

^{1}H NMR (CDCl$_3$): δ$_H$ 8.02 (d, $^3J_{HH}$ = 8.7 Hz, 2H, Ar CH), 7.44 (d, $^3J_{HH}$ = 8.7 Hz, 2H, Ar CH), 6.55 (dd, $^3J_{HH}$ = 10.1 Hz, $^5J_{HF}$ = 1.7 Hz, 1H, A-ring HC=CH), 6.47 (t, $^4J_{HH}$ = 2.1 Hz, 1H, A-ring C=CH), 6.27 (dd, $^3J_{HH}$ = 10.1 Hz, $^4J_{HH}$ = 2.1 Hz, 1H, A-ring HC=CH), 5.46 (dddd, $^2J_{HF}$ = 49.4 Hz, $^3J_{HH}$ = 10.7, 6.1 Hz, $^4J_{HH}$ = 2.1 Hz, 1H, CHF), 5.25 (d, $^2J_{HH}$ = 17.1 Hz, 1H, CH$_2$OBz), 4.92 (d, $^2J_{HH}$ = 17.1 Hz, 1H, CH$_2$OBz), 3.36 (t, $^3J_{HH}$ = 2.0 Hz, 1H, C-ring C-O-CH), 3.16-3.07 (m, 1H, D-ring CHCH$_3$), 2.71-2.62 (m, 1H, B-ring CH$_2$), 2.49 (s, 1H, OH), 2.44 (dd, $^2J_{HH}$ = 14.6 Hz, $^3J_{HH}$ = 2.0 Hz, 1H, C-ring CH$_2$), 2.38-2.31 (m, 1H, B/C ring junction CH), 2.00 (dd, $^2J_{HH}$ = 14.6 Hz, $^3J_{HH}$ = 2.0 Hz, 1H, C-ring CH$_2$), 1.88 (td, $^3J_{HH}$ = 11.1, 8.6 Hz, 1H, C/D ring junction), 1.71-1.64 (m, 2H, B-ring CH$_2$, D-ring CH$_2$), 1.43 (s, 3H, A/B ring junction CH$_3$), 1.38 (ddd, $^2J_{HH}$ = 12.8 Hz, $^3J_{HH}$ = 8.6, 4.6 Hz, 1H, D-ring CH$_2$), 0.99 (s, 3H, C/D ring junction CH$_3$), 0.94 (d, $^3J_{HH}$ = 7.2 Hz, D-ring CH$_3$).

$^{13}C\{^1H\}$ NMR (CDCl$_3$): δ_C 203.5, 184.8, 164.9, 160.1 (d, $^2J_{CF}$ = 14.5 Hz), 150.9, 139.4, 130.8, 128.3, 127.8, 127.3, 121.1 (d, $^3J_{CF}$ = 11.2 Hz), 90.1, 85.7 (d, $^1J_{CF}$ = 181.2 Hz), 67.8, 65.3, 62.6, 48.9, 47.1, 43.2, 37.5 (d, $^2J_{CF}$ = 19.6 Hz), 34.9, 32.6, 32.6, 30.0, 22.9, 16.7, 14.0.

^{19}F NMR (CDCl$_3$): δ_F-184.2 (ddd, $^2J_{HF}$ = 49.4 Hz, $^3J_{HF}$ = 15.8, 10.4 Hz)

IR: 2941, 1724, 1666, 1628, 1404, 1265, 1132, 1078, 1016 cm^{-1}.

HPLC: t$_R$ 3.371 min,

m/z (LC/MS MDAP ES+): t$_R$ 18.63 min, [M-HF] calculated 508.2, observed 508.2 ([M-HF]$^+$).

M.P. (MeCN/Water) 193 °C (decomposition).

6.4.3.9. Synthesis of 2-((4aS,4bS,5aS,6aS,7R,8R)-2-((4-acetoxybenzoyl)oxy)-7-hydroxy-4a,6a,8-trimethyl-4a,5a,6,6a,7,8,9,9a,9b,10-decahydrocyclopenta[1,2]phenanthro[4,4a-b]oxiren-7-yl)-2-oxoethyl methyl terephthalate (161a):
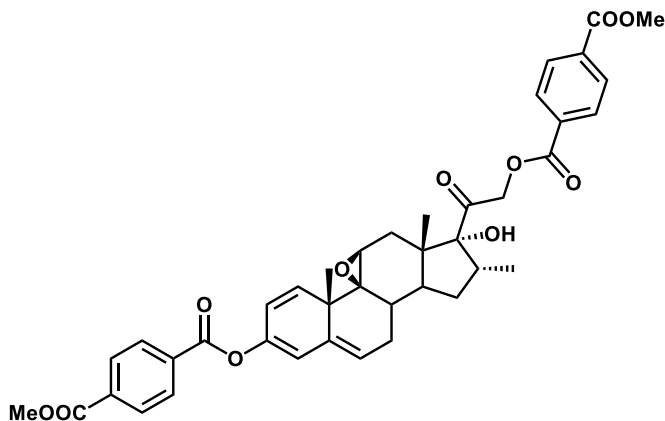
Prepared according to general procedure I. The desired compound precipitated from the reaction mixture and was collected by filtration, washed with 2:1 MeCN:water and dried *in vacuo* to yield 8.83 g of the title compound (79%) as an off-white solid.

^1H NMR (CDCl$_3$): δ_H 8.18-8.08 (m, 8H, Ar CH), 5.98 (d, $^4J_{HH}$ = 1.8 Hz, A-ring C=CH), 5.84 (dd, $^3J_{HH}$ = 7.7, 2.9 Hz, 1H, B-ring C=CH), 5.82 (dd, $^3J_{HH}$ = 10.4 Hz, $^4J_{HH}$ = 1.8 Hz, 1H, A-ring HC=CH), 5.54 (d, $^3J_{HH}$ = 10.4 Hz, 1H, A-ring HC=CH), 5.32 (d, $^2J_{HH}$ = 17.2 Hz, 1H, CH$_2$OBz), 4.98 (d, $^2J_{HH}$ = 17.2 Hz, 1H, CH$_2$OBz), 3.97 (s, 3H, COOCH$_3$), 3.96 (s, 3H, COOCH$_3$), 3.15 (t, $^3J_{HH}$ = 2.4 Hz, 1H, C-ring C-O-CH), 3.13-3.03 (m, 1H, D-ring CHCH$_3$), 2.88 (ddd, $^2J_{HH}$ = 18.1

Hz, $^3J_{HH}$ = 9.3, 2.9 Hz, 1H, B-ring CH$_2$), 2.45 (dd, $^2J_{HH}$ = 15.2 Hz, $^3J_{HH}$ = 2.4 Hz, 1H, C-ring CH$_2$), 2.37 (s, 1H, OH), 2.28 (dd, $^3J_{HH}$ = 12.5, 9.3 Hz, 1H, B/C ring junction CH), 2.18 (dd, $^2J_{HH}$ = 18.1 Hz, $^3J_{HH}$ = 7.7 Hz, 1H, B-ring CH$_2$), 1.97 (dd, $^2J_{HH}$ = 15.2 Hz, $^3J_{HH}$ = 2.4 Hz, C-ring CH$_2$), 1.95-1.87 (m, 1H, C/D ring junction CH), 1.75-1.66 (m, 1H, D-ring CH$_2$), 1.38 (ddd, $^2J_{HH}$ = 13.0 Hz, $^3J_{HH}$ = 8.5, 4.9 Hz, 1H, D-ring CH$_2$), 1.30 (s, 3H, A/B ring junction CH$_3$), 1.00 (s, 3H, C/D ring junction CH$_3$), 0.94 (d, $^3J_{HH}$ = 7.1 Hz, 3H, D-ring CH$_3$).

^{13}C{^{1}H} NMR (CDCl$_3$): δ_C 204.1, 166.2, 166.1, 165.4, 163.9, 144.2, 139.7, 134.8, 134.4, 134.2, 133.2, 133.2, 130.0, 129.9, 129.7, 129.6, 126.1, 120.0, 113.9, 91.0, 68.4, 66.0, 64.0, 52.5, 52.4, 48.4, 47.7, 41.8, 35.5, 33.4, 31.3, 29.9, 26.9, 20.5, 16.8, 14.5.

IR: 1715, 1269, 1252, 1151, 1138, 1115, 1020 cm^{-1}.

HPLC: t_R 4.067 min,

m/z (LC/MS ES+): t_R 10.167 min, [M+H] calculated 697.3, observed 697.3 ([M+H]$^+$).

M.P. (MeCN/Water) 171-173 °C (decomposition).

6.4.3.10. Synthesis of 2-((4aS,4bS,5aS,6aS,7R,8R,11S)-11-fluoro-7-hydroxy-4a,6a,8-trimethyl-2-oxo-2,4a,5a,6,6a,7,8,9,9a,9b,10,11-dodecahydrocyclopenta[1,2]phenanthro[4,4a-b]oxiren-7-yl)-2-oxoethyl methyl terephthalate (6α-161):
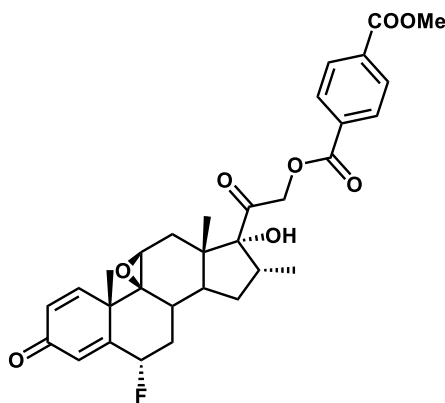
Prepared according to general procedure K. Combined reaction mixtures from kinetic runs of compound **161a** were concentrated to yield crude white solid. Compound **6α-161** was isolated by suspending the crude solid in 2:1 1 M aqueous NaHCO$_3$

solution:MeCN and shaking for 3 hours at room temperature. Compound **6α-161** was collected by filtration and the white solid washed with water to yield a pure analytical sample.

¹H NMR (CDCl₃): δ_H 8.15 (d, $^3J_{HH}$ = 8.8 Hz, 2H, Ar CH), 8.12 (d, $^3J_{HH}$ = 8.8 Hz, 2H, Ar CH), 6.55 (dd, $^3J_{HH}$ = 10.2 Hz, $^5J_{HF}$ = 1.2 Hz, 1H, A-ring HC=CH), 6.47 (t, $^4J_{HH}$ = 1.8 Hz, 1H, A-ring C=CH), 6.27 (dd, $^3J_{HH}$ = 10.1 Hz, $^4J_{HH}$ = 1.8 Hz, 1H, A-ring HC=CH), 5.46 (dddd, $^2J_{HF}$ = 49.2 Hz, $^3J_{HH}$ = 10.6. 5.9 Hz, $^4J_{HH}$ = 1.8 Hz, 1H, CHF), 5.27 (d, $^2J_{HH}$ = 17.1 Hz, 1H, CH₂OBz), 4.97 (d, $^2J_{HH}$ = 17.1 Hz, 1H, CH₂OBz), 3.96 (s, 3H, COOCH₃), 3.36 (t, $^3J_{HH}$ = 2.4 Hz, 1H, C-ring C-O-CH), 3.17-3.07 (m, 1H, D-ring CHCH₃), 2.72-2.63 (m, 1H, B-ring CH₂), 2.45 (dd, $^2J_{HH}$ = 14.9 Hz, $^3J_{HH}$ = 2.4 Hz, 1H, C-ring CH₂), 2.40 (s, 1H, OH), 2.35 (td, $^3J_{HH}$ = 10.9, 7.0 Hz, 1H, B/C ring junction CH), 2.01 (dd, $^2J_{HH}$ = 14.6 Hz, $^3J_{HH}$ = 2.4 Hz, 1H, C-ring CH₂), 1.88 (td, $^3J_{HH}$ = 10.9 Hz, 8.4 Hz, C/D ring junction CH), 1.72-1.62 (m, 2H, B-ring CH₂, D-ring CH₂), 1.44 (s, 3H, A/B ring junction CH₃), 1.39 (ddd, $^2J_{HH}$ = 12.8 Hz, $^3J_{HH}$ = 8.4, 4.6 Hz, 1H, D-ring CH₂), 1.00 (s, 3H, C/D ring junction CH₃), 0.94 (d, $^3J_{HH}$ = 7.2 Hz, 3H, D-ring CH₃).

¹³C{¹H} NMR (CDCl₃): δ_C 203.4, 184.8, 165.7, 164.9, 160.1 (d, $^2J_{CF}$ = 14.3 Hz), 150.9, 133.7, 132.6, 129.3, 129.1, 127.8, 121.1 (d, $^3J_{CF}$ = 11.6 Hz), 90.1, 85.7 (d, $^1J_{CF}$ = 181.2 Hz), 67.7, 65.3, 62.6, 52.0, 49.0, 47.2, 43.2 (d, $^3J_{CF}$ = 4.6 Hz), 37.5 (d, $^2J_{CF}$ = 19.5 Hz), 34.9, 32.7, 32.6, 30.0, 22.9, 16.7, 14.0.

¹⁹F NMR (CDCl₃): δ_F-184.2 (ddd, $^2J_{HF}$ = 49.2 Hz, $^3J_{HF}$ = 15.6, 10.4 Hz)

IR: 2941, 1720, 1665, 1624, 1408, 1261, 1119, 1103, 1078, 1020 cm⁻¹.

HPLC: t_R 3.315 min,

m/z (LC/MS MDAP ES+): t_R 14.99 min, [M-HF] calculated 532.2, observed 532.2 ([M-HF]).

M.P. (MeCN/Water) 219-220 °C (decomposition).

6.4.3.11. **Synthesis of 2-((4aS,4bS,5aS,6aS,7R,8R)-7-hydroxy-4a,6a,8-trimethyl-2-((4-nitrobenzoyl)oxy)-4a,5a,6,6a,7,8,9,9a,9b,10-decahydrocyclopenta[1,2]phenanthro[4,4a-b]oxiren-7-yl)-2-oxoethyl 4-nitrobenzoate (162a):**
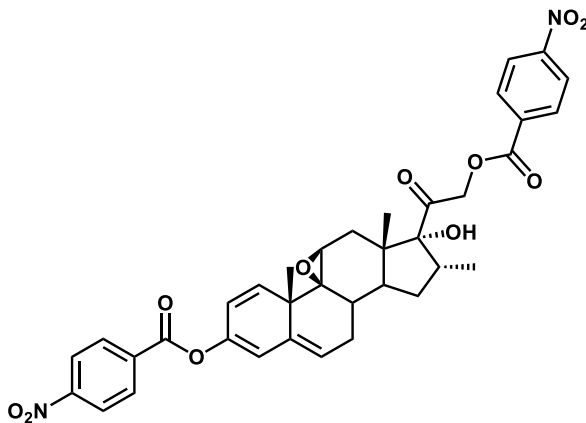
Prepared according to general procedure I. Reaction mixture was diluted with CH_2Cl_2 and extracted with saturated aqueous $CuSO_4$ solution. The organic phase was collected and concentrated. The oily residue was diluted with acetone and 2:1 MeCN:water added resulting in the precipitation of a pale yellow solid. The precipitate was collected *via* filtration and washed with 2:1 MeCN:water and the solid collected and dried *in vacuo* to yield 1.82 g of the title compound (17%).

^{1}H NMR (CDCl$_3$): δ_H 8.35-8.26 (m, 8H, Ar CH), 6.00 (d, $^4J_{HH}$ = 2.0 Hz, 1H, A-ring C=CH), 5.87 (dd, $^3J_{HH}$ = 7.4, 2.9 Hz, 1H, B-ring C=CH), 5.82 (dd, $^3J_{HH}$ = 10.4 Hz, $^4J_{HH}$ = 2.0 Hz, 1H, A-ring HC=CH), 5.56 (d, $^3J_{HH}$ = 10.4 Hz, 1H, A-ring HC=CH), 5.34 (d, $^2J_{HH}$ = 17.2 Hz, 1H, CH$_2$OBz), 5.03 (d, $^2J_{HH}$ = 17.2 Hz, 1H, CH$_2$OBz), 3.15 (t, $^3J_{HH}$ = 2.1 Hz, 1H, C-ring C-O-CH), 3.13-3.04 (m, 1H, D-ring CHCH$_3$), 2.89 (ddd, $^2J_{HH}$ = 18.1 Hz, $^3J_{HH}$ = 9.2, 2.9 Hz, 1H, B-ring CH$_2$), 2.45 (dd, $^2J_{HH}$ = 14.9 Hz, $^3J_{HH}$ = 2.1 Hz, 1H, C-ring CH$_2$), 2.29 (dd, $^3J_{HH}$ = 12.4, 9.2 Hz, 1H, B/C ring junction CH), 2.19 (apparent dd, $^2J_{HH}$ = 18.1 Hz, $^3J_{HH}$ = 7.4 Hz, 2H, B-ring CH$_2$, OH), 1.98 (dd, $^2J_{HH}$ = 14.9 Hz, $^3J_{HH}$ = 2.1 Hz, 1H, C-ring CH$_2$), 1.89 (td, $^3J_{HH}$ = 12.4, 8.5 Hz, 1H, C/D ring junction CH), 1.76-1.67 (m, 1H, D-ring CH$_2$), 1.39 (ddd, $^2J_{HH}$ = 13.0 Hz, $^3J_{HH}$ = 8.4, 4.8 Hz, 1H, D-ring CH$_2$), 1.31 (s, 3H, A/B ring junction CH$_3$), 0.99 (s, 3H, C/D ring junction CH$_3$), 0.95 (d, $^3J_{HH}$ = 7.1 Hz, 3H, D-ring CH$_3$).

¹³C{¹H} NMR (CDCl₃): δ_C 203.7, 164.3, 162.9, 150.9, 150.7, 144.1, 139.6, 135.0, 134.8, 134.8, 131.1, 131.0, 126.6, 123.7, 123.6, 119.7, 114.0, 91.0, 68.9, 66.0, 63.9, 48.4, 47.7, 41.8, 35.6, 33.4, 31.3, 29.9, 27.0, 20.5, 16.8, 14.5.

IR: 2980, 2970, 1715, 1267, 1138, 1117, 1105, 1061, 1022 cm⁻¹.

HPLC: t_R 4.022 min,

m/z (LC/MS ES-): t_R 9.903 min, [M-H] calculated 669.2, observed 669.2 ([M-H]⁻).

M.P. (MeCN/Water) 175-177 °C (decomposition).

6.4.3.12. Synthesis of 2-((4aS,4bS,5aS,6aS,7R,8R,11S)-11-fluoro-7-hydroxy-4a,6a,8-trimethyl-2-oxo-2,4a,5a,6,6a,7,8,9,9a,9b,10,11-dodecahydrocyclopenta[1,2]phenanthro[4,4a-b]oxiren-7-yl)-2-oxoethyl 4-nitrobenzoate (6α-162):
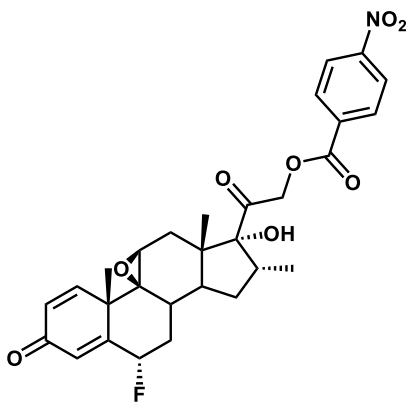
Prepared according to general procedure K. Combined reaction mixtures from kinetic runs of compound **162** were concentrated to yield crude white solid. Compound **6α-162** was isolated by suspending the crude solid in 2:1 1 M aqueous NaHCO₃ solution:MeCN and shaking for 3 hours at room temperature. Compound **6α-162** was collected by filtration and the white solid washed with water to yield a pure analytical sample.

¹H NMR (CDCl₃): δ_H 8.32 (d, ³J_HH = 9.0 Hz, 2H, Ar CH), 8.26 (d, ³J_HH = 9.0 Hz, 2H, Ar CH), 6.56 (dd, ³J_HH = 10.1 Hz, ⁵J_HF = 1.3 Hz, 1H, A-ring HC=CH), 6.47 (t, ⁴J_HH = 1.8 Hz, 1H, A-ring C=CH), 6.28 (dd, ³J_HH = 10.1 Hz, ⁴J_HH = 1.8 Hz, 1H, A-ring HC=CH), 5.46 (dddd, ²J_HF = 49.4 Hz, ³J_HH = 10.5, 5.9 Hz, ⁴J_HH = 1.8 Hz, 1H, CHF), 5.29 (d, ²J_HH = 17.2 Hz, 1H, CH₂OBz), 5.02

(d, $^2J_{HH}$ = 17.2 Hz, 1H, CH$_2$OBz), 3.37 (t, $^3J_{HH}$ = 2.3 Hz, 1H, C-ring C-O-CH), 3.17-3.08 (m, 1H, D-ring CHCH$_3$), 2.72-2.63 (m, 1H, B-ring CH$_2$), 2.46 (dd, $^2J_{HH}$ = 15.0 Hz, $^3J_{HH}$ = 2.3 Hz, 1H, C-ring CH$_2$), 2.40-2.30 (m, 2H, B/C ring junction CH, OH), 2.02 (dd, $^2J_{HH}$ = 15.0 Hz, $^3J_{HH}$ = 2.1 Hz, 1H, C-ring CH$_2$), 1.88 (td, $^3J_{HH}$ = 11.4, 8.6 Hz, 1H, C/D ring junction CH), 1.73-1.62 (m, 2H, B-ring CH$_2$, D-ring CH$_2$), 1.44 (s, 3H, A/B ring junction CH$_3$), 1.39 (ddd, $^2J_{HH}$ = 12.8 Hz, $^3J_{HH}$ = 8.4, 4.6 Hz, 1H, D-ring CH$_2$), 0.99 (s, 3H, C/D ring junction CH$_3$), 0.95 (d, $^3J_{HH}$ = 7.2 Hz, 3H, D-ring CH$_3$).

^{13}C{^{1}H} NMR (CDCl$_3$): δ$_C$ 203.0, 184.8, 163.8, 160.0 (d, $^2J_{CF}$ = 14.4 Hz), 150.8, 150.2, 134.3, 130.5, 127.9, 123.1, 121.2 (d, $^3J_{CF}$ = 11.6 Hz), 90.1, 85.7 (d, $^1J_{CF}$ = 181.2 Hz), 68.4, 65.3, 62.6, 49.0, 47.3, 43.2, (d, $^3J_{CF}$ = 5.4 Hz), 37.4 (d, $^2J_{CF}$ = 19.6 Hz), 35.0, 32.6 (d, $^4J_{CF}$ = 9.7 Hz), 32.5, 30.0, 22.9, 16.6, 13.9.

^{19}F NMR (CDCl$_3$): δ$_F$-184.0 (ddd, $^2J_{HF}$ = 49.4 Hz, $^3J_{HF}$ = 15.2, 10.5 Hz)

IR: 2941, 1742, 1722, 1665, 1624, 1528, 1344, 1275, 1121, 1107, 1074 cm^{-1}.

HPLC: t_R 3.329 min,

m/z (LC/MS MDAP ES+): t_R 15.05 min, [M-HF] calculated 519.2, observed 519.2 ([M-HF]).

M.P. (MeCN/Water) 227-228 °C (decomposition).

7. Computational Details

Calculations were carried out using Gaussian 09[232] software (Rev. D.01) on the Archie-West HPC at the University of Strathclyde.[233] All calculations used the SMD solvent model (acetonitrile solvation). Calculations were carried out without symmetry constraints. The nature of all stationary points was confirmed using frequency calculations.

8. Appendix

8.1. ^{1}H and ^{19}F NMR Spectra of Compound 102

Compound **102** 400.03 MHz ^{1}H
NMR spectrum CDCl$_3$

Compound **102** 376.46 MHz ^{19}F
NMR spectrum CDCl$_3$

8.2. ^{1}H and 1^{9}F NMR Spectra for Compound 107-ax

Compound **107-ax** 400.13 MHz ^{1}H
NMR spectrum CDCl$_3$

Compound **107-ax** 376.46 MHz
^{19}F NMR spectrum CDCl$_3$
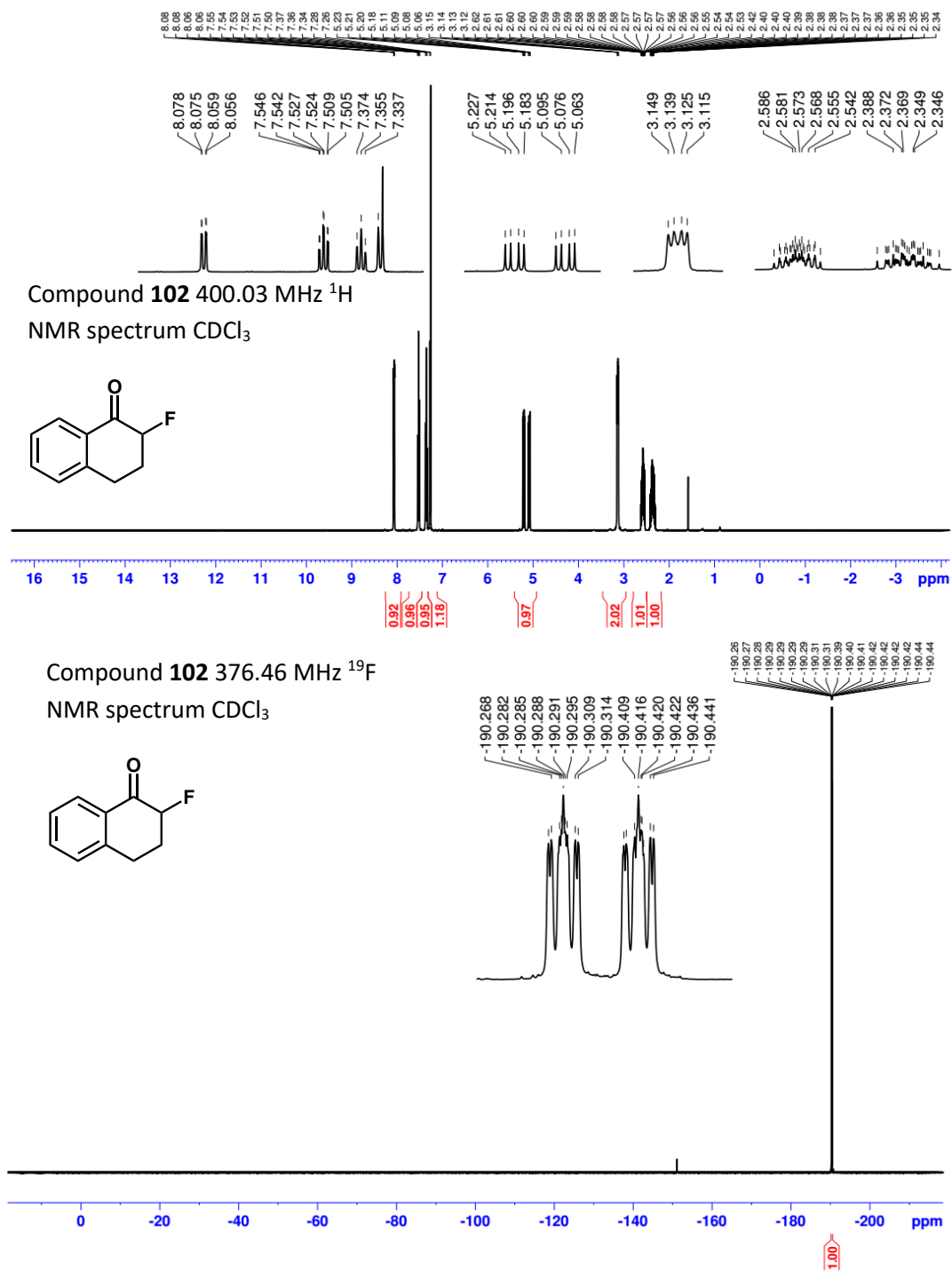
8.3. ^{1}H and ^{19}F NMR Spectra for Compound 107-eq

Compound **107-eq** 400.13 MHz
^{1}H NMR spectrum CDCl$_3$
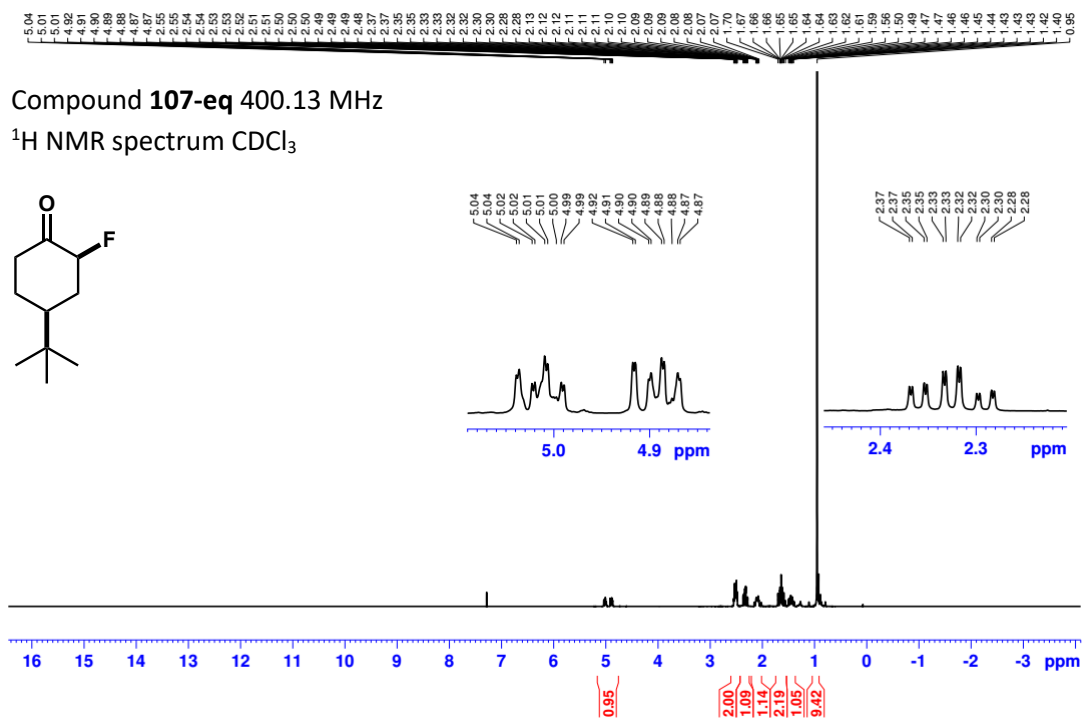
Compound **107-eq** 376.46 MHz
^{19}F NMR spectrum CDCl$_3$
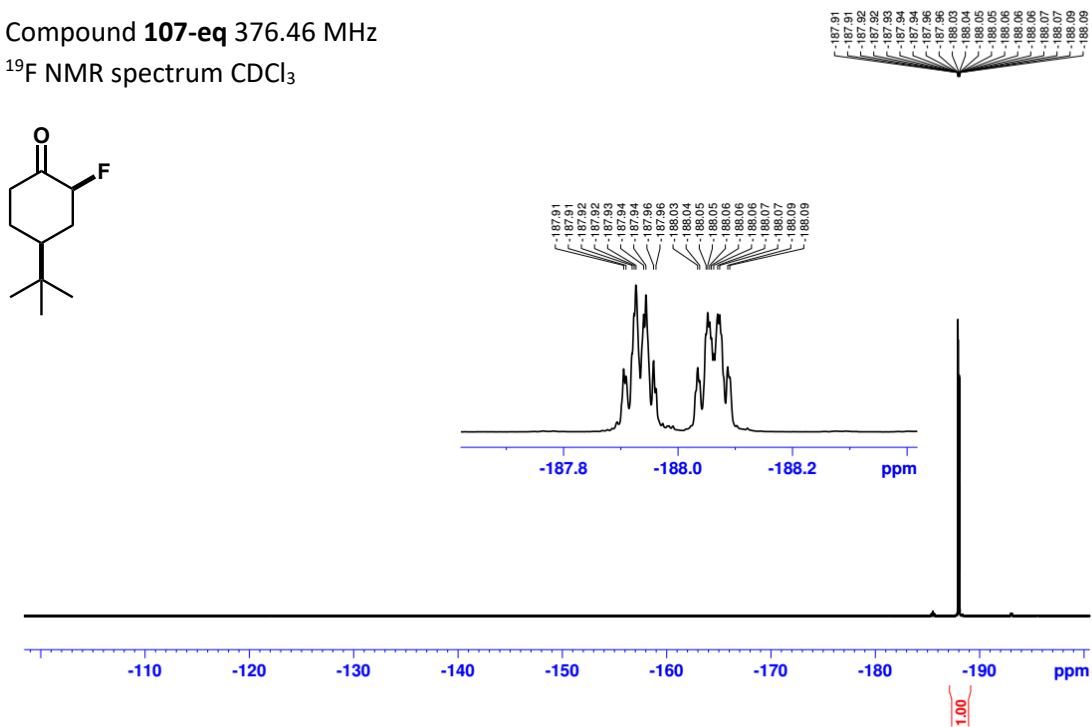
8.4. ^{1}H and ^{19}F NMR Spectra for Compound 117

Compound **117** 400.13 MHz ^{1}H
NMR spectrum CDCl$_3$

Compound **117** 376.46 MHz ^{19}F
NMR spectrum CDCl$_3$

8.5. ^{1}H and ^{19}F NMR Spectra for Compound 120a

Compound **120a** 400.13 MHz ^{1}H
NMR spectrum CDCl$_3$

Compound **120a** 376.46 MHz ^{19}F
NMR spectrum CDCl$_3$

8.6. ^{1}H and ^{19}F NMR Spectra for Compound β-151

Compound **β-151** 400.13 MHz ^{1}H NMR spectrum CDCl$_3$

Compound **β-151** 376.46 MHz ^{19}F NMR spectrum CDCl$_3$

Compound α-151 400.13 MHz ^{1}H
NMR spectrum CDCl₃
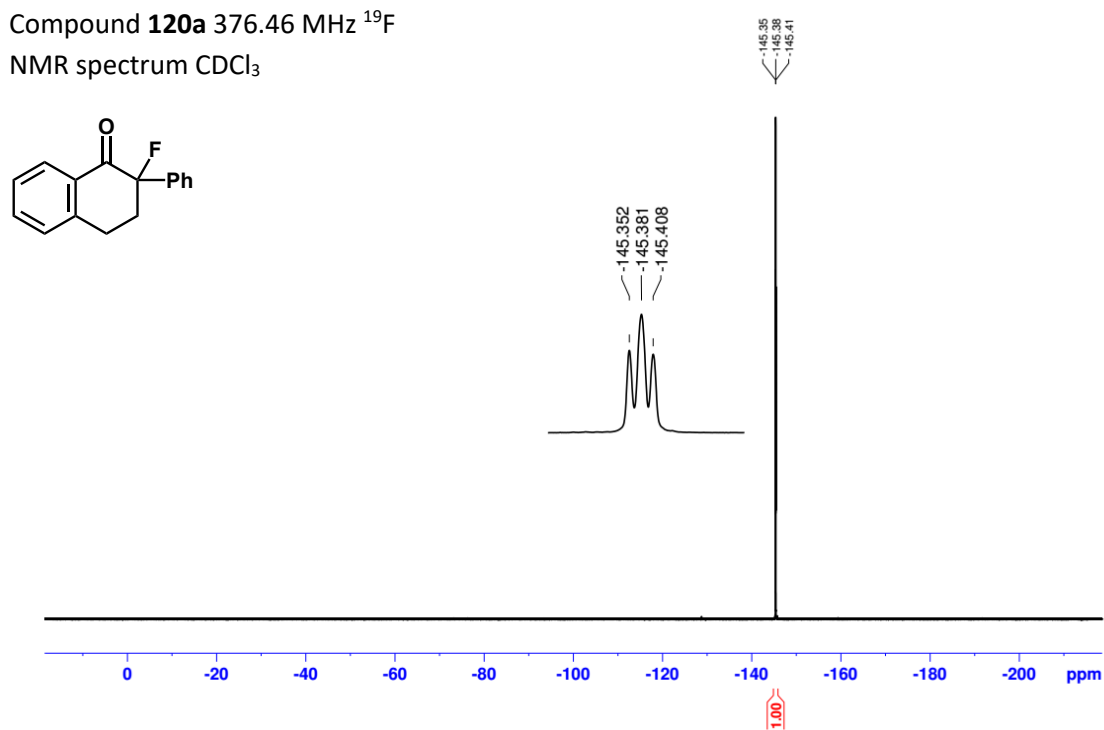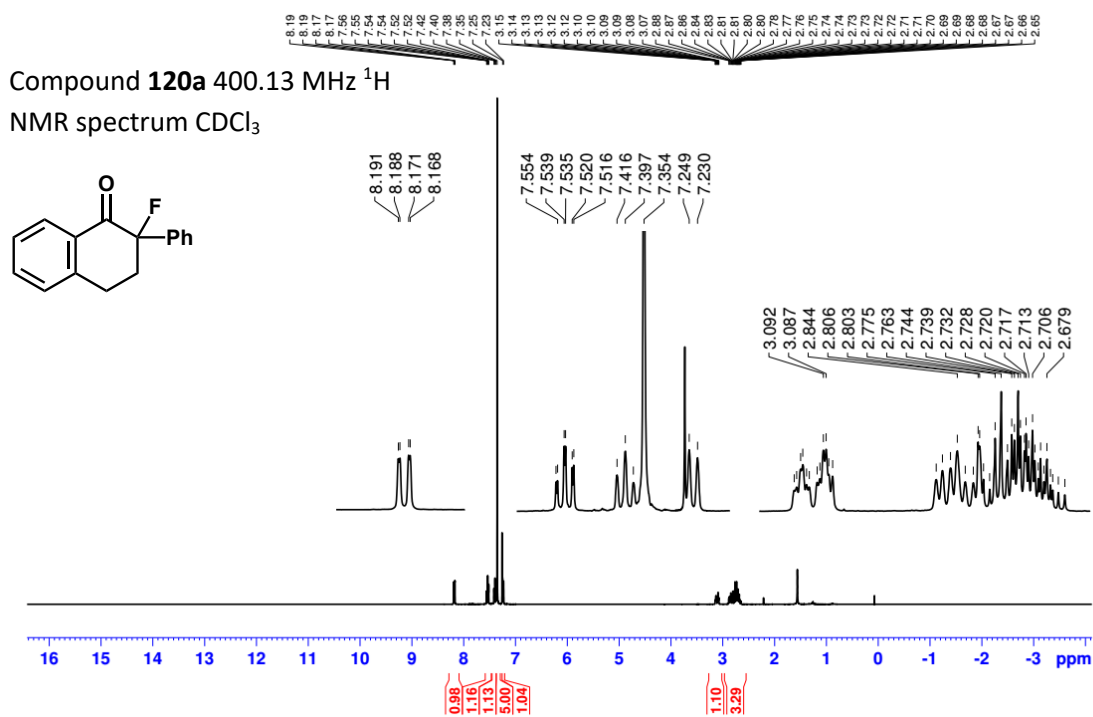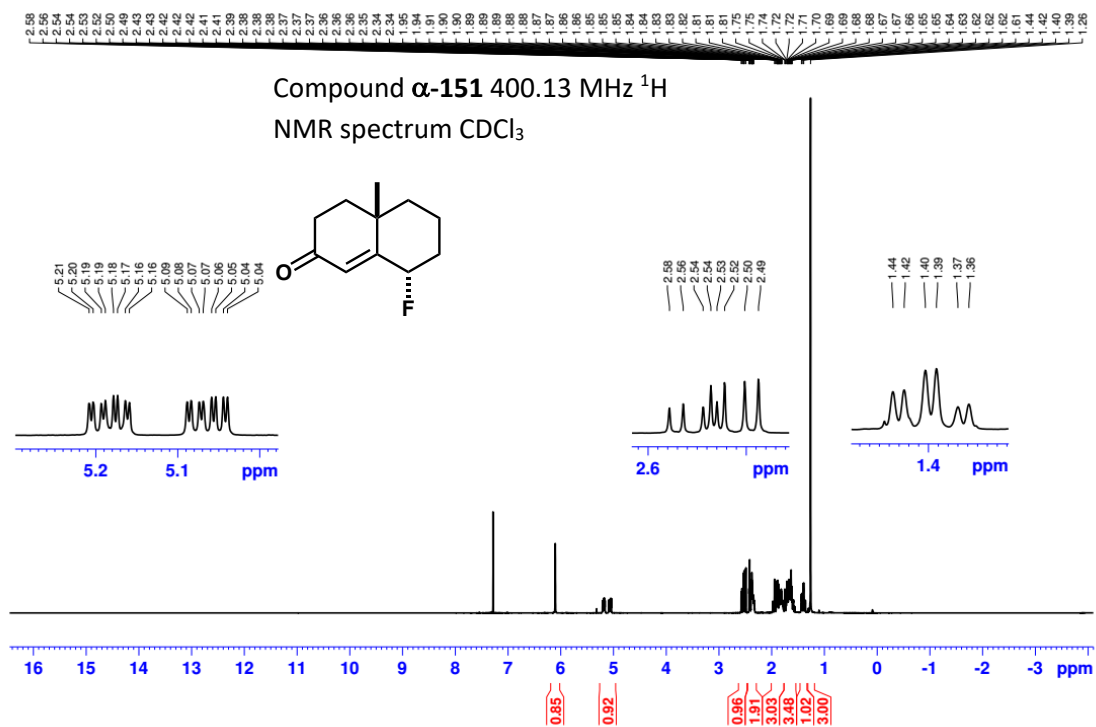
Compound α-151 376.46 MHz ^{19}F
NMR spectrum CDCl₃

8.8.   ¹H and ¹⁹F NMR Spectra for Compound 6α-99

Compound **6α-99** 400.13 MHz ¹H NMR spectrum CDCl₃

Compound **6α-99** 470.54 MHz ¹⁹F NMR spectrum CDCl₃

8.9.   ¹H and ¹⁹F NMR Spectra for Compound 6β-99

Compound **6β-99** 400.03 MHz ¹H NMR spectrum CDCl₃
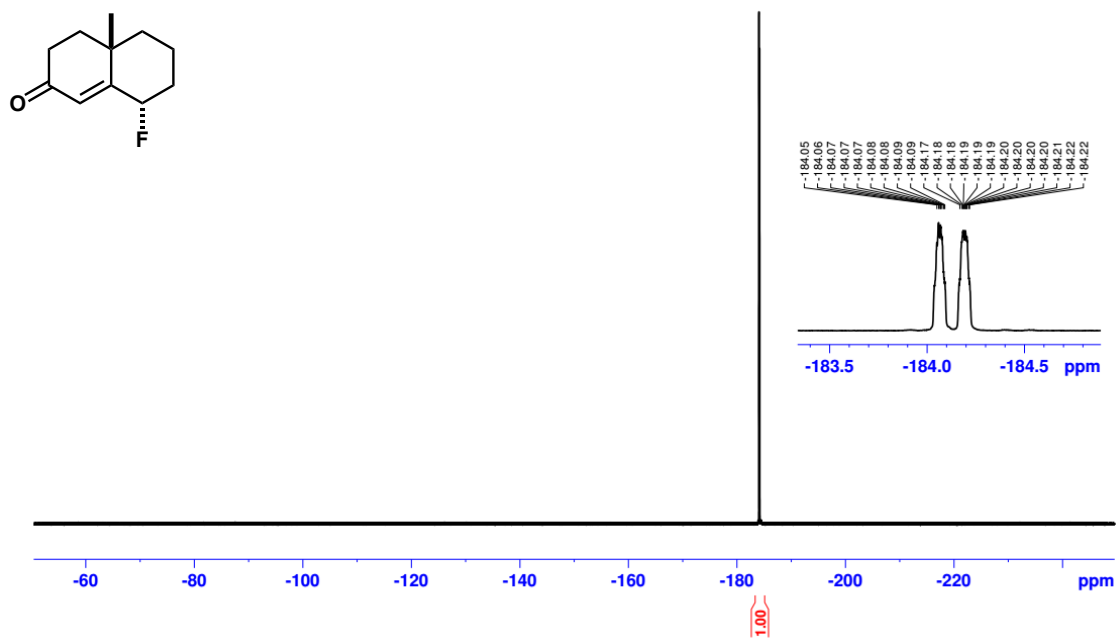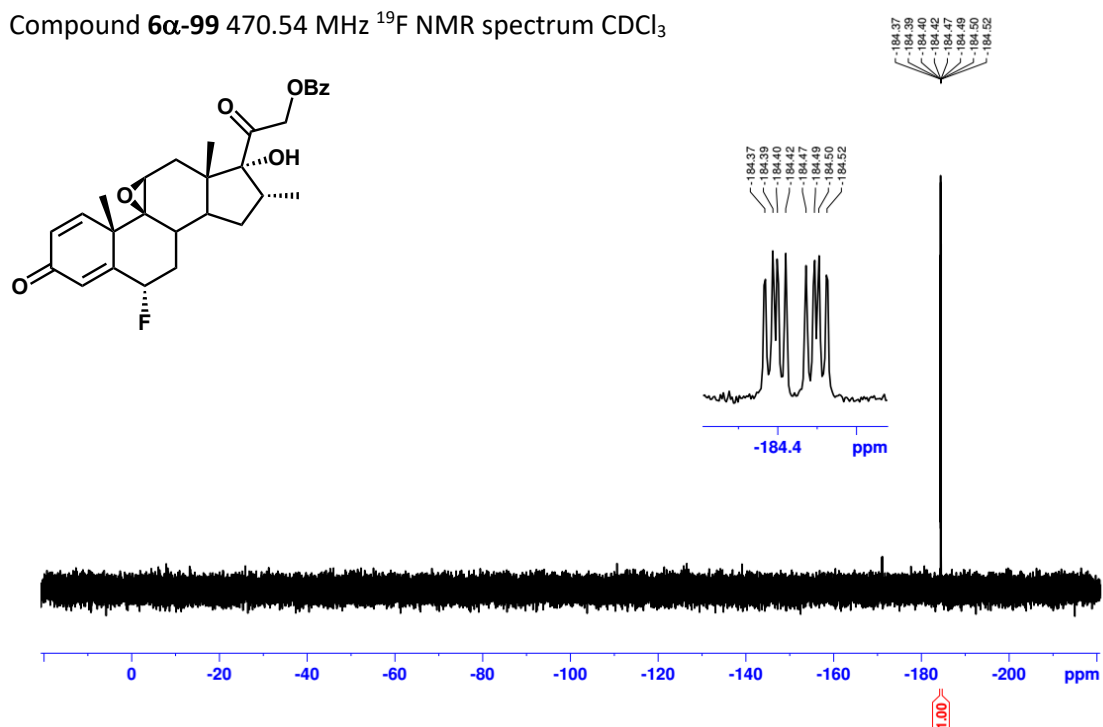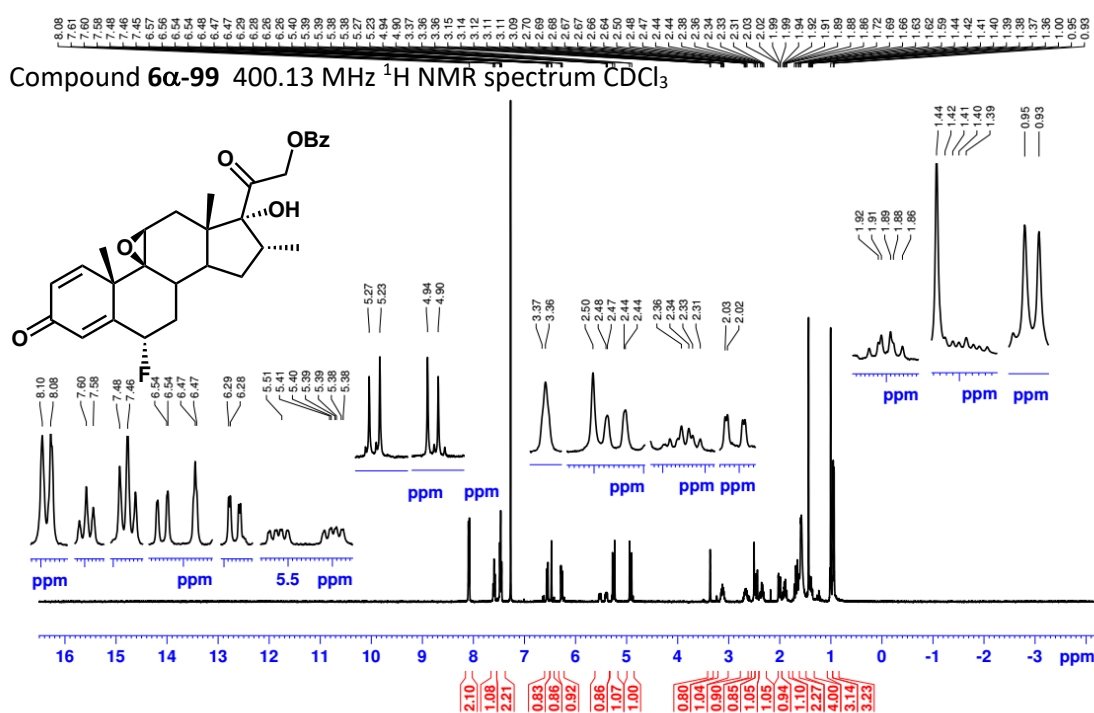
Compound **6β-99** 470.54 MHz ¹⁹F NMR spectrum CDCl₃
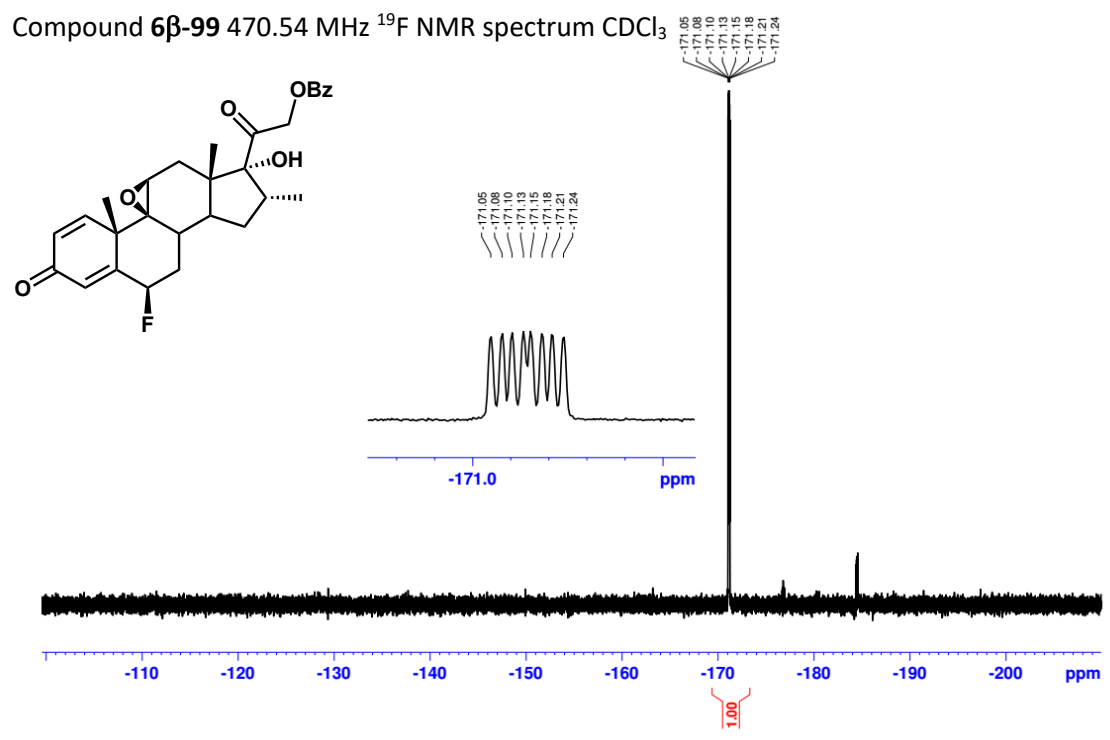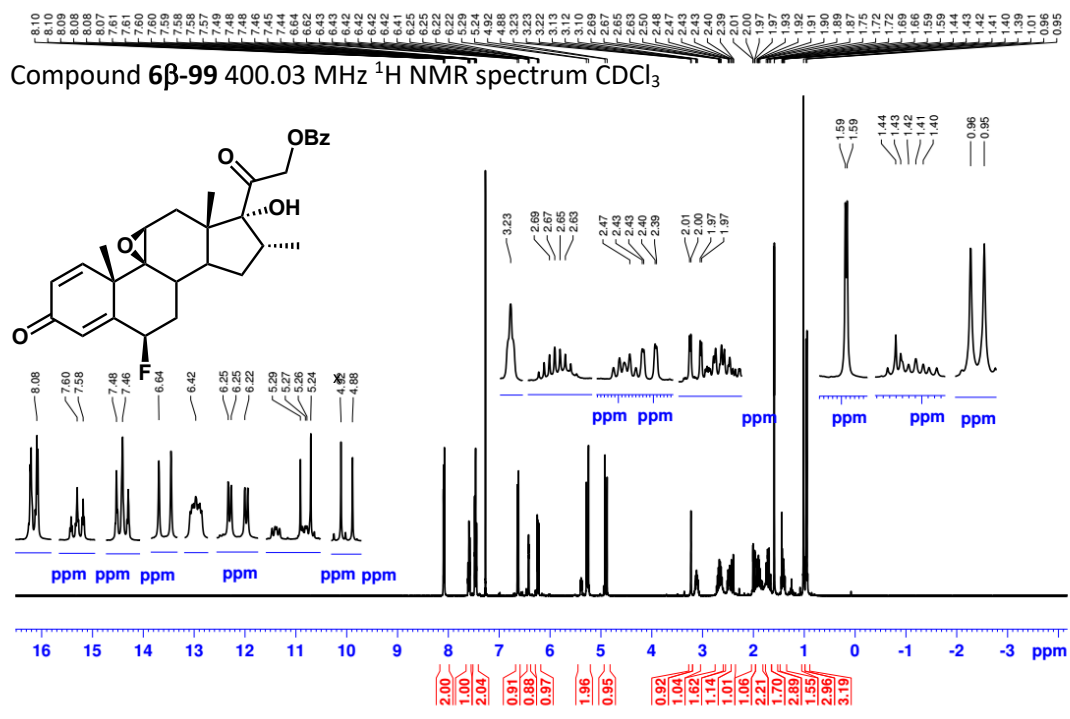
8.10. ^{19}F NMR Spectrum of Pure Isolated 138a

Compound **138a** 376.46 MHz ^{19}F
NMR spectrum CDCl$_3$
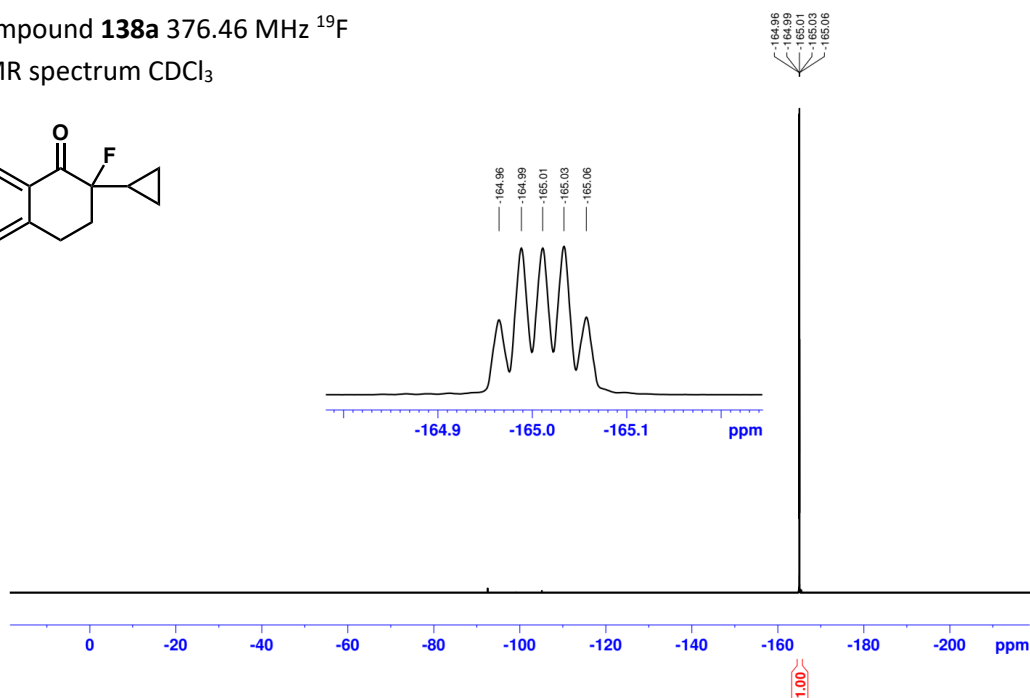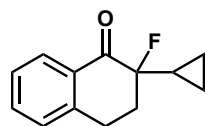
8.11. ^{19}F NMR Spectrum of Sample of 138a in CDCl$_3$ after 3 weeks
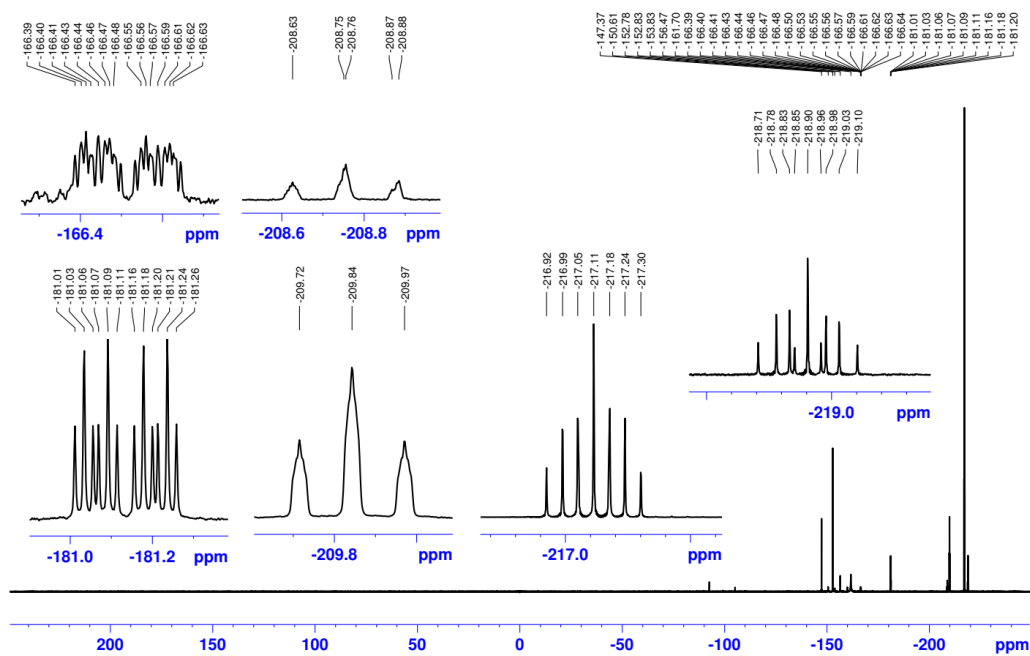
Compound **138a** sample after 3 weeks 376.46 MHz ^{19}F NMR spectrum CDCl$_3$

8.12. Crude ¹H NMR Spectrum of Attempted Synthesis of 148 using Benzoyl Chloride in Pyridine

Compound **148** crude reaction mixture 400.13 MHz ¹H NMR spectrum CDCl₃
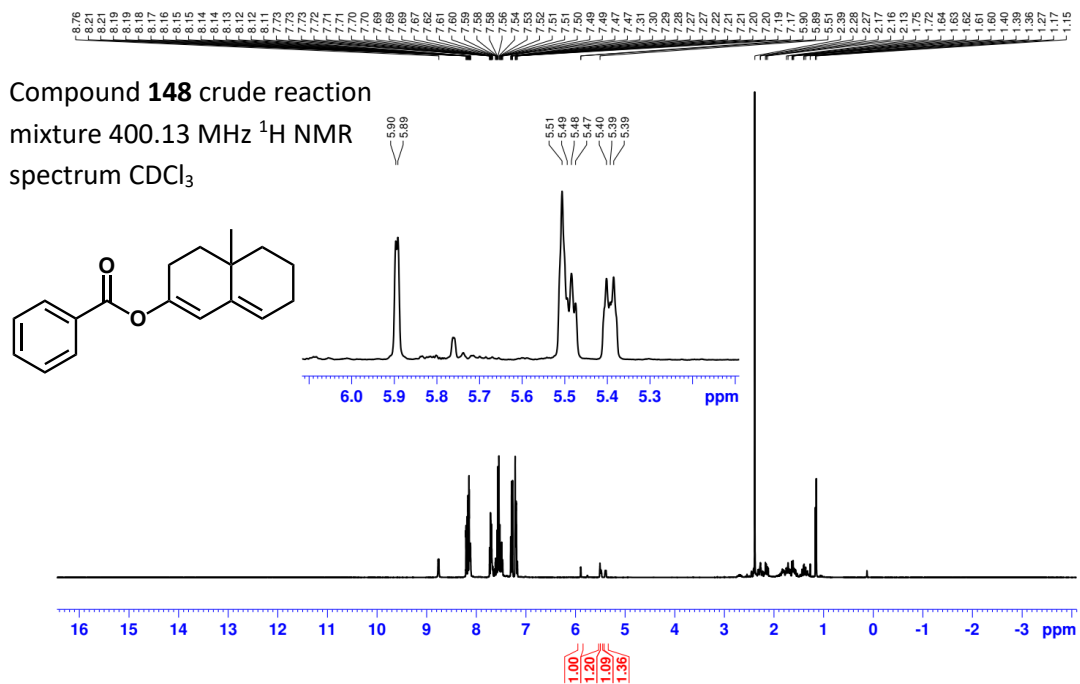
8.13. ¹H NMR Spectrum of Isolated 148

Compound **148** 400.13 MHz ¹H NMR spectrum CDCl₃
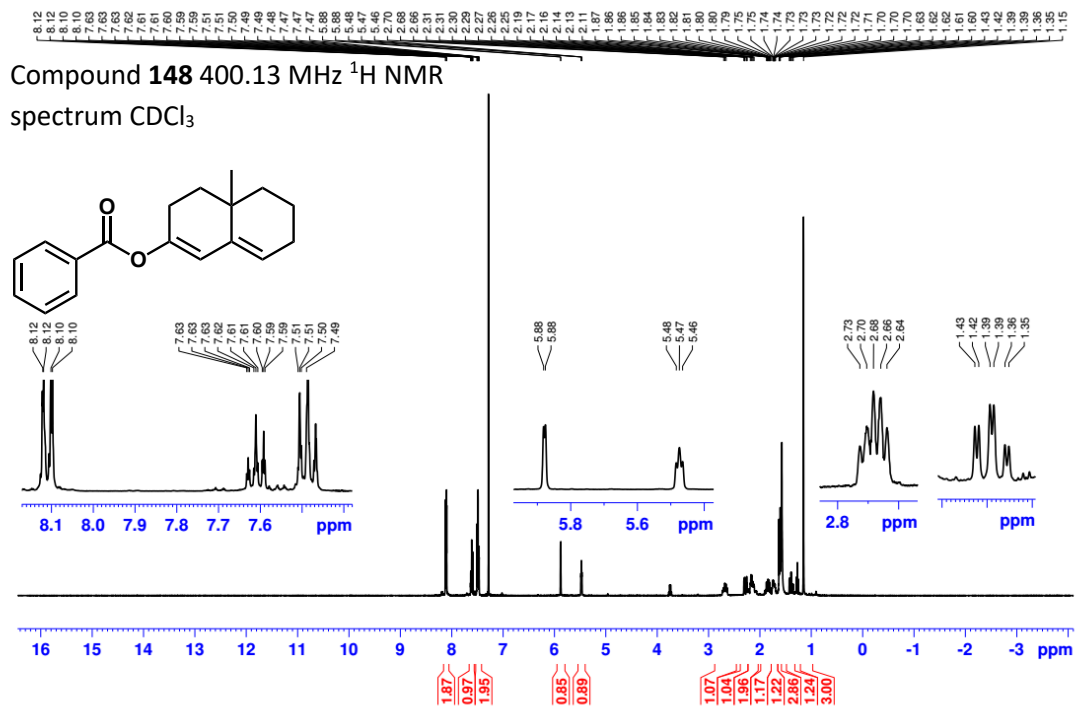
8.14. Crude ^{1}H NMR Spectrum of Attempted Synthesis of 156

Compound **156** crude reaction mixture 400.13 MHz ^{1}H NMR spectrum CDCl$_3$
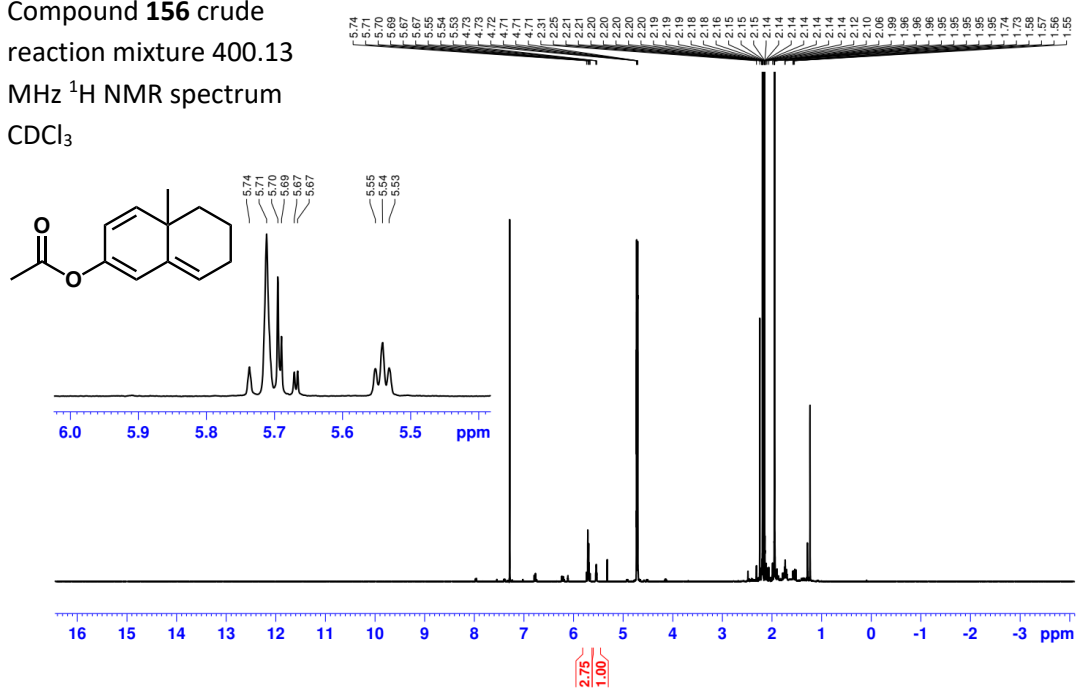
8.15. Crude ^{1}H NMR Spectrum of Attempted Synthesis of 157

Compound **157** crude reaction mixture 400.13 MHz ^{1}H NMR spectrum CDCl$_3$
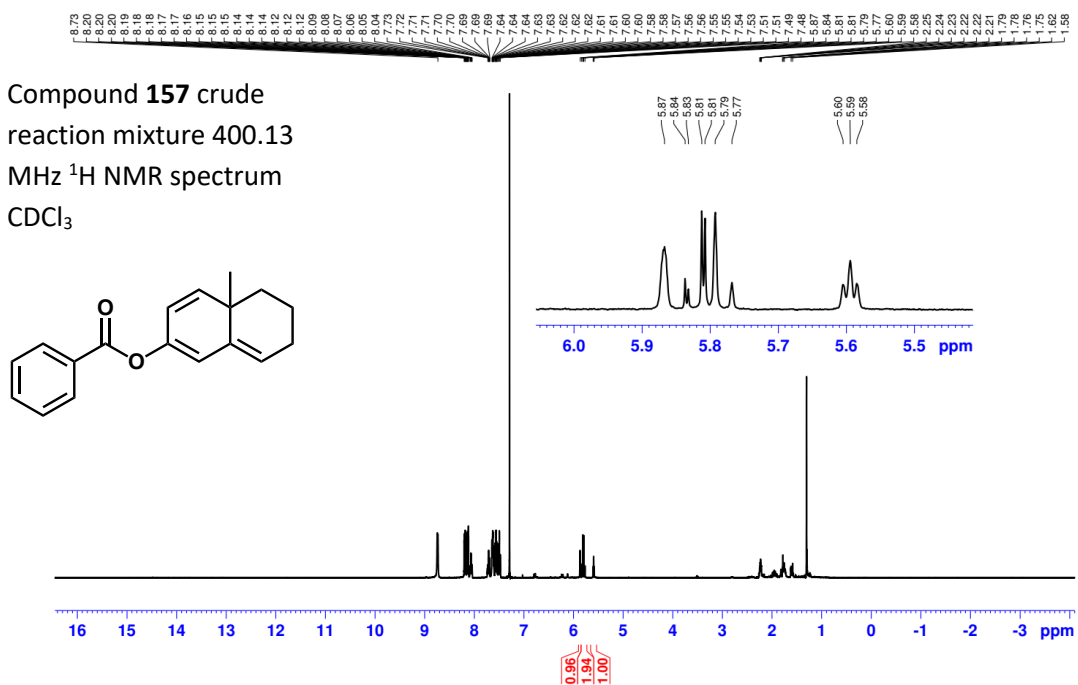
8.16. Representative ^{1}H NMR Kinetic Spectra for the Fluorination of Compound 100

t = 0 s

t = 120 s

t = 6210 s
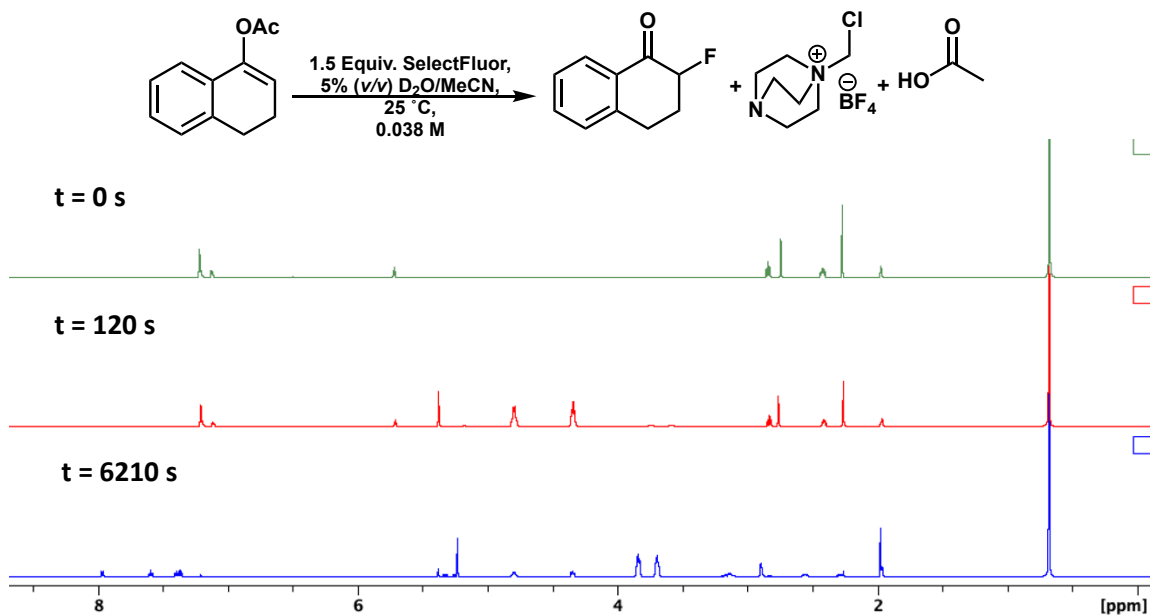
8.17. Representative ^{1}H NMR Kinetic Spectra for the Fluorination of Compound 108

t = 0 s

t = 120 s

t = 6000 s
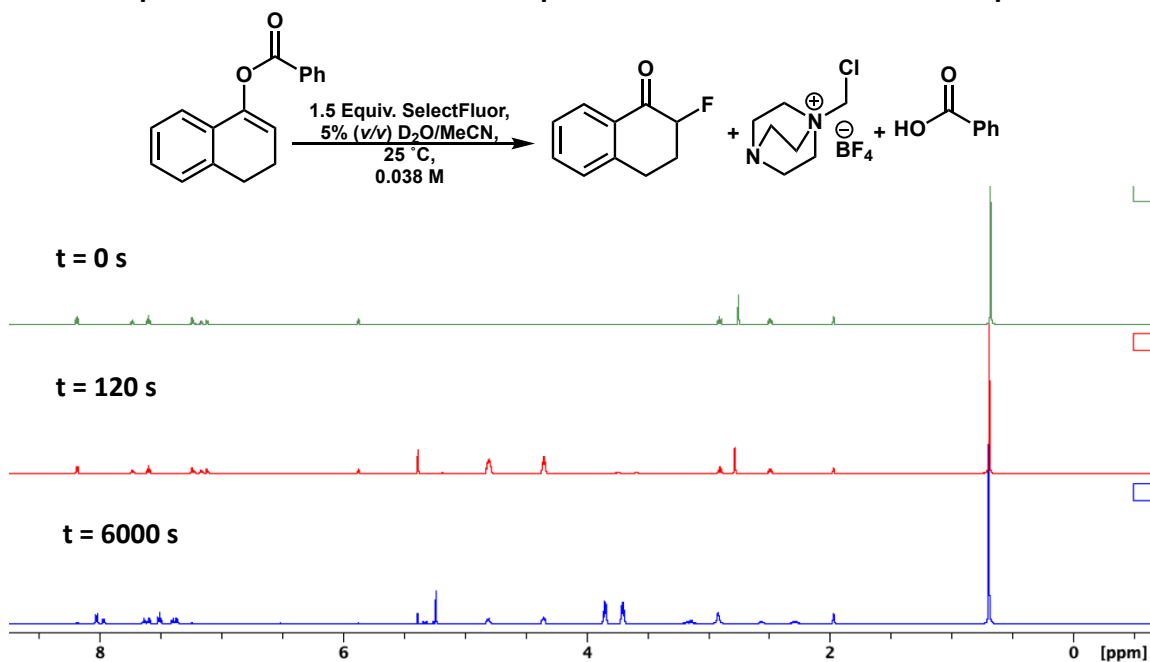
8.18. Representative ^{1}H NMR Kinetic Spectra for the Fluorination of Compound 120
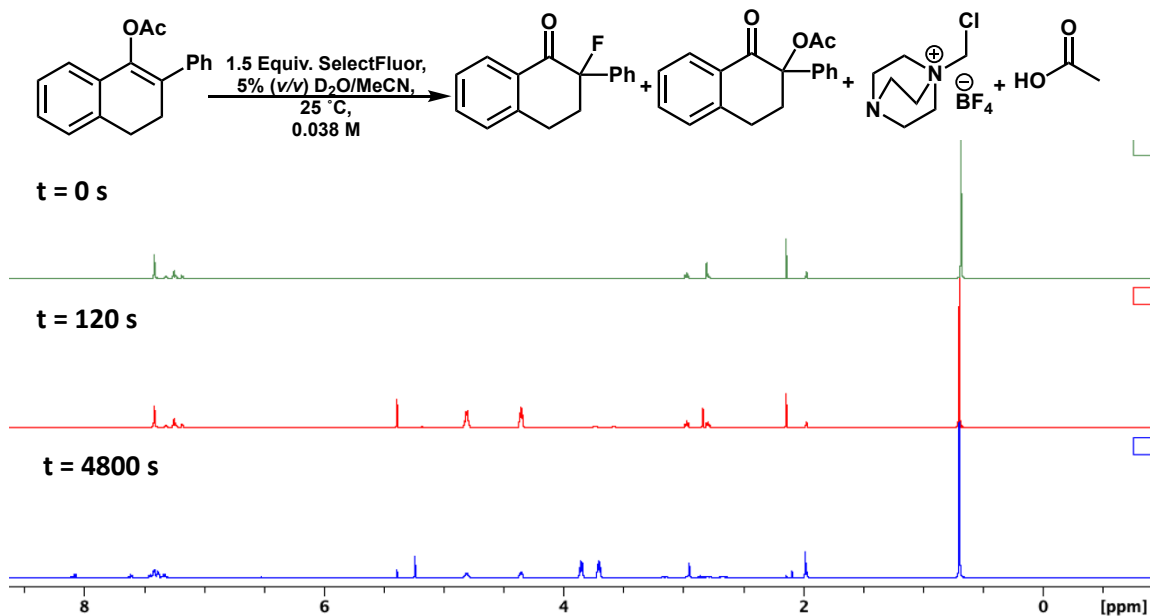
8.19. X-Ray Crystal Data for Compound 117

Table 1. Crystal data and structure refinement for nelson_wood.

Identification code	nelson_wood
Empirical formula	$C_{10}H_8BrFO$
Formula weight	243.07
Temperature	173(2) K
Wavelength	0.71073 Å
Crystal system	Monoclinic
Space group	P 2$_1$/c
Unit cell dimensions	a = 8.6420(4) Å α= 90°.
	b = 18.2587(8) Å β= 109.483(5)°.
	c = 6.0825(3) Å γ = 90°.
Volume	904.81(8) Å^3
Z	4
Density (calculated)	1.784 Mg/m^3
Absorption coefficient	4.511 mm^{-1}

F(000)	480			
Crystal size	0.5 x 0.2 x 0.18 mm^3			
Theta range for data collection	3.352 to 27.494°.			
Index ranges	-11<=h<=10, -23<=k<=23, -7<=l<=6			
Reflections collected	4499			
Independent reflections	2069 [R(int) = 0.0236]			
Completeness to theta = 27.000°	99.8 %			
Absorption correction	Analytical			
Max. and min. transmission	0.53 and 0.19			
Refinement method	Full-matrix least-squares on F^2			
Data / restraints / parameters	2069 / 0 / 118			
Goodness-of-fit on F^2	1.021			
Final R indices [I>2sigma(I)]	R1 = 0.0355, wR2 = 0.0686			
R indices (all data)	R1 = 0.0531, wR2 = 0.0747			
Extinction coefficient	n/a			
Largest diff. peak and hole	0.533 and -0.504 e.Å^{-3}			

Atomic coordinates (x 10^4) and equivalent isotropic displacement parameters (Å^2 x 10^3) for nelson_wood. U(eq) is defined as one third of the trace of the orthogonalized U^{ij} tensor.

_____

	x	y	z	U(eq)
Br(1)	1904(1)	205(1)	-1303(1)	43(1)
F(1)	315(2)	1452(1)	-1018(3)	42(1)
O(1)	2638(2)	1995(1)	-2445(3)	34(1)
C(1)	1852(3)	1182(2)	50(4)	27(1)
C(2)	3089(3)	1622(1)	-694(4)	23(1)
C(3)	4815(3)	1562(1)	853(4)	22(1)
C(4)	5230(3)	1220(1)	3034(4)	22(1)
C(5)	3945(3)	863(2)	3851(4)	28(1)
C(6)	2222(3)	1146(2)	2629(4)	27(1)
C(7)	6035(3)	1870(2)	108(4)	26(1)

C(8)	7646(3)	1842(2)	1504(5)	32(1)
C(9)	8066(3)	1512(2)	3677(5)	31(1)
C(10)	6872(3)	1210(2)	4437(5)	29(1)

Bond lengths [Å] and angles [°] for nelson_wood.

_____

Br(1)-C(1)	1.972(3)
F(1)-C(1)	1.361(3)
O(1)-C(2)	1.213(3)
C(1)-C(6)	1.495(3)
C(1)-C(2)	1.522(4)
C(2)-C(3)	1.478(3)
C(3)-C(7)	1.397(4)
C(3)-C(4)	1.401(3)
C(4)-C(10)	1.391(4)
C(4)-C(5)	1.509(4)
C(5)-C(6)	1.516(4)
C(5)-H(5A)	0.9900
C(5)-H(5B)	0.9900
C(6)-H(6A)	0.9900
C(6)-H(6B)	0.9900
C(7)-C(8)	1.369(4)
C(7)-H(7)	0.9500
C(8)-C(9)	1.386(4)
C(8)-H(8)	0.9500
C(9)-C(10)	1.380(4)
C(9)-H(9)	0.9500
C(10)-H(10)	0.9500
F(1)-C(1)-C(6)	110.5(2)
F(1)-C(1)-C(2)	109.8(2)
C(6)-C(1)-C(2)	114.2(2)
F(1)-C(1)-Br(1)	106.40(17)
C(6)-C(1)-Br(1)	111.77(19)

C(2)-C(1)-Br(1)	103.73(16)
O(1)-C(2)-C(3)	124.1(2)
O(1)-C(2)-C(1)	120.3(2)
C(3)-C(2)-C(1)	115.6(2)
C(7)-C(3)-C(4)	120.3(2)
C(7)-C(3)-C(2)	118.3(2)
C(4)-C(3)-C(2)	121.4(2)
C(10)-C(4)-C(3)	118.3(2)
C(10)-C(4)-C(5)	120.3(2)
C(3)-C(4)-C(5)	121.4(2)
C(4)-C(5)-C(6)	113.7(2)
C(4)-C(5)-H(5A)	108.8
C(6)-C(5)-H(5A)	108.8
C(4)-C(5)-H(5B)	108.8
C(6)-C(5)-H(5B)	108.8
H(5A)-C(5)-H(5B)	107.7
C(1)-C(6)-C(5)	111.2(2)
C(1)-C(6)-H(6A)	109.4
C(5)-C(6)-H(6A)	109.4
C(1)-C(6)-H(6B)	109.4
C(5)-C(6)-H(6B)	109.4
H(6A)-C(6)-H(6B)	108.0
C(8)-C(7)-C(3)	120.3(2)
C(8)-C(7)-H(7)	119.8
C(3)-C(7)-H(7)	119.8
C(7)-C(8)-C(9)	119.8(3)
C(7)-C(8)-H(8)	120.1
C(9)-C(8)-H(8)	120.1
C(10)-C(9)-C(8)	120.4(3)
C(10)-C(9)-H(9)	119.8
C(8)-C(9)-H(9)	119.8
C(9)-C(10)-C(4)	120.9(2)
C(9)-C(10)-H(10)	119.6
C(4)-C(10)-H(10)	119.6

Symmetry transformations used to generate equivalent atoms:

Anisotropic displacement parameters (Å^2 x 10^3)for nelson_wood. The anisotropic displacement factor exponent takes the form: $-2\pi^2$ [h^2 a^{*2} U^{11} + ... + 2 h k a* b* U^{12}]

	U^{11}	U^{22}	U^{33}	U^{23}	U^{13}	U^{12}
Br(1)	48(1)	39(1)	46(1)	-19(1)	21(1)	-15(1)
F(1)	22(1)	69(1)	32(1)	-1(1)	5(1)	10(1)
O(1)	39(1)	39(1)	19(1)	5(1)	5(1)	5(1)
C(1)	22(1)	33(2)	25(1)	-5(1)	6(1)	4(1)
C(2)	30(1)	22(1)	18(1)	-5(1)	8(1)	3(1)
C(3)	26(1)	20(1)	19(1)	-3(1)	7(1)	2(1)
C(4)	26(1)	21(1)	20(1)	-1(1)	7(1)	4(1)
C(5)	30(2)	29(2)	26(1)	6(1)	10(1)	1(1)
C(6)	28(1)	31(2)	25(1)	0(1)	13(1)	2(1)
C(7)	32(2)	28(2)	22(1)	0(1)	13(1)	5(1)
C(8)	29(2)	31(2)	41(2)	0(1)	20(1)	2(1)
C(9)	24(1)	32(2)	32(2)	-3(1)	6(1)	5(1)
C(10)	31(2)	29(2)	24(1)	2(1)	8(1)	8(1)

Hydrogen coordinates (x 10^4) and isotropic displacement parameters (Å^2x 10^3) for nelson_wood.

	x	y	z	U(eq)
H(5A)	4231	945	5549	34

H(5B)	3962	328	3592	34
H(6A)	1420	819	2978	33
H(6B)	2108	1640	3227	33
H(7)	5745	2100	-1375	32
H(8)	8474	2047	985	38
H(9)	9184	1495	4649	37
H(10)	7175	991	5939	34

Torsion angles [°] for nelson_wood.

_____

F(1)-C(1)-C(2)-O(1)	-18.8(3)
C(6)-C(1)-C(2)-O(1)	-143.5(3)
Br(1)-C(1)-C(2)-O(1)	94.6(2)
F(1)-C(1)-C(2)-C(3)	160.7(2)
C(6)-C(1)-C(2)-C(3)	36.0(3)
Br(1)-C(1)-C(2)-C(3)	-85.9(2)
O(1)-C(2)-C(3)-C(7)	-9.1(4)
C(1)-C(2)-C(3)-C(7)	171.4(2)
O(1)-C(2)-C(3)-C(4)	169.7(2)
C(1)-C(2)-C(3)-C(4)	-9.8(3)
C(7)-C(3)-C(4)-C(10)	1.3(4)
C(2)-C(3)-C(4)-C(10)	-177.5(2)
C(7)-C(3)-C(4)-C(5)	-178.1(2)
C(2)-C(3)-C(4)-C(5)	3.2(4)
C(10)-C(4)-C(5)-C(6)	158.8(2)
C(3)-C(4)-C(5)-C(6)	-21.9(4)
F(1)-C(1)-C(6)-C(5)	-178.7(2)
C(2)-C(1)-C(6)-C(5)	-54.4(3)
Br(1)-C(1)-C(6)-C(5)	63.0(3)
C(4)-C(5)-C(6)-C(1)	46.6(3)
C(4)-C(3)-C(7)-C(8)	-0.2(4)
C(2)-C(3)-C(7)-C(8)	178.6(2)
C(3)-C(7)-C(8)-C(9)	-0.6(4)
C(7)-C(8)-C(9)-C(10)	0.3(4)

C(8)-C(9)-C(10)-C(4)	0.8(4)
C(3)-C(4)-C(10)-C(9)	-1.6(4)
C(5)-C(4)-C(10)-C(9)	177.8(3)

9.   References

1   World Health Organisation Essential Medicines List, http://www.who.int/medicines/publications/essentialmedicines/en/ (accessed October 2018).

2   Y. Zhou, J. Wang, Z. Gu, S. Wang, W. Zhu, J. L. Aceña, V. A. Soloshonok, K. Izawa and H. Liu, *Chem. Rev.*, 2016, **116**, 422–518.

3   N. A. McGrath, M. Brichacek and J. T. Njardarson, *J. Chem. Educ.*, 2010, **87**, 1348–1349.

4   E. A. Ilardi, E. Vitaku and J. T. Njardarson, *J. Med. Chem.*, 2014, **57**, 2832–2842.

5   ChEMBL, https://www.ebi.ac.uk/chembl/drugstore, (accessed October 2018).

6   M. Stefek, V. Snirc, P. O. Djoubissie, M. Majekova, V. Demopoulos, L. Rackova, Z. Bezakova, C. Karasu, V. Carbone and O. El-Kabbani, *Bioorg. Med. Chem.*, 2008, **16**, 4908–4920.

7   A. Kaptein, A. Oubrie, E. De Zwart, N. Hoogenboom, J. De Wit, B. Van De Kar, M. Van Hoek, G. Vogel, V. De Kimpe, C. Schultz-Fademrecht, J. Borsboom, M. Van Zeeland, J. Versteegh, B. Kazemier, J. De Roos, F. Wijnands, J. Dulos, M. Jaeger, P. Leandro-Garcia and T. Barf, *Bioorg. Med. Chem. Lett.*, 2011, **21**, 3823–3827.

8   Z. Li, S. Rao, J. R. Gever, K. Widjaja, S. B. Prusiner and B. M. Silber, *ACS Med. Chem. Lett.*, 2013, **4**, 647–650.

9   M. Morgenthaler, E. Schweizer, A. Hoffmann-Röder, F. Benini, R. E. Martin, G.

Jaeschke, B. Wagner, H. Fischer, S. Bendels, D. Zimmerli, J. Schneider, F. Diederich, M. Kansy and K. Müller, *ChemMedChem*, 2007, **2**, 1100–1115.

10   C. Jamieson, E. M. Moir, Z. Rankovic and G. Wishart, *J. Med. Chem.*, 2006, **49**, 5029–5046.

11   J. J. Matasi, J. P. Caldwell, H. Zhang, A. Fawzi, G. A. Higgins, M. E. Cohen-Williams, G. B. Varty and D. B. Tulshian, *Bioorg. Med. Chem. Lett.*, 2005, **15**, 3675–3678.

12   Y. J. Choi, J. H. Seo and K. J. Shin, *Bioorg. Med. Chem. Lett.*, 2014, **24**, 880–883.

13   P. Kirsch, *Modern Fluoroorganic Chemistry: Synthesis, Reactivity, Applications*, Ed. 2, Wiley-VCH, Weinheim, 2013.

14   H. H. Jensen, L. Lyngbye, A. Jensen and M. Bols, *Chem. Eur. J.*, 2002, **8**, 1218–1226.

15   D. C. Lankin, N. S. Chandrakumar, S. N. Rao, D. P. Spangler and J. P. Snyder, *J. Am. Chem. Soc.*, 1993, **115**, 3356–3357.

16   A. Sun, D. C. Lankin, K. Hardcastle and J. P. Snyder, *Chem. Eur. J.*, 2005, **11**, 1579–1591.

17   M. B. Van Niel, I. Collins, M. S. Beer, H. B. Broughton, S. K. F. Cheng, S. C. Goodacre, A. Heald, K. L. Locker, A. M. MacLeod, D. Morrison, C. R. Moyes, D. O'Connor, A. Pike, M. Rowley, M. G. N. Russell, B. Sohal, J. A. Stanton, S. Thomas, H. Verrier, A. P. Watt and J. L. Castro, *J. Med. Chem.*, 1999, **42**, 2087–2104.

18   C. D. Cox, P. J. Coleman, M. J. Breslin, D. B. Whitman, R. M. Garbaccio, M. E. Fraley, C. A. Buser, E. S. Walsh, K. Hamilton, M. D. Schaber, R. B. Lobell, W. Tao, J. P. Davide, R. E. Diehl, M. T. Abrams, V. J. South, H. E. Huber, M. Torrent, T. Prueksaritanont, C. Li, D. E. Slaughter, E. Mahan, C. Fernandez-Metzler, Y. Yan, L. C. Kuo, N. E. Kohl and G. D. Hartman, *J. Med. Chem.*, 2008, **51**, 4239–4252.

19   B. Hulin, S. Cabral, M. G. Lopaze, M. A. Van Volkenburg, K. M. Andrews and J. C. Parker, *Bioorganic Med. Chem. Lett.*, 2005, **15**, 4770–4773.

20   H.-J. Böhm, D. Banner, S. Bendels, M. Kansy, B. Kuhn, K. Müller, U. Obst-Sander and M. Stahl, *ChemBioChem*, 2004, **5**, 637–43.

21   R. Vogel, F. Siebert, E. C. Y. Yan, T. P. Sakmar, A. Hirshfeld and M. Sheves, *J. Am. Chem. Soc.*, 2006, **128**, 10503–10512.

22   T. H. Maren and C. W. Conroy, *J. Biol. Chem.*, 1993, **268**, 26233–26239.

23   D. O'Hagan, *Chem. Soc. Rev.*, 2008, **37**, 308–19.

24   J. W. Banks, A. S. Batsanov, J. A. K. Howard, D. O'Hagan, H. S. Rzepa and S. Martin-Santamaria, *J. Chem. Soc. Perkin Trans. 2*, 1999, 2409–2411.

25   B. J. van der Veken, S. Truyen, W. A. Herrebout and G. Watkins, *J. Mol. Struct.*, 1993, **293**, 55–58.

26   R. J. Abraham, A. D. Jones, M. A. Warne, R. Rittner and C. F. Tormena, *J. Chem. Soc. Perkin Trans. 2*, 1996, 533–539.

27   H. V. Phan and J. R. Durig, *J. Mol. Struct. Theochem*, 1990, **209**, 333–347.

28   Y. Sasaki, A. Niida, T. Tsuji, A. Shigenaga, N. Fujii and A. Otaka, *J. Org. Chem.*, 2006, **71**, 4969–4979.

29   S. Couve-Bonnaire, D. Cahard and X. Pannecoucke, *Org. Biomol. Chem.*, 2007, **5**, 1151.

30   T. Allmendinger, P. Furet and E. Hungerbühler, *Tetrahedron Lett.*, 1990, **31**, 7297–7300.

31   T. Allmendinger, E. Felder and E. Hungarbühler, *Tetrahedron Lett.*, 1990, **31**, 7301–7304.

32   T. Allmendinger, C. Angst and H. Karfunkel, *J. Fluor. Chem.*, 1995, **72**, 247–253.

33   S. Couve-Bonnaire, D. Cahard and X. Pannecoucke, *Org. Biomol. Chem.*, 2007, **5**, 1151.

34   N. E. J. Gooseman, D. O'Hagan, M. J. G. Peach, A. M. Z. Slawin, D. J. Tozer and R. J. Young, *Angew. Chem. Int. Ed.*, 2007, **46**, 5904–5908.

35   I. Yamamoto, M. J. T. Jordan, N. Gavande, M. R. Doddareddy, M. Chebib and L. Hunter, *Chem. Commun.*, 2012, **48**, 829–831.

36   L. Hunter, S. Butler and S. B. Ludbrook, *Org. Biomol. Chem.*, 2012, **10**, 8911.

37   L. Hunter, K. A. Jolliffe, M. J. T. Jordan, P. Jensen and R. B. Macquart, *Chem. Eur. J.*, 2011, **17**, 2340–2343.

38   X.-G. Hu, D. S. Thomas, R. Griffith and L. Hunter, *Angew. Chem. Int. Ed.*, 2014, **53**, 6176–6179.

39   C. Ionescu and M. R. Caira, *Drug Metabolism: Current Concepts*, Springer, Dordrecht, 2005.

40   S. B. Rosenblum, T. Huynh, A. Afonso, H. R. Davis, N. Yumibe, J. W. Clader and D. A. Burnett, *J. Med. Chem.*, 1998, **41**, 973–980.

41   I. E. Bush and V. B. Mahesh, *Biochem. J.*, 1964, **93**, 236–55.

42   S. M. Abel, D. J. Back, J. L. Maggs and B. K. Park, *J. Steriod Biochem. Mol. Biol.*, 1993, **46**, 833–839.

43   T.-C. Chou, H. Dong, A. Rivkin, F. Yoshimura, A. E. Gabarda, Y. S. Cho, W. P. Tong and S. J. Danishefsky, *Angew. Chem. Int. Ed.*, 2003, **42**, 4762–4767.

44   L. Xing, D. C. Blakemore, A. Narayanan, R. Unwalla, F. Lovering, R. A. Denny, H. Zhou and M. E. Bunnage, *ChemMedChem*, 2015, **10**, 715–726.

45   J. Fried, D. K. Mitra, M. Nagarajan and M. M. Mehrotra, *J. Med. Chem.*, 1980, **23**, 234–237.

46   L. Li, J. Liu, L. Zhu, S. Cutler, H. Hasegawa, B. Shan and J. C. Medina, *Bioorg. Med. Chem. Lett.*, 2006, **16**, 1638–42.

47   M. W. Rowbottom, R. Faraoni, Q. Chao, B. T. Campbell, A. G. Lai, E. Setti, M. Ezawa, K. G. Sprankle, S. Abraham, L. Tran, B. Struss, M. Gibney, R. C. Armstrong, R. N. Gunawardane, R. R. Nepomuceno, I. Valenta, H. Hua, M. F. Gardner, M. D. Cramer, D. Gitnick, D. E. Insko, J. L. Apuy, S. Jones-Bolin, A. K. Ghose, T. Herbertz, M. A. Ator, B. D. Dorsey, B. Ruggeri, M. Williams, S. Bhagwat, J. James and M. W. Holladay, *J. Med. Chem.*, 2012, **55**, 1082–1105.

48   H. Sun, C. E. Keefer and D. O. Scott, *Drug Metab. Lett.*, 2011, **5**, 232–242.

49   S. S. Stokes, M. Gowravaram, H. Huynh, M. Lu, G. B. Mullen, B. Chen, R. Albert, T. J. O'Shea, M. T. Rooney, H. Hu, J. V. Newman and S. D. Mills, *Bioorg. Med. Chem. Lett.*, 2012, **22**, 85–89.

50   C. S. Burgey, K. A. Robinson, T. A. Lyle, P. G. Nantermet, H. G. Selnick, R. C. A. Isaacs, S. D. Lewis, B. J. Lucas, J. A. Krueger, R. Singh, C. Miller-Stein, R. B. White, B. Wong, E. A. Lyle, M. T. Stranieri, J. J. Cook, D. R. McMasters, J. M. Pellicore, S. Pal, A. A. Wallace, F. C. Clayton, D. Bohn, D. C. Welsh, J. J. Lynch, Y. Yan, Z. Chen, L. Kuo, S. J. Gardell, J. A. Shafer and J. P. Vacca, *Bioorg. Med. Chem. Lett.*, 2003, **13**, 1353–1357.

51   C. S. Burgey, K. A. Robinson, T. A. Lyle, P. E. J. Sanderson, S. D. Lewis, B. J. Lucas, J. A. Krueger, R. Singh, C. Miller-Stein, R. B. White, B. Wong, E. A. Lyle, P. D. Williams, C. A. Coburn, B. D. Dorsey, J. C. Barrow, M. T. Stranieri, M. A. Holahan, G. R. Sitko, J. J. Cook, D. R. McMasters, C. M. McDonough, W. M. Sanders, A. A. Wallace, F. C. Clayton, D. Bohn, Y. M. Leonard, T. J. Detwiler, J. J. Lynch, Y. Yan, Z.

Chen, L. Kuo, S. J. Gardell, J. A. Shafer and J. P. Vacca, *J. Med. Chem.*, 2003, **46**, 461–473.

52   D. A. Dixon and B. E. Smart, *J. Phys. Chem.*, 1991, **95**, 1609–1612.

53   J. A. K. Howard, V. J. Hoy, D. O'Hagan and G. T. Smith, *Tetrahedron*, 1996, **52**, 12613–12622.

54   M. Nishio, Y. Umezawa, M. Hirota and Y. Takeuchi, *Tetrahedron*, 1995, **51**, 8665–8701.

55   L. Kang, S. E. Novick, Q. Gou, L. Spada, M. Vallejo-Lopez and W. Caminati, *J. Mol. Spec.*, 2014, **297**, 32–34.

56   K. Müller, C. Faeh and F. Diederich, *Science*, 2007, **317**, 1881–1886.

57   R. Paulini, K. Müller and F. Diederich, *Angew. Chem. Int. Ed.*, 2005, **44**, 1788–1805.

58   D. Cantacuzene, K. L. Kirk, D. H. McCulloh and C. R. Creveling, *Science*, 1979, **204**, 1217–9.

59   T. Nose, Y. Shimohigashi, M. Ohno, T. Costa, N. Shimizu and Y. Ogino, *Biochem. Biophys. Res. Commun.*, 1993, **193**, 694–699.

60   A. Matsushima, T. Fujita, T. Nose and Y. Shimohigashi, *J. Biochem.*, 2000, **128**, 225–232.

61   M. B. V. Roberts, *Biology: A Functional Approach*, Ed. 3, Nelson, Cheltenham, 1986.

62   C. H. Yeh, K. Hogg and J. I. Weitz, *Arterioscler. Thromb. Vasc. Biol.*, 2015, **35**, 1056–1065.

63   J. A. Olsen, D. W. Banner, P. Seiler, B. Wagner, T. Tschopp, U. Obst-Sander, M.

Kansy, K. Müller and F. Diederich, *ChemBioChem*, 2004, **5**, 666–675.

64   O. Jacobson, D. O. Kiesewetter and X. Chen, *Bioconjug. Chem.*, 2015, **26**, 1–18.

65   O. Warburg, *Science*, 1956, **123**, 309–314.

66   S. Vallabhajosula, *Semin. Nucl. Med.*, 2007, **37**, 400–419.

67   C. Sioka, A. Fotopoulos and A. P. Kyritsis, *Eur. J. Nucl. Med. Mol. Imaging*, 2010, **37**, 1594–1603.

68   R. Y. Moore, A. L. Whone and D. J. Brooks, *Neurobiol. Dis.*, 2008, **29**, 381–390.

69   J. R. Barrio, S. C. Huang and M. E. Phelps, *Biochem Pharmacol*, 1997, **54**, 341–8.

70   D. Elmenhorst, P. T. Meyer, A. Matusch, O. H. Winz and A. Bauer, *J. Nucl. Med.*, 2012, **53**, 1723–9.

71   J. Fried and E. F. Sabo, *J. Am. Chem. Soc.*, 1954, **76**, 1455–1456.

72   E. A. Ilardi, E. Vitaku and J. T. Njardarson, *J. Med. Chem.*, 2014, **57**, 2832–2842.

73   J. Kirschbaum, in *Analytical Profiles of Drug Substances*, 1978, pp. 251–275.

74   S.-H. Cho, H. J. Park, J. H. Lee, J.-A. Do, S. Heo, J. H. Jo and S. Cho, *J. Pharm. Biomed. Anal.*, 2015, **111**, 138–146.

75   M. P. O'Leary, C. Roehrborn, G. Andriole, C. Nickel, P. Boyle and K. Höfner, *BJU Int.*, 2003, **92**, 262–266.

76   S. Bernstein, R. H. Lenhard, W. S. Allen, M. Heller, R. Littell, S. M. Stolar, L. I. Feldman and R. H. Blank, *J. Am. Chem. Soc.*, 1956, **78**, 5693–5694.

77   J. S. Mills, A. Bowers, C. Djerassi and H. J. Ringold, *J. Am. Chem. Soc.*, 1960, **82**, 3399–3404.

78   Fluticasone   Propionate, DrugBank, http://www.drugbank.ca/drugs/DB00588, (accessed February 2019).

79   WebMD, http://www.webmd.com/drugs/2/drug-20538/advair-diskusinhalation/details, (accessed February 2019).

80   G. H. Phillipps, E. J. Bailey, B. M. Bain, R. A. Borella, J. B. Buckton, J. C. Clark, A. E. Doherty, A. F. English, H. Fazakerley, S. B. Laing, E. Lane-Allman, J. D. Robinson, P. E. Sandford, P. J. Sharratt, I. P. Steeples, R. D. Stonehouse and C. Williamson, *J. Med. Chem.*, 1994, **37**, 3717–3729.

81   Fluticasone Furoate, DrugBank, http://www.drugbank.ca/drugs/DB08906, (accessed February 2019).

82   K. Biggadike, S. J. Coote and R. K. Nice, WO0212265, 2002.

83   K. Biggadike, P. Jones and J. J. Payne, WO0212266A1, 2002.

84   K. Solanki, R. Z. Bavadia, D. P. Patel, D. J. Patel, T. C. Shah and M. K. Singh, WO2012029077A2, 2012.

85   M. B. Berry, M. J. Hughes, D. Parry-Jones and S. J. Skittrall, WO2007144363A2, 2007.

86   J. J. Partridge and D. S. Walker, WO03012427A2, 2003.

87   S. J. Coote, R. K. Nice and M. D. Wipperman, WO03066653A2, 2003.

88   H. H. Claassen, H. Selig and J. G. Malm, *J. Am. Chem. Soc.*, 1962, **84**, 3593–3593.

89   M. Shaw, H. H. Hyman and R. Filler, *J. Am. Chem. Soc.*, 1969, **91**, 1563–1565.

90   M. A. Tius, *Tetrahedron*, 1995, **51**, 6605–6634.

91   N. Bartlett and F. O. Sladky, *Chem. Commun.*, 1968, 1046.

92   Xenon difluoride, Sigma Aldrich, https://www.sigmaaldrich.com/catalog/product/aldrich/394505?lang=en&region=GB, (accessed February 2019).

93   H. M. Kissman, A. M. Small and M. J. Weiss, *J. Am. Chem. Soc.*, 1960, **82**, 2312–2317.

94   P. G. Urben and Akzo-Nobel, *Bretherick's handbook of reactive chemical hazards*, Ed. 6, Butterworth-Heinemann, Oxford, 1999.

95   M. Tada, T. Matsuzawa, K. Yamaguchi, Y. Abe, H. Fukuda, M. Itoh, H. Sugiyama, T. Ido and T. Takahashi, *Carbohydr. Res.*, 1987, **161**, 314–317.

96   A. S. Kiselyov, *Chem. Soc. Rev.*, 2005, **34**, 1031–1037.

97   H. Meinert, *Zeitschrift für Chemie*, 2010, **5**, 64–64.

98   T. Umemoto and G. Tomizawa, *Tetrahedron Lett.*, 1987, **28**, 2705–2708.

99   T. Umemoto, S. Fukami, G. Tomizawa, K. Harasawa, K. Kawada and K. Tomita, *J. Am. Chem. Soc.*, 1990, **112**, 8563–8575.

100   K. Tomita and K. Kawada, *Org. Synth.*, 1990, **8**, 129.

101   *N*-Fluoropyridinium triflate, Sigma Aldrich, https://www.sigmaaldrich.com/catalog/product/aldrich/323659?lang=en&region=GB , (accessed February 2019).

102   *N*-Fluoropyridinium tetrafluoroborate, Sigma Aldrich, https://www.sigmaaldrich.com/catalog/product/aldrich/377260?lang=en&region=GB, (accessed February 2019).

103   R. E. Banks, M. K. Besheesh and R. G. Pritchard, *Acta Crystallogr. Sect. C Cryst. Struct. Commun.*, 2003, **59**, m141–m143.

104   T. Holm, I. Crossland, L. Eberson, E. Sjöstrand, I. Lagerlund and L. Ehrenberg, *Acta Chem. Scand.*, 1971, **25**, 59–69.

105   H. Yamataka, Y. Kawafuji, K. Nagareda, N. Miyano and T. Hanafusa, *J. Org. Chem.*, 1989, **54**, 4706–4708.

106   P. T. Nyffeler, S. G. Durón, M. D. Burkart, S. P. Vincent and C.-H. Wong, *Angew. Chem. Int. Ed.*, 2005, **44**, 192–212.

107   T. M. Bockman, K. Y. Lee and J. K. Kochi, *J. Chem. Soc. Perkin Trans. 2*, 1992, **1542**, 1581.

108   K. Y. Lee and J. K. Kochi, *J. Chem. Soc. Perkin Trans. 2*, 1992, 1011.

109   S. Ito, A. Satoh, Y. Nagatomi, Y. Hirata, G. Suzuki, T. Kimura, A. Satow, S. Maehara, H. Hikichi, M. Hata, H. Kawamoto and H. Ohta, *Bioorg. Med. Chem.*, 2008, **16**, 9817–9829.

110   J. Roppe, N. D. Smith, D. Huang, L. Tehrani, B. Wang, J. Anderson, J. Brodkin, J. Chung, X. Jiang, C. King, B. Munoz, M. A. Varney, P. Prasit and N. D. P. Cosford, *J. Med. Chem.*, 2004, **47**, 4645–4648.

111   A. S. Kiselyov, *Tetrahedron Lett.*, 2005, **46**, 4851–4854.

112   A. S. Kiselyov, *Tetrahedron Lett.*, 2006, **47**, 2631–2634.

113   T. Umemoto, G. Tomizawa, H. Hachisuka and M. Kitano, *J. Fluor. Chem.*, 1996, **77**, 161–168.

114   R. E. Banks, R. A. Du Boisson, W. D. Morton and E. Tsiliopoulos, *J. Chem. Soc., Perkin Trans. 1*, 1988, 2805–2811.

115   SelectFluor, Sigma Aldrich, https://www.sigmaaldrich.com/catalog/product/aldrich/439479?lang=en&regio

n=GB, (accessed February 2019).

116   R. E. Banks, *J. Fluor. Chem.*, 1998, **87**, 1–17.

117   A. Solladié-Cavallo, L. Jierry, A. Klein, M. Schmitt and R. Welter, *Tetrahedron: Asymmetry*, 2004, **15**, 3891–3898.

118   S. J. Dixon, K. M. Lemberg, M. R. Lamprecht, R. Skouta, E. M. Zaitsev, C. E. Gleason, D. N. Patel, A. J. Bauer, A. M. Cantley, W. S. Yang, B. Morrison and B. R. Stockwell, *Cell*, 2012, **149**, 1060–1072.

119   B. R. Stockwell, W. S. Yang and M. Larraufie, WO2015109009A1, 2015.

120   S. L. Acebedo, J. A. Ramírez and L. R. Galagovsky, *Steroids*, 2009, **74**, 435–440.

121   V. Rauniyar, a. D. Lackner, G. L. Hamilton and F. D. Toste, *Science*, 2011, **334**, 1681–1684.

122   H. Egami, J. Asada, K. Sato, D. Hashizume, Y. Kawato and Y. Hamashima, *J. Am. Chem. Soc.*, 2015, 5–8.

123   G. Stavber, M. Zupan and S. Stavber, *Synlett*, 2009, **2009**, 589–594.

124   K. K. Laali and G. I. Borodkin, *J. Chem. Soc. Perkin Trans. 2*, 2002, 953–957.

125   J. Baudoux, A.-F. Salit, D. Cahard and J.-C. Plaquevent, *Tetrahedron Lett.*, 2002, **43**, 6573–6574.

126   C. Baudequin, J.-C. Plaquevent, C. Audouard and D. Cahard, *Green Chem.*, 2002, **4**, 584–586.

127   M. R. P. Heravi, *J. Fluor. Chem.*, 2008, **129**, 217–221.

128   J. Pavlinac, M. Zupan and S. Stavber, *Molecules*, 2009, **14**, 2394–2409.

129   Y. A. Serguchev, L. F. Lourie, M. V. Ponomarenko, E. B. Rusanov and N. V.

Ignat'ev, *Tetrahedron Lett.*, 2011, **52**, 5166–5169.

130   L. F. Lourie, Y. A. Serguchev, M. V. Ponomarenko, E. B. Rusanov, M. V. Vovk and N. V. Ignat'ev, *Tetrahedron*, 2013, **69**, 833–838.

131   R. P. Bogautdinov, A. F. Fidarov, S. N. Morozkina, A. A. Zolotarev, G. L. Starova, S. I. Selivanov and A. G. Shavva, *J. Fluor. Chem.*, 2014, **168**, 218–222.

132   L. F. Lourie, Y. A. Serguchev, A. V. Bentya, M. V. Ponomarenko, E. B. Rusanov, M. V. Vovk, A. A. Fokin and N. V. Ignat'ev, *J. Fluor. Chem.*, 2015, **179**, 42–47.

133   A. S. Reddy and K. K. Laali, *Tetrahedron Lett.*, 2015, **56**, 5495–5499.

134   M. R. P. Heravi, *J. Fluor. Chem.*, 2008, **129**, 217–221.

135   S. P. Vincent, M. D. Burkart, C.-Y. Tsai, Z. Zhang and C.-H. Wong, *J. Org. Chem.*, 1999, **64**, 5264–5279.

136   X. Zhang, Y. Liao, R. Qian, H. Wang and Y. Guo, *Org. Lett.*, 2005, **7**, 3877–3880.

137   C. M. Whitehouse, R. N. Dreyer, M. Yamashita and J. B. Fenn, *Anal. Chem.*, 1985, **57**, 675–679.

138   R. Bertani, R. Seraglia, D. Favretto, R. A. Michelin, M. Mozzon, S. M. Sbovata and A. Sassi, *Inorganica Chim. Acta*, 2003, **356**, 357–364.

139   Y. A. Serguchev, M. V. Ponomarenko, L. F. Lourie and A. A. Fokin, *J. Phys. Org. Chem.*, 2011, **24**, 407–413.

140   Y. A. Serguchev, M. V Ponomarenko, L. F. Lourie and A. N. Chernega, *J. Fluor. Chem.*, 2003, **123**, 207–215.

141   M. Zupan, A. Gregorcic and A. Pollak, *J. Org. Chem.*, 1977, **42**, 1562–1566.

142   R. A. Sadykov, V. N. Yakovlev, R. G. Bulgakov, V. P. Kazakov, G. A. Tolstikov and A.

I. Kruppa, *J. Organomet. Chem.*, 1989, **377**, 1–8.

143   T. B. Patrick, S. Khazaeli, S. Nadji, K. Hering-Smith and D. Reif, *J. Org. Chem.*, 1993, **58**, 705–708.

144   C. a. Ramsden and R. G. Smith, *Org. Lett.*, 1999, **1**, 1591–1594.

145   Z. Li, Z. Wang, L. Zhu, X. Tan and C. Li, *J. Am. Chem. Soc.*, 2014, **136**, 16439–16443.

146   C. Sandford, R. Rasappan and V. K. Aggarwal, *J. Am. Chem. Soc.*, 2015, **137**, 10100–10103.

147   S.-W. Wu and F. Liu, *Org. Lett.*, 2016, **18**, 3642–3645.

148   A. Hassner, E. S. Ferdinandi and R. J. Isbister, *J. Am. Chem. Soc.*, 1970, **92**, 1672–1675.

149   S.-W. Wu, J.-L. Liu and F. Liu, *Chem. Commun.*, 2017, **53**, 12321–12324.

150   D. S. Timofeeva, A. R. Ofial and H. Mayr, *J. Am. Chem. Soc.*, 2018, **140**, 11474–11486.

151   W. W. Schoeller, J. Niemann and P. Rademacher, *J. Chem. Soc. Perkin Trans. 2*, 1988, 369.

152   A. G. Gilicinski, G. P. Pez, R. G. Syvret and G. S. Lal, *J. Fluor. Chem.*, 1992, **59**, 157–162.

153   N. Rozatian, I. W. Ashworth, G. Sandford and D. R. W. Hodgson, *Chem. Sci.*, 2018, **9**, 8692–8702.

154   Selectfluor II, Manchester Organics, http://www.manchesterorganics.com/C24036, (accessed February 2019).

155   X. Zhang, S. Guo and P. Tang, *Org. Chem. Front.*, 2015, **2**, 806–810.

156   T. F. Campbell and C. E. Stephens, *J. Fluor. Chem.*, 2006, **127**, 1591–1594.

157   D. Cahard, C. Audouard, J.-C. Plaquevent and N. Roques, *Org. Lett.*, 2000, **2**, 3699–3701.

158   N. Shibata, E. Suzuki, T. Asahi and M. Shiro, *J. Am. Chem. Soc.*, 2001, **123**, 7001–7009.

159   N. Shibata, T. Ishimaru, E. Suzuki and K. L. Kirk, *J. Org. Chem.*, 2003, **68**, 2494–2497.

160   T. Fukuzumi, N. Shibata, M. Sugiura, S. Nakamura and T. Toru, *J. Fluor. Chem.*, 2006, **127**, 548–551.

161   B. Mohar, D. Sterk, L. Ferron and D. Cahard, *Tetrahedron Lett.*, 2005, **46**, 5029–5031.

162   T. Yamamoto, Y. Suzuki, E. Ito, E. Tokunaga and N. Shibata, *Org. Lett.*, 2011, **13**, 470–473.

163   J. R. Wolstenhulme, J. Rosenqvist, O. Lozano, J. Ilupeju, N. Wurz, K. M. Engle, G. W. Pidgeon, P. R. Moore, G. Sandford and V. Gouverneur, *Angew. Chem. Int. Ed.*, 2013, **52**, 9796–9800.

164   B. Thierry, C. Audouard, J.-C. Plaquevent and D. Cahard, *Synlett*, 2004, **2004**, 0856–0860.

165   N. Shibata, T. Ishimaru, M. Nakamura and T. Toru, *Synlett*, 2004, 2509–2512.

166   S. Singh, D. D. DesMarteau, S. S. Zuberi, M. Witz and H. N. Huang, *J. Am. Chem. Soc.*, 1987, **109**, 7194–7196.

167   E. Differding, G. M. Rüegg and R. W. Lang, *Tetrahedron Lett.*, 1991, **32**, 1779–

1782.

168 E. Differding and G. M. Rüegg, *Tetrahedron Lett.*, 1991, **32**, 3815–3818.

169 E. Differding and M. Wehrli, *Tetrahedron Lett.*, 1991, **32**, 3819–3822.

170 A. J. Poss, M. Van Der Puy, D. Nalewajek, G. A. Shia, W. J. Wagner and R. L. Frenette, *J. Org. Chem.*, 1991, 5962–5964.

171 G. S. Lal, *J. Org. Chem.*, 1993, **58**, 2791–2796.

172 V. Reydellet-Casey, D. J. Knoechel and P. M. Herrinton, *Org Proc Res Dev*, 1997, **1**, 217–221.

173 V. V. Bogert and B. M. Bloom, US2961441, 1960.

174 D. E. Ayer, C. A. Schlagel and G. L. Flynn, US3980778, 1976.

175 G. Cainelli, A. Umani-Ronchi, M. Contento, S. Sandri and M. Da Col, US6369218, 2002.

176 F. La Loggia and M. Da Col, US20020062021A1, 2002.

177 P. MacDonald and P. Rossetto, WO2004052911, 2004.

178 S. Grassi, S. Mascheroni and R. Giani, US20140179914A1, 2014.

179 C. Sandford, R. Rasappan and V. K. Aggarwal, *J. Am. Chem. Soc.*, 2015, **137**, 10100–10103.

180 E. Laurent, R. Tardivel and H. Thiebault, *Tetrahedron Lett.*, 1983, **24**, 903–906.

181 V. M. Vlasov, *Russ. Chem. Rev.*, 2006, **75**, 765–796.

182 D. A. Singleton, A. A. Thomas and C. Biochemistry, *Reactions Rates of Isotopic Molecules*, UTC, 1995, vol. 117.

183   A. Goldblum and R. Mechoulam, *J. Chem. Soc. Perkin Trans. 1*, 1977, 1889.

184   T. Poisson, V. Dalla, C. Papamicaël, G. Dupas, F. Marsais and V. Levacher, *Synlett*, 2007, **2007**, 0381–0386.

185   F. De Vleeschouwer, V. Van Speybroeck, M. Waroquier, P. Geerlings and F. De Proft, *J. Org. Chem.*, 2008, **73**, 9109–9120.

186   X. Creary, *J. Am. Chem. Soc.*, 1981, **103**, 2463–2465.

187   T. B. Phan, C. Nolte, S. Kobayashi, A. R. Ofial and H. Mayr, *J. Am. Chem. Soc.*, 2009, **131**, 11392–11401.

188   B. Liu and S. Thayumanavan, *J. Am. Chem. Soc.*, 2017, **139**, 2306–2317.

189   S. Minegishi, S. Kobayashi and H. Mayr, *J. Am. Chem. Soc.*, 2004, **126**, 5174–5181.

190   Y-H. Pan and J. B. Stothers, *Can. J. Chem.*, 1967, **45**, 2943.

191   M. D. Struble, M. T. Scerba, M. Siegler and T. Lectka, *Science (80-.).*, 2013, **340**, 57–60.

192   C. R. Pitts, M. G. Holl and T. Lectka, *Angew. Chem. Int. Ed.*, 2018, **57**, 1924–1927.

193   M. D. Struble, M. G. Holl, M. T. Scerba, M. A. Siegler and T. Lectka, *J. Am. Chem. Soc.*, 2015, **137**, 11476–11490.

194   C. R. Pitts, M. G. Holl and T. Lectka, *Angew. Chem. Int. Ed.*, 2018, **57**, 1924–1927.

195   M. G. Holl, C. R. Pitts and T. Lectka, *Angew. Chem. Int. Ed.*, 2018, **57**, 2758–2766.

196   D. Griller and K. U. Ingold, *Acc. Chem. Res.*, 1980, **13**, 317–323.

197   A. Advance, D. Griller, K. U. Ingold, M. Newcomb, S. U. Park, A. G. Glenn, . B Manek, T. R. Varick, C. Ha, X. Yue, C. C. Johnson, K. E. Liu, S. J. Lippard and J. K. Atkinson, *J. Am. Chem. Soc*, 1994, **13**, 30.

198   M. Newcomb, D. L. Chestney and L. Tadic, *Acta Biol. Med. Ger*, 1992, **114**, 9209–9214.

199   M. Newcomb, *Tetrahedron*, 1993, **49**, 1151–1176.

200   J. M. Tanko, R. E. Drumright, N. Kamrudin Suleman and L. E. Brammer, *J. Am. Chem. Soc*, 1994, **116**, 1785–1791.

201   K. W. Shimkin, P. G. Gildner and D. A. Watson, *Org. Lett.*, 2016, **18**, 988–991.

202   Z. Li, Z. Wang, L. Zhu, X. Tan and C. Li, *J. Am. Chem. Soc.*, 2014, **136**, 16439–16443.

203   G. N. Maw and R. K. Boeckman Jr, *Org. Synth.*, 1992, **70**, 35.

204   W. J. A. Vandenheuvel and E. S. Wallis, *J. Org. Chem.*, 1962, **27**, 1233–1237.

205   C. J. Cramer and D. G. Truhlar, *Acc. Chem. Res.*, 2008, **41**, 760–768.

206   T. Yamakawa and T. Fukuyama, *Org. Synth.*, 2010, **87**, 126.

207   B. Basdevant and C. Y. Legault, *J. Org. Chem.*, 2015, **80**, 6897–6902.

208   A. Dalla Cort, *J. Org. Chem.*, 1991, **56**, 6708–6709.

209   D. F. Shellhamer, D. L. Carter, M. C. Chiaco, T. E. Harris, R. D. Henderson, W. S. C. Low, B. T. Metcalf, M. C. Willis, V. L. Heasley and R. D. Chapman, *J. Chem. Soc. Perkin Trans. 2*, 1991, 401.

210   J. Liu, J. Chan, C. M. Bryant, P. A. Duspara, E. E. Lee, D. Powell, H. Yang, Z. Liu, C. Walpole, E. Roberts and R. A. Batey, *Tetrahedron Lett.*, 2012, **53**, 2971–2975.

211   K. K. Laali, A. Jamalian and C. Zhao, *Tetrahedron Lett.*, 2014, **55**, 6643–6646.

212   M. Fujita, W. H. Kim, Y. Sakanishi, K. Fujiwara, S. Hirayama, T. Okuyama, Y. Ohki, K. Tatsumi and Y. Yoshioka, *J. Am. Chem. Soc.*, 2004, **126**, 7548–7558.

213   J. T. Welch and K. W. Seper, *J. Org. Chem.*, 1988, **53**, 2991–2999.

214   S. Sato, M. Yoshida and S. Hara, *Synthesis*, 2005, 2602–2605.

215   M. P. Dwyer, K. M. Keertikar, C. A. Coburn, H. Wu, B. Hu, B. Zhong, C. Zhang, Z. Dan, WO2012040924 (A1), 2012.

216   K. G. Rutherford and C. L. Stevens, *J. Am. Chem. Soc.*, 1955, **77**, 3278–3280.

217   H. Hofmann, H.-J. Haberstroh, B. Appler, B. Meyer and H. Herterich, *Chem. Ber.*, 1975, **108**, 3596–3610.

218   S.-Q. Qiu, Y.-H. Xu and T.-P. Loh, *Org. Lett.*, 2015, **17**, 3462–3465.

219   Y. Guo, B. Twamley and J. M. Shreeve, *Org. Biomol. Chem.*, 2009, **7**, 1716.

220   T. Sugimoto, N. Nakamura, M. Nojima and S. Kusabayashi, *J. Org. Chem.*, 1991, **56**, 1672–1674.

221   C. Guo, R.-W. Wang, Y. Guo and F.-L. Qing, *J. Fluor. Chem.*, 2012, **133**, 86–96.

222   S. Buksha, G. S. Coumbarides, M. Dingjan, J. Eames, M. J. Suggate and N. Weerasooriya, *J. Label. Compd. Radiopharm.*, 2005, **48**, 337–352.

223   É. Bélanger, K. Cantin, O. Messe, M. Tremblay and J.-F. Paquin, *J. Am. Chem. Soc.*, 2007, **129**, 1034–1035.

224   M. Hayashi, M. Shibuya and Y. Iwabuchi, *Org. Lett.*, 2012, **14**, 154–157.

225   F. E. Ziegler and K. J. Hwang, *J. Org. Chem.*, 1983, **48**, 3349–3351.

226   J. B. P. A. Wijnberg, J. Vader and A. De Groot, *J. Org. Chem.*, 1983, **48**, 4380–4387.

227   T. Umemoto, K. Tomita, K. Kawada and K. Tomisawa, EP0204535A1, 1986.

228   M. Tischler, G. Gal and G. A. Stein, *Org. Synth.*, 1959, **39**, 27.

229   B. R. Davis, *J. Chem. Soc. Perkin Trans. 1*, 1979, 1–5.

230   S. M. Bloom, *J. Am. Chem. Soc.*, 1958, **80**, 6280–6283.

231   K. Thangaraj, P. C. Srinivasan and S. Swaminathan, *Synthesis (Stuttg).*, 1982, **1982**, 855–857.

232   Frisch, M. J.; Trucks, G. W.; Schlegel, H. B.; Scuseria, G. E.; Robb, M. A.; Cheeseman, J. R.; Scalmani, G.; Barone, V.; Mennucci, B.; Petersson, G. A.; Nakatsuji, H.; Caricato, M.; Li, X.; Hratchian, H. P.; Izmaylov, A. F.; Bloino, J.; Zheng, J.; Sonnenberg, L.; Hada, M.; Ehara, M.; Toyota, K.; Fukuda, R.; Hasegawa, J.; Ishida, M.; Nakajima, T.; Honda, Y.; Kitao, O.; Nakai, T.; Vreven, T.; Montgomery, J. A.; Peralta, J. E.; Ogliaro, F.; Bearpark, M.; Heyd, J. J.; Brothers, E.; Kudin, K. N.; Staroverov, V. N.; Kobayashi, R.; Normand, J.; Raghavachari, K.; Rendell, A.; Burant, J. C.; Iyengar, S. S.; Tomasi, J.; Cossi, M.; Rega, N.; Millam, J. M.; Klene, M.; Knox, J. E.; Cross, J. B.; Bakken, V.; Adamo, C.; Jaramillo, J.; Gomperts, R.; Stratmann, R. E.; Yazyev, O.; Austin, A. J.; Cammi, C.; Pomelli, C.; Ochterski, J. W.; Martin, R. L.; Morokuma, K.; Zakrzewski, V. G.; Voth, G. A.; Salvador, P.; Dannenberg, J. J.; Dapprich, S.; Daniels, A. D.; Farkas, O.; Foresman, J. B.; Ortiz, J. V.; Cioslowski, J.; Fox, D. J.: Gaussian 09. Revision D.01. Gaussian, Inc.: Wallingford CT, 2009.

233   Archie-WeSt, https://www.archie-west.ac.uk/ (accessed February 2019).